UNCLASSIFIED

AD NUMBER
ADC020845
CLASSIFICATION CHANGES
TO: unclassified
FROM: confidential
LIMITATION CHANGES
TO: Approved for public release, distribution unlimited
FROM: Controlling DoD Organization. Naval Ocean Systems Center, San Diego, CA 92152.
AUTHORITY
ONR ltr, 31 Jan 2006; ONR ltr, 31 Jan 2006

THIS PAGE IS UNCLASSIFIED

CONFIDENTIAL

NOSC

LEVEL II

NOSC TR 467

NOSC TR 467

ADC020845

Technical Report 467

PROPAGATION LOSS ASSESSMENT OF THE BEARING STAKE EXERCISE (U)

MA Pedersen and GS Yee
RR Gardner, Project Technical Director

Research and Development Dept., January — May 1977

(16) X0 75505

(17) X0 76510 11

(10) Melvin A. Pedersen
Grant S. Yee R.R. Gardner

DTIC
ELECTE
MAR 2 6 1980

28 SEPTEMBER 1979

(12) 245

Classified by: OPNAVINST S5513.5-03
Review on: 8 October 1994

"NATIONAL SECURITY INFORMATION"

"Unauthorized Disclosure Subject to Criminal Sanctions"

DDC FILE COPY

NAVAL OCEAN SYSTEMS CENTER
SAN DIEGO, CALIFORNIA 92152

CONFIDENTIAL

393 159

80 2 8 50

NAVAL OCEAN SYSTEMS CENTER, SAN DIEGO, CA 92152

AN ACTIVITY OF THE NAVAL MATERIAL COMMAND

SL GUILLE, CAPT, USN
Commander

HL BLOCD
Technical Director

ADMINISTRATIVE INFORMATION (U)

(U) The work in this report, sponsored by the Naval Electronic Systems Command (PME-124), was performed from January through May 1977.

Released by
N. O. Booth, Head
Environmental Acoustics Division

Under authority of
J. D. Hightower, Head
Environmental Sciences Department

ACKNOWLEDGMENTS (U)

(U) The authors acknowledge the excellent contributions and performance of all BEARING STAKE field personnel involved in the collection of the acoustic data vital to this propagation loss assessment report. In particular, the authors thank Western Electric Company for providing the data from the deep bottom-mounted arrays and Dr. Steven K. Mitchell (Applied Research Laboratories, Austin, Texas) for the supporting bottom-reflection loss information. Without these data, the analyses and assessments contained in this report would not have been possible.

(U) Special acknowledgment is extended to the many members of NOSC involved in the preparation of this report. Dr. Richard Bannister (Exchange Scientist from New Zealand) provided all the inputs to the source-depth dependence assessment and Richard T. Bachman provided all the bathymetric profiles in the appendix. Rawson F. Hosmer, DeWayne White, and Dr. John Northrop performed the bulk of the data reduction and computer programming analyses of the data contained in this report. Their contributions and the assistance of all others in preparing this report are gratefully acknowledged.

SECURITY CLASSIFICATION OF THIS PAGE *(When Data Entered)*

REPORT DOCUMENTATION PAGE

READ INSTRUCTIONS BEFORE COMPLETING FORM

1. REPORT NUMBER: NOSC Technical Report 467 (TR 467) / 2. GOVT ACCESSION NO.	3. RECIPIENT'S CATALOG NUMBER
4. TITLE *(and Subtitle)*: PROPAGATION LOSS ASSESSMENT OF THE BEARING STAKE EXERCISE (U)	5. TYPE OF REPORT & PERIOD COVERED: R&D: Jan–May 1977
	6. PERFORMING ORG. REPORT NUMBER
7. AUTHOR*(s)*: Melvin A. Pedersen and Grant S. Yee	8. CONTRACT OR GRANT NUMBER*(s)*
9. PERFORMING ORGANIZATION NAME AND ADDRESS: Naval Ocean Systems Center, San Diego, California 92152	10. PROGRAM ELEMENT, PROJECT, TASK AREA & WORK UNIT NUMBERS: 63788N, X0755-0S, X0765104
11. CONTROLLING OFFICE NAME AND ADDRESS: Naval Electronic Systems Command (PME - 124)	12. REPORT DATE: 28 September 1979
	13. NUMBER OF PAGES: 242
14 MONITORING AGENCY NAME & ADDRESS*(if different from Controlling Office)*	15. SECURITY CLASS. *(of this report)*: Confidential
	15a. DECLASSIFICATION/DOWNGRADING SCHEDULE: Review on: 8 October 1994

16. DISTRIBUTION STATEMENT *(of this Report)*

17. DISTRIBUTION STATEMENT *(of the abstract entered in Block 20, if different from Report)*

18 SUPPLEMENTARY NOTES

19. KEY WORDS *(Continue on reverse side if necessary and identify by block number)*

Acoustic surveillance
Ambient noise
Propagation
Reflectivity

20. ABSTRACT *(Continue on reverse side if necessary and identify by block number)*

(C) This report is an acoustic propagation loss assessment for the Northwest Indian Ocean based upon propagation loss data collected in support of BEARING STAKE acoustic measurements. The BEARING STAKE exercise was conducted by NOSC at five sites in the Northwest Indian Ocean between January and May 1977.

DD FORM 1 JAN 73 1473 EDITION OF 1 NOV 65 IS OBSOLETE
S/N 0102-LF-014-6601

CONFIDENTIAL

SECURITY CLASSIFICATION OF THIS PAGE *(When Data Entered)*

EXECUTIVE SUMMARY (U)

(C) The BEARING STAKE exercise was an acoustic measurements program that was conducted at five selected sites in the Northwest Indian Ocean during the period of January through May 1977. The major objective of BEARING STAKE was to collect acoustic data to determine the variability in the acoustic environment and to provide inputs to systems performance evaluation models. The program was sponsored by the Naval Electronic Systems Command (PME-124).

(C) This report contains an overall assessment of the propagation loss data collected during BEARING STAKE at the following sites in the Northwest Indian Ocean: Site 1A/1B (Gulf of Oman), Sites 2 and 3 (central Arabian Sea), Site 4 (western Somali Basin), and Site 5 (southern Arabian Sea).

(C) The BEARING STAKE exercise was successful in terms of collecting, analyzing, and interpreting acoustic data. The lesson learned from this exercise is that an acoustic measurement program, such as BEARING STAKE, should be conducted in ocean areas where the deployment of surveillance systems is being considered. Although theoretical models have been developed to predict the propagation losses for surveillance systems in specified locations, these predictions are only as good as the environmental acoustic inputs to the models.

PROPAGATION LOSS ASSESSMENT RESULTS (U)

1. (C) Propagation losses were unexpectedly low for the basins of the Northwest Indian Ocean such as the Indus Fan, Gulf of Oman, and Somali Basin. These low propagation losses correlated well with measurements of low bottom loss in BEARING STAKE. With the exception of high-loss ridge areas, such as the Carlsberg Ridge and Owen Ridge, propagation loss will not be the limiting factor in system performance. Performance will depend more on other acoustic variables such as the noise background and signal coherence.

2. (C) For bottom-limited areas such as the Gulf of Oman and the Indus Fan, the receiver depth with minimum propagation loss is at the ocean floor. However, a 2–3-dB improvement in signal-to-noise ratio may result if the receiver is suspended somewhat off the ocean floor; e.g., 30 m off the floor at 25 Hz.

3. (C) The placement of surveillance receivers on the high-loss ridges bounding a low-loss, bottom-limited basin is not an optimal choice. For example, the choice of sites for the Indus Fan should not be limited to the periphery of the fan but should include midbasin locations which are removed from shipping lanes to minimize shipping noise.

4. (C) Experimental data and results of normal mode theory indicate that the number of multipaths is much larger in bottom-limited areas than in convergence zone areas. This result suggests that array beamforming will pose more of a problem in the Indian Ocean than in the deep Pacific and Atlantic.

5. (C) Site 4, in the Somali Basin, differed from the other BEARING STAKE sites in that there was a slight depth excess. Strong convergence zones were observed at 290 Hz but not at 25 Hz. The receivers measuring the lowest propagation losses were located on the Chain Ridge. At 140 and 290 Hz the receiver with the lowest loss was 400 m above the floor of the basin, whereas at 25 Hz the receiver was 1050 m above the floor. The

acoustic results indicate a very complicated dependence on frequency, receiver depth, depth excess, and season of the year. Critical decisions as to a surveillance site configuration in the Somali Basin should be held in abeyance until theoretical studies on the dependence of the mentioned variables are completed and verified by additional experimental measurements.

6. (C) The azimuthal dependence of propagation loss at a given BEARING STAKE site was larger than the difference between the events of lowest propagation loss at the various sites.

7. (C) The only significant dependence on source depth in the experimental data was the high propagation loss associated with an 18-m source depth at 20 Hz. The effect has been modeled accurately by both normal mode and ray theory and is a result of cancellation effects near the ocean surface (commonly known as the surface decoupling effect).

8. (C) The events with the highest propagation losses were generally associated with bathymetric features with high bottom loss. The highest propagation losses measured in BEARING STAKE occurred for the events which ran west of the Owen Ridge.

9. (C) On the basis of the propagation loss results for the three sites associated with the Indus Fan, the area was divided into two bottom loss regimes – a low-loss regime to the south and a somewhat higher-loss regime to the north.

10. (C) Comparisons of the BEARING STAKE experimental data and results with three propagation loss models (ASTRAL, RAY WAVE, and FACT) indicate that with some minor modifications the ASTRAL model is well suited for the prediction of mean propagation loss in a bottom-limited environment such as BEARING STAKE.

11. (C) Comparisons of the event of lowest propagation loss at each site with the familiar Eleuthera Reference Propagation Loss Curve show that for 25 Hz the measured loss at all available ranges for all five sites was less than the reference by as much as 13 dB. For 140 Hz, for all sites except Site 2, the losses were less than the reference by as much as 6 dB. Site 2 values varied from 1 dB smaller at short ranges to 2 dB larger at ranges beyond 300 km. For 290 Hz, the losses were greater than the reference by as much as 3 dB for Sites 1B and 3 and 9 dB for Site 2 At Site 4 the losses were less than the reference by as much as 4 dB, and at Site 5 the losses were comparable at short ranges and exceeded the reference by 3 dB at ranges beyond 550 km.

12. (U) The major portion of the propagation loss data collected during BEARING STAKE was found to be reliable, consistent, and valid. There were a few identifiable data sets at each site which were in error and/or questionable. These data sets were not used to influence the conclusions of this assessment report.

13. (C) It can be concluded, from the propagation loss assessment of BEARING STAKE, that propagation loss in the Northwest Indian Ocean will not adversely affect the performance of surveillance array systems operating in the area. How well a system will perform in the area will depend on other acoustic parameters such as signal coherence, noise background, and signal processing techniques.

PREFACE (U)

(C) The BEARING STAKE exercise was conducted by the Naval Ocean Systems Center (NOSC) under the sponsorship of the Naval Electronic Systems Command (PME-124) at five sites in the Northwest Indian Ocean between January and May 1977. Dr. Robert R. Gardner (NOSC) was the Technical Director of the overall BEARING STAKE operation. This report is an acoustic propagation loss assessment for the Northwest Indian Ocean based upon propagation loss data collected in support of BEARING STAKE acoustic measurements.

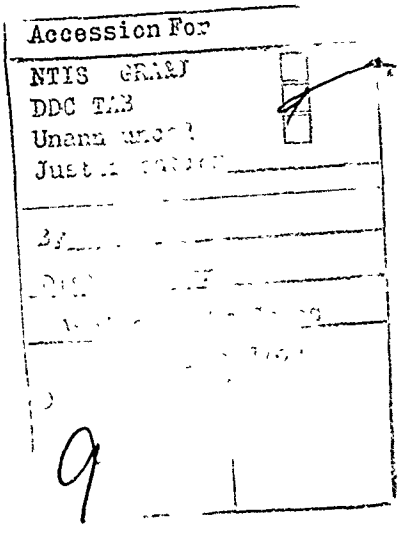

CONTENTS (U)

ILLUSTRATIONS (U)

TABLES (U)

1.0 (U) INTRODUCTION

(U) The BEARING STAKE exercise was a major acoustic survey program conducted in the Northwest Indian Ocean from January through May 1977. The program was sponsored by the Naval Electronic Systems Command (PME-124). The survey was designed to collect acoustic data to determine the variability in the acoustic environment, provide inputs to performance models, and provide acoustic data for assessing surveillance systems options in selected areas of the Indian Ocean.

(C) The survey utilized near-surface, midwater, and bottom-mounted receivers/arrays to collect the necessary data to perform assessments of the following environmental acoustic properties in the Indian Ocean:

- Propagation loss versus frequency and depth
- Noise (omnidirectional, directional, ambient)
- Bottom interaction
- Wavefront coherence
- Environment

(C) This report presents the propagation loss assessment of the BEARING STAKE exercise based upon the data collected at five selected sites in the Northwest Indian Ocean as shown in figure 1. Assessments of the other acoustic properties are being made by the principal investigators involved and will be reported accordingly in other reports. These assessments will provide to surveillance system designers heretofore unavailable acoustic data required to assess the performance of passive surveillance systems in the Indian Ocean.

(U) This report is an assessment of the propagation loss at each site and an overall propagation loss assessment of the operating areas as a whole.

(U) The operational aspects of the BEARING STAKE exercise, measurement procedures, and equipment descriptions will be mentioned only briefly in this report. Detailed exercise planning documents, systems descriptions, and preliminary results of data processing and analyses are contained in references 1–5.

(U) The data for this report came from the various activities that participated in BEARING STAKE. The Applied Research Laboratories, Austin, Texas (ARL), provided

---

1. "Acoustic Survey Program: Planning Document (U)," S-2105-76, Naval Undersea Center, 15 June 1976. (SECRET)
2. "Technical Specifications for Project BEARING STAKE Acoustic Survey (U)," TS 196-76, Western Electric Company, 18 November 1976. (SECRET)
3. "Supplements to Technical Specifications for BEARING STAKE (U)," 00S-4061-76, Naval Undersea Center, 17 December 1976. (SECRET)
4. "BEARING STAKE Data Analysis Plan (U)," 00S-1055-77, Naval Ocean Systems Center, May 1977. (SECRET)
5. "BEARING STAKE Exercise: Preliminary Results (U)," by the Principal Scientific Investigators, Naval Ocean Systems Center TR 169, 31 October 1978. (CONFIDENTIAL)

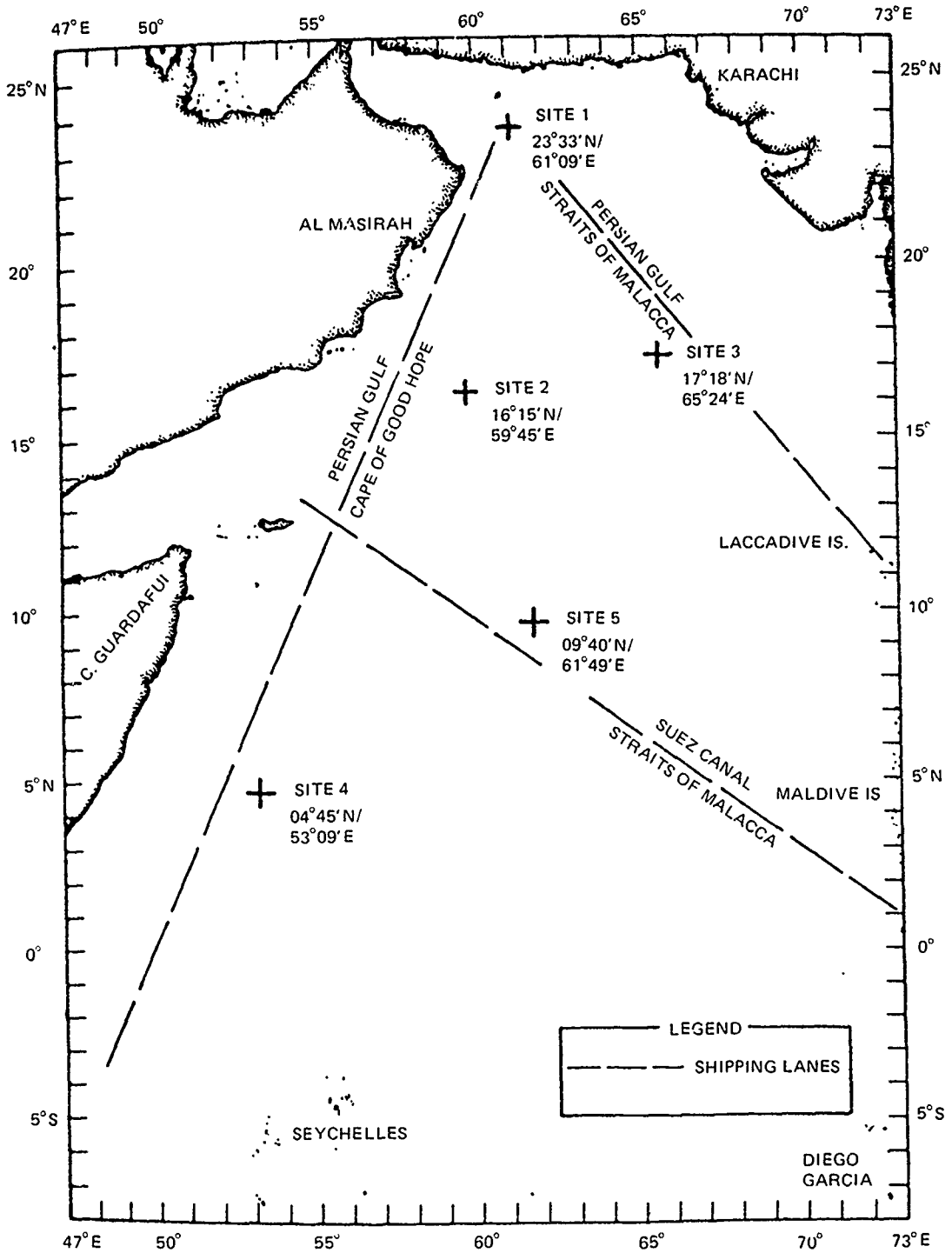

Figure 1. (C) BEARING STAKE site locations. (U)

propagation loss and bottom loss data (ref 6 and 7) as measured with the acoustic data capsule (ACODAC) and the bottom-moored system (BMS). Western Electric Company (WECo) provided propagation loss data (ref 8) as measured by the bottom-mounted array (BMA). The Naval Ocean Research and Development Activity (NORDA) provided measured sound speed profiles. Propagation loss data from the Ocean Acoustic Measurement System (OAMS) towed array and the Long Acoustic Towed Array (LATA) were provided by in-house NOSC personnel. All their contributions aided greatly in the preparation of this report.

(U) The bathymetry along the track/direction of the propagation loss runs for all five BEARING STAKE sites is contained in appendix A. The bathymetry is included in this report because of the principal role it plays in assessing propagation loss.

(U) Other equally important factors, such as sound speed profiles, bottom loss, and ambient noise data, that are used in the assessment of propagation loss are (or will be) reported in other BEARING STAKE reports. Only the results of the propagation loss measurements are presented here. However, data will be presented in detail whenever needed to clarify and/or substantiate conclusions reached.

(C) This report discusses, first, the data reduction methodology used to determine the variability, consistency, errors, and validity of the BEARING STAKE propagation loss data at all five sites. Propagation loss assessments are then presented for each site. The assessments are, in general, based upon receiver depth, frequency, range, bathymetry, and source depth and the effect of these on propagation loss. An overall propagation loss assessment based upon the results from the five sites is then presented as well as recommendations for future measurements that should be made in the Indian Ocean to substantiate the conclusions reached in this report.

---

6. "BEARING STAKE – Vertical ACODAC Acoustic Measurements Data Report (U)," ARL-TR-78-8, Applied Research Laboratories, The University of Texas at Austin, 15 February 1978. (CONFIDENTIAL)
7. "Analysis of Acoustic Bottom Interaction in BEARING STAKE (U)." by S. K. Mitchell, K. C. Focke, J. J. Lemmon, and M. M. McSwain, ARL-TR-78-52, November 1978. (CONFIDENTIAL)
8. "Project BEARING STAKE Transmission Loss, Omnidirectional Ambient Noise from Bottomed Arrays (U)," by J. T. Osborne, Western Electric Company, Greensborough, North Carolina, 5 May 1978. (CONFIDENTIAL)

2.0 (U) ANALYSIS METHODOLOGY

(U) During BEARING STAKE, propagation loss measurements were conducted at each of the five sites to obtain the data required to provide for the propagation loss assessment contained in this report. The data from a total of 47 propagation loss runs were analyzed for this report. Primary receivers used in collecting the data were the bottom-mounted array (BMA) and the acoustic data capsule (ACODAC).

(U) The data were made available to NOSC in the form of digital magnetic tapes and plotted paper charts. The BMA data came from WECo and the ACODAC data from ARL/UT. As might be expected from an exercise of the magnitude of BEARING STAKE, the total volume of data collected could easily become overwhelming and unmanageable.

(C) For example, figure 2 presents the basic propagation loss data for a bottomed hydrophone at Site 1B (event 1BP1) at a frequency of 25 Hz. The dots represent the ARL produced observations from the ACODAC and the crosses represent the WECo BMA data. The example is representative of hundreds of such plots that would be produced if the data were plotted point by point.

(U) Therefore, a decision was made to compress the data into a more manageable format. There were two main reasons for doing data compression. The first was to reduce the experimental data to integral ranges which facilitated the comparison of data sets with each other as well as with propagation models. The second was to reduce the scatter in the data. The original experimental data contained the phasing effects of multipaths, whereas propagation models rely on incoherent addition of multipaths. Compression reduces the data to a state more compatible with that of the models.

2.1 (U) DATA COMPRESSION

(C) As detailed in the test plans (ref 1), the acoustic projectors used in BEARING STAKE were cycled to give a 2-minute off period every 10 minutes. Thus, there are 10-minute sets of propagation data with 2-minute gaps between sequential data sets for a given run. The WECo method of data reduction was to manually read the data recorded on graphic recorders at 2-minute intervals and store the information on magnetic tape. The ARL method was to digitally process the data with an output at 1-minute intervals. However, in order to avoid the necessity for precise coordination of the ARL digital processor with the source cycle, the initial and final outputs for a 10-minute interval data set were rejected. Hence, for each 10-minute data set, WECo typically had five observations and ARL had eight. For a typical propagation loss run, the total number of data points amounted to 1300.

(U) In order to analyze the experimental data, it was necessary to use smoothing techniques, as meaningful comparisons of raw data such as shown in figure 2 are almost impossible. The principal smoothing method of the raw data to compress the vast volumes of data in simple representations was to average the raw CW and SUS data in 50-km range bins (or 30° bearing bins).

(C) In the case of radial events, the raw data were averaged in 50-km range bins centered at integral multiples of 50 km. Thus, the 50-km bin covers the interval from 25 to 75 km, the 100-km bin covers the interval from 75 to 125 km, etc. The squared pressure corresponding to each propagation loss observation in the bin was summed, divided by the

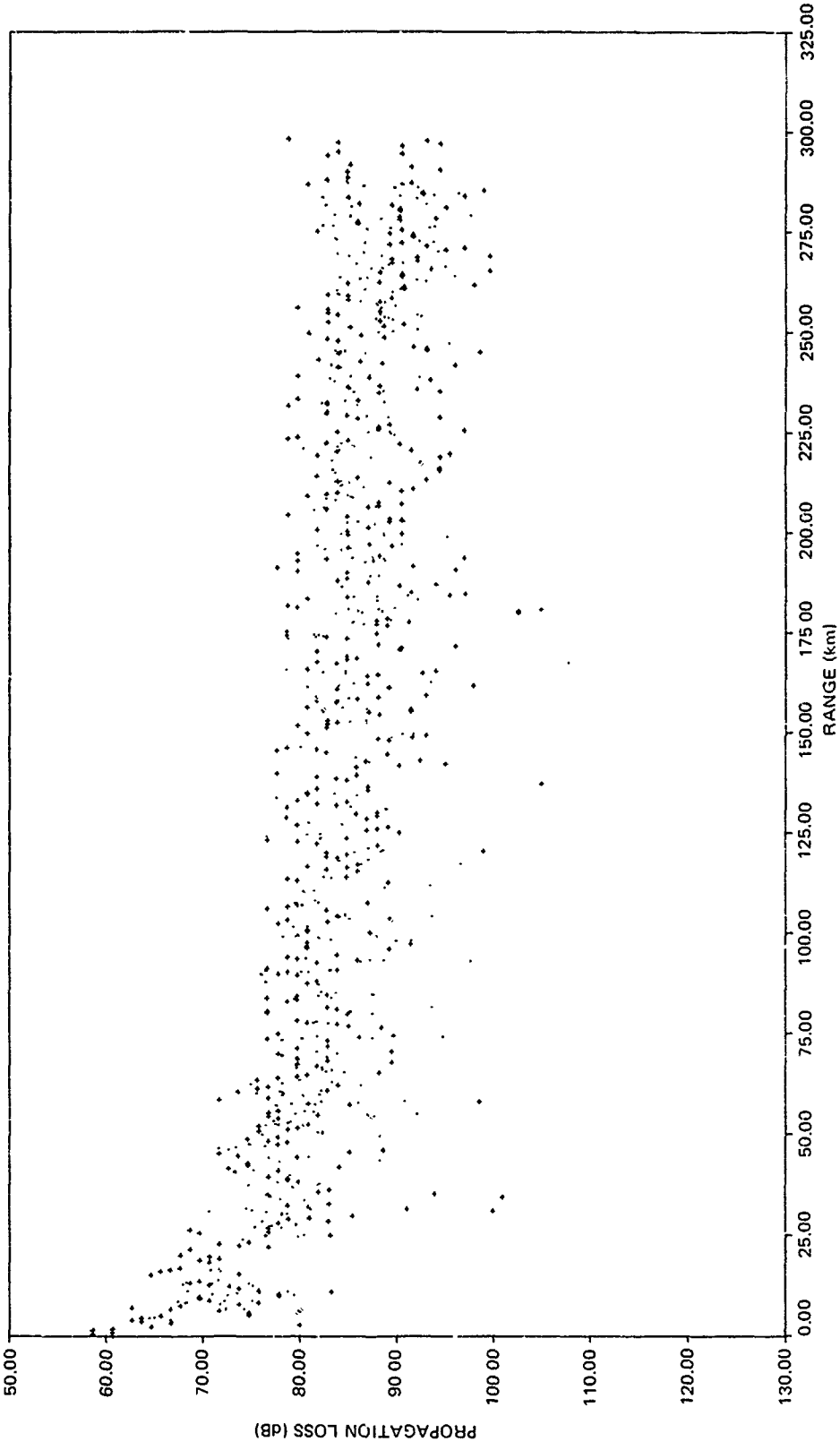

Figure 2. (C) Propagation loss as a function of range at Site 1B for 25 Hz. (C)

number of observations, and then converted to dB to obtain an average propagation loss for the bin. This choice of mean squared pressure is based on fundamental physical principles of conservation of energy and is commensurate with theoretical propagation loss models such as ASTRAL or RAY WAVE, which incoherently add the squared pressures of multipath contributions. Many examples of this type of data smoothing are presented throughout this report. For example, figure 3 shows the smoothed results of the data shown in figure 2.

(C) In the case of circular runs made at constant range (arc events), the raw data were averaged in 30° bearing bins centered at integral multiples of 30° in azimuth. This bin size was chosen so that the number of observations (about 70) per bin was comparable to that for the 50-km range bins.

(C) Another method of data smoothing was to obtain averages of the CW data in 2-km range bins. The main purpose of this method was to facilitate a comparison of the data with propagation models. The mean of the squared pressure level for each 10-minute data set was determined and then, by using linear interpolation, the mean at even integral range increments of 2 km was determined and converted to propagation loss. The results of this compression technique on the data (shown in figure 2) are plotted in figure 4. The crosses of figure 4 are the WECo data, whereas the circles are the ARL data from the ACODAC. This run covered a range interval of about 298 km and a time interval of about 23 hours and 15 minutes. In this example, the 10-minute data sets are about 2.1 km apart. Thus, the range increments of 2 km are compatible with the data sampling rate. This method not only smoothed but reduced the data to integral ranges, which facilitated comparison of data sets with each other and with theoretical propagation models.

(C) The data smoothing just described proved very useful for assessing propagation losses at convergence zones for Site 4. However, for the remaining sites, which were bottom

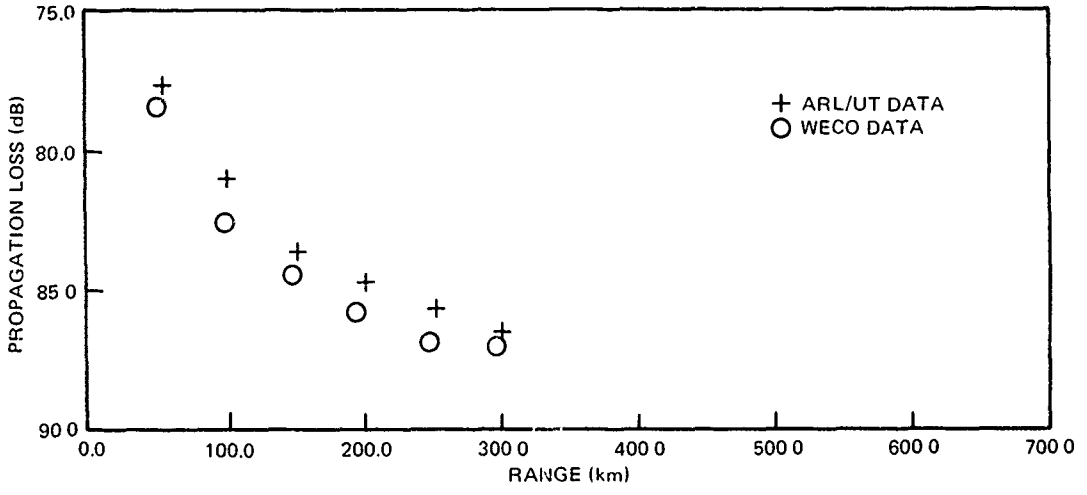

Figure 3. (C) Example of data compression results for data increments of 50 km. (U)

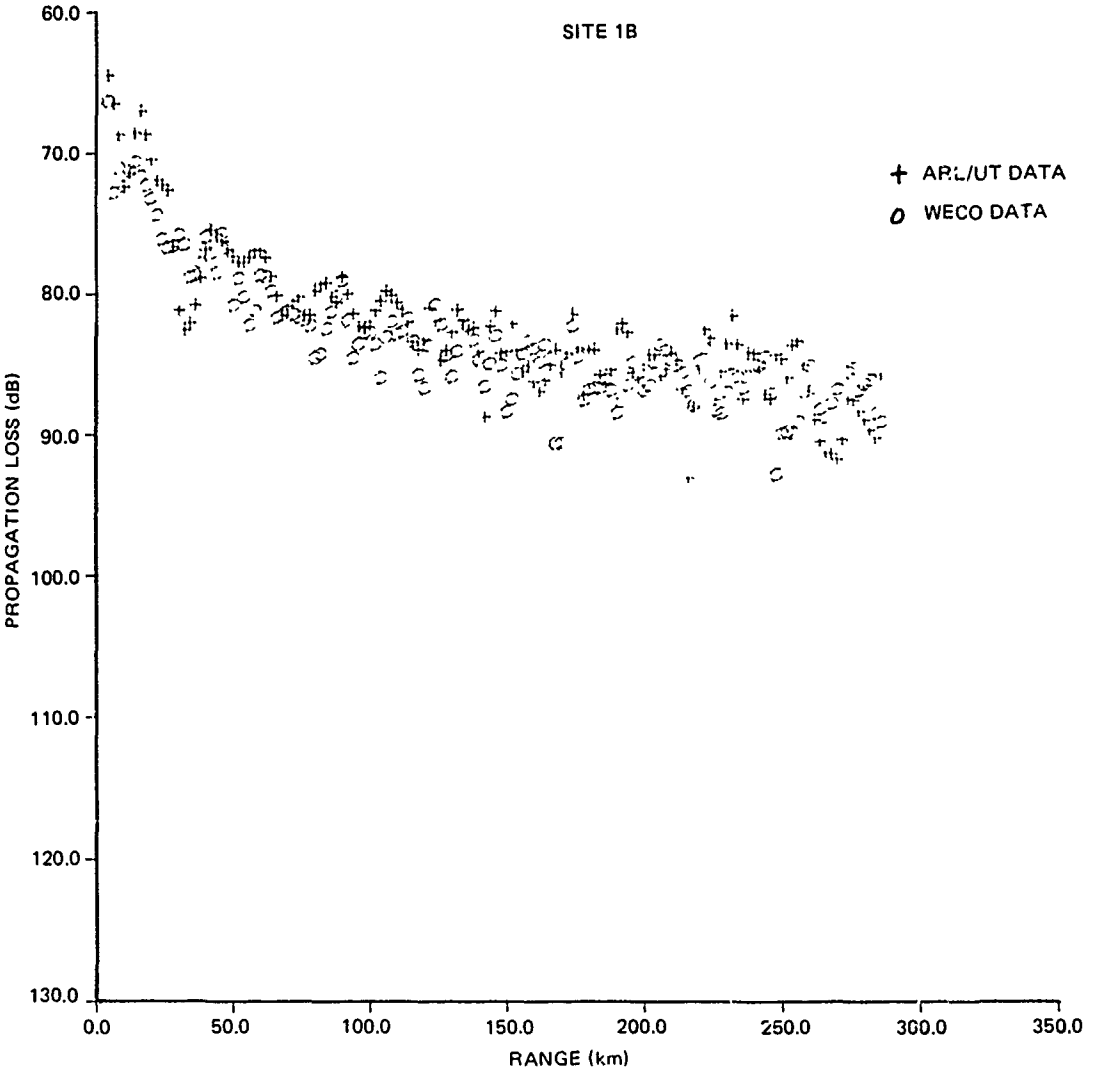

Figure 4. (C) Example of data compression results to reduce scatter of propagation loss data. (U)

limited, present incoherent models of propagation loss do not predict the fine structure which is preserved in the 2-km bin treatment of experimental data. As will be seen in the section on Data Variability in this report, a NOSC normal mode model run indicated that the problem is primarily statistical in nature. The bin size is dictated by the accuracy desired in the average propagation loss and the variance of the raw data.

(U) All the CW data of BEARING STAKE for this report on propagation loss were reduced in the above manner. The type of compression illustrated in figure 3 is used throughout this report. It preserves the basic trends with range and allows ready comparison between many data sets. For example, figure 3 indicates that the average propagation loss for WECo hydrophone 8 is consistently lower than that of the bottomed ACODAC.

The average propagation loss is about 1 dB less for the WECo hydrophone. This type of comparison is obscured by the scatter of data points in figures 2 and 4.

(U) In the remaining sections of this report, plots similar to that of figure 3 will be presented. The range is always an integral multiple of 50 km. Some of the plotted points may be slightly offset from these exact ranges. (The plot program offsets the range slightly so that different symbols can be identified more easily.)

(U) The data from the SUS runs were also compressed to produce plots similar to that of figure 3. However, since the SUS data were relatively sparse in range, the first stage compression was omitted and the means of the pressure squared of the raw data points were determined only over range increments of 50 km.

2.2 (U) DATA CONSISTENCY

(U) Since this report on propagation loss assessment takes into account the data from WECo and ARL/UT of propagation loss measurements from CW and SUS sources, an analysis was conducted to determine the consistency of the collected data. The analysis consisted of three separate studies:

1. WECo data only
2. Comparison of SUS and CW events
3. Comparison of SUS data at different source depths

2.2.1 (U) WECo Data

(C) Independent sets of WECo data for Sites 1 and 3 were first examined to determine which data sets were taken under comparable conditions. It was found that the comparable-condition data were too sparse to determine whether there were significant differences in the accuracy at various frequencies of the CW and SUS events, or in the accuracy at different sites. However, when all available data of this type were combined, some interesting results emerged. The combined data consist of a total of 18 independent evaluations. Of these, nine evaluations (50%) differed by no more than 0.3 dB, 12 evaluations (67%) differed by nor more than 0.5 dB; 16 evaluations (75%) differed by no more than 0.8 dB; and 18 evaluations (100%) differed by no more than 1 dB. These results demonstrate that the manner in which WECo data are processed is remarkably consistent. They also demonstrate that the process of calculating averages of the pressure squared over 50 km or 30° bins is very robust. Despite the huge variation in the raw data, propagation loss differences of less than 1 dB can be meaningful.

(C) Many factors contribute to the differences in propagation loss for various receivers measured under comparable conditions. One factor is a statistical error. A later section in this report on propagation loss variance shows that the typical standard error of the means for a 50-km range bin is about 0.6 dB for both CW and ship SUS events. However, this number does not represent the statistical error of an evaluation because the 18 evaluations were based on from 7 to 24 bins. This reduces the statistical component of a typical evaluation to something on the order of 0.2 dB. Other contributing factors are

errors in hydrophone response and system calibration. Any inconsistency in the manner in which the various receiver channels were processed also contributes. A final source of difference is that the measurements are not strictly "comparable" in that they are not made under identical conditions – some of the difference is "real" in terms of a somewhat different geometry.

(C) This analysis provides a good assessment of the receiver system error. The data suggest that an absolute difference (in propagation loss between two receivers as obtained by averaging over range or bearing bins) which exceeds 1 dB is significant. This difference represents a "real" difference above and beyond that attributed to receiver system errors. On the other hand, an absolute difference which is smaller than 0.3 dB is most likely due to statistical or receiver system error. An absolute difference which lies between 0.3 and 1.0 dB is more likely to be "real" but could reasonably be attributed to receiver system error.

2.2.2 (U) SUS and CW Comparison

(U) There are two different types of comparisons which involve the SUS data. The first type compares SUS data with CW data, whereas the second type compares SUS data at different source depths. Table 1 (A and B) shows the propagation loss differences that resulted from these two types of comparisons.

Table 1A. (C) Propagation loss differences (dB) between 91-m SUS depth events and the corresponding CW event over the same track. (U)

Site	BMA Rcvr Number	Frequency (Hz)		
		Low	140	300
1A	C*	0.2 dB	-0.8 dB	3.0 dB
1B	C	0.3	3.2	4.2
2	3	1.2	-8.0	-15.5
2	7	2.5	-4.2	–
3	C	1.0	1.5	0.3
4	1	2.7	3.2	–
4	3	2.7	2.5	4.8
4	7	2.8	1.3	–
5	5	1.8	-2.0	1.0
Median		1.4	1.1	2.0

*Values are averaged over available bottomed receivers.

Table 1B. (C) Propagation loss differences (dB) between 91-m and 243-m depth sources for SUS events. (U)

	Frequency (Hz)			
Event	20	50	140	290
1AS1	2.8	-0.4	1.6	4.1
1BS1	1.9	0.3	3.0	4.6
2S1	2.6	-1.6	0.1	2.6
2S2	6.8	1.4	1.0	3.0
3S1	2.7	-0.4	2.4	3.6
3S2	2.3	-0.2	2.3	2.0
4S1	3.6	-1.1	0.4	1.0
5S1	2.9	-1.2	2.3	2.3
Median	2.7	-0.4	1.9	2.8

(C) At each site, there were a CW event and a SUS event which ran over the same bathymetry (within navigation errors). Table 1A shows the propagation loss difference between the SUS event and that of the CW event based on the average loss over the available bins. The first column indicates the sites and the second column indicates the BMA receiver which was used to obtain the data. The "C" in the second column means that an average was taken over all available bottomed receivers. The median value shown is the value taken over the various sites and considers only the low value at Sites 2 and 4 where multiple receivers were present. The main value of table 1A is as a consistency check in the data for the various sites. For example, the results at Site 2 for 140 and 300 Hz are completely out of line with the results for the other sites. (As discussed later in the Site 2 assessment section of this report, investigations show that the 140- and 290-Hz data from event 2P1 at Site 2 are probably in error.) However, the low-frequency data for Site 2 falls in line with the data for the other sites.

(C) All the low-frequency data are quire consistent. The maximum difference from the median value is only 1.4 dB. For the low-frequency data, the source depths are comparable. However, the SUS data were analyzed at 20 Hz and the CW data at 25 Hz at all sites except Site 5, where the frequency was 22 Hz. It is believed that the median value of 1.4 dB at the low frequency represents a difference in source levels rather than a difference in propagation loss. The difference between the true and assumed source levels appears to be 1.5 dB larger for the CW source than for the 91-m SUS charges.

(C) Consider next the data at 140 and 300 Hz. If we discount the Site 2 data, the values at Site 5 for 140 and 300 Hz appear to be out of line. Again, this may have been caused by a relative difference in source level. There is also an effect of different source depths in that the CW source depth was 18 m whereas the SUS depths were 91 m.

(U) Considering all the factors involved, such as different types of processing and the source levels of the SUS and CW sources, the agreement of the CW and SUS results seems reasonable.

2.2.3 (U) Comparison of SUS Data

(C) This discussion describes the results of a comparison of the data from different source depths for SUS events. Table 1B shows the propagation loss differences between the 91- and 243-m SUS depths for all the ship SUS events. The median of the differences at each frequency listed is also given.

(C) First, note that the largest difference at any frequency from its corresponding median value is 4.1 dB for event 2S2 at 20 Hz. The next largest difference is only 1.8 dB. It is apparent that the 20-Hz data for event 2S2 are in error.

(C) A detailed analysis was made to determine whether the 91- or 243-m source depth data, or both, were in error. The analysis was accomplished in the following manner.

Step 1. (C) The propagation loss differences between 20 and 50 Hz at 91 and 243 m were compared for two events at Site 3 (events 3S1 and 3S2). The values obtained from both events were 3.7 dB at 91 m and 6.5 dB at 243 m.

Step 2. (C) Corresponding propagation loss differences for event 2S2 were 40 dB at 91 m and 9.2 dB at 243 m. Thus, the losses for the 91-m SUS depth in event 2S2 appear to be correct (4.0 dB vice 3.7 dB in step 1).

Step 3. (C) If we accept the median value of 2.7 dB shown in table 1B for 20 Hz and the 6.8-dB value for event 2S2, we can conclude that the 243-m SUS depth data are in error by 4.1 dB.

Step 4. (C) Furthermore, the value for event 2S2 at 50 Hz in table 1B appears to be out of line with the values for the other events. The median value at 50 Hz in table 1B indicates that the losses for the 243-m SUS data may be larger by 1.8 dB. With these loss adjustments determined by the differences between 20 and 50 Hz, the estimate of the true difference for the 243-m SUS data for event 2S2 becomes 9.2 (step 2) – 4.1 (step 3) + 1.8, which equals 6.9 dB. This estimate is in excellent agreement with the 6.5-dB value obtained in step 1.

Step 5. (C) The difference between the Site 3 values found in step 1 was 6.5 – 3.7 = 2.8 dB. If the adjusted value (6.9) found in step 4 for the 243-m SUS is used, the difference value for step 2 is 6.9 – 4.0 = 2.9 dB.

(C) Thus, the above analysis shows that the 20-Hz data for event 2S2 are indeed in error and require corrective measures before being assessed.

(C) Table 1B shows that the numerically smallest entries are for event 2S1 at 50 and 140 Hz. This suggests that the relative SUS values at these frequencies may be off by about 2 dB. The entries for Site 4 are at or near the numerically smallest values after discounting event 2S1. This is not surprising, since Site 4 had convergence zone propagation conditions.

(C) Consider, now, the numerical values of the median values of table 1B. Note that the negative values at 50 Hz are consistently out of line with the data at the other frequencies. We certainly cannot attribute this to some delicate quirk of propagation properties which occurs at all the sites. On the contrary, table 1B provides strong evidence that at least some (if not all) of the SUS source levels are in error. In a comparison of theory and experimental results at Site 1 (section 3.6.1) the analysis suggests how the SUS

source levels should be adjusted. The comparisons indicated that the 91- and 243-m source levels were 1.4 and 4.3 dB too low, respectively, at 20 Hz and 2.3 and 1.6 dB too high at 50 Hz. With these adjustments for source levels, the medians of table 1B become −0.2 and −1.1 dB at 20 and 50 Hz, respectively. The differences between the adjusted medians at 20 and 50 Hz now lie within statistical and experimental errors. At the present time, there is no theoretical basis for judging the differences at 140 and 300 Hz and determining whether the median values represent true differences in propagation loss or source levels as was the apparent case for 20 and 50 Hz.

2.3 (U) DATA VARIABILITY

(C) One of the surprising properties of most BEARING STAKE data was their variability. With the exception of some convergence zone data at the higher frequencies at Site 4, the variability between successive observations dominated (or at least obscured) trends in the data. The plots of raw CW data, appearing in the WECo data report (ref 8), show a jumbled and ragged band about 15 dB wide. It became apparent that in order to compare such data sets it was necessary to reduce the scatter in the raw data by computing averages and compressing the data as described previously in this report.

2.3.1 (U) Variability of CW Data

(U) Although the first examination of the raw CW data indicated excessive variability, subsequent analysis (see appendix B) has shown the measured results to be typical of propagation involving a large number of multipaths. The discussion herein is concerned with the statistical distribution of data points in a range (or bearing) bin after data compression. The aspect of this distribution which has been evaluated is the second moment about the mean, otherwise known as the variance. The variance was calculated by squaring the dB differences between the propagation loss of the observations and the average propagation loss for the bin, summing these squares, and then dividing by the number of observations. The square root of the variance (called the standard deviation) was then calculated. Note that this process involves working with the dB values of the observations. This is in contrast to the process of calculating the average propagation loss which averaged the pressure squared, in which the pressure was expressed in linear rather than dB units. This hybrid approach of determining the means from linear units but expressing the distribution in dB units follows standard practice for treating this type of data.

(U) A standard deviation was calculated as described above, corresponding to each mean for all the range and bearing bins. The standard deviations for all the BEARING STAKE CW events were examined. These standard deviations were quite variable from sample to sample. They had to be treated statistically by pooling large numbers of samples. There appeared to be no consistent trend with range except in the 25–75-km range bin. The standard deviation seemed somewhat larger in this bin than in other range bins. The data for this range bin were deleted and the remaining data were investigated further.

(U) There appeared, in most cases, to be little dependence on the events at a particular site. Thus, the data for all events at each site were pooled. Median values of these pooled standard deviations were determined for each of the five sites and each of the three

frequencies. Medians were chosen here as an estimate of the mean rather than arithmetic averages because one "sour" data point in a data set can result in an inordinately large standard deviation. Such sour data points would have relatively minor effect on the median as compared to the arithmetic average.

(C) Investigation of these median values showed that there was no significant dependence on frequency or site for data from Sites 1A, 1B, 2, and 3. Pooling of the frequency data produced standard deviations of 5.3, 5.4, 5.1, and 5.3 dB for Sites 1A, 1B, 2, and 3, respectively. Pooling the site data produced standard deviations of 5.3, 5.1, and 5.4 dB for frequencies of 25, 140, and 290 Hz, respectively. A standard deviation of 5.3 dB appears to be a good characteristic value for all three frequencies and for Sites 1A, 1B, 2, and 3. This value was based on a total of 374 determinations of standard deviation over various frequencies and range and bearing bins.

(C) The median values obtained for Site 4 were 5.2, 5.8, and 6.7 dB for frequencies of 25, 140, and 290 Hz, respectively. The numbers of determinations of standard deviation on which these medians were based were, respectively, 120, 87, and 87. The value of 5.2 dB for 25 Hz agrees well with the 5.3-dB characteristic value for Sites 1A, 1B, 2, and 3. However, the values for 140 and 290 Hz were significantly higher. This is readily explained in terms of the convergence zone structure at Site 4. There was little evidence of zones at 25 Hz whereas the convergence zones at 290 Hz were very prominent. The presence of convergence zones significantly increased the standard deviation in a 50-km bin. (Indeed, it is not apparent that a division into 50-km bins is a satisfactory means of treating convergence zone data.)

(C) The median values obtained for Site 5 were 4.65, 4.56, and 4.50 dB for frequencies of 25, 140, and 290 Hz, respectively. The numbers of determinations of standard deviation on which these medians were based were respectively 96, 62, and 62. There appeared to be no significant dependence on frequency. However, the values at Site 5 were significantly smaller than the characteristic value for other sites by about 0.7 dB. The reason for this difference is not known at this writing.

(C) Standard deviations were also computed for ACODAC data. The median values obtained for Site 1B were 5.0, 5.0, and 7.5 dB for frequencies of 25, 140, and 290 Hz, respecitvely. The number of determinations in which these medians were based is 40. The median values obtained for Site 4 were 4.8, 5.0, and 5.8 for frequencies of 25, 140, and 290 Hz, respectively. The numbers of determinations on which these medians were based were 96, 92, and 92, respectively.

(C) Comparison of the above ACODAC results with the WECo results indicates some systematic differences. The median value of 7.5 dB for 290 Hz at Site 1B is completely out of line with all other measurements. This gives further cause to suspect these data. (The mean propagation losses of this data set also appear out of line.) Once this piece of data is rejected, the remaining ACODAC data are consistently lower than their WECo counterparts. This may be due to the fact that the ACODAC data were obtained by using an integration process which averages out some of the variability.

(C) Earlier it was mentioned that the standard deviation seemed somewhat larger in the 25–75-km bin than in other range bins. This observation was tested by pooling all the data for this bin for Sites 1A, 1B, 2, and 3. The median standard deviation, based on 87 values, was 5.6 dB and is indeed higher than the 5.3-dB characteristic value for other bins. This higher value can be attributed to the larger trend with range in the data associated with

this bin. To show this, consider first the contribution that a linear trend with range can make. If the total trend across a bin is Δ dB, then the trend contributes an amount $\Delta^2/12$ to the variance. If 5.3 dB is a measure of standard deviation with no trend, then the standard deviation with Δ trend is

$$\sqrt{(5.3)^2 + \Delta^2/12}$$

Now the difference between the propagation loss at 75 km and at 25 km for the standard Eleuthera reference is 9 dB. This trend superimposed on a standard deviation of 5.3 dB yields a standard deviation of 5.9 dB. This is in reasonable agreement with the measured value of 5.6 dB. Indeed, the measured value one place above the median is 5.8 dB, which is in good agreement with the theoretical estimate.

(C) The question now arises as to whether the effect of a trend can be detected in the measured data for other range bins. For example, the difference between the propagation loss at 125 km and at 75 km for the Eleuthera reference is 4.5 dB. This trend superimposed on a standard deviation of 5.3 dB yields a standard deviation of 5.5 dB as an estimate for the 100-km bin. The data for this bin for Sites 1A, 1B, 2, and 3 were pooled. The median standard deviation based on 87 values was 5.3 dB, the same as the characteristic median for all bins (excluding the 50-km bin). The contribution due to the trend is apparently too small to detect in the data. The difference between the propagation loss at 175 km and at 125 km for the Eleuthera reference is 2.5 dB. This yields a standard deviation of 5.35 dB as an estimate for the 150-km bin. Thus, the estimated increase in standard deviation due to a trend is nil at the 150-km and larger range bins.

(C) Theoretical results on standard deviations are available from two different approaches. In the first approach, Dyer (ref 9) investigated the statistics of propagation loss based on the randomness of individual propagation paths and obtained a predicted standard deviation of 5.6 dB. In the second approach, the normal mode propagation model for Site 1B, as discussed in appendix B, was utilized. This normal mode model calculated the theoretical propagation loss for range increments of 100 m at 25 Hz. Each range bin, 50 km wide, contained 499 data points. The propagation loss corresponding to the average pressure squared was computed for the usual bins. The standard deviation of the data in each bin was calculated. Values obtained for the 50-km through 250-km bins were, respectively, 5.44, 5.57, 6.22, 5.41, and 6.33 dB. The average of these five values is 5.79 dB, which is slightly larger than Dyer's value of 5.6 dB. Since the mode determined values contain a range trend across each bin, they were expected to be somewhat larger than Dyer's value. These limited mode calculations indicated that the standard deviation can vary as much as 0.92 dB between adjacent bins even under idealized conditions. It is evident that more investigation needs to be done with the mode theory approach in order to determine a "typical" standard deviation and to establish an expected distribution about this typical value. Such an investigation should "de-trend" the range dependence to produce estimates unbiased by it.

---

9. "Statistics of Sound Propagation in the Ocean," by Ira Dyer, J. Acoustic Soc. Amer., vol. 48, no. 1 (part 2), p. 337–345, July 1970

(C) Both Dyer's value of 5.6 dB and the averaged mode estimate of 5.8 dB are larger than the characteristic experimental value of 5.3 dB. This may have been due to the manner in which the WECo data were read from strip chart recorders. However, their procedures remain to be critically assessed.

(C) Before closing the discussion of variability of the CW data, a few more results of the normal mode computation for Site 1B are pertinent. At a frequency of 25 Hz, a 10-dB fade (rapid increase in loss due to phasing) in the propagation loss data occurred on the average every 1.4 km for the 25–75-km range bin. This beat distance increased with range and was, for example, 2.0 km for the 225–275-km range bin. Now the nominal range interval between successive WECo experimental observations was 494 m for Site 1B. Thus, the experimental data were undersampled with only three or four measurements over the beat distance. Normal mode calculations were also made at 50 Hz. At this frequency, a 10-dB beat in the propagation loss data occurred on the average every 0.8 km for the 25–75-km range bin and every 1.3 km for the 225–275-km range bin. The distance between successive beats decreased with increasing frequency. At frequencies of 140 and 290 Hz, it is likely that the experimental data were sampled less often than once over the beat distance.

(C) It is apparent why the raw CW data appear as a jumbled and ragged band devoid of any structure except for a general increase in loss with increasing range. The normal mode calculation exhibits a similar lack of structure. Indeed, the modal result is even more jumbled and ragged than the experimental data. The experimental data represent a nearly random statistical sampling which is sparse compared to the theoretical beat distance. In summary, the variability of the experimental data is not excessive, as it appears at first exposure. The experimental variability is only slightly smaller than that predicted by normal mode theory, which takes into account the coherent addition of large numbers of propagation paths.

2.3.2 (U) Variability of SUS Data

(C) The variance of propagation loss for the SUS events made by the source ship (S events) was investigated for shot depths of 91 and 243 m. The same data analysis was used as described for the CW events with standard deviations calculated in 50-km range bins. For these shot depths the typical number of shots in a bin was 13. The analysis could not be applied to the 18-m shots because the number of shots varied from 0 to 4 per bin and was not adequate for this purpose.

(C) It was obvious from the data that the standard deviations for the shots were much smaller than for the CW data; i.e., in the range of 1–3 dB as compared to 5.3 dB for the CW data. This result is not unexpected, because the CW data were processed in a 1-Hz band whereas the shots were processed in 7% bands of the center frequency. For the shots the phasing effects of the multipaths are smoothed by the processing bandwidth.

(C) In contrast to the CW standard deviations the shot results were frequency dependent, in that they increased with increasing frequency. This dependence probably results from the variable bandwidth for each frequency. Some nonlinear process must be involved here, because it is not obvious why the variance should depend on frequency for proportional bandwidths.

(C) The variance was also slightly higher for the 243-m as compared to the 91-m shots. This may be attributed to the fact that the 243-m source is generally not bottom

limited whereas the 91-m source is generally bottom limited. The presence of convergence zones tends to increase the variance in 50-km bins as already discussed.

(C) Sites 1A, 1B, 2, and 3 could not be assessed individually because the number of samples at any one site would be too small. Since the CW data indicated that these sites could be pooled, the shot data were pooled as well. As with the CW data the 25–75-km bin was excluded and these data were treated separately.

(C) As in the case of the CW data, median values for the standard deviations of various sets of range bins were determined. The pooled data for Sites 1A, 1B, 2, and 3 yielded standard deviations of 0.9, 1.5, 2.4, and 2.4 dB at respective frequencies of 20, 50, 140, and 300 Hz for the 91-m shots. Corresponding values for the 243-m shots were 1.2, 1.6, 2.2, and 2.5 dB. Note that all values are monotonic, increasing with frequency, and that three of the four values are larger for the 243-m shots. These medians are based on between 25 and 60 determinations of standard deviation.

(C) Median values obtained for Site 4 were 1.3, 2.1, and 2.2 for respective frequencies of 20, 50, and 140 Hz for the 91-m shots Corresponding values for the 243-m shots were 2.5, 2.5, and 3.0. Medians were based on 20 to 25 determinations. These data display the same type of dependence on frequency and source depth as the data for the other sites. Note also that in five out of six cases the Site 4 data are larger than their counterparts at other sites. This is in agreement with the CW results, which were larger at Site 4 and can be attributed to stronger convergence zones at Site 4.

(C) Median values at 50 Hz based on 20 determinations at Site 5 were 1.1 and 1.3 dB for respective shot depths of 91 and 243 m. (The sample sizes were too small at other frequencies.) These values are significantly lower than their counterparts (1.5 and 1.6 dB) at Sites 1A, 1B, 2, and 3. This is in agreement with the CW results discussed previously. The fact that lower values were obtained from both CW and SUS events strongly suggests that the effect is somehow related to the Site 5 environment and is not due to some processing quirk at Site 5.

(C) The standard deviations in the 25–75-km range bin were pooled for Sites 1A, 1B, 2, and 3. The only frequency for which there were an adequate number of bins (in this case 18) was 50 Hz. The median values were 2.9 and 2.6 dB for respective shot depths of 91 and 243 m. These values are significantly higher than their counterparts in other range bins, 1.5 and 1.6 dB. Again, this larger value may be attributed to the trend across this range bin. If the effect of the trend were estimated by the Eleuthera reference value of 9 dB, as was done for the CW results, values of 3.0 and 3.1 dB for respective shot depths of 91 and 243 m would result. The value for 91 m is in excellent agreement with the measured value of 2.9 dB. Agreement is not good at 243 m. However, the measured value of 2.6 dB may be slightly low, because it is 0.3 dB smaller than the measured value for 91 m and for most of the other data sets the standard deviations are larger for 243 m than for 91 m.

(C) The smaller variances for the shot data allow reliable average values in the 50-km bins to be obtained with a smaller number of observations. For example, consider the typical CW standard deviation of 5.3 dB with 70 observations. This combination results in a standard error of the mean of 0.63 dB. The corresponding value of a typical shot standard deviation of 2.0 dB with 13 observations is 0.55 dB. Thus, the reliability of averages based on 13 shots is comparable to that of averages based on 70 CW observations, provided, of course, that the 13 shots are reasonably well distributed in the 50-km bin.

(U) To conclude the discussion of data variability, a few examples of the statistical distribution of range bin data about the mean are in order. These distributions, as well as the corresponding accumulative distributions, have been plotted for a very limited sampling

of the 50-km range bins. With the exception of Site 4 data, which contains prominent convergence zones, these distributions appear to have characteristic shapes. No attempt was made to fit statistical distribution functions to the data. Considering the large spread in measured values of the standard deviation, a determination of the distribution function is beyond the scope of the present work. However, it should be noted that these distribution functions are a necessary adjunct to the ASTRAL propagation model for the system performance evaluation of bottom-limited regimes. The ASTRAL model provides only a mean value for the propagation loss and some knowledge of the expected distribution about the mean is necessary.

(C) Figure 5 presents a histogram for the 150-km range bin for event 1BP1 at 25 Hz for the bottomed receiver, ACODAC 13 (see fig 2). This histogram was prepared by a computer program which counted the number of observations in 0.5-dB bins and normalized by the number of observations. For example, in figure 5, 10.83% of the observations fall within ±0.25 dB of the mean, while 14.17% have propagation losses which are between 0.25 and 9.75 dB greater than the mean. This 150-km range bin was the bin with the largest standard deviation (5.4 dB) of five available bins. This standard deviation is somewhat larger than the median value of 5.0 dB for Site 1B ACODAC data at 25 Hz. The histogram may be regarded as an estimator of the true statistical distribution function of the data.

(C) Figure 6 is the counterpart of figure 5 for the 200-km range bin. This was the bin with the smallest standard deviation (3.4 dB).

(C) Figure 7 presents the cumulative distributions for all five 50-km range bins of figure 3. For example, consider the cumulative distribution for the 150-km range bin. Figure 7 shows that about 6% of the data have losses which are smaller than the mean by 5 dB, about 42% of the data were less than or equal to the mean, and 93% of the data were less than 10 dB greater than the mean. The standard deviations are also given for each range bin. The curve marked "all" is a composite of the distributions for each range bin. It was obtained by summing the bin distribution functions and normalizing to the total number of observations.

(U) Figure 8 represents the theoretical cumulative distributions obtained by normal mode model results for Site 1B with range increments of 100 m. Comparing the experimental (fig 7) and theoretical distributions, we see that the left-hand tails of the curves are very similar. However, the right-hand tail of the theoretical distribution generally extends to higher losses than that of the experiment. This right-hand tail of high losses is responsible for the higher standard deviation of the theory as compared to experiment.

(U) Present plans call for an in-depth investigation of the BEARING STAKE distribution functions. The main objective of the analysis will be to determine the statistical distribution functions which best fit various subsets of the experimental data. The analyses of standard deviations previously presented herein will provide guidance for this investigation.

2.4 (U) VALIDITY OF DATA SETS

(U) Although the major portion of the propagation loss data collected during BEARING STAKE was found to be reliable and consistent, there were a few data sets at four of the five sites that appeared to be in error or which were regarded with varying degrees of suspicion as to their validity. The technique used for determining suspect data sets was to examine the particular data set as a member in a matrix consisting of similar data sets. Inconsistencies in propagation loss differences between receiver depths, frequencies,

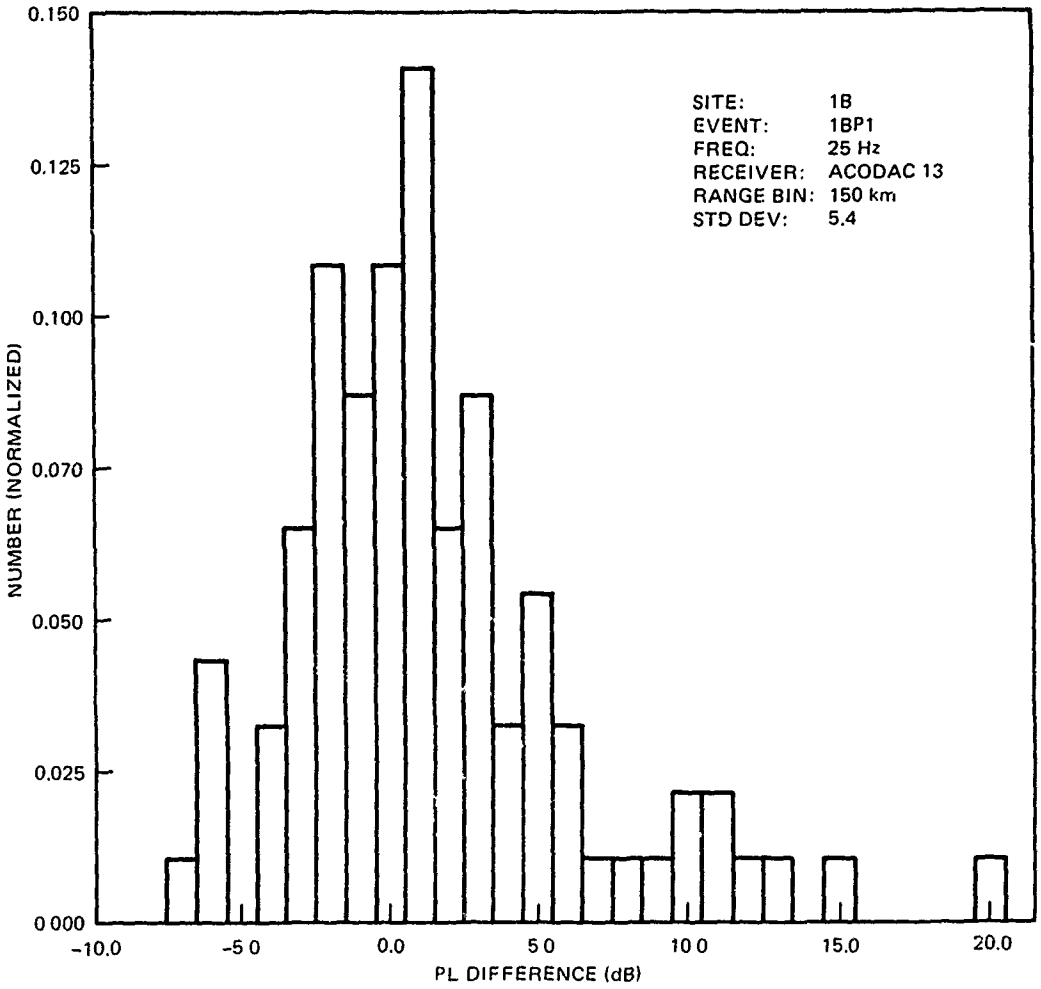

Figure 5. (C) Histogram for the 150-km range-bin data points for event 1BP1 at 25 Hz. (C)

events at one site, and sites flagged potential errors. Questionable data sets are identified in the individual site assessments of this report.

(U) The quality of some of the acoustic data provided in BEARING STAKE was a source of considerable frustration to the analyst. Plans and delivery schedules were made, understandably, under the assumption that the data would be perfect and would not have to be subjected to further examination for correctness. Such was not the case, although, in retrospect, most of the data were good. Considerable time and effort were expended in ferreting out bad or questionable data sets. The point here is not to berate the overall quality of the data. The errors uncovered were reasonable in terms of the vast volumes of data involved in the entire BEARING STAKE exercise. It should be recognized, however, that the chances of error are increased when different activities are involved in collecting data and transcriptions of the data must be made. In order to minimize some of the problems

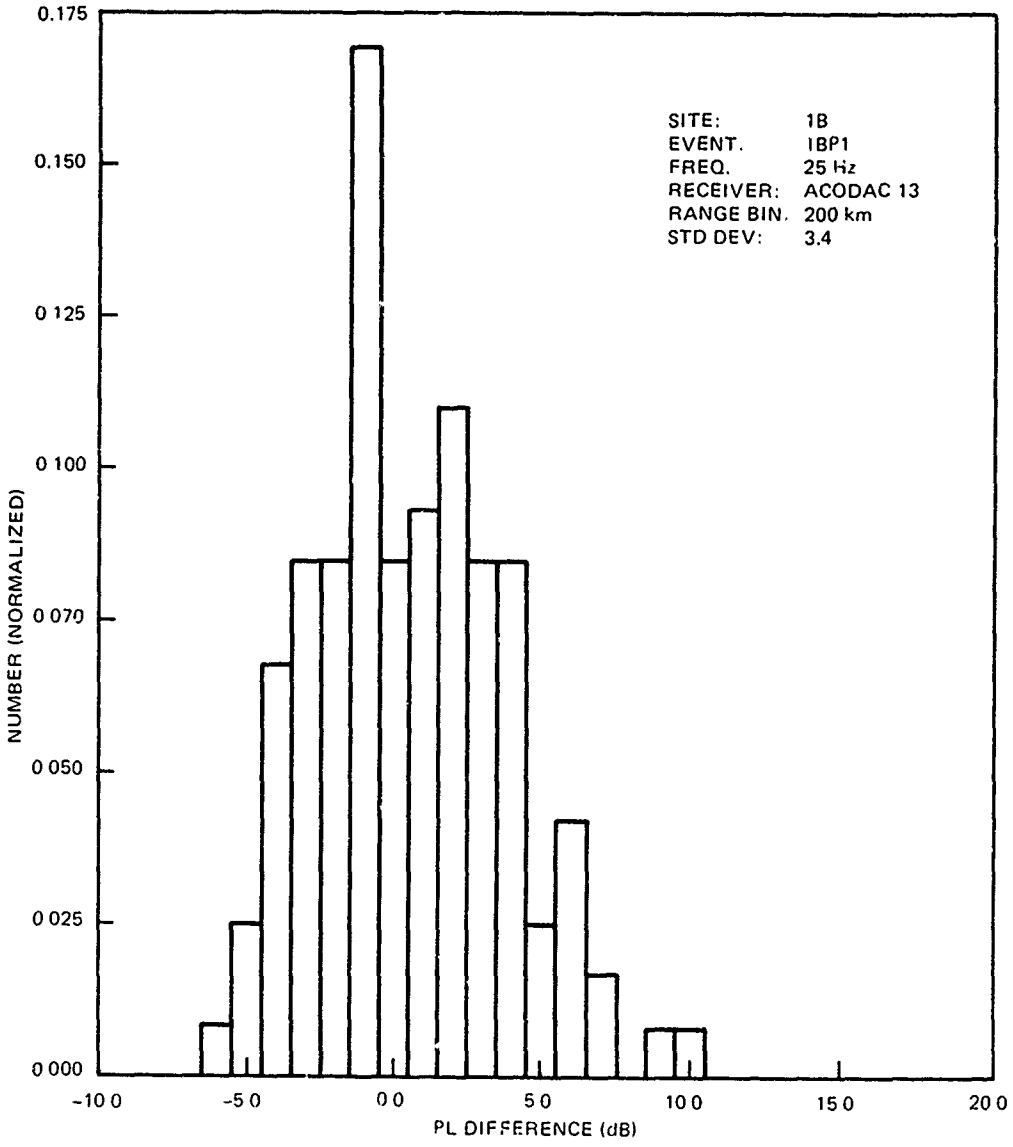

Figure 6. (C) Histogram for the 200-km range-bin data points for event 1BP1 at 25 Hz. (C)

encountered in BEARING STAKE, several procedures are recommended that should be followed when the data collection/reduction is performed by one activity and the data analysis by another.

- An allocation of time and effort should be included for both data collector and analyst for the purpose of checking the quality of the data. Provision should be made for at least one iteration between data collector and analyst.
- Contact between data collector and analyst should not be limited to handing over and accepting the reduced data.

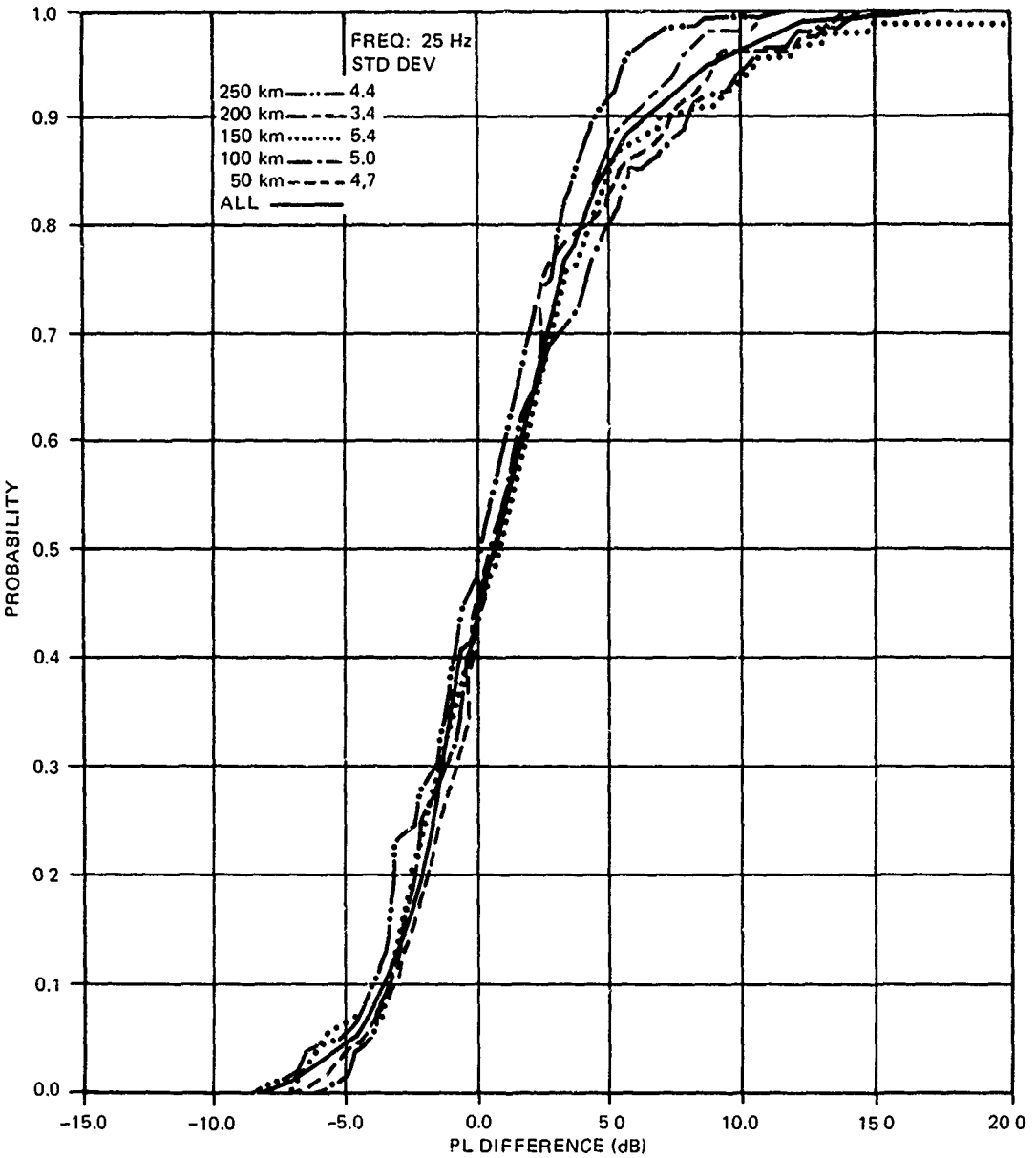

Figure 7. (C) Cumulative distributions for all five 50-km range-bins of event 1BP1. (U)

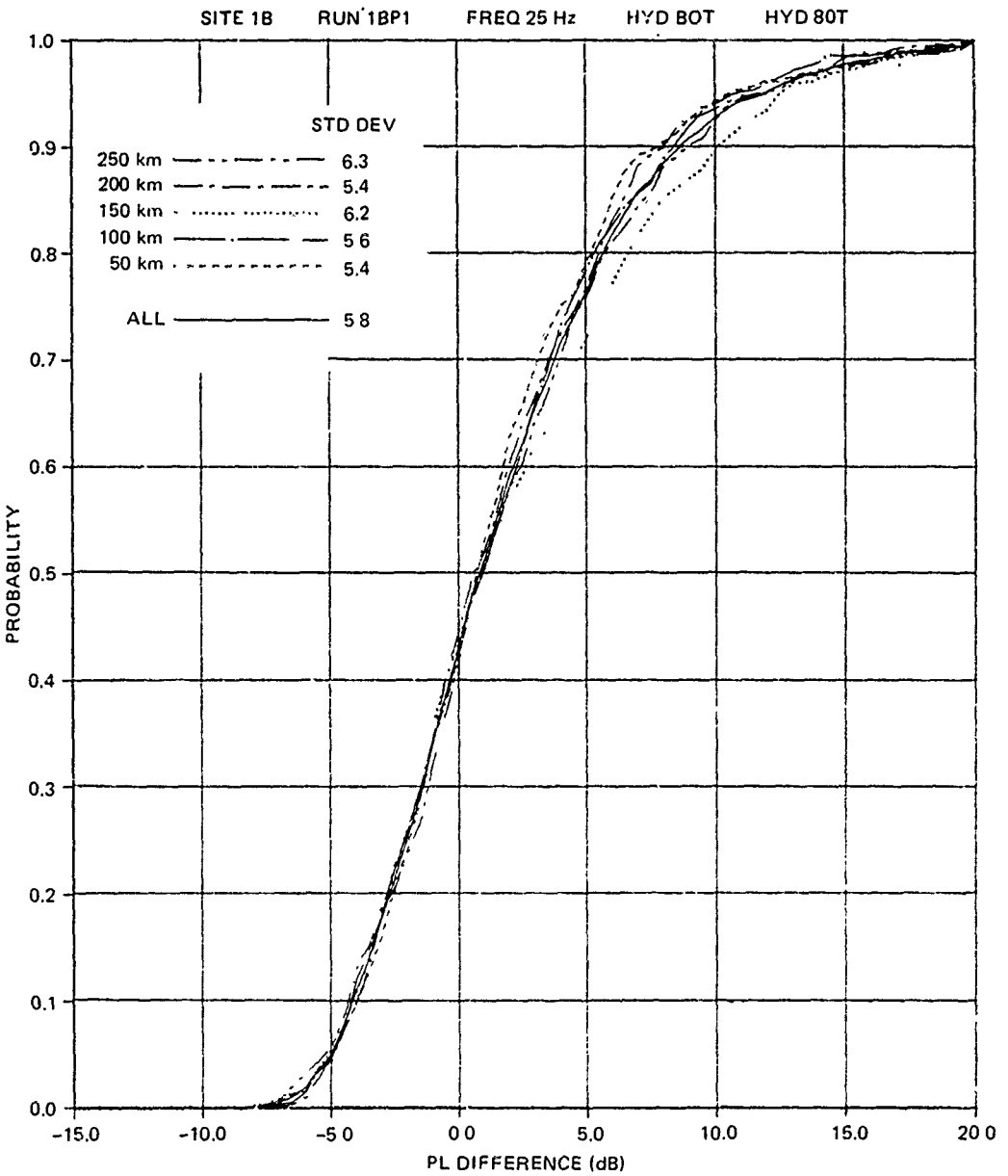

Figure 8. (C) Theoretical cumulative distributions obtained by normal mode model results for event 1BP1 using range increments of 100 m. (U)

- The data collector should be responsible for checking their data for errors or poter tial errors.

(U) There are several good examples of events illustrating the need for interaction between data collector and analyst. The initial propagation loss data for the ACODAC at Site 4 is one example. The data were analyzed at NOSC and the ACODAC propagation losses appeared exceptionally high when compared to the BMA data. The differences between the ACODAC and BMA data increased as a function of frequency. Moreover, the differences progressively increased with time in that the ACODAC losses got larger with successive event. Early comparisons of the ACODAC data with theoretical models also showed unbelievably large discrepancies in the ACODAC experimental data. ARL/UT, the processor of the ACODAC data, was notified of these findings and they proceeded to re-examine the original analog recordings of the ACODAC. ARL/UT determined that the initial calibrate of the system at Site 4 was good but that subsequent calibrates showed a progressive deterioration of the tape drive stability. The bandwidths used in the initial processing were found to be too narrow, particularly at the high frequencies. Subsequently, ARL/UT reprocessed the tapes through bandwidths commensurate with the instability of the tape drive. The data appearing in this report are the result of this reprocessing.

(C) Another example is the exceptionally low experimental propagation losses at 25 Hz compared to the results of several models that were found in the early analyses of the data. This led to a revision of bottom losses by ARL/UT and also to the realization that a reappraisal of source levels is necessary.

(U) In addition to the comparison with models, there are two other ways in which the validity of suspect data sets may be determined. The first is an examination of processing procedures to determine that receiver sensitivities, source levels, calibrates, attenuator settings, etc, were correct. The second is processing analog tape data for receiver depths which were not included in the original processing.

(U) The limitation of the discussion of questionable data to a few data sets at each site in this report does not mean that data sets not mentioned are correct. The discussion is limited to flagrant cases. Analysis with models and the processing of additional BMA data may well uncover additional anomalous data which may be subject to further examination. No attempt was made in this report to examine individual data points for the CW events. The analysis was confined to examination of entire data sets. An analysis of the statistical distribution functions scheduled for FY80 will no doubt uncover individual "sour" observations which cannot be detected in an examination of averaged data points.

3.0 (U) SITE 1 ASSESSMENT

3.1 (U) INTRODUCTION

(C) Site 1 was located at the mouth of the Gulf of Oman. The water depth at the site was 3353 m and offered, bathymetrically, a flat seafloor to ranges of 277.8 km (150 nmi) to the east and west, and much longer ranges in a narrow corridor into the Arabian Sea to the south. Site 1 was occupied twice – once in January 1977 (Site 1A) and once in February 1977 (Site 1B). For the purposes of this report, the propagation loss assessment for each time the site was occupied is discussed herein as a Site 1 occurrence and the site is referred to as Site 1A or 1B when needed to clarify a point.

(U) Figure 9 shows the physical configuration of the BMA installed at Site 1A. Also included in the figure is the array configuration before installation on the seafloor. Figure 10 shows the BMA configuration installed at Site 1B.

(U) The geometry of the various propagation loss measurement runs (which consisted of towed projector source runs and explosive sources (SUS) dropped from aircraft and ships) for Site 1 is shown in figure 11. The runs conducted during 1A and 1B are identified as such in the figure.

(C) Typical and representative sound speed profiles taken at various ranges from the bottom-mounted array (BMA) on all runs at Site 1 (1A and 1B) are shown in figures 12 and 13, respectively. All detailed sound speed profiles obtained at Site 1, as well as the profiles obtained at the other four sites, were provided by the Naval Ocean Research and Development Activity (NORDA) and reported in reference 10. Although the two tests at Site 1 were conducted about a month apart (February and March), their sound speed profiles were quite similar. The most noticeable difference was a slight surface duct for 1A (fig 12). Otherwise, both profiles show that Site 1 was bottom limited for shallow sources.

(C) Tables 2 and 3 summarize the propagation loss data measured at Site 1 from the projector tow runs with the CW source and the explosive charge (SUS) runs (table 2 is for 1A, and table 3 is for 1B). Similar tables are presented for the other four sites in their respective assessment sections contained in this report Each table contains the following.

1. (C) The receiving hydrophone number and depth of the bottom-mounted array (BMA) and, when applicable, the ACODAC receiving system.

2. (C) Run identification and range covered. The run identification consists of three parts: site, type of run, and run number. The type of run is indicated by a letter – "P" for projector tow (CW), "S" for SUS charge dropped by ship, or "A" for aircraft SUS drop. For example, 1BP5 indicates that the run was at Site 1B, the source was the CW projector, and the run was run 5 of a series. The range covered was either a short line run or a circular run. For example, "10 – 165 km" indicates an opening run starting at 10 km and ending at 165 km from the receiver. A closing run could appear as "210 – 6 km." The term "Circular 139 km" indicates a circular run at a radius of 139 km from the receiver.

3. (C) Frequency, source depth, and the hydrophone(s) which recorded the data.

---

10. "BEARING STAKE Exercise: Sound Speed and Other Environmental Variability (U)," by D. F. Fenner and W. J. Cronin, Jr., NORDA Report 18, September 1978. (CONFIDENTIAL)

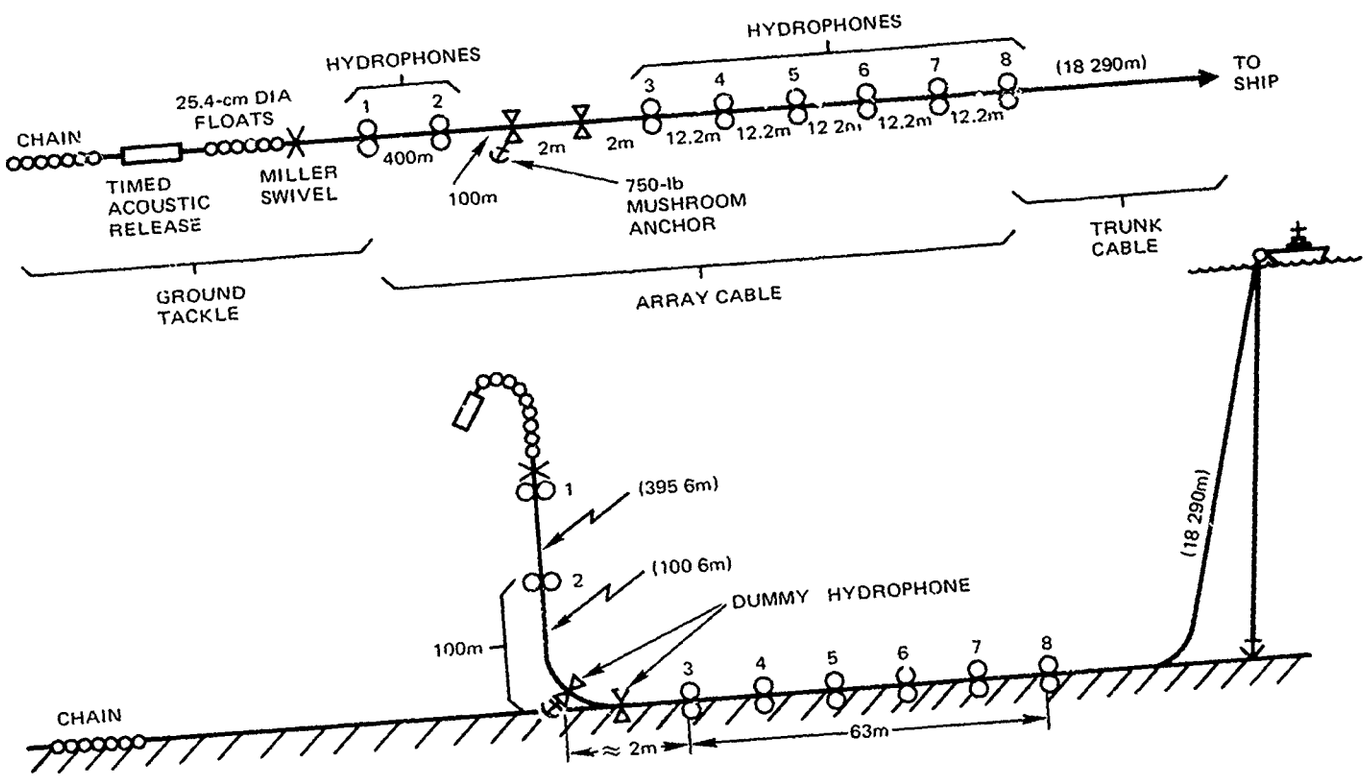

TOP – ARRAY CONFIGURATION BEFORE INSTALLATION
BOTTOM – ARRAY CONFIGURATION AFTER INSTALLATION AND ACOUSTIC RELEASE OPERATES

Figure 9. (U) Physical configuration of the BMA installed at Site 1A. (U)

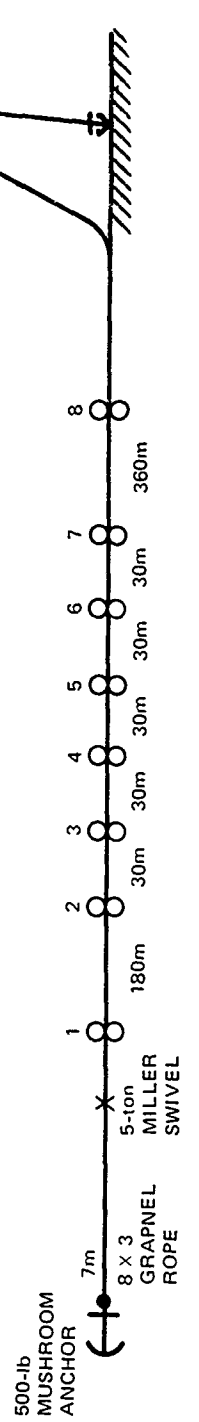

Figure 10. (U) BMA configuration at Site 1B. (U)

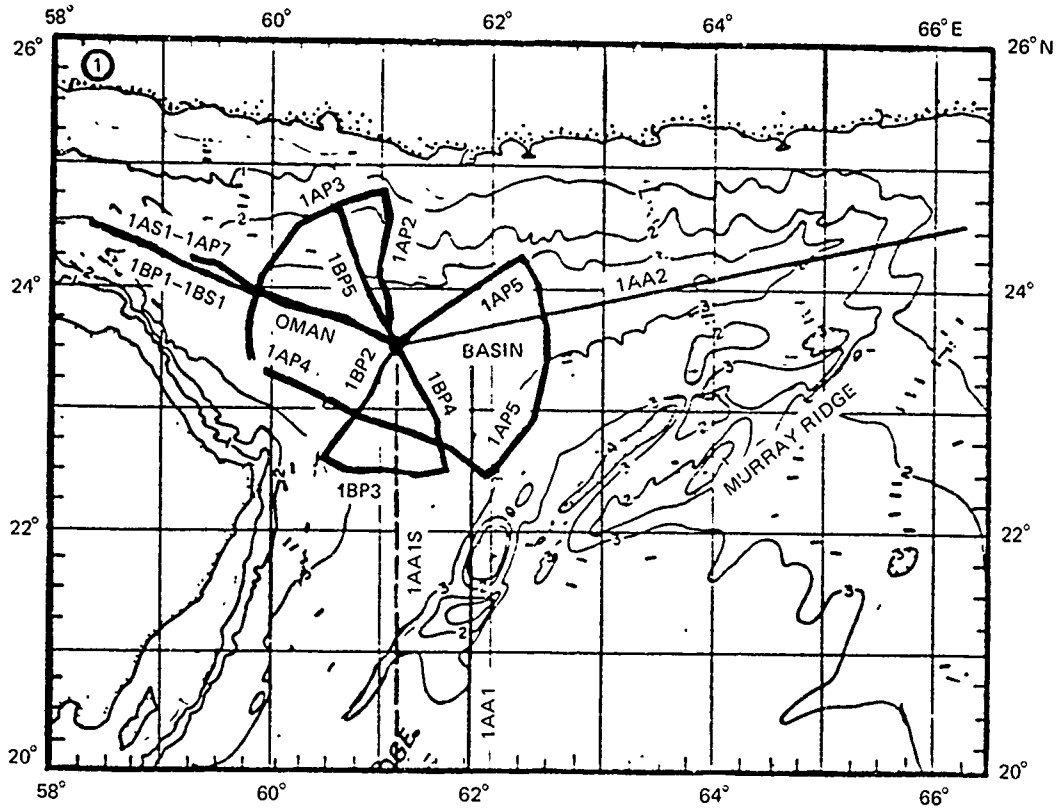

Figure 11. (C) Geometry of events conducted at Site 1 (1A and 1B). (U)

(U) The propagation loss assessment of Site 1 in this section discusses the dependence of the propagation loss in regard to the following variables:

1. The selection of receiving hydrophones of the BMA to measure data
2. Receiver depth
3. Optimum receiver depths for bottom-limited environments
4. Comparison of events or runs
5. Range and frequency

Questionable data sets for Site 1 are presented and an assessment of Site 1, based upon the experimental data, is summarized. Finally, recommendations for further data processing of data from Site 1 are suggested.

3.2 (U) DEPENDENCE ON BMA RECEIVING HYDROPHONES

(U) At Sites 1 and 3, WECo processed data from two to four receivers which were mounted on a nearly flat bottom and in close proximity to each other. This analysis of the dependence on the BMA receiving hydrophones used at each site is important because it

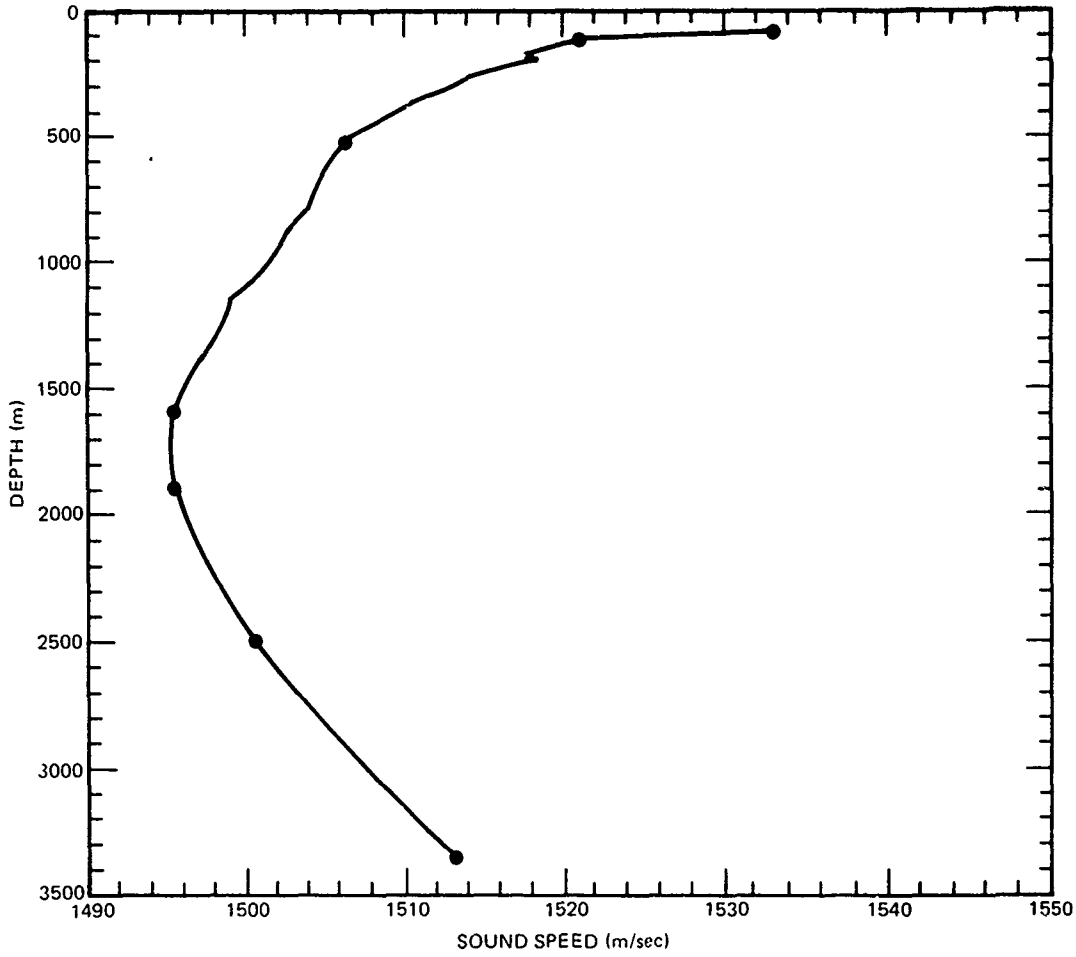

Figure 12. (U) Representative sound speed profile for Site 1A. (U)

indicates whether or not independent sets of WECo data taken under comparable conditions are consistent.

(U) To determine the dependence of the BMA receivers used to measure propagation loss, the data from each receiver used were averaged for each 50-km range bin (or 30° bearing bin). The differences between the averages of pairs of receivers were calculated and then a grand average difference was computed by averaging the individual differences between all available range and bearing bins. To minimize the effect of environmental differences between receivers, each receiver was paired with its closest neighbor in range. When only three receivers were available, the middle receiver was chosen as a reference and was compared with each of the other two receivers.

(C) At Site 1A, data were reduced for three BMA receiving hydrophones mounted on the ocean floor. The hydrophones were numbers 3, 5, and 8 (see fig 9). Comparisons of

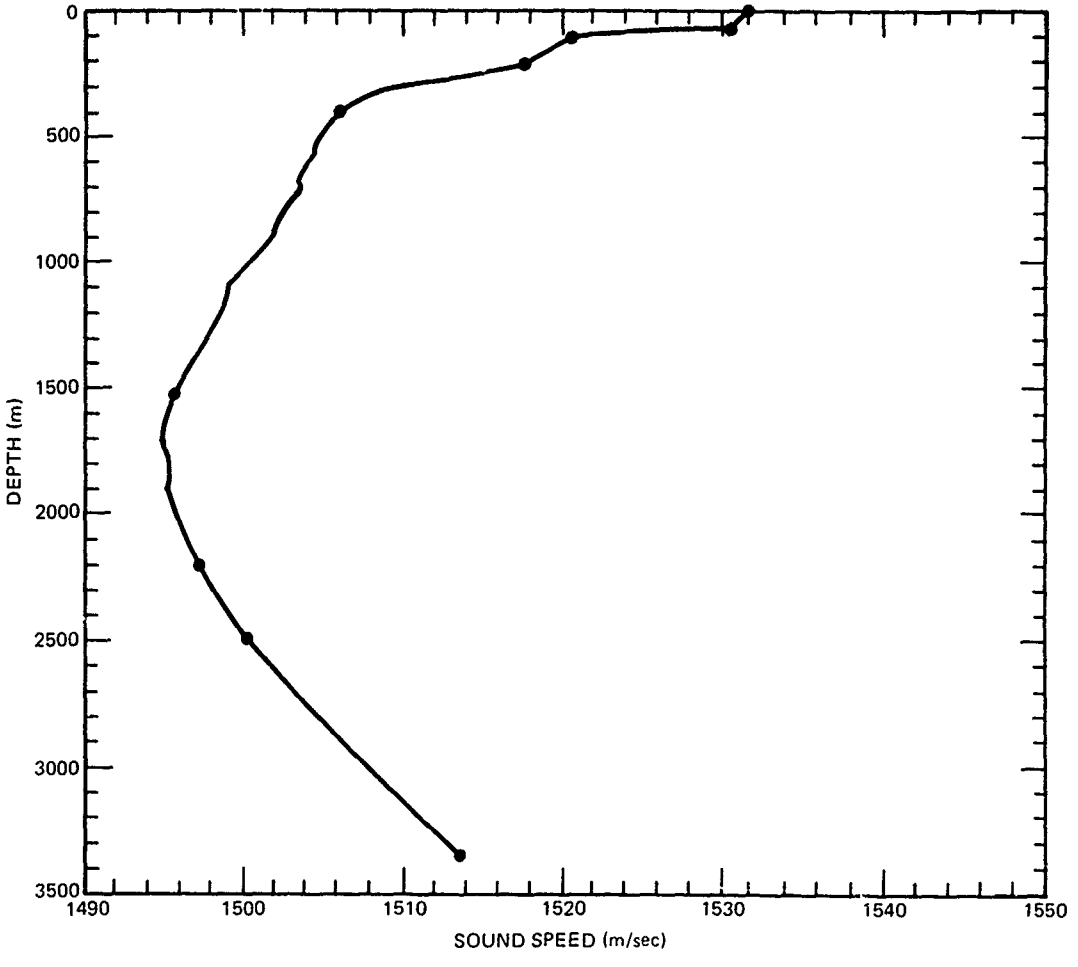

Figure 13. (U) Representative sound speed profile for Site 1B. (U)

propagation loss were made (based on four CW events) between number 5 and both numbers 8 and 3. The range displacement between receiver 8 and receiver 5 was about 40 metres. The range displacement between numbers 3 and 5 was about 24 metres. The depth displacement for both comparisons was only 1 metre. The analysis showed that receivers 8 and 3 had low-frequency (25 Hz nominal) propagation losses which were, respectively, 1.0 and 0.5 dB greater than those of number 5. The differences for number 8 were based on three range bins and 13 bearing bins. The differences for number 3 were based on three range bins and four bearing bins. A Student's t-test of the results indicated that the differences were significant at better than the 95% level.

(C) In addition, data were available from SUS event 1AS1 for receivers 8 and 5. Comparisons of propagation losses were made for both the 91- and 243-m shot depths. The 18-m shot depth data were too sparse for reliable comparisons. The 91- and 243-m shot data were treated as independent samples with four range bins available for each shot depth.

Table 2. (C) Summary of the propagation loss data set from the BMA collected at Site 1A from the projector (P) and SUS runs. (U)

BMA Hydrophone No Depth (m)		1 2854	2 3249	5 3350	8 3351
Freq (Hz)	Source Depth (m)				
Run 1AP2: 9-167 km					
39	91	X		X	X
140	18			X	
290	18			X	
Run 1AP3: Circular 139 km					
39	91	X		X	X
140	18			X	
290	18			X	
Run 1AP4: Circular 237 km					
39	91	X		X	X
140	18			X	
290	18			X	
Run 1AP5: Circular 148 km					
25	91	X		X	X
140	18			X	
290	18			X	
Run 1AP7: 0-200 km					
25	84	X		X	X
140	18			X	
290	18			X	
*Run 1AS1, 1AA1, 1AA3					
20				X	
50		X	X	X	X
140				X	
290				X	

These were SUS runs. SUS depths were 18, 91, 243 m for ship runs (s) and only 18 and 91 m for aircraft runs (A).

*Runs 1AS1: 207-0 km, Run 1AA1: 352-70 km, Run 1AA3: 0-579 km

Table 3. (C) Summary of the propagation loss data set from the BMA and ACODAC collected at Site 1B from the projector (P) and SUS runs. (U)

BMA Hydrophone No. / Depth (m)		1	2	5	8	ACODAC			
		2854	3249	3350	3351	496	1685	3321	3351
Source Freq (Hz)	Depth (m)								
Run 1BP1: 298 - 0 km									
25	102	X		X	X	X	X	X	X
140	18	X		X	X	X	X	X	X
290	18			X	X	X	X	X	X
Run 1BP2: 263 - 0 km									
25	100			X	X	X	X	X	X
140	18	X		X	X	X	X	X	X
290	18	X		X	X	X	X	X	X
Run 1BP3: Circular 130 km									
25	103					X	X	X	X
140	18	X		X	X	X	X	X	X
290	18			X	X	X	X	X	X
Run 1BP4: 0 - 132 km									
25	102	X		X	X	X	X	X	X
140	18	X		X	X	X	X	X	X
290	18			X	X	X	X	X	X
Run 1BP5: 0 - 137 km									
25	102	X		X	X	X	X	X	X
140	18	X		X	X	X	X	X	X
290	18			X	X	X	X	X	X
Run 1BS1: 0 - 292 km									
20				X					
50				X	X				
140				X	X				
290				X	X				

This was a SUS run. SUS depths were 18, 91, and 244 m for all frequencies.

Based upon these eight bins, the propagation loss at 50 Hz was 0.4 dB greater for receiver 8 than for receiver 5. Student's t-test indicated that the difference was also significant at better than the 95% level.

(C) At Site 1B, data were reduced for three BMA receivers (1, 5, and 8) which were mounted on the ocean floor as shown in figure 10. The range displacement between receiver 8 and receiver 5 was about 430 m. The range displacement between receiver 1 and receiver 5 was about 270 m. Corresponding depth displacements were 7 and 3 m. Comparisons of propagation loss were made based on five CW events and a total of 11 range bins and 2 bearing bins. Receiver 8 had losses which were −0.2, 0.7, and −0.8 dB greater than those of receiver 5 at respective frequencies of 20, 140, and 290 Hz. Receiver 1 had losses which were −0.1 and 0.3 dB greater than those of receiver 5 at respective frequencies of 25 and 140 Hz. Student's t-test indicated that the two smallest absolute differences are not statistically significant whereas the three largest absolute differences are significant at better than the 95% level.

(C) Propagation loss data from SUS event 1BS1 for receivers 8 and 5 were compared for shot depths of 91 and 243 m covering a total of 12 range bins. Receiver 8 had losses which were −0.2, 0.3, and −0.6 dB greater than those of receiver 5 at frequencies of 50, 140, and 300 Hz, respectively.

(U) On the basis of the above analyses, it was concluded that the Student's t-tests for the Site 1 WECo data indicated that (although the differences were at most 1 dB) there was, in most cases, a significant statistical dependence on which BMA receiving hydrophone was used to determine propagation loss. These differences are most likely due to minor calibration errors in the receiver system, although we cannot absolutely rule out minor differences in the actual propagation paths to the various receiving hydrophones.

(C) At Site 1B, additional comparisons were made between the measured propagation losses from a bottomed ACODAC receiver and WECo receivers 1, 5, and 8. The ACODAC was in close proximity to the WECo receivers. An average WECo value, based on the three receivers, was calculated for each 50-km range bin. Differences between the ACODAC value and the average WECo value were determined for each range bin. These differences were then averaged for 11 range bins that were available. The ACODAC propagation losses were 1.5, 2.6, and 4.6 dB higher than the WECo propagation losses for frequencies of 25, 140, and 290 Hz, respectively. Student's t-test, calculated on the basis of the 11 samples, yielded values in excess of 6, which indicates that the differences are all highly significant. The reason for these differences between the ACODAC data and WECo data is not known, and they should be investigated further. However, the fact that the difference increases with increasing frequency suggests a difference in processing techniques rather than a calibration error as calibration errors would be random as to frequency.

3.3 (U) DEPENDENCE ON RECEIVER DEPTH

(U) At all BEARING STAKE sites, except Site 3, data were available for more than one receiver depth. One of the most important features to establish at each site is the dependence of propagation loss on receiver depth; i.e., which receiver depth was best and by how many dB. The treatment of experimental data presented herein for Site 1 is essentially the same as that to be presented for the other sites. Hence, the discussion of the data analyses, both experimental and theoretical, will be more extensive in this section and not repeated again when assessing the propagation loss for the other sites.

(U) The receiver depth dependence for the CW events at Site 1A is given in table 4. Two of the BMA receiving hydrophones (numbers 1 and 2) were suspended above the seafloor. Receiver 1 was 496 m off the floor and receiver 2 was 100 m off the floor. Receivers 3, 5, and 8 were bottomed on the ocean floor.

Table 4. (C) Propagation loss differences between the average value of the three bottomed receivers and other receivers for Site 1A CW events. Receiver 2 was used, but the data are not available. (U)

		Event		
BMA Receiver Number	Receiver Depth (m)	1AP7 25 Hz	1AP3 39 Hz	1AP5 25 Hz
1	2855	2.0	0.2	2.4
2	3251	—	—	—
3, 5, 8	3351	0	0	0

(C) As shown in table 4, and in all other tables to follow presenting receiver depth dependence, the losses are normalized to that of one receiver depth or, as in the present case, the average of the receivers at one depth. For each event, the propagation loss difference between receiver depths is averaged over the available range bins. For example, the difference between receiver 1 and the average over the bottomed receivers was 2.0 dB for event 1AP7. The value was obtained by computing the dB differences for each of the four range bins of event 1AP7 and calculating the arithmetic average of these differences. Similarly, the values for event 1AP3 and event 1AP5 were obtained by averaging differences over four and three bearing bins, respectively.

(C) Thus, in the tables presenting receiver dependence, the propagation losses will be referenced to the receiver depth with lowest loss. In the case of table 4, all the entries in the data column are seen to be positive, indicating higher loss than the reference. In some special situations, the receiver with the lowest loss may not be the reference. In that situation, there will be negative entries indicating that such a receiver has a lower loss than the reference.

(U) The dashed lines shown in table 4 following BMA receiver 2 indicate that data were not available for that receiver for this analysis. From table 4 it is seen that the bottomed receivers had less loss than the suspended receiver for the events and frequencies indicated.

(C) Table 5 presents the receiver depth dependence results for the SUS events at Site 1A for 50 Hz. The aircraft SUS events used only two source depths (18 and 91 m) whereas the ship SUS events also included a source depth of 243 m. The table shows the results of a ship SUS event (1AS1) and the aircraft SUS events (1AA1, 1AA2). Event 1AA2 is divided into two parts in the table. The data from the 100–350-km range bins are designated in the table as "1AA2,1" and the data from the 400–600-km range bins as "1AA2,2." Analysis of table 5 indicates that the receiver depth dependence made a significant change with range in event 1AA2. The table shows receiver 5 with the lowest propagation loss except for event "1AA2,2," which shows that receiver 2 had the lowest loss.

Table 5. (C) Propagation loss differences between the BMA receiver with lowest propagation loss and other BMA receivers for Site 1A SUS events at 50 Hz. (C)

Event	BMA Hydrophone Number	SUS Depth (m) 18	91	243
1AS1	1	1.9	2.7	2.2
	2	2.6	1.2	1.7
	5	0	0	0
	8	0.2	0.4	0.4
1AA1	1	3.2	4.3	No Data
	2	4.0	1.9	
	5	0	0	
	8	2.4	1.6	
1AA2, 1 (100—350 km)	1	3.7	3.8	No Data
	2	2.1	1.4	
	5	0	0	
	8	1.7	1.5	
1AA2, 2 (400—600 km)	1	1.2	1.8	No Data
	2	0	0	
	5	1.2	2.5	
	8	2.5	2.5	

(C) At Site 1B, receiver depth dependence for the CW events conducted at the site was based on data from the ACODAC system. Data from 4 of the 13 receiving hydrophones of the ACODAC were processed. These were ACODAC 2, 6, and 10, which were suspended above the seafloor at respective depths of 496, 1685, and 3321 m, and ACODAC 13, which was on the ocean floor at 3351 m. The results of comparing each of the suspended receivers with the bottomed receiver are shown in table 6. The values in the table were obtained by averaging over five range bins for event 1BP1, three bearing bins for event 1BP3, and two range bins each for events 1BP2, 1BP4, and 1BP5. At frequencies of 25 and 140 Hz, the receiver with the lowest loss is generally number 10. At 290 Hz, it appears that number 2 has the lowest loss.

(U) The results shown in the preceding tables are best explained after a discussion of a normal mode computer program utilized in this assessment report.

Table 6. (C) Propagation loss differences between the bottomed ACODAC receiver (13) and the other ACODAC receivers for Site 1B CW events. The negative values indicate the propagation loss was less than the bottomed receiver. (U)

ACODAC Receiver Number	Receiver Depth (m)	Event	Frequency (Hz)		
			25	140	290
2	496	1BP1	2.8	2.0	−1.0
6	1685		2.6	3.0	0.6
10	3321		−0.3	−0.6	−0.5
13	3351		0	0	0
2	496	1BP2	3.2	0.4	−2.0
6	1685		2.9	1.8	1.0
10	3321		−0.9	−1.0	−0.6
13	3351		0	0	0
2	496	1BP4	2.4	1.8	−0.8
6	1685		2.3	1.8	0.4
10	3321		−0.3	−1.0	0.4
13	3351		0	0	0
2	496	1BP5	1.4	2.8	−1.6
6	1685		0.7	2.4	−1.9
10	3321		−1.0	−1.4	−2.6
13	3351		0	0	0
2	496	1BP3	1.2	4.3	3.0
6	1685		1.4	4.5	3.8
10	3321		1.2	1.5	3.0
13	3351		0	0	0

3.3.1 (U) Normal Mode Discussion

(U) The normal mode program was used to investigate the dependence on receiver depth not only to verify the experimental data but also to establish the receiver depth dependence over the entire water column.

(C) Figures 14 through 19 present the receiver depth dependence for frequencies of 25 and 50 Hz. The source depths are 18, 91, and 243 m, which correspond to the standard

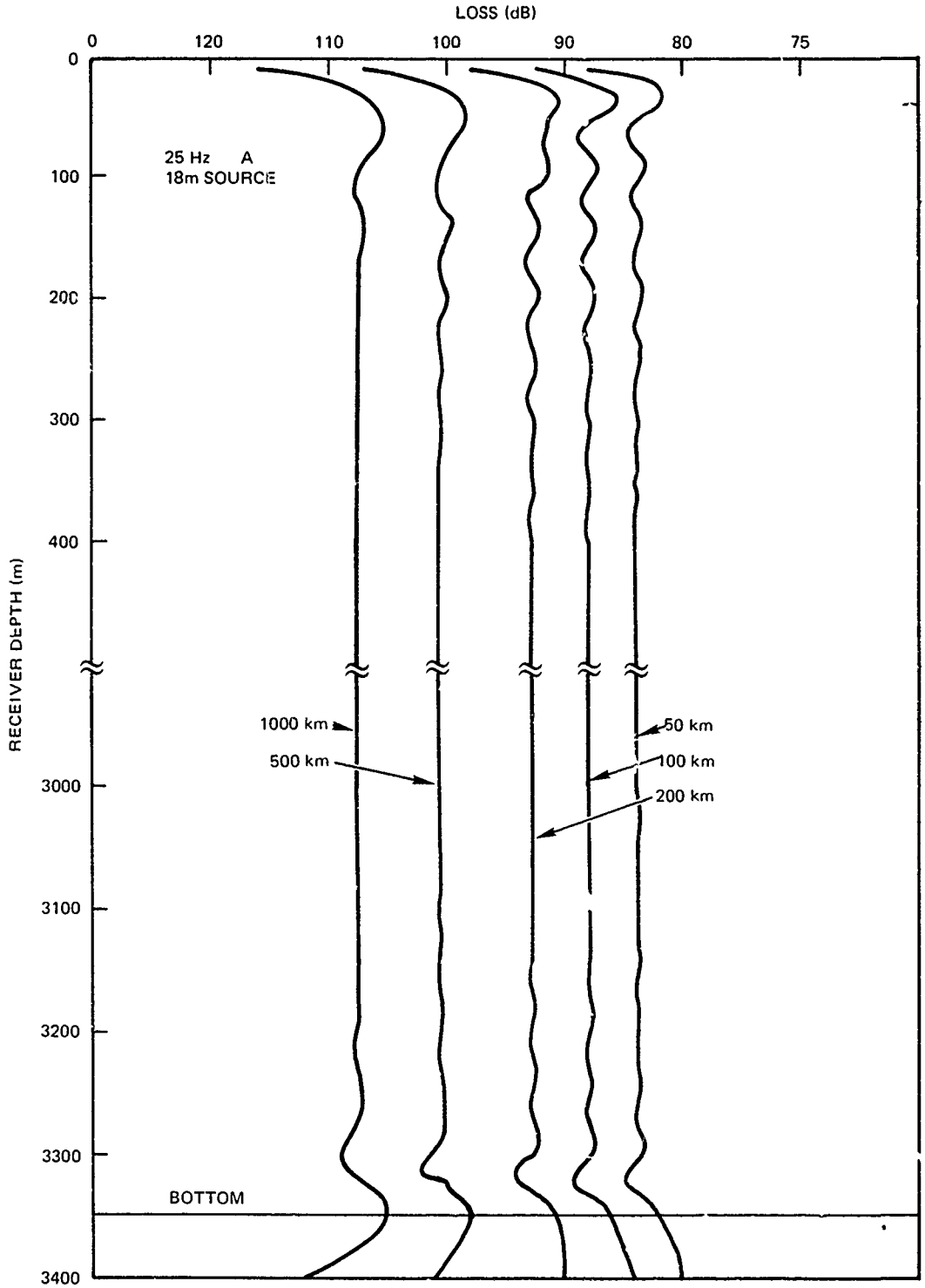

Figure 14. (C) Theoretical propagation loss as a function of receiver depth for 25 Hz for a source depth of 18 m. (C)

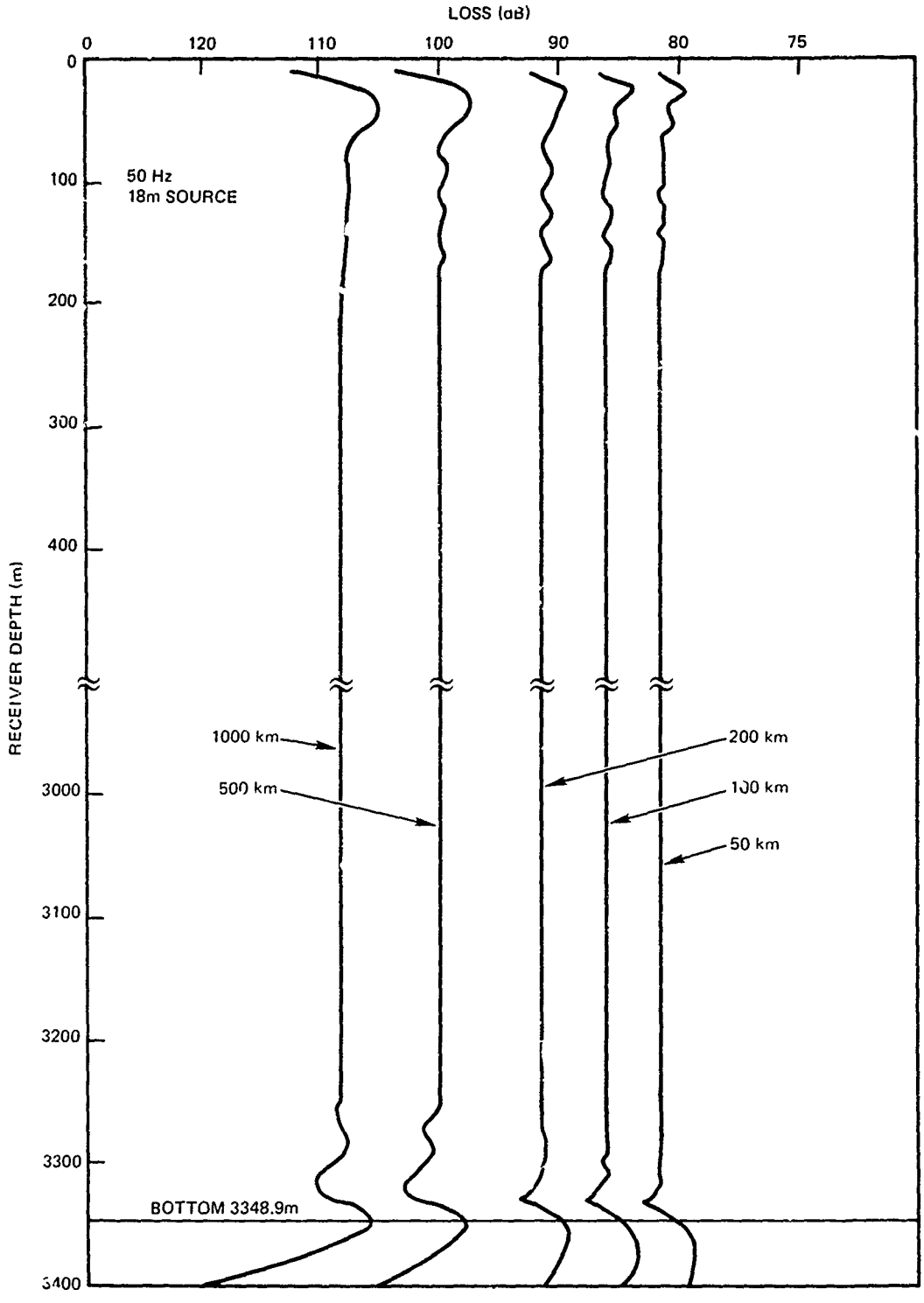

Figure 15. (C) Theoretical propagation loss as a function of receiver depth for 50 Hz for a source depth of 18 m. (C)

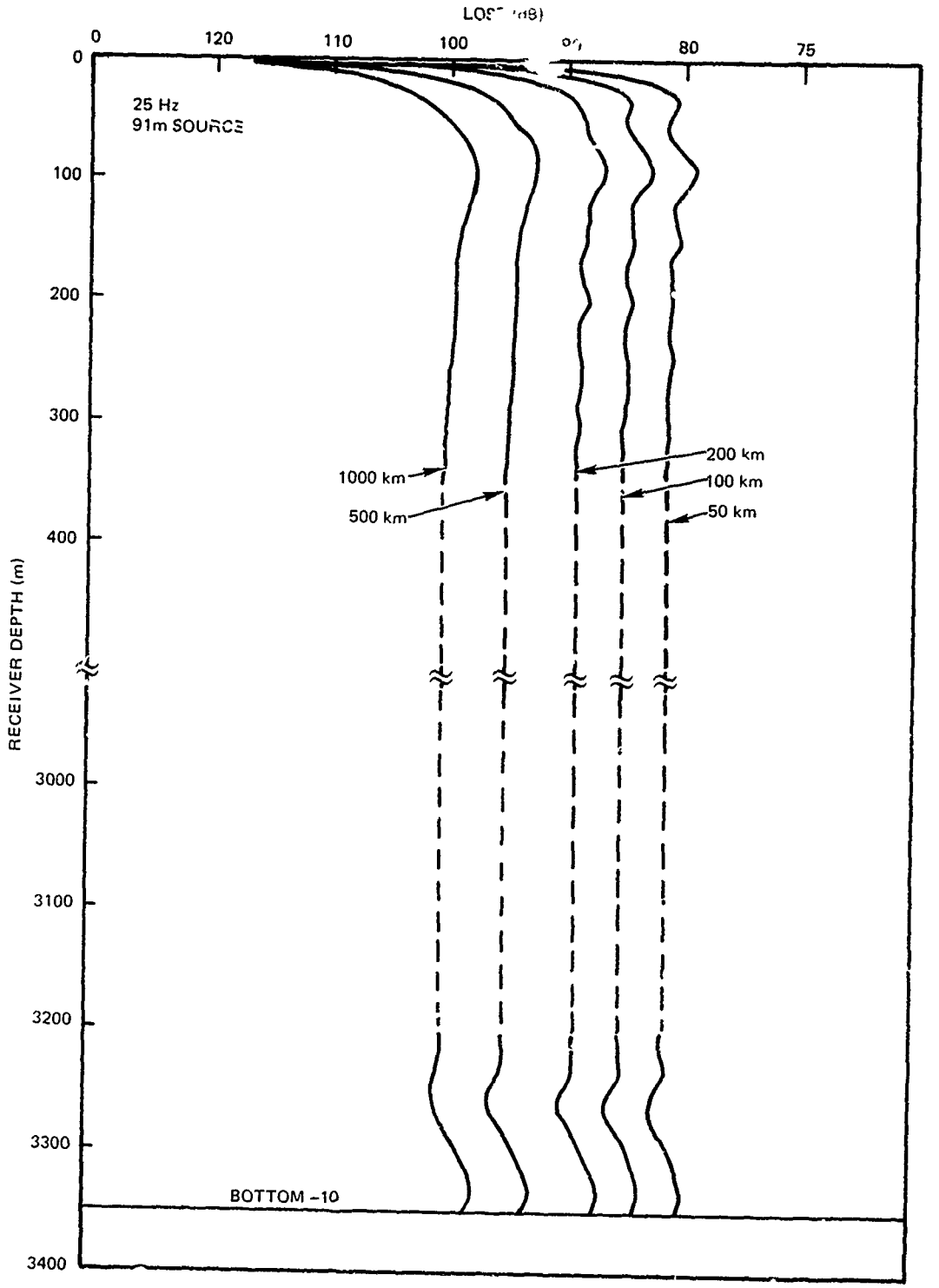

Figure 16. (C) Theoretical propagation loss as a function of receiver depth for 25 Hz for a source depth of 91 m. (C)

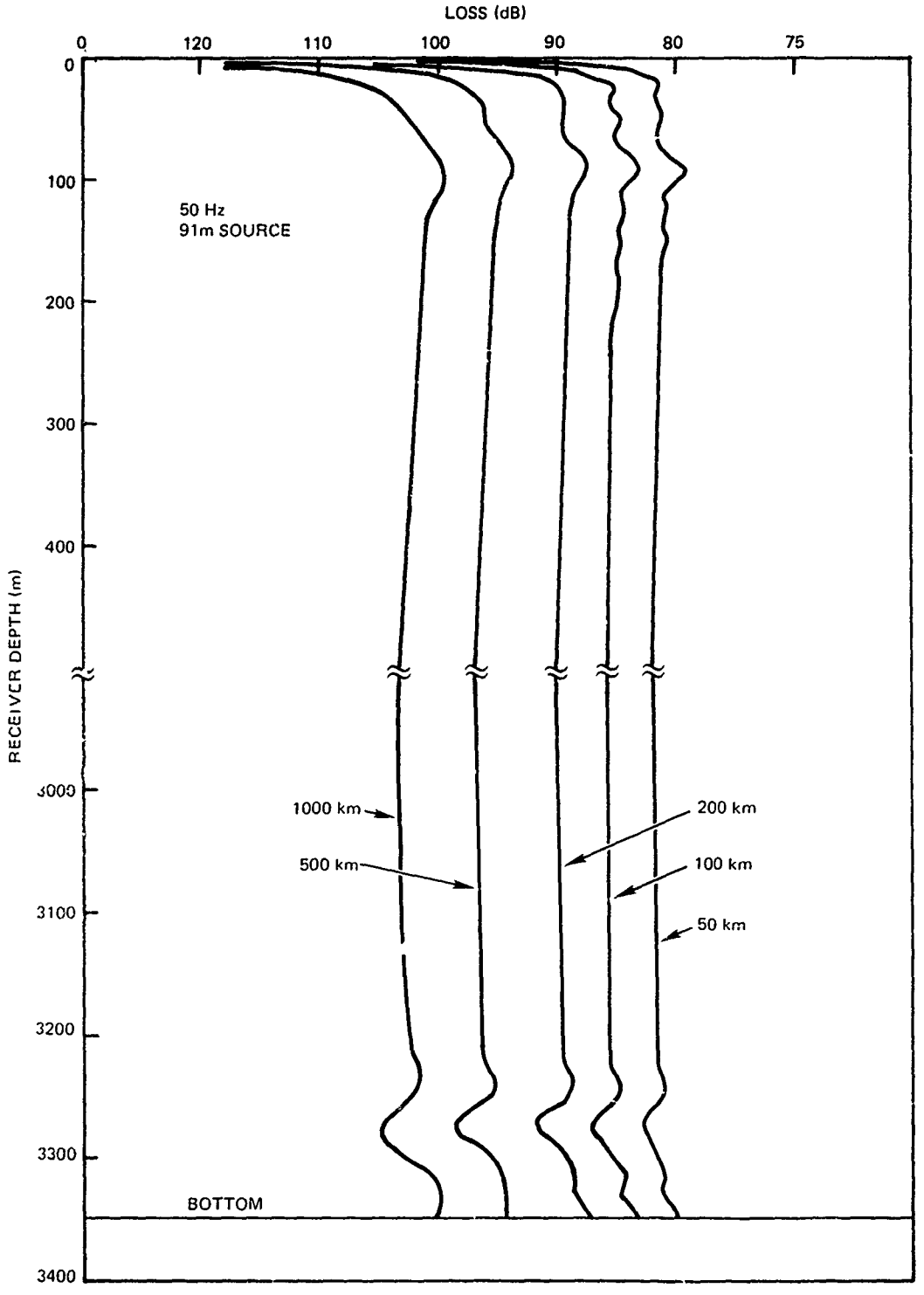

Figure 17. (C) Theoretical propagation loss as a function of receiver depth for 50 Hz for a source depth of 91 m. (C)

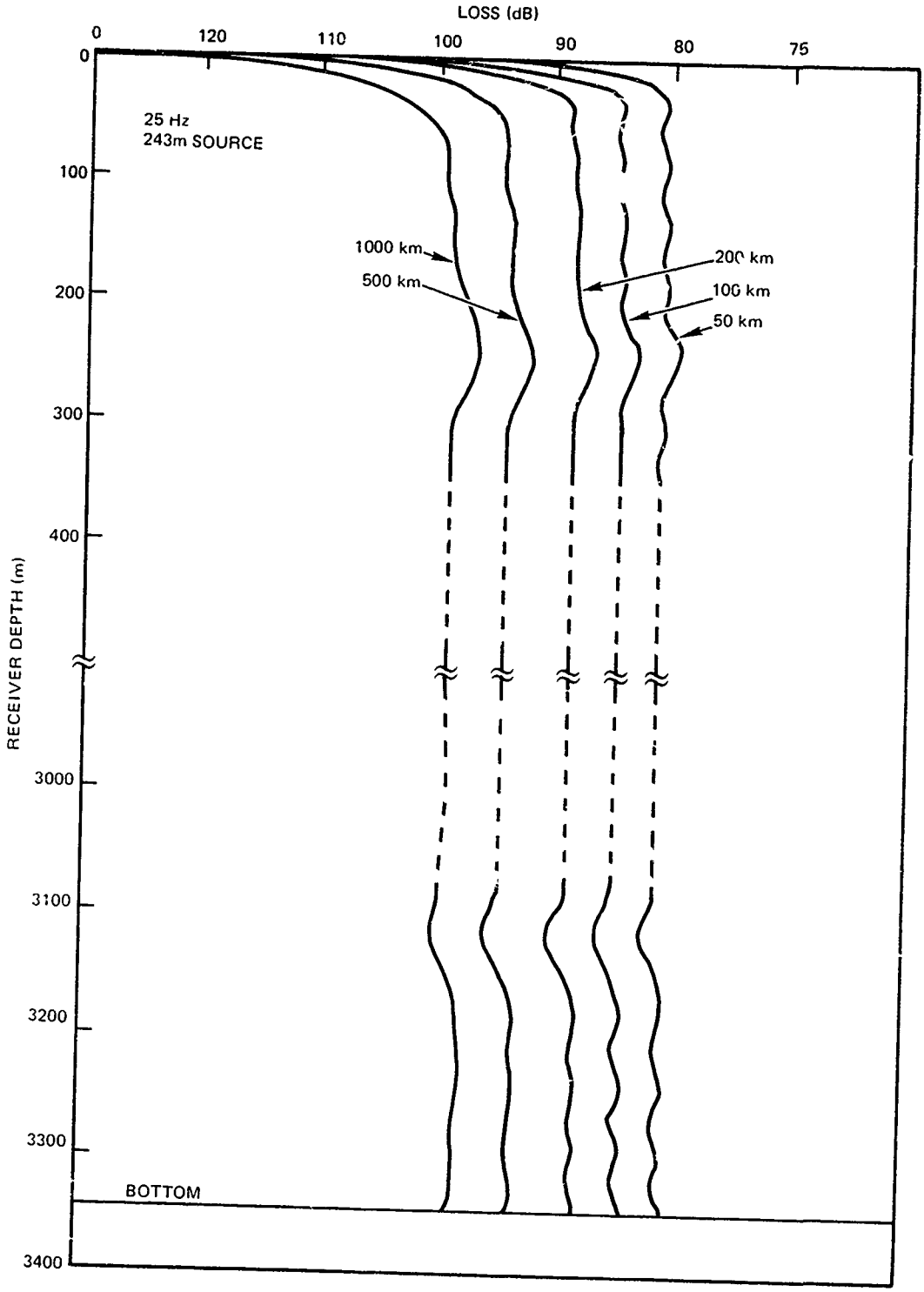

Figure 18. (C) Theoretical propagation loss as a function of receiver depth for 25 Hz for a source depth of 243 m. (C)

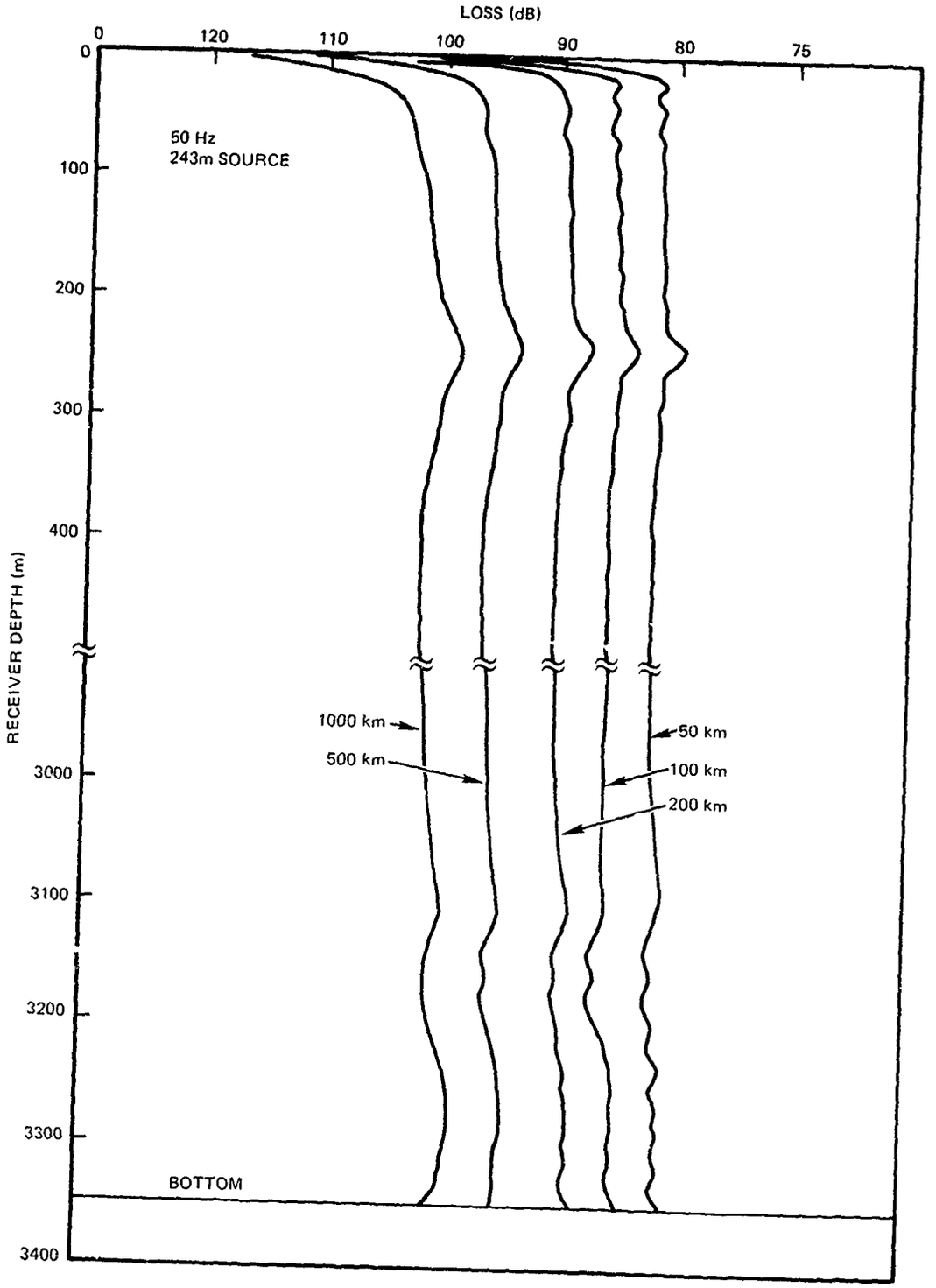

Figure 19. (C) Theoretical propagation loss as a function of receiver depth for 50 Hz for a source depth of 243 m. (C)

SUS source depths in BEARING STAKE. Propagation loss is shown as a function of receiver depth at fixed ranges of 50, 100, 200, 500, and 1000 km. In these computations, the normal modes are added in random phase at the given ranges. This procedure averages out the detailed structure of the phased acoustic field and produces a good representation of the depth structure. This structure is an incoherent combination of the depth structure of individual normal modes. The combined structure changes with range somewhat because the contribution of individual modes is affected by the mode attenuation. In figures 14 through 19, there are scale breaks at 500 and 2900 m. The region between 500 and 2900 m shows very little change and was not plotted in detail. However, the maximum value of propagation loss in this interval is indicated between the scale breaks.

(C) The important features of figures 14 through 19 are summarized in table 7, which presents the propagation loss at key depths minus the propagation loss at the ocean bottom. In the table, depth numbers 2 to 5, 7, and 9 represent receiver depths at which experimental data were taken at Site 1. The other depth numbers correspond to certain critical depths and are best discussed by an examination of the figures progressing downward from the ocean surface. Depth 1 represents the minimum propagation loss for receiver depths less than 500 m. For figures 16 through 19, this is a receiver depth equal to the source depth.

(C) For figures 14 and 15, the minimum loss depth is the surface decoupling depth. The surface decoupling depth is defined as the depth of the first (shallowest) antinode of the mode depth structure. This depth of minimum propagation loss is a well known phenomenon and is discussed in reference 11. Reference 11 also presents ray theory models of surface decoupling depths and decoupling losses, and describes the loss for receivers (or sources) at depths shallower than the surface decoupling depth. Simply stated, the receiver depth with minimum loss above the sound channel axis is the same as the source depth when the source depth is deeper than the surface decoupling depth. When the source depth is shallower than the surface decoupling depth, the minimum loss receiver depth is the same as the surface decoupling depth.

(C) Note in figure 14 that the decoupling depth at 25 Hz is about 30 m at 50-km range and increases to about 55 m at 1000-km range. This increase in depth with increasing range occurs because the steeper-angle arrivals dominate at shorter ranges; the steeper the angle, the smaller the decoupling depth. At long ranges, the bottom loss at steep angles strips out these arrivals and the lower-angle arrivals dominate. These lower angles have larger decoupling depths.

(C) Comparison of figures 14 and 15 shows that the decoupling depth decreases with increasing frequency. At 50 Hz (fig 15) the decoupling depth is 20 m at 50-km range and 35 m at 1000-km range.

(U) Thus, surface decoupling depths play a prominent role in the propagation effects from near-surface sources.

(C) Referring back to table 7, now that the salient features of surface decoupling depths have been discussed, we see that the minimum loss entries for depth 1 are negative except for the 18-m source depth at 1000-km range at 25 Hz. The propagation loss for depth 1 is generally less than 1 dB smaller than the loss for the bottomed receiver except for the 243-m source depth at 1000-km range, in which case the difference in loss is about 2 dB.

---

11. "Low Frequency Propagation Effects for Source or Receiver Near the Ocean Surface (U)," by M. A. Pedersen, D. F. Gordon, and D. White, NUC TP 488, September 1975

Table 7. (C) Propagation loss differences between key receiver depths and a bottomed receiver as calculated from normal mode model of Site 1B. (U)

		Source Depth (m)	18								91								243							
		Range (km)	50		100		200		1000		50		100		200		1000		50		100		200		1000	
		Freq (Hz)	25	50	25	50	25	50	25	50	25	50	25	50	25	50	25	50	25	50	25	50	25	50	25	50
Depth Number	Depth Descriptor																									
1	Minimun Loss		-0.8	-0.7	-0.5	-0 4	-0 3	-0.2	0 2	-0.2	-0 7	-0.3	-0.7	-0 3	-0.5	-0.4	-0.5	-1.0	-0.7	-0 3	-0.8	-0.7	-0.8	-0.8	-1.7	-2.2
2	ACODAC 2		1 7	1.8	1 9	1.2	2.2	2 5	2 9	3.2	1 8	2.5	1 9	2.7	2.2	2 7	2.3	2.6	1.6	1.9	1 6	1.9	1.6	1 9	0.8	0.9
3	ACODAC 6		1 9	2 0	2.1	2 3	2.4	2 7	3 2	3 6	2.2	2.9	2.3	3.1	2.6	3 2	2.8	3 3	2.1	2.4	2.1	2.5	2.1	2 6	1.7	2.0
4	ACODAC 1		1.8	1 8	2.0	2.1	2.2	2.5	2.8	3.2	1.8	2 4	1.9	2.6	2.2	2 6	2.2	2.5	1.5	1.8	1.5	1.9	1 4	1.8	1.4	0 8
5	BMA 2		1.6	1 7	1 8	1 °	2 1	2.3	2 2	3 0	2 1	1 4	2.2	2.5	2.6	1.5	2.6	1.7	0.2	1.1	0.1	0.8	0.0	0.4	-1.2	-1 7
6	Maximum Loss		3 0	3.0	3.4	3.5	3.8	4.1	4.0	5.5	2.6	3 4	2.8	3.7	3.1	4.0	2.6	4.0	2 7	1.9	2.7	1.9	2.7	1.6	1.4	0 1
7	ACODAC 10		3 0	3.0	3 4	3.5	3.6	3.9	2 3	2.4	0 2	1.4	0.1	1.4	0.1	1.1	-0 7	-0.2	1.0	0.4	0.9	0 4	0.6	0 3	-0.8	-1.3
8	Minimum Loss		–	–	–	–	–	–	–	–	-0.3	–	-0 3	–	-0.3	–	-0.8	-0 7	–	–	–	–	–	–	–	–
9	Bottom		0	0	0	0	0	0	0	0	0	0	0	0	0	0	0	0	0	0	0	0	0	0	0	0
10	Spread		3.8	3 7	3.9	3.9	4.1	4 3	4 0	5.7	3.3	3 7	3.5	4.0	3 6	4.4	3.6	5 0	3 4	2.9	3.5	3.2	3 5	3.4	3.4	4.2

CONFIDENTIAL

CONFIDENTIAL

(C) The sound speed model of table 7 utilized a sound speed at the 243-m source depth of 0.2 m/s less than that at the ocean bottom. At 243-m depth there are some acoustic paths which are not bottom reflected and have lower attenuation losses than those steeper-angle paths which must reflect from the bottom to reach the bottomed receiver. Hence, it is not surprising that the propagation loss at long ranges for a receiver at 243-m depth is as much as 2 dB less than for a receiver at the ocean bottom.

(C) In the normal mode model calculations which resulted in the curves shown in figures 14 through 19, there was a broad flat relative maximum in propagation loss for intermediate depths. The maximum loss occurred at the sound speed axis, which was at approximately 1900 m. In the depth interval from 1500 to 2000 m, the maximum loss values for figures 14 through 19 were within 0.1 dB of each other. Depth 3 (ACODAC 6) at 1685 m falls into this interval. Thus, the entries in table 7 for depth 3 represent somewhat greater losses than at the ocean bottom, with values ranging from 1.7 to 3.6 dB. Depth 2 (ACODAC 2) at 496-m depth has somewhat smaller propagation losses than depth 3 and has greater losses than at the bottom. Depth 2 loss values range from 0.8 to 3.2 dB.

(C) Another feature of the depth structure curves is the "notch" of maximum loss which appears in figures 14 through 17 slightly above the ocean bottom. The losses associated with this notch are given in table 7 under depth 6. For example, the notch in figure 17 at a range of 1000 km appears at a depth 75 m above the ocean bottom and is listed in table 7 with a propagation loss which is 4.0 dB greater than at the ocean bottom. In figures 18 and 19, in which the notch is not apparent, the values entered in table 7 for the 243-m source are for the largest loss for receiver depths below 3100 m.

(U) The notch plays a significant role in the consideration of optimum receiver depths for bottom-limited propagation. However, the importance of this notch with respect to source depth and frequency is best discussed after a physical interpretation of what causes the notch is presented.

(U) Assume a receiver is suspended near, but off, the ocean bottom. Couched in terms of ray theory, a ray headed downward toward the receiver will be out of phase with a ray which has reflected from the ocean bottom and headed upward to the receiver, and destructive interference will result. This interference occurs at depths below the notch. It is beyond the scope of this report to model exactly where the notch occurs. However, notch behavior is somewhat analogous to surface decoupling behavior since both concern interference phenomena between upgoing and downgoing rays. Thus, we should expect the notch to be closer to the bottom for steep-angle propagation paths and, also, for higher frequencies This is indeed the case.

(C) In figures 14, 15, 16, and 17, the above-bottom depth of the notch for ranges from 50 to 1000 km varies from 29 to 49 m, 18 to 37 m, 85 to 100 m, and 75 to 80 m, respectively. Note that the notch is always closer to the bottom at 50 Hz than at 25 Hz. The notch is also closer to the bottom at shorter ranges corresponding to steeper propagation paths. Additionally, the notch is closer to the bottom for the 18-m source depth because the dominant paths are steeper for the 18-m depth than for the 91-m depth. This is a very important feature and is discussed later in this report.

(C) Again returning to the discussion of table 7, the maximum losses for depth 6 range 2.6 to 5.5 dB greater than the losses for the bottomed receiver for source depths of 18 and 91 m. Depth 4, the BMA receiver 496 m off the bottom, is well above the notch depth. Depth 5, the BMA receiver 100 m off the bottom, is slightly above the notch for the

91-m source depth at 50 Hz. This receiver is well above the notch for the other given conditions. Depth 7, the ACODAC receiver 30 m off the bottom, is critically located with respect to the notch for the 18-m source depth in the following manner. At 25 Hz, depth 7 is in the notch for the 50- and 100-km ranges. At 50 Hz, it is located below the notch at the 50-, 100-, and 200-km ranges, in the notch at 500-km range, and above the notch at 1000-km range.

(C) The last major feature of interest is the relative minimum in propagation loss which appears just above the bottom at all ranges in figure 16 and at ranges of 500 and 1000 km in figure 17. These values are listed in table 7 under depth 8. For example, in figure 16 at 1000-km range, the propagation loss at a depth about 20 m off the bottom is 0.8 dB less than that for a bottomed receiver. This relative minimum in propagation loss appears to be related to the fact that the phase shift on bottom reflection is negative for the dominant arrivals. The upgoing and dowgoing arrivals are exactly in phase for a short distance above the bottom where the positive phase change due to travel-time difference equals the negative phase shift upon reflection at the bottom.

(C) The last entry in table 7, depth 10, is the dB spread over the other depth numbers. It represents the difference between the maximum and minimum propagation loss for receiver depths from the surface decoupling depth to the ocean bottom. The important feature of this entry is the small dependence on receiver depth. Values range from 2.9 to 5.7 dB, with 79% falling between 3.2 and 4.2 dB.

3.3.2 (U) Discussion of Receiver Depth Dependence

(C) The results of experiment and theory pertaining to receiver depth dependence for Site 1A are presented for comparison in table 8. The table shows the experimental propagation loss differences between the suspended BMA receivers and the bottomed receiver as well as the differences determined by normal mode theory. The experimental result at 25 Hz is a weighted average of the differences for events 1AP7 and 1AP5 shown previously in table 4. The experimental results at 50 Hz were obtained from event 1AS1 of table 5 by subtracting the average of receivers 5 and 8 (0.2) from the entries for receivers 1 and 2. The normal mode results in table 8 were determined from the results of table 7. These theoretical results represent weighted averages taken over the range of the experimental results.

(C) The agreement between experiment and theory for BMA receiver 1 is quite remarkable; they are within 0.2 dB of each other. The agreement is not quite as good for BMA receiver 2, but certainly acceptable. Notice that both theory and experiment yielded somewhat smaller differences for BMA receiver 2 when compared to BMA receiver 1 at 50 Hz. It is unfortunate that there were no processed data at 25 Hz for BMA receiver 2, since they would have provided an excellent check of the normal mode theory, which had predicted a larger value for BMA 2 than for BMA 1 at 25 Hz.

(C) Table 9 shows the difference between the bottomed receiver and other ACODAC receivers for Site 1B as determined by experiment and normal mode theory. Each experimental result is a weighted average of the number of range bins used in the events shown in table 7. The normal mode results of table 9 were derived from computations for a source depth of 102 m, which was appropriate for the CW source at 25 Hz. Agreement between

Table 8. (C) Propagation loss differences between the bottomed BMA receiver and other receivers at Site 1A for both experimental data and normal mode theoretical results. (U)

		Experimental			Normal Mode		
Source Depth (m)		91	91	243	91	91	243
Frequency (Hz)		25	50	50	25	50	50
BMA Receiver							
Number	Depth (m)						
1	2855	2.2	2.5	2.0	2.0	2.6	1.9
2	3251	—	1.0	1.5	2.4	1.5	0.6
3, 5, 8	3351	0	0	0	0	0	0

Table 9. (C) Propagation loss differences between bottomed ACODAC receiver and other ACODAC receivers at Site 1B for experimental data and normal mode results. The source depth is 102 m. (U)

		Experimental			Normal Mode	
Frequency (Hz) ⟶		25	140	290	25	50
ACODAC Receiver						
Number	Depth (m)					
2	496	2.3	2.3	−0.3	1.6	2.3
6	1685	2.1	2.9	1.0	2.0	2.7
10	3321	−0.2	−0.4	0.1	−0.2	0.9
13	3351	0	0	0	0	0

the experimental and theoretical results at 25 Hz for Site 1B is again quite good. The experimental data even appear to verify a relative minimum in propagation loss about 30 m off the bottom. Normal mode results for 50 Hz are also shown in table 9. The purpose of this calculation was to determine whether or not there were drastic changes in the propagation loss difference with frequency. As can be seen in table 9, the 50-Hz results appear similar to the experimental results at 140 Hz for ACODAC 2 and 5. Normal mode calculations were not made at higher frequencies than 50 Hz because the large number of modes generated by the program required more computer core storage than was available.

(C) The experimental depth dependence at 290 Hz shown in table 9 is quite different from that at 25 and 140 Hz. However, the 290-Hz data are suspect on three different counts. The first is the different character of the depth dependence shown in table 9. The second is that the propagation loss for ACODAC 13 at 290 Hz was 4.6 dB greater than for two bottom-mounted BMA hydrophones (discussed in the preceding section on Dependence of BMA Receiving Hydrophones). The third is that the variance of the 290-Hz data set was found to be significantly higher (50% higher) than for 25 and 140 Hz. In fact, the variance of the 290-Hz data set was larger than the variance of any other BEARING STAKE data set for all sites and frequencies. Any one of the above three anomalies might be accepted, but taken together they cast strong doubts on the data set.

(C) From this discussion on dependence of receiver depth, we can conclude that if differences of several dB in propagation loss are of small concern any receiver depth which avoids the near-surface region would be suitable at Site 1. The maximum variation in propagation loss with receiver depth for Site 1 was no more than 5 dB. This limit in variation applies only to source depths no deeper than 243 m. For deeper source depths near the axis of minimum velocity, the propagation conditions cease to be bottom limited, and near-axial receiver depths would have a distinct advantage over near-bottom receivers.

3.4 (U) OPTIMUM RECEIVER DEPTHS FOR BOTTOM-LIMITED ENVIRONMENTS

(C) This section is a discussion of optimum receiver depths based on the normal mode analysis of Site 1B. Although it remains to be verified, the general results contained in the discussion will apply to other bottom-limited areas with low bottom loss; in particular, the Indus Fan.

(C) If optimal receiver depths are desired, there are several choices. The minimum propagation loss often occurs at a receiver whose depth is the same as the source depth. However, this is not a practical choice for a fixed installation and, moreover, requires knowledge of the source depth. The smallest propagation loss below the sound speed axis occurs at the ocean bottom or slightly above it. In any case, as shown previously in table 6, the propagation loss at the ocean bottom is within 1 dB of the minimum propagation loss. Thus, bottom-mounted receivers are a good practical choice from the standpoint of minimum propagation loss.

(C) From the standpoint of signal-to-noise ratio, there is perhaps an even better choice. The noise generated by distant shipping may be reduced by positioning the receiver in the propagation loss "notch" described earlier for shallow sources. Computations for a source depth of 6 m are plotted in figures 20 and 21, and they show that the notch is in the identical location as for a source depth of 18 m (fig 22). The implication is that if the source is in the surface decoupling region, the location of the notch is independent of source depth. The reason for this property is that the dominant arrival angles apparently do not change significantly with source depth in this region. In contrast, for source depths below the surface decoupling region, the location of the notch shifts with source depths. Thus, a notch should occur at the same depth in the noise field from surface vessels of various drafts, and appear at different depths if a target submarine is deeper than the decoupling depth.

(C) The above concept is illustrated in figure 20 which depicts the propagation loss difference between a noise source at 6-m depth and a target source at 91-m depth at a frequency of 25 Hz. The target is assumed to be at a fixed range of 200 km. The difference in propagation loss is shown as a function of receiver depth from the ocean bottom. Each curve represents a different range for the noise source, starting at 50 km and progressing in increments of 50 km to a maximum range of 1000 km. The difference in propagation loss can be interpreted as signal-to-noise ratio for noise and target sources of equal strength. Thus, the magnitudes shown in figure 20 are not too meaningful; it is the relative values as a function of receiver depth which are important, as this applies not only to noise sources of various levels but also to multiple noise sources. For example, consider a receiver depth 30 m off the ocean bottom as shown by the horizontal line in figure 20. This depth is near optimum for noise generated at about 100-km range. For the noise ranges of figure 20, this receiver depth represents a 2.5–3.0-dB improvement in SNR from that for a receiver on the ocean bottom.

(C) Furthermore, note that the relative maximum of the curves in figure 20 moves increasingly above the ocean bottom as the noise range increases. This is because the notch, as illustrated previously in figure 14, shoals as range increases. Note also that there is a relative minimum in the curves which occurs about 93 m off the ocean bottom. This depth corresponds to the notch in figure 16 at 200-km range for a target depth of 91 m. The depth and noise of the target will affect the depth of this relative minimum. However, there will be no appreciable effect on the relative maximum as long as the target depth is below the surface decoupling depth.

(C) Figure 21 is similar to figure 20 except the range of the noise source is fixed at 200 km and the range of the target is allowed to vary. In this case, the relative maximum of the curves is independent of target range.

(C) Figure 22 is similar to figure 21 except the noise depth is 18 m rather than 6 m. The shapes of the curves in both figures are almost identical. The magnitudes differ because the propagation loss for the 6-m noise source is greater (because of surface decoupling) than that for the 18-m noise source.

(C) Figure 23 shows the loss curves for the same noise and target depths used to generate figure 20. Frequency is 50 Hz instead of 25 Hz. The horizontal line is for a receiver depth 18 m off the ocean bottom and is the optimal depth for noise at a range of 300 km. This depth represents a 1.5–3.5-dB improvement in SNR from that of a receiver on the ocean bottom.

(C) Several drawbacks in this discussion of optimizing SNR become apparent in analyzing figures 20 and 23. The first is that the optimum receiver depth moves with frequency. Thus, we must either optimize for a particular frequency or else use multiple depths, with each depth optimized for the frequency of interest. Another drawback is that in figure 23 the optimum depth appears to be more severely dependent on range than that of figure 20. This may not be a significant drawback if the predominant shipping noise can be predictable in range.

(U) Finally, in this discussion of optimizing SNR, the method of noise reduction relies on the fact that the principal arrival angles at the ocean bottom are different for shallow sources and deep sources. The process of slope enhancement (wherein the slope of the ocean bottom converts noise arrivals from steep to shallower angles) will tend to degrade this method. Experimental measurements of noise are necessary to determine this degradation.

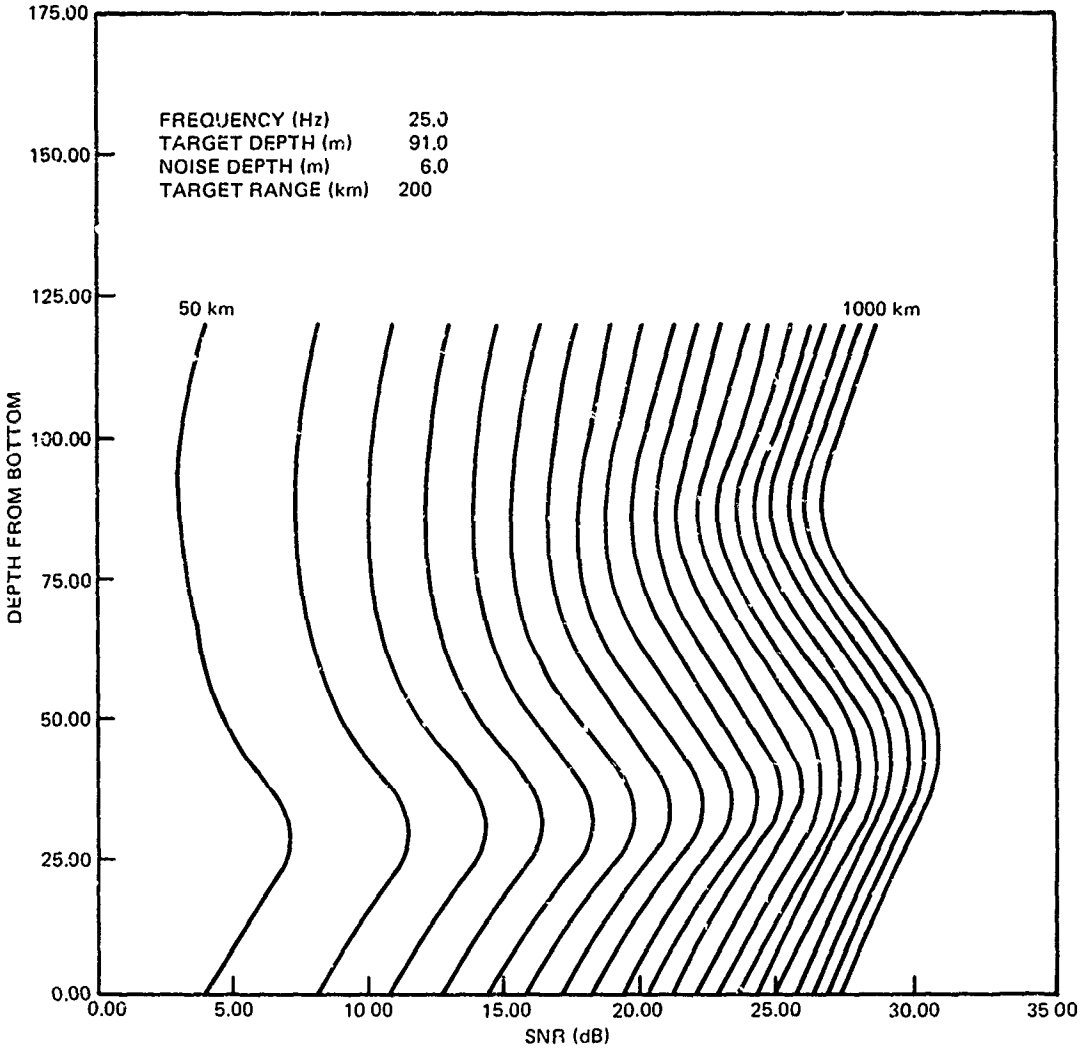

Figure 20. (C) SNR for a noise source at 6-m depth and a target source at 91-m depth for 25 Hz. The SNR is shown as a function of receiver depth from the ocean bottom. Range of the target is fixed while the range of the noise source varies (C)

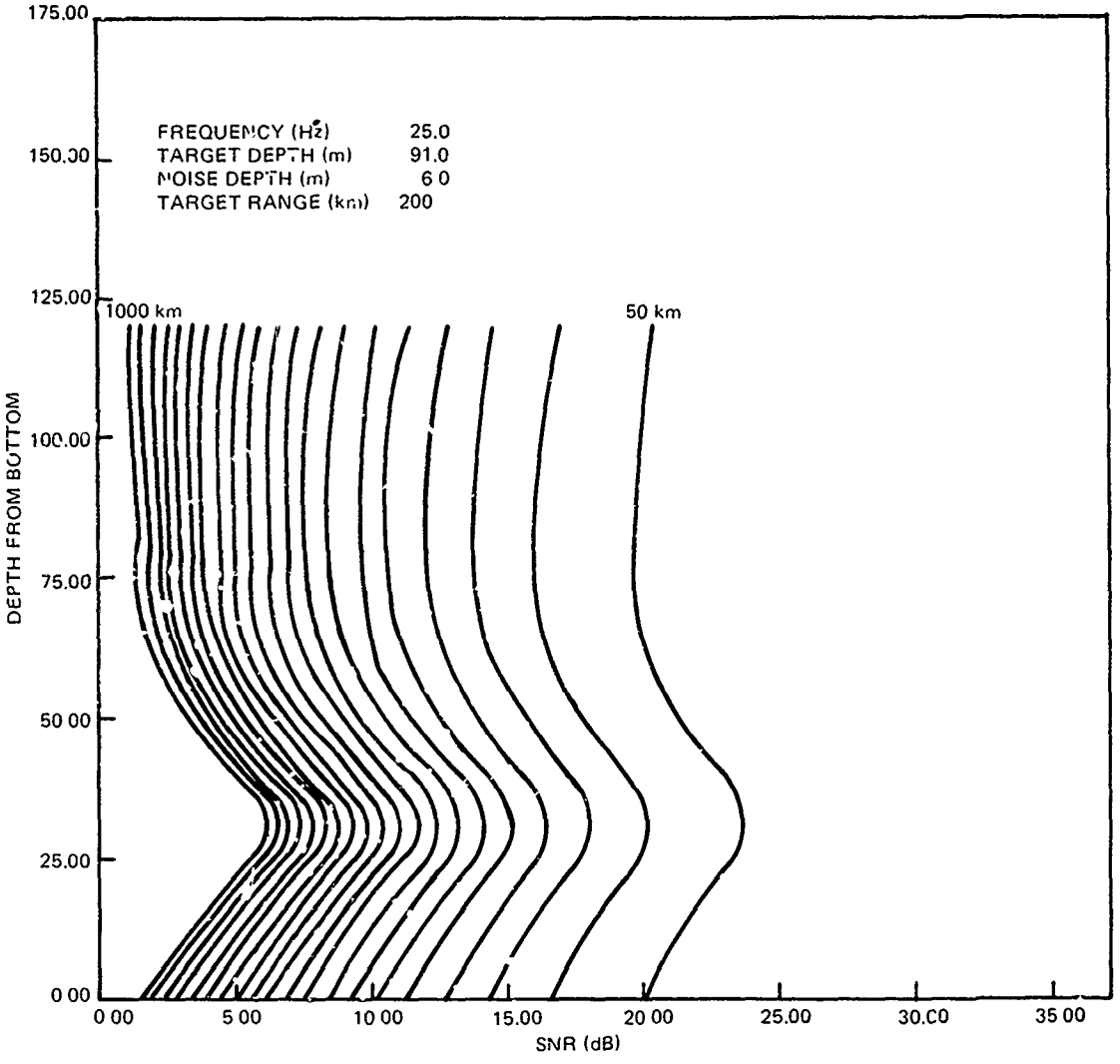

Figure 21. (C) SNR for a noise source at 6-m depth and a target source at 91-m depth for 25 Hz. Range of the noise source is fixed while the range of the target varies. (C)

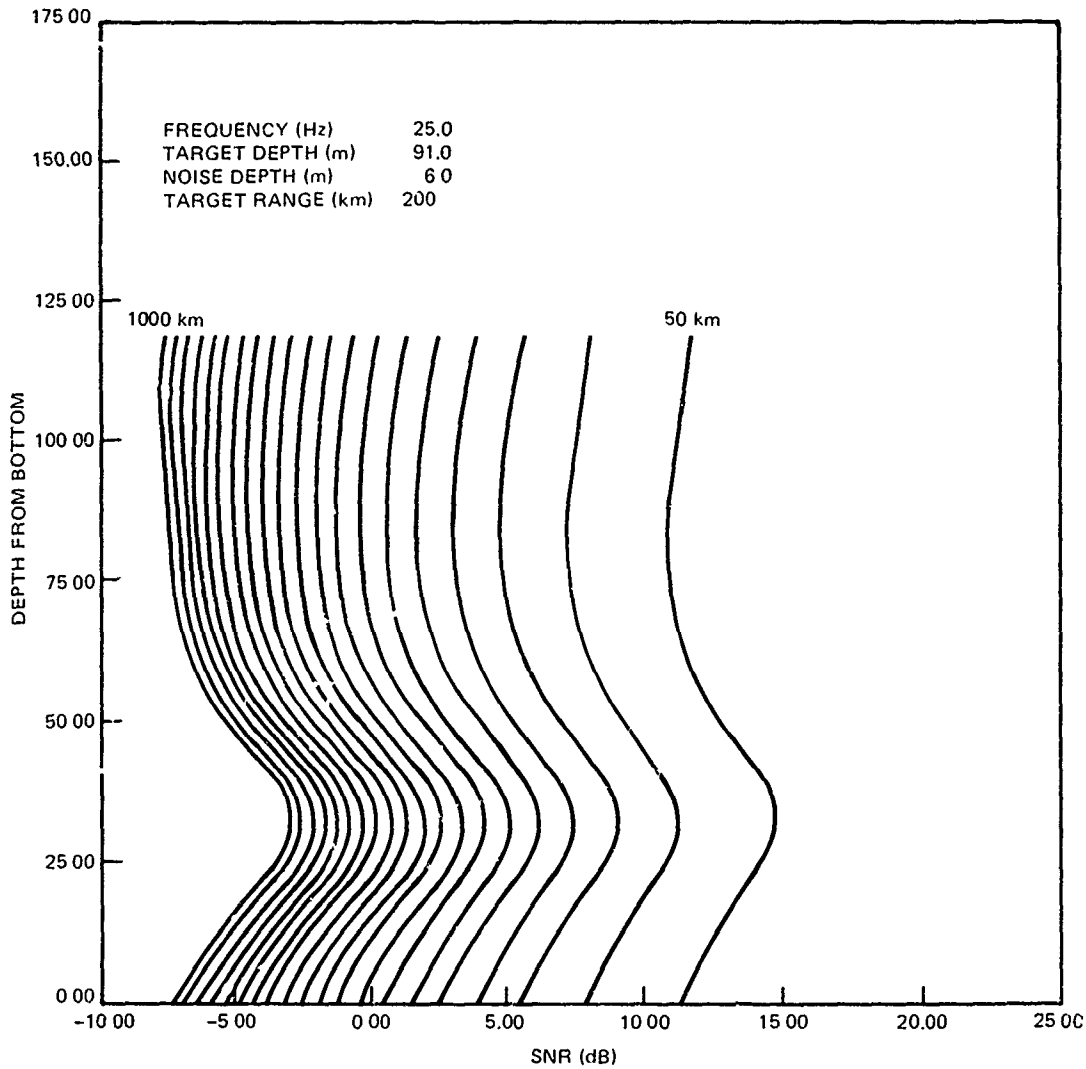

Figure 22. (C) SNR for a noise source at 18-m depth and a target source at 91-m depth for 25 Hz. Range of the noise source is fixed while the range of the target varies. (C)

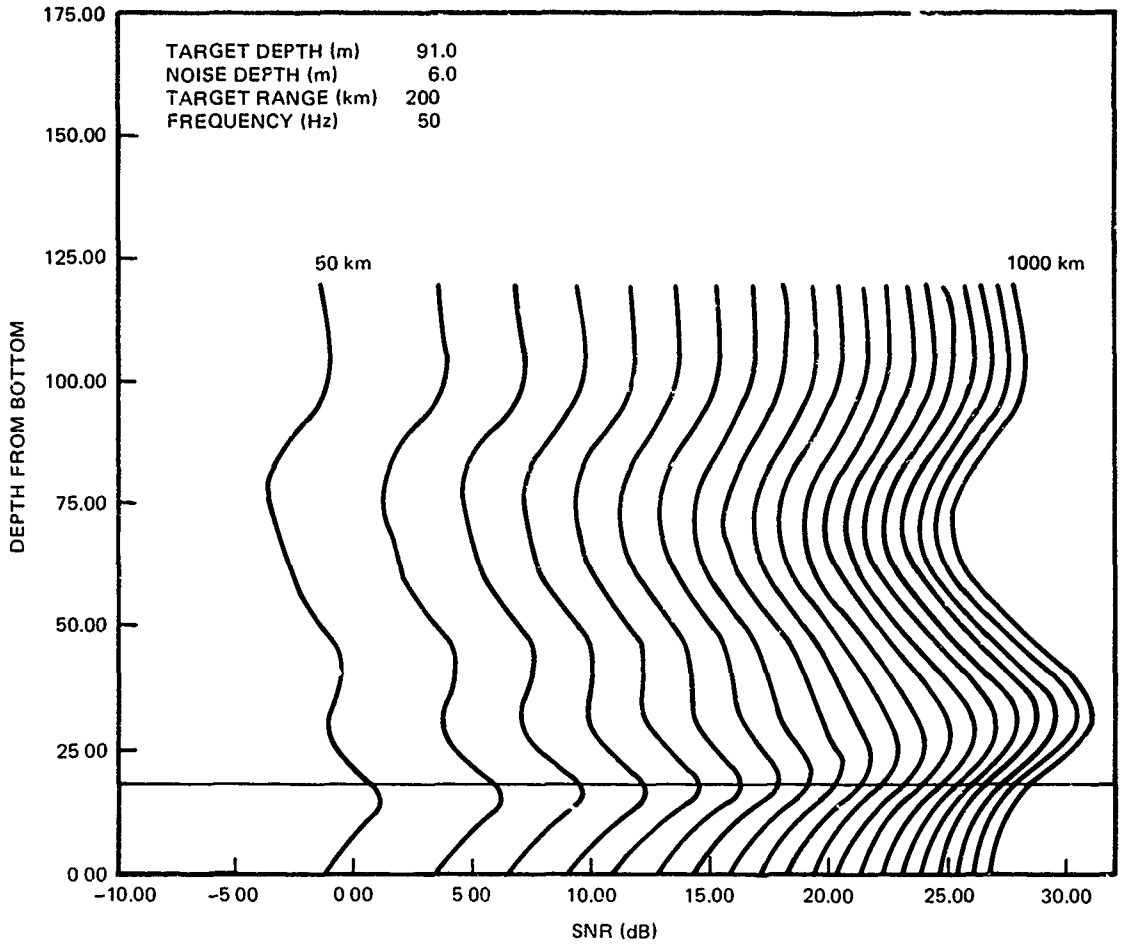

Figure 23. (C) SNR for a noise source at 6-m depth and a target source at 91-m depth for 50 Hz. Range of the target is fixed while the range of the noise source varies. (C)

3.5 (U) DEPENDENCE ON EVENTS

(C) In the assessment of propagation loss for each BEARING STAKE test site, it is important not only to determine the best receiver depth at a site but also to show the differences (if any) in propagation characteristics between various events conducted at a given site. This comparison between events will give indications of how homogeneous (or inhomogeneous) the propagation is in different directions from the location of the receiver. The best receiver depth for each event will be used as the basis for comparison of propagation loss. In the case of SUS events, the 91-m SUS depth will always be used for all frequencies. The 18-m SUS depth data are too sparse to use for comparison of events.

(U) Figures 24, 25, 26, and 27 show propagation loss for the receiver with lowest propagation loss as a function of range for all the events conducted at Site 1 (1A and 1B). The receivers at this site were BMA receivers on the ocean bottom. Figure 24 shows

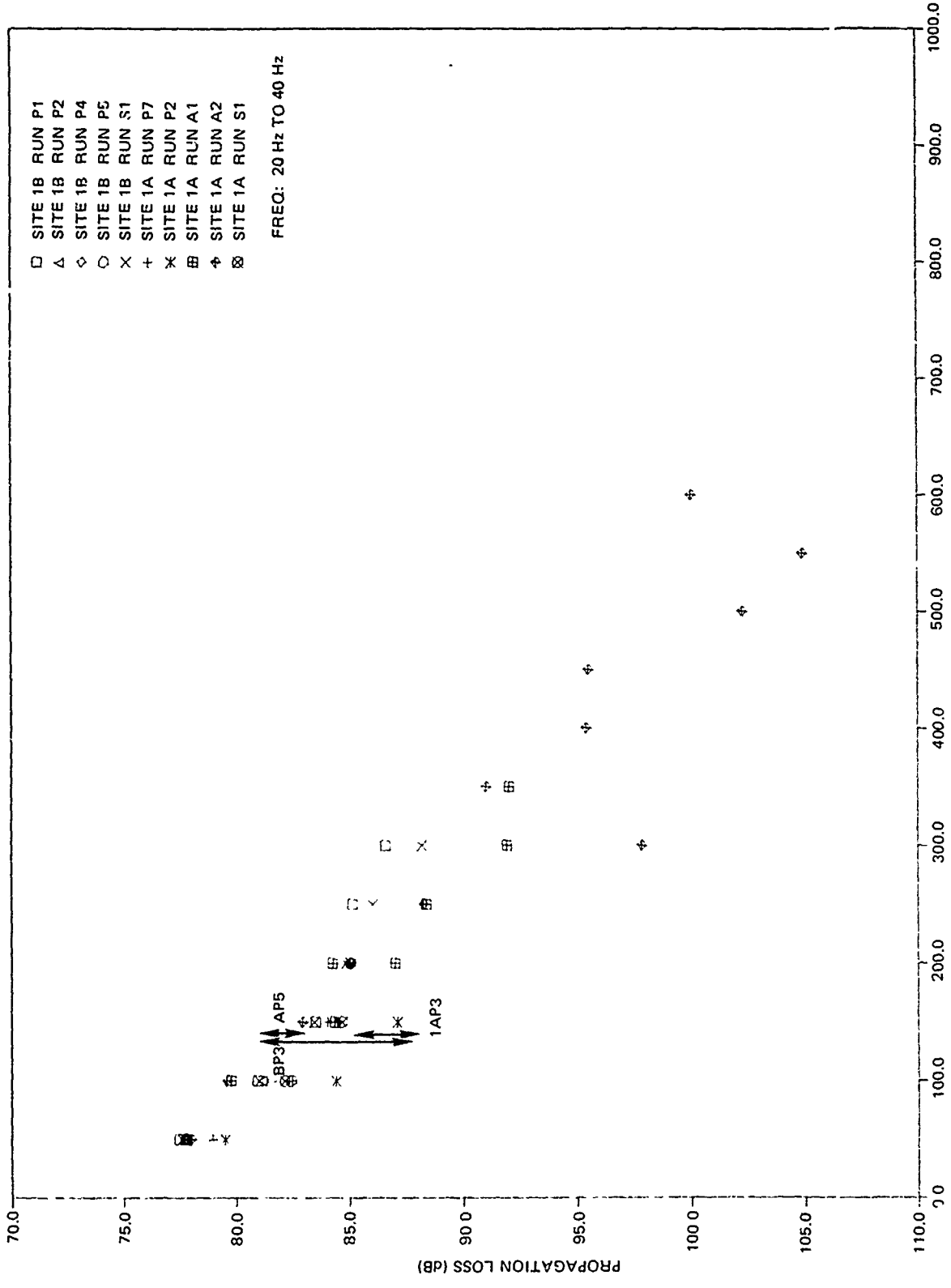

Figure 24. (C) Propagation loss of the receiver with the lowest propagation loss at 20–40 Hz as a function of range for all the events conducted at Site 1. (C)

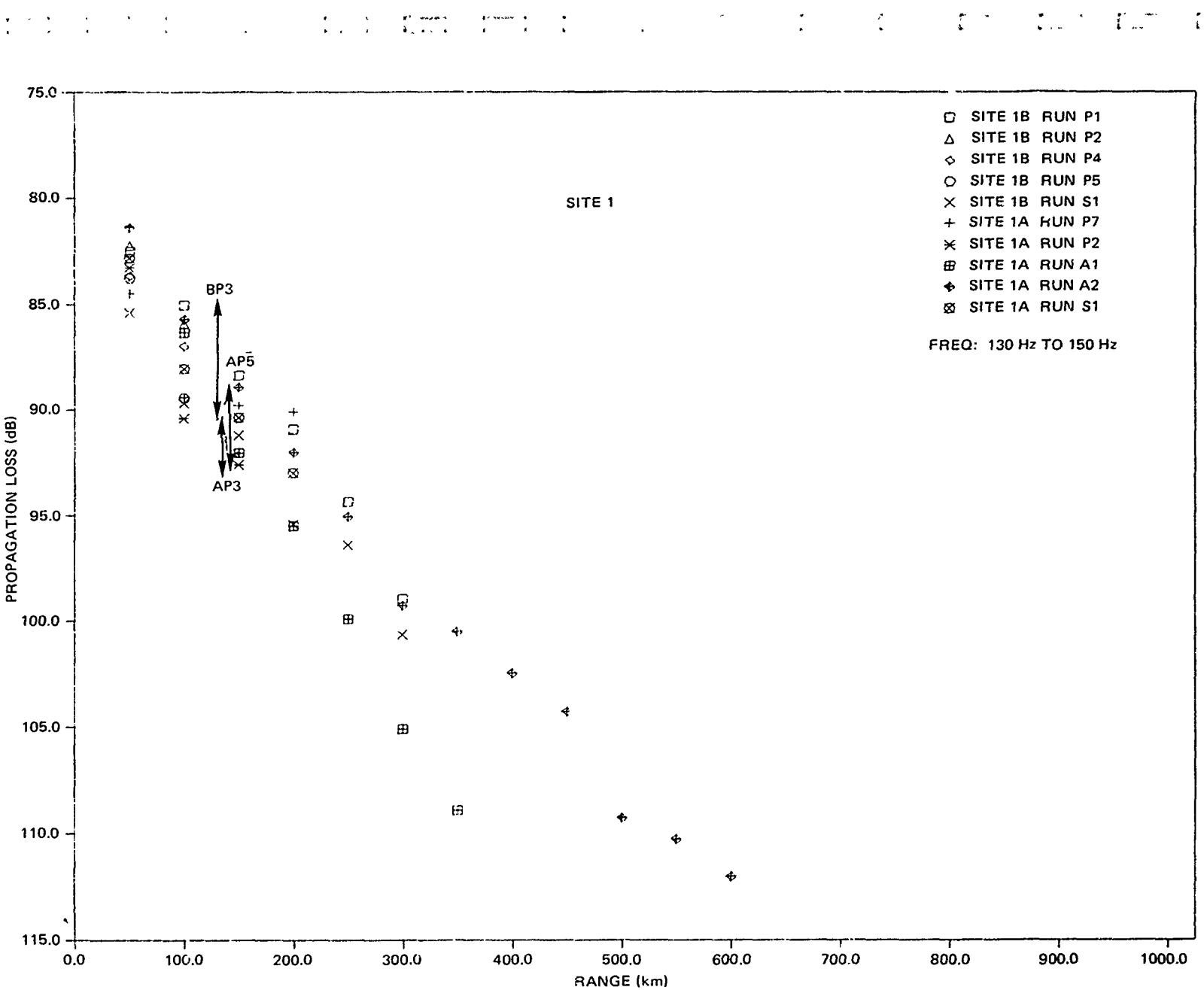

Figure 25. (C) Propagation loss of the receiver with the lowest propagation loss at 130–150 Hz as a function of range for all the events conducted at Site 1. (C)

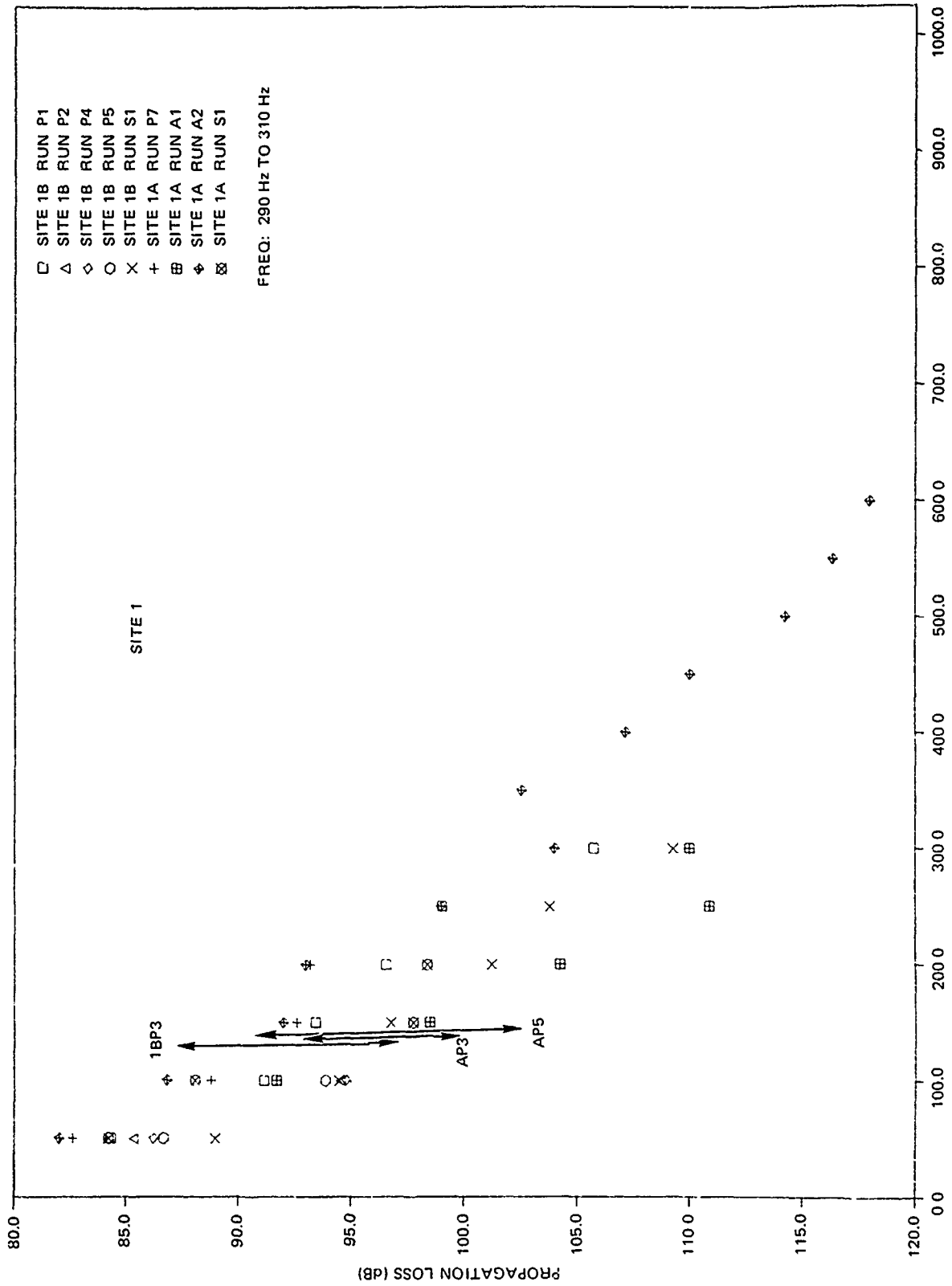

Figure 26. (C) Propagation loss of the receiver with the lowest propagation loss at 290–310 Hz as a function of range for all the events conducted at Site 1. (C)

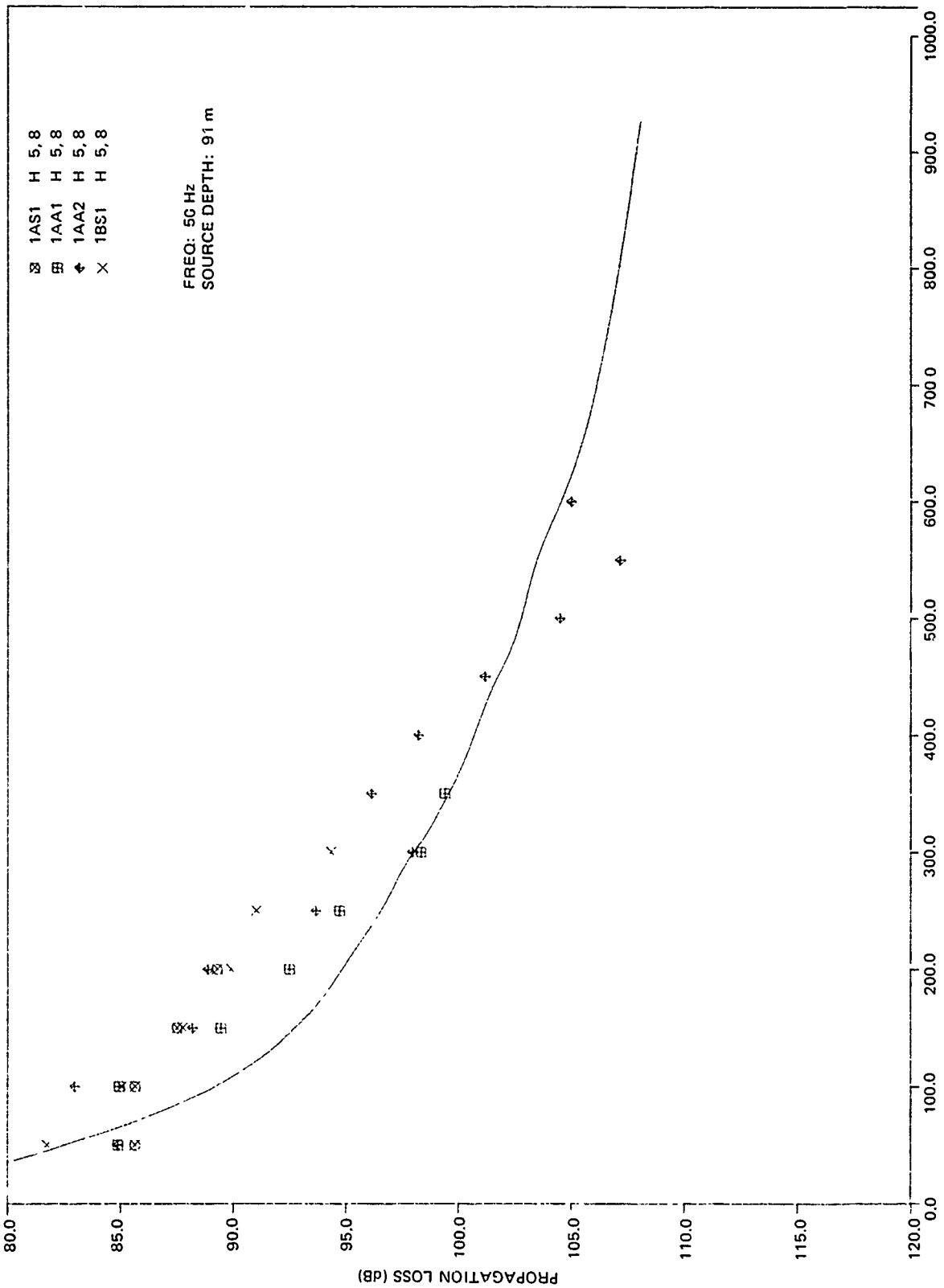

Figure 27. (C) Propagation loss of the receiver with the lowest propagation loss at 50 Hz as a function of range for all the SUS events conducted at Site 1. Also shown is the Eleuthera Reference Propagation Loss Curve. (C)

propagation loss for frequencies between 20 and 40 Hz. Figure 25 covers the frequencies between 130 and 150 Hz and figure 26 the frequencies between 290 and 310 Hz. Figure 27 shows only the propagation loss at 50 Hz and is based on SUS events only. The curve plotted along with the 50-Hz results is the Eleuthera reference. The results at other frequencies will be compared to this reference later in this report.

(U) The spread of values for the arc or circular events is plotted at the nominal range of these events and noted as such in figures 24 to 26.

(U) In order to assess the dependence of events at Site 1, the events were ranked according to propagation loss for each frequency. However, before the rankings were made, the validity of the propagation loss data and results had to be considered.

(C) For instance, in event 1AA1, only the data points out to and including 150 km were used to determine its ranking because analysis of the bathymetry for the event showed that the event was not conducted as planned. The test plan called for the event to proceed due north to the receiver location along the track, labeled 1AA1S in figure 11. The bathymetric profile for this event (appendix *A*, fig *A-1*) indicated that there were deviations from the plan and that the event was radial only from 150 km to the receiver. This made the event very complicated and ill suited for good quantitative measures of propagation loss beyond 150-km range.

(U) There were other complications which made a rigorous comparison between events difficult. One was the fact that the SUS data had somewhat higher loss than the corresponding CW data. This was discussed earlier in the Data Consistency section of the report.

(C) Another complication was that at Site 1B, the source was operated at 102-m depth and the source depth at Site 1A was 91 m.

(C) Finally, at Site 1A, the CW sources at 140 and 290 Hz were operated at 24-m depth rather than the 18-m depth used at Site 1B and all the other sites.

(C) The ranking of the Site 1 radial events, complications notwithstanding, is shown in table 10. The table shows the ranking of the various events for low frequency (20–40), 140, 290, and 50 Hz. The best events, in terms of low propagation loss overall for all four frequencies, are 1BP1 and 1AA2. It is difficult to say for certain which of the two events is best because the levels of 1AA2 should be raised somewhat to account for typical differences between SUS and CW events. Both events were conducted over essentially flat bottoms from 250 km to the receiver. (See appendix A for bathymetric profiles of all the events conducted in BEARING STAKE.)

(C) The three next best events in the overall ranking are 1AA1, 1BP2, and 1BP4. As shown in figure 11, all three events had a southerly direction from the basin center. The bathymetric profiles for events 1AA1, 1BP2, and 1BP4 were essentially flat out to ranges of 220, 75, and 75 km, respectively. For the latter two events, there was only a slight rise in bathymetry.

(C) Finally, the events with the largest overall propagation losses are 1BP5 and 1AP2. These two events ran in a northerly direction from the basin center and proceeded up the continental shelf (see fig 11). The bathymetric profiles of the events were essentially flat out to about 65 km and then proceeded abruptly up the continental rise with slopes as high as 5°.

(C) The arc (or circular) events at Site 1 support the ranking of events in table 10. The highest propagation losses occurred in event 1AP3 due north of the receiver location,

Table 10. (C) Ranking of events at Site 1. The dash (—) indicates that the data were not processed for the particular event and frequency. (U)

Rank	Low (20 - 40 Hz)	140 Hz	290 Hz	50 Hz
1	1BP1	1BP1	1AA2	1AA2
2	1AA2	1AA2	1AP7	1BS1
3	1AA1	1BP2	1BP1	1AA1
4	1BS1	1AA1	1AS1	1AS1
5	1BP2	1AS1	1AA1	—
6	1BP4	1BP4	1BP2	—
7	1BP5	1BP5	1BP4	—
8	1AP7	1AP7	1BP5	—
9	1AS1	1AP2	1BS1	—
10	1AP2	1BS5	—	—

where the ocean bottom shallows to less than 1500 m. Similarly, the highest losses for event 1AP5 occurred at the northernmost section of the event, where the bottom shallows to about 2500 m. For event 1AP5, exceptionally high losses occurred at 290 Hz (see fig 26) and appear too great to justify on the basis of bathymetry alone. It is not clear, at the present time, why larger losses occur at 290 Hz for event 1AP5 than for event 1AP3, which penetrated further up the continental rise.

(U) The losses for the final arc event 1BP3 appear to be comparable to the range bin results of the radial events. In general, the higher losses for event 1BP3 are along the end which connects to event 1BP4, with the lower losses connecting to event 1BP2. Note that 1BP4 is ranked lower than 1BP2 in table 10.

(C) Thus, the propagation characteristics of Site 1, located in the Oman Basin, can be summed up as follows

1. (C) The lowest losses occur along the floor of the basin.

2. (C) Somewhat higher losses occur in the southern portion of the basin, where the bottom shallows.

3. (C) The largest losses occur to the north of the basin towards the continental rise.

(U) As mentioned before, the rankings in table 10 were based on propagation losses for each event. There were four events – 1AP7, 1AS1, 1BP1, and 1BS1 – which ran over essentially the same bathymetry. We should assume that the propagation losses would be about the same and that, in rank order, these four events would be clustered. However, this was not the case, as can be seen by the spread in their rankings in table 10.

(U) A detailed analysis of the four events was made to determine the cause for the spread in ranking. The analysis consisted of four tests made between the various data sets to

help determine a logical explanation for the spread. (These tests were utilized for analysis of events at the other sites whenever applicable.)

(C) Test 1 was a comparison between the propagation losses between the SUS and CW events at Site 1A and, also, at Site 1B. Although there may have been variations between the sound speed profiles for each event that may have had some effect on propagation, these variations were considered to be insignificant to the analysis at hand. The propagation loss differences between the SUS (1AS1) and the CW (1AP7) events at Site 1A were 0.2, –0.8, and 3.0 dB for 25, 140, and 300 Hz, respectively. Corresponding values for Site 1B were 0.3, 3.2, and 4.2 dB. Typical values obtained for all sites were 1.4, 1.1, and 2.0 dB for the same respective frequencies.

(C) Test 2 was a comparison between the propagation loss of the 91-m depth and the 243-m depth SUS shots. The propagation loss differences for SUS event 1AS1 were 2.8, –0.4, 1.6, and 4.1 dB for 20, 50, 140, and 300 Hz, respectively. Corresponding values for event 1BS1 at Site 1B were 1.9, 0.3, 3.0, and 4.6 dB. The typical values for all SUS events at all sites were 2.7, –0.4, 1.9, and 2.8 dB for the respective frequencies.

(C) Test 3 was a comparison between the propagation loss for CW events 1AP7 and 1BP1. The loss differences between the two events were 0.9, [illegible] and 1.6 dB for 25, 140, and 290 Hz respectively.

(C) Test 4 was a comparison of the propagation loss difference between SUS events 1AS1 and 1BS1 for 91- and 243-m depth. The differences for the 91-m depth shots were 0.7, –0.1, –2.5, and –2.2 dB for 20, 50, 140, and 300 Hz, respectively. The corresponding values for the 243-m depth shots were 0, 0.3, –0.3, and –1.9, respectively.

(U) The negative values of the results in the above four tests indicate that the first event mentioned in each test had less loss than the second event.

(C) In analyzing the results of the above four tests at frequencies of 20, 25, and 50 Hz, it was noted that the differences all lie within the experimental error which could be attributed to receiver system errors. Thus, at these frequencies, propagation loss differences between Site 1A and 1B are not significant. The differences between the SUS and CW events were typical to those at other sites and were within the experimental error.

(C) In contrast, the data at 140 and 290 Hz are in conflict with one another. Test 3 indicates that propagation conditions were better at Site 1B than at Site 1A at 140 Hz and worse at 290 Hz, whereas test 4 indicates that both frequencies were better at Site 1A. There is obviously some error in the propagation loss results. To determine whether errors existed, some reasonable assumptions were made to see what changes could be made in adjusting propagation loss which would bring the results into line within experimental error.

(C) At 140 Hz, the ranking of events in table 10 has 1BP1 and 1AS1 near the top of the rankings. Assume that the losses for these two events are correct. If the assumption is made that the propagation losses for events 1BS1 and 1AP7 are 2.0 dB too high, there is agreement then with the typical site result of test 1 to within ±0.1 dB. These assumed errors in propagation loss yield a value of 2.0 dB for test 3 and –2.0 dB for test 4 for the 91-m depth shots. These values are within the experimental error of 2.6 and –2.5 dB. Consider then the 243-m shot data at 140 Hz. Test 2 indicates that the difference between 91- and 243-m shots for event 1AS1 is typical of other sites. Thus, the propagation losses for 243-m shots for event 1AS1 are correct. Now, assume that the propagation losses for the 243-m shots for event 1BS1 are 0.3 dB too high. This assumption leads to a value for test 4 of 0.3 dB within experimental error of the measured value. It also leads to an adjusted value

for test 2 of 3.0 dB (experimental value) minus 2.0 dB (assumed correction at 91 m) plus 0.3 dB (assumed correction at 243 m), which equals 1.3 dB; this is within experimental error of the typical value of 1.9 dB.

(C) At 290 Hz, consider the following assumptions which were derived by minimizing the various errors: losses for 1BP1 are correct and losses are too high for events 1BS1, 1AP7, and 1AS1 by 2.4, −1.0, and 0.6 dB, respectively. These assumptions lead to a value of −1.0 dB for test 3 compared to a measured value of −1.6 and to a value of −1.8 dB for test 4 compared to a measured value of −2.2 dB. Test 1 for Site 1A leads to a value of 1.4 dB (3.0 − 0.6 − 1.0) compared to a typical site value of 2.0 dB. Test 1 for Site 1B leads to a value of 1.8 dB (4.2 − 2.4) compared to a typical site value of 2.0 dB.

(C) Furthermore, consider the 243-m shot depth at 290 Hz. Assume that the losses for events 1BS1 and 1AS1 are 0.9 and −0.8 dB too large, respectively. These assumptions lead to a value for test 4 of −1.7 dB compared to a measured value of −1.9 dB. Test 2 for Site 1A leads to an adjusted value of 2.5 dB (4.1 − 2.4 + 0.8) compared to the typical site value of 2.8 dB. Test 2 for Site 1B leads to an adjusted value of 3.1 dB (4.6 − 2.4 + 0.9) compared to the typical site value of 2.8 dB. Thus, the assumptions at 290 Hz have led to adjusted values which agree within experimental error of the measured values for all four tests.

(C) In summary, the event with the largest error, at 140 and 290 Hz, is 1BS1. Estimated errors for 91-m depth are 2.0 and 2.4 dB, respectively, at 140 and 290 Hz, which explains the low ranking of this event in table 10. Corresponding errors for 243-m depth are 0.3 and 0.9 dB. The estimated errors for event 1AP7 are 2.0 and −1.0 dB, respectively, at 140 and 290 Hz, which explains the relatively low ranking of the event at 140 Hz and the relative high ranking at 290 Hz in the table. The losses for event 1AS1 appear to be correct at 140 Hz and too high at 290 Hz by 0.6 and 0.9 dB for the 91- and 243-m depths, respectively. The losses for event 1BP1 appear correct at both 140 and 290 Hz.

(C) All the above estimates are based on the hypothesis that the propagation conditions at Site 1A were not significantly different than at Site 1B. In any case, it is believed that the levels at 140 and 290 Hz for the 91-m shots in event 1BS1, and the 140-Hz levels in 1AP7, are definitely in error by about 2.0 dB. The 243-m shot data at 290 Hz in events 1BS1 and 1AS1 are possibly in error by about 1.0 dB and the 290-Hz data for event 1AP7 are possibly in error by 1.0 dB.

3.6 (U) DEPENDENCE ON RANGE AND FREQUENCY

(U) In this section, comparisons of the best event at Site 1 for each of the frequencies are made with the Eleuthera reference (hereafter referred to as the "reference"). The discussion is somewhat abbreviated herein since a subsequent section in this report provides a detailed analysis of the data based upon the collective sites.

(C) The propagation loss at Site 1A and 1B is listed in tables 11 and 12, respectfully, for the CW event with lowest propagation loss at frequencies of 25, 140, and 290 Hz, and for the SUS event at 50 Hz.

(C) The propagation loss values for 25, 140, and 290 Hz are plotted and compared to the reference in figure 28. The slope of the 25-Hz losses is much less than that of the reference and suffers 12-dB less propagation loss at the maximum range shown. The slope of the 140-Hz losses is slightly less than that of the reference; loss values for Site 1B range from

Table 11. (C) Propagation loss results of the best CW events at Site 1A. (U)

Range (km)	Propagation Loss (dB) Event: 1AP7 Freq: 25Hz	Event: 1AP7 Freq: 140Hz	Event: 1AP7 Freq: 290Hz	Event: 1AA2 Freq: 50Hz
50	78.8	84.5	82.6	—
100	82.0	89.4	88.8	83.6
150	83.7	89.8	92.6	88.2
200	—	—	—	88.9

Table 12. (C) Propagation loss results of the best CW events at Site 1B. (U)

Range (km)	Propagation Loss (dB) Event: 1BP1 Freq: 25Hz	Event: 1BP1 Freq: 140Hz	Event: 1BP1 Freq: 290Hz	Event: 1BS1 Freq: 50Hz
50	77.5	82.5	84.3	81.7
100	80.9	85.0	91.2	85.0
150	83.5	88.4	93.4	87.8
200	84.2	91.0	96.6	89.9
250	85.2	94.4	99.0	91.0

0 to 4 dB less while the loss values for Site 1A straddle the reference. However, as previously discussed, these losses are estimated to be 2 dB too high and are suspect. The slope at 290 Hz is comparable to that of the reference, with loss values for Site 1B larger than those of the reference by 1 to 2.5 dB. The loss values for Site 1A are less than 1 dB smaller than those of the reference but are suspect because these losses are estimated as being 1 dB too low.

(C) The 50-Hz data were compared with the reference previously in figure 27. Event 1AA2 was not compared beyond 200-km range because of the seamount crossing previously discussed. The 50-Hz losses appear comparable to those of the reference when slopes are compared. However, the losses for event 1AA2 are from 4 to 6.5 dB less than those of the reference, and the losses for event 1BS1 are from 0.5 to 5.5 dB less. In comparing frequency data, it must be recalled that the 50-Hz data are from SUS events while the other frequencies are for CW events, and that the SUS data are not as reliable as the CW data because the SUS sampling was sparser.

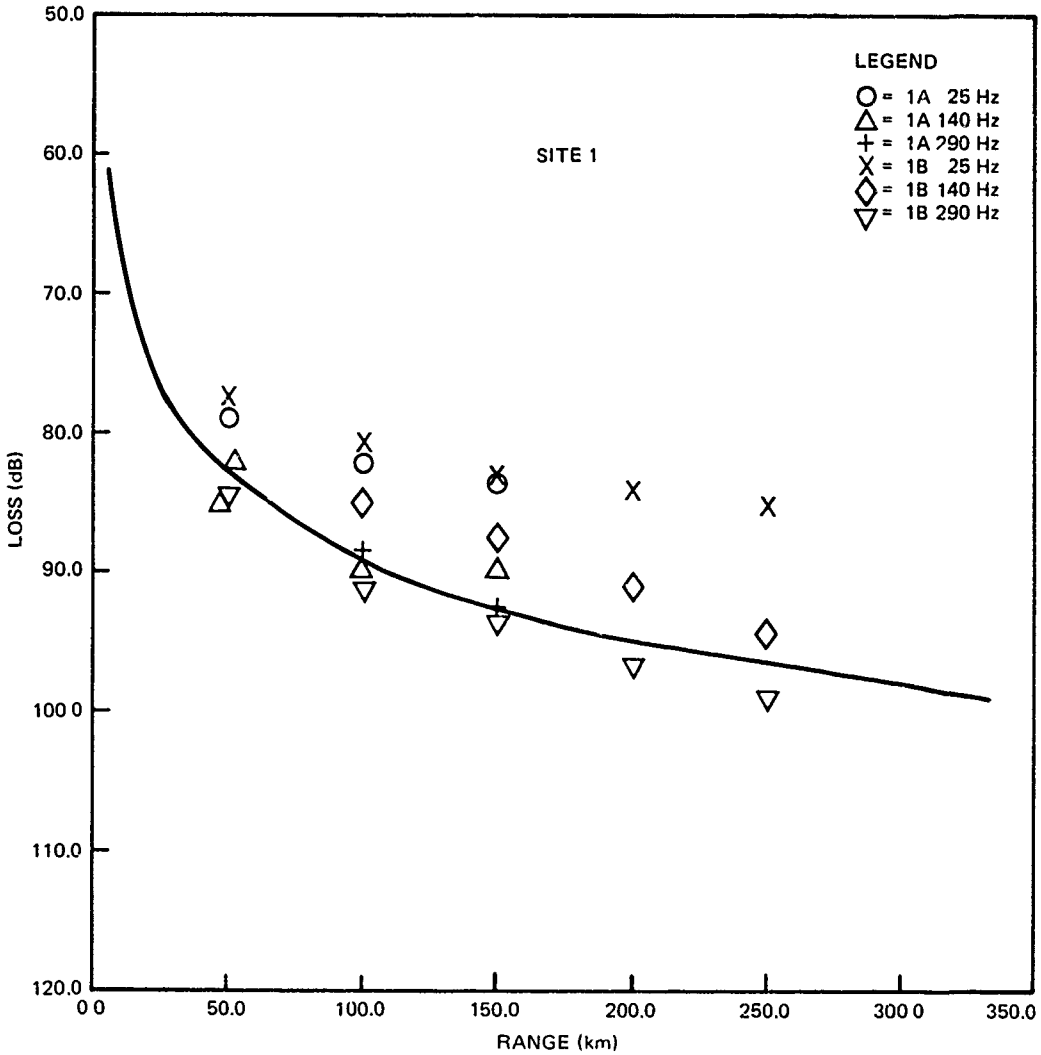

Figure 28. (C) Propagation loss curves for 25, 140, and 290 Hz plotted against the Eleuthera reference curve. (C)

3.6.1 (U) Comparison of Experimental Results with Theory

(U) This section is unique to Site 1 and is concerned with a comparison between the experimental and theoretical dependence of propagation loss on range and on source depths at low frequency. It has already been shown that the normal mode model gave good agreement with experiment in the dependence of propagation loss on receiver depth.

(C) Figure 29 shows propagation loss at 25 Hz as a function of range for various theoretical and experimental data from Site 1. The particular event used in this case is event 1BP1. The BMA experimental results are based on the average for three bottomed

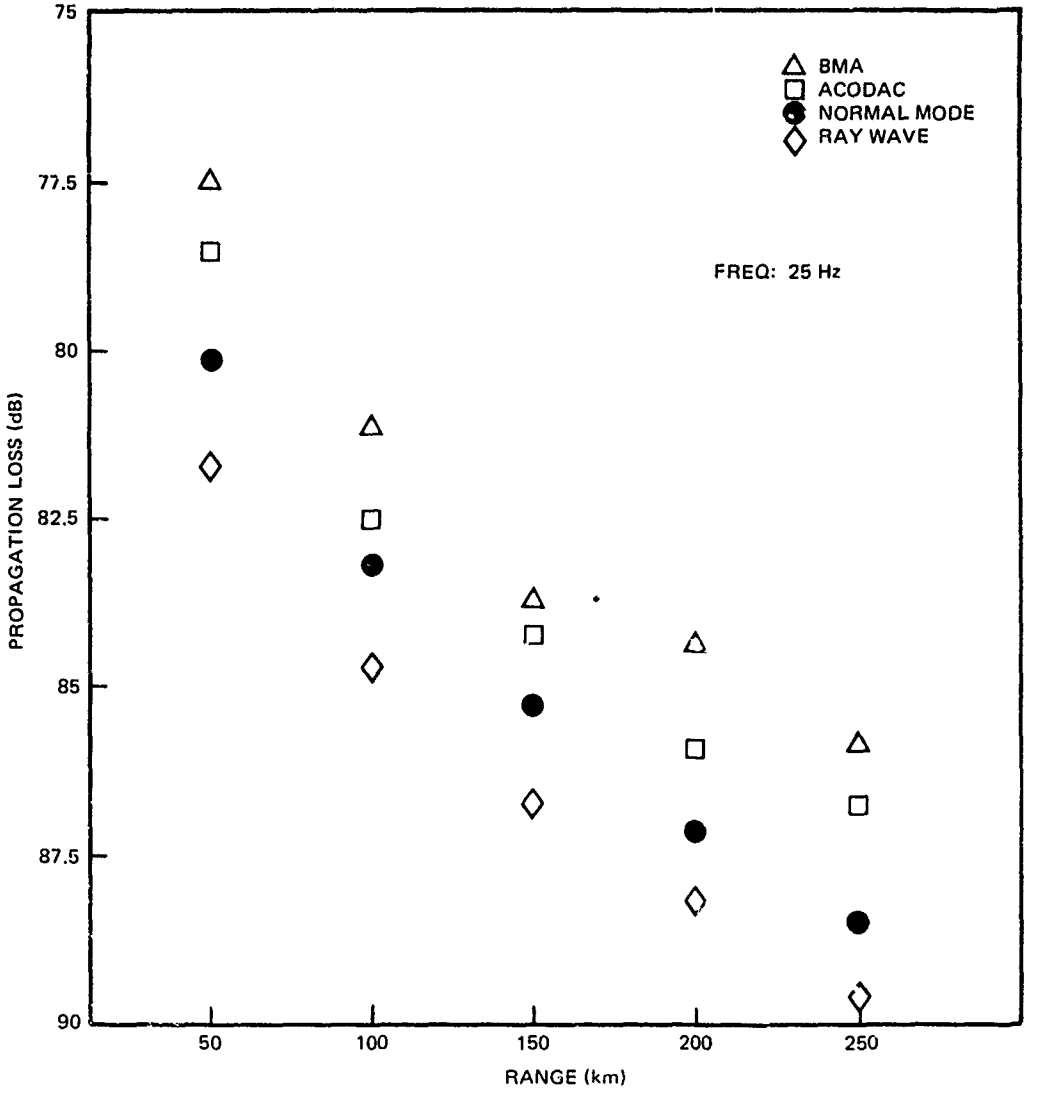

Figure 29. (C) Propagation loss as a function of range for various theoretical and experimental data results from Site 1. (U)

receivers and the values listed in table 12 under the 25-Hz column. The ACODAC experimental results are from receiver 13 mounted on the ocean bottom and were obtained by p^2 averaging of the raw ACODAC data. The normal mode theoretical calculations are based on coherent calculations for propagation loss. The normal mode results were p^2 averaged in 50-km range bins, converted to propagation loss, and plotted. The normal mode model was also used to calculate reflection coefficients at the ocean bottom. By using these coefficients and a representative sound speed profile for Site 1B, propagation losses were computed with the RAY WAVE model at 2-km range intervals. The RAY WAVE data were also p^2 averaged in 50-km range bins and plotted in figure 29. This procedure allows a comparison between normal mode and RAY WAVE for a comparable environmental input.

(C) Statistical analysis of the data shows that the differences between experiment and model results in figure 29 are not range dependent. The average experimental losses for the five range bins are 2.6 and 1.3 dB smaller than losses arrived at by mode theory for the BMA and ACODAC data, respectively. Corresponding standard errors of the mean were 0.5 and 0.4 dB.

(C) Figure 19 shows also that the experimental losses are about 4 to 5 dB less than those predicted by the RAY WAVE model. This discrepancy was investigated and is discussed in detail in the section of this report entitled "Propagation Loss Model Assessment." In brief, the investigation identified four separate factors, each of which could reduce the discrepancy between experiment and theory by 1 or 2 dB. These four factors were:

1. (C) The bottom loss values used in the models were too high.
2. (C) The models sum up the energy incoherently.
3. (C) A biasing in data processing procedures of the different receiving systems.
4. (C) Errors in estimations of source levels.

(U) The above four factors are presently being thoroughly examined to determine their influence as related to the general comparison between experiment and models at the various BEARING STAKE sites. It should be noted that factors 1 and 2 are corrections to the model inputs or modes and factors 3 and 4 represent corrections to the experimental data. When the study is completed, the entire problem of the discrepancy between the CW experimental results and theory will be re-examined and assessed. An assessment, however, can be made of the SUS events as compared with normal mode theory.

(C) Figure 30 compares the experimental propagation loss results from the SUS data for 20 Hz at Site 1B with propagation losses from the normal mode model. The experimental values represent averaged values in 50-km range bias. The normal mode results were calculated by adding modes in random phase rather than averaging the coherent results in bins, to allow for calculations of propagation loss as a continuous function of range. The random phase addition preserves the standing wave patterns (which include bottom and surface effects), which are not preserved in incoherent ray theory models without some special provision.

(C) Values for the standard shot depths of 18, 19, and 243 m are presented in figure 30. All the data are for bottomed BMA receivers. In comparing experiment to theory, the shot data for event 1AA2 beyond 200-km range were not included in the analysis because of a seamount obstruction. Similarly, the data for event 1AA1 beyond 150 km were not included because of a ridge.

(C) Figure 31 is the counterpart for 50 Hz of figure 30. Analysis of the differences between theory and experiment shows that there appear to be no significant trend with range and no appreciable dependence on event. The data for all available range bins and all events were combined to produce an average difference between theory and experiment for each source depth and each frequency.

(C) Table 13 presents the results of the analysis. The average difference values represent range-independent offsets between theory and experiment. The relatively small values of the standard errors contain all residual range and event dependence and indicate that the offsets are statistically significant. The 18- and 91-m values at each frequency are based on independent data from 16 range bins while the 243-m values are based on 10

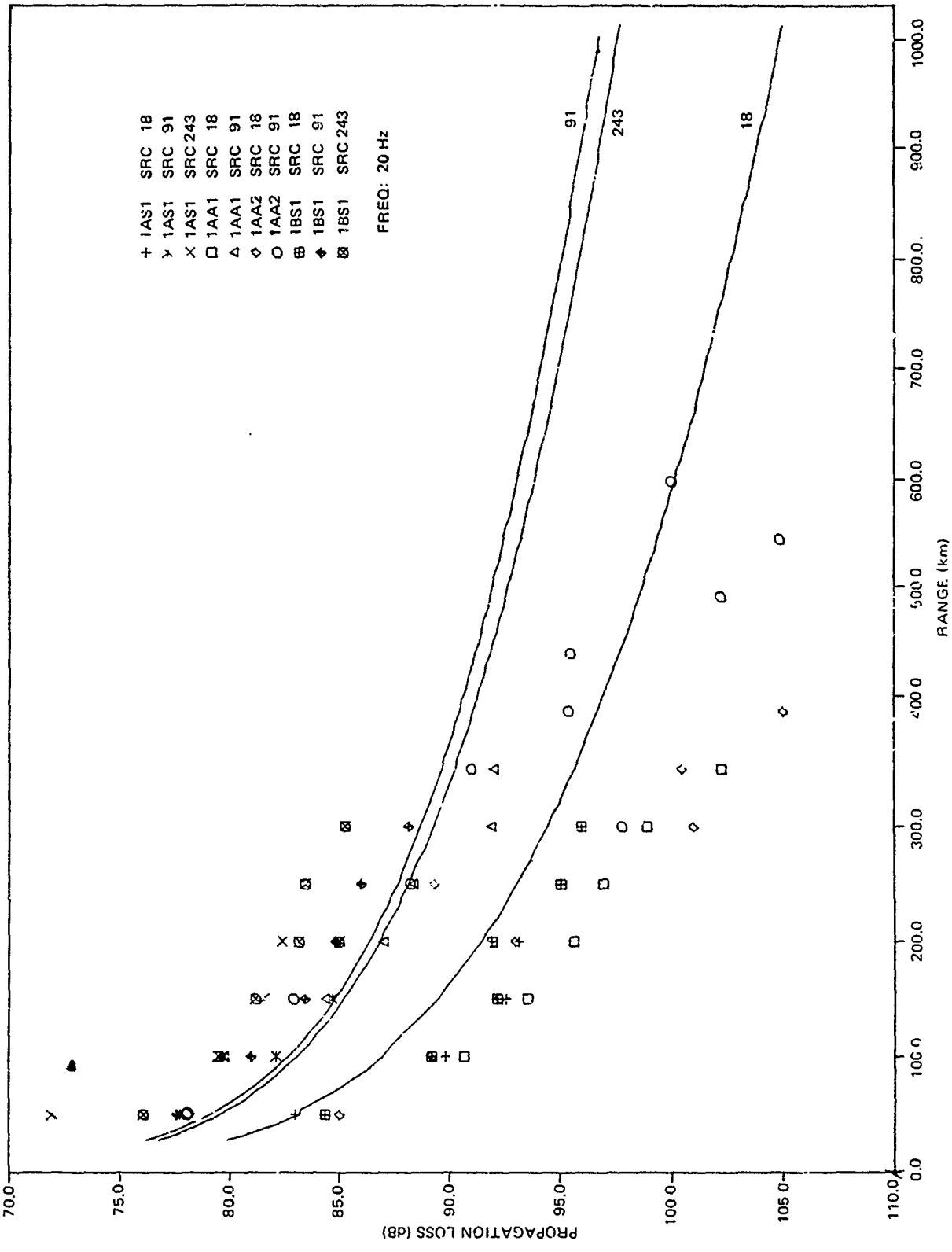

Figure 30. (C) Comparison of experimental propagation loss results from SUS data for 20 Hz at Site 1B with propagation losses from the normal mode model. (C)

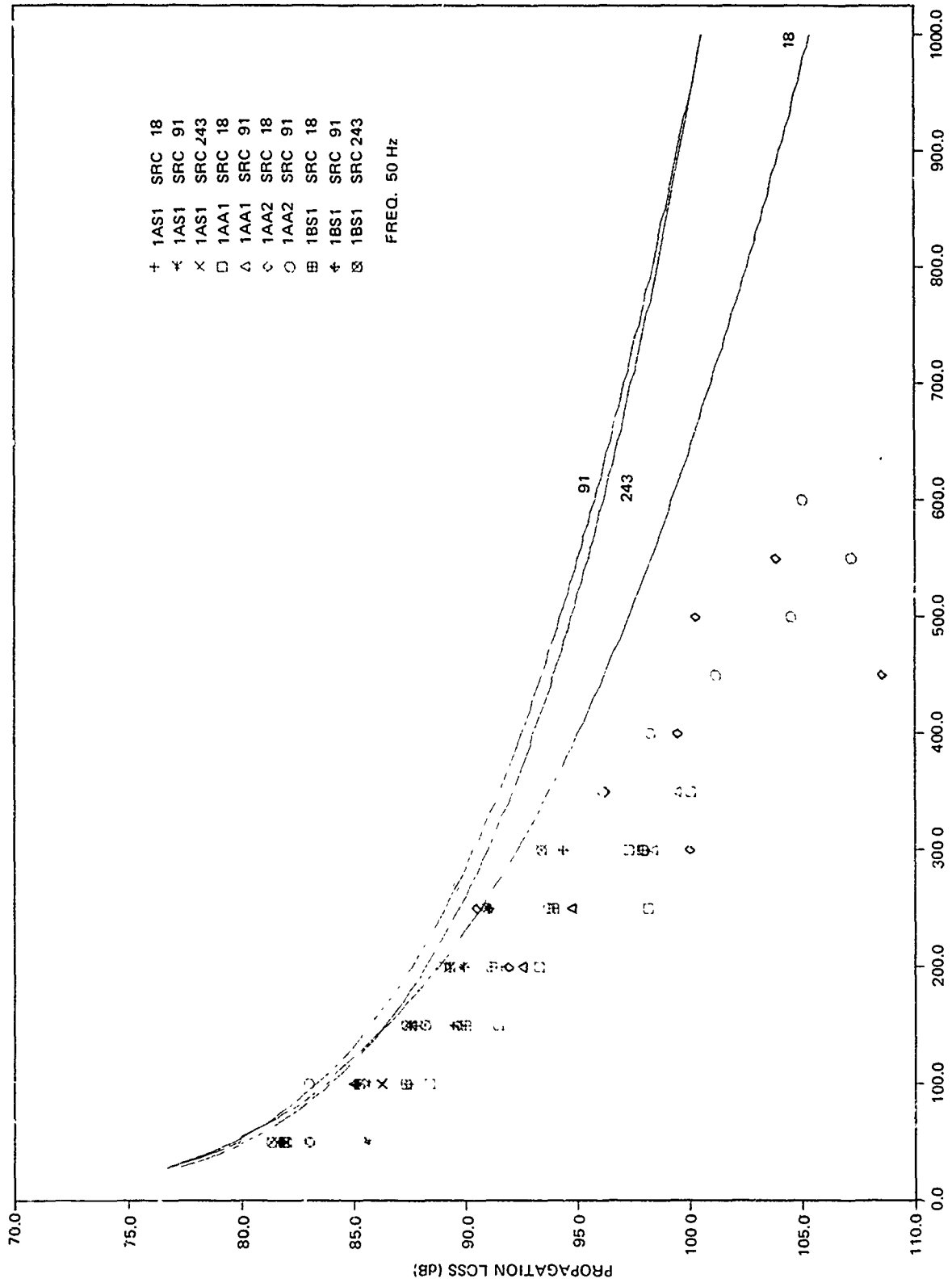

Figure 31. (C) Comparison of experimental propagation loss results from SUS data for 50 Hz at Site 1B with propagation losses from the normal mode model. (C)

Table 13. (C) The average difference between theoretical and experimental propagation losses for SUS events at Site 1. Standard errors of the mean are also shown. (U)

Frequency:	20Hz			50Hz		
Sus Depth (m):	18	91	243	18	91	243
Theory Minus Experiment:	−1.8	1.4	4.3	−2.8	−2.3	−1.6
Standard Error:	0.2	0.4	0.3	0.3	0.3	0.1

range bins. The negative values for 50 Hz are evident from figure 31, where almost all the experimental results lie below the theoretical curves. The results suggest that the source levels used to convert the 50-Hz data to propagation loss may be from 1.6 to 2.8 dB too high, depending on source depth.

(C) The behavior at 20 Hz is somewhat more complicated. Here the source levels for the 18-m shots appear to be 1.8 dB too high, whereas those for 91 m and 243 m appear to be, respectively, 1.4 and 4.3 dB too low. The differences in table 13 may not necessarily all be due to source level errors. Other effects which produce a systematic bias can also be contribute. However, table 13 indicates that systematic biases do occur and it is suggested that shot source levels should be subjected to further examination. An earlier section of this report summarizing the experimental differences between 91- and 243-m data demonstrates conclusively that the source levels used for SUS data are in error.

(C) Some salient features of the theoretical curves in figures 30 and 31 deserve mentioning. Note that the theoretical propagation loss for the 91-m source depth is less than that for the 243-m source depth. At first, the result was viewed with some alarm for it had been anticipated that the 243-m source depth would have the smaller loss (a deeper source would have rays with lower grazing angles at the bottom and hence lower losses). This theoretical result is explained in part by figure 32 for a fixed receiver depth. This figure presents propagation loss versus source depth for a receiver on the ocean bottom. In all cases the source depth with smallest propagation loss also occurs on the ocean bottom. Thus, this property obeys the previous rule of thumb that the lowest propagation loss generally occurs when source and receiver are at the same depth. A somewhat more surprising result is that the optimum source depth above the axis occurs at the surface decoupling depth; i.e., at the depth of the first (shallowest) antinode for the dominant arrivals. This optimum depth takes advantage of the reinforcement of arrivals which occurs when they are in phase somewhat below the ocean surface. The 25-Hz frequency of figure 32 lies between the 20- and 50-Hz cases of figures 30 and 31. Nonetheless, figure 32 indicates that the 91-m shots are closer to the decoupling depth and hence have lower propagation loss than the 243-m shots. Indeed, a source depth of about 45 m would be optimal for ranges of 50 to 200 km in figure 32.

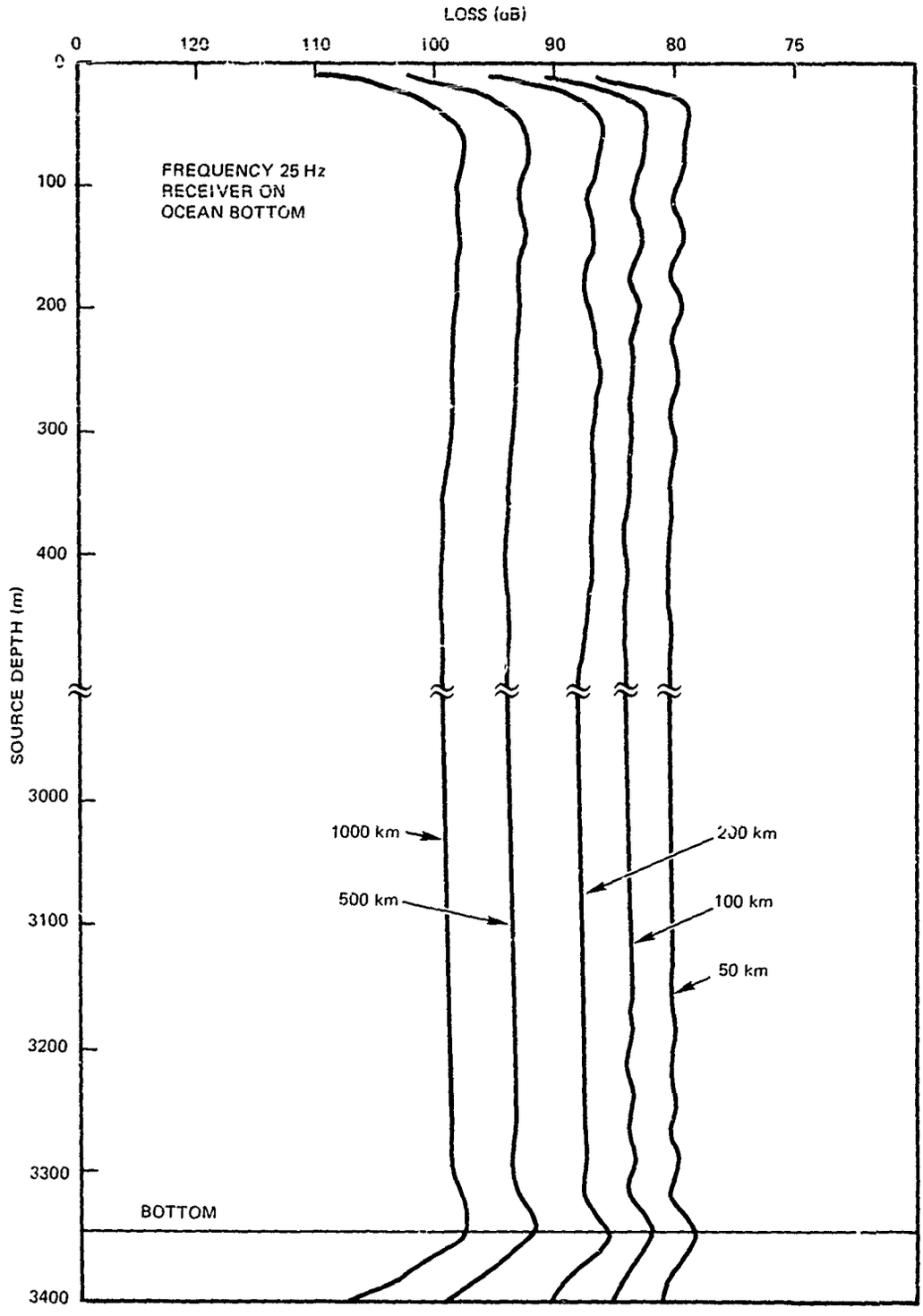

Figure 32. (C) Propagation loss versus source depth for a receiver on the ocean bottom. (U)

(C) Note also in figure 30 that the 18-m curve diverges from the 91- and 243-m curves with opening range. This effect is typical of most of the experimental data for BEARING STAKE. At short ranges, the steeper-angle arrivals dominate and there is less surface decoupling effect for an 18-m source depth. Thus, at short ranges the 18-m results lie closer to the 91- and 243-m depths, which are below the surface decoupling region. At longer ranges, the steep-angle arrivals are stripped out by the bottom and the dominant arrivals are low-angle rays and have a greater decoupling loss. A similar effect is noted in figure 31. The effect is much smaller because at 50 Hz the decoupling loss at 18 m is minimal.

(C) As for the source depths used for the low-frequency projector tow runs in BEARING STAKE, the nominal tow depth of 91 m (300 ft) for the CW source was a good choice. Figure 32 shows that variation in source depth was not critical for most depths deeper than 50 m. The source log recorded aboard the tow ship indicated the source depth varied from 77 to 102 m during the exercise. It is only at Site 4 that the exact CW source depth could be critical because of near-bottom limiting conditions. The predicted insensitivity of source depth allows us to directly compare CW results for different site and event without having to consider the fact that the source depth of the low-frequency CW source was variable.

(U) Thus, good agreement between experiment and theory has been shown for receiver depth dependence (tables 8 and 9) Comparisons between experimental and theoretical dependence on range and source depth were found in agreement, subject to possible changes in source level. The remaining task is to examine the data for evidence of the high-propagation-loss "notch" which appears off the ocean bottom as shown in figure 32 and was discussed earlier in this report.

(C) The notch represents a critical interaction between both source and receiver depth and frequency. There were only two receiver depths which could provide data – WECo BMA receiver 2, at Site 1A, which is 100 m off the bottom, and ACODAC receiver 10, at Site 1B, which was 30 m off the bottom. The WECo receiver was close to the notch of figure 16 for 25 Hz, at 91-m source depth. Unfortunately, WECo only processed this receiver for shots at 50 Hz. However, the ACODAC receiver was ideally situated in the notch of figure 14 for 25 Hz at 18-m source depth. Unfortunately, there were problems with the experimental data set. The bottomed ACODAC could not be processed for shots because of instrumentation considerations, and the shots available from the other ACODAC receivers were very sparse because much of the shot data had to be rejected because of overloads.

(C) Figures 33, 34, and 35 for 20, 25, and 50 Hz, respectively, represent our best effort at treating the ACODAC data for event 1BS1 at Site 1B. These plots present the difference in propagation loss between 18- and 91-m shots as a function of range. The curves represent the normal mode results for the three ACODAC receivers. The experimental data were obtained by p^2 averaging, in 50-km bins, the data that were not overloaded for each source depth, and then plotting the difference between the 18- and 91-m averages. Since the theoretical values were so close for ACODAC 2 at 496-m depth and ACODAC 6 at 1685-m depth, the experimental data were lumped and plotted as circles in figures 33, 34, and 35. Whereas the quality of the data leaves something to be desired, a definite pattern emerges when we consider further differences which take into account the offsets in the data.

(C) These differences are summarized in table 14. The second column represents the average difference between the normal mode results of ACODAC 10 and the average

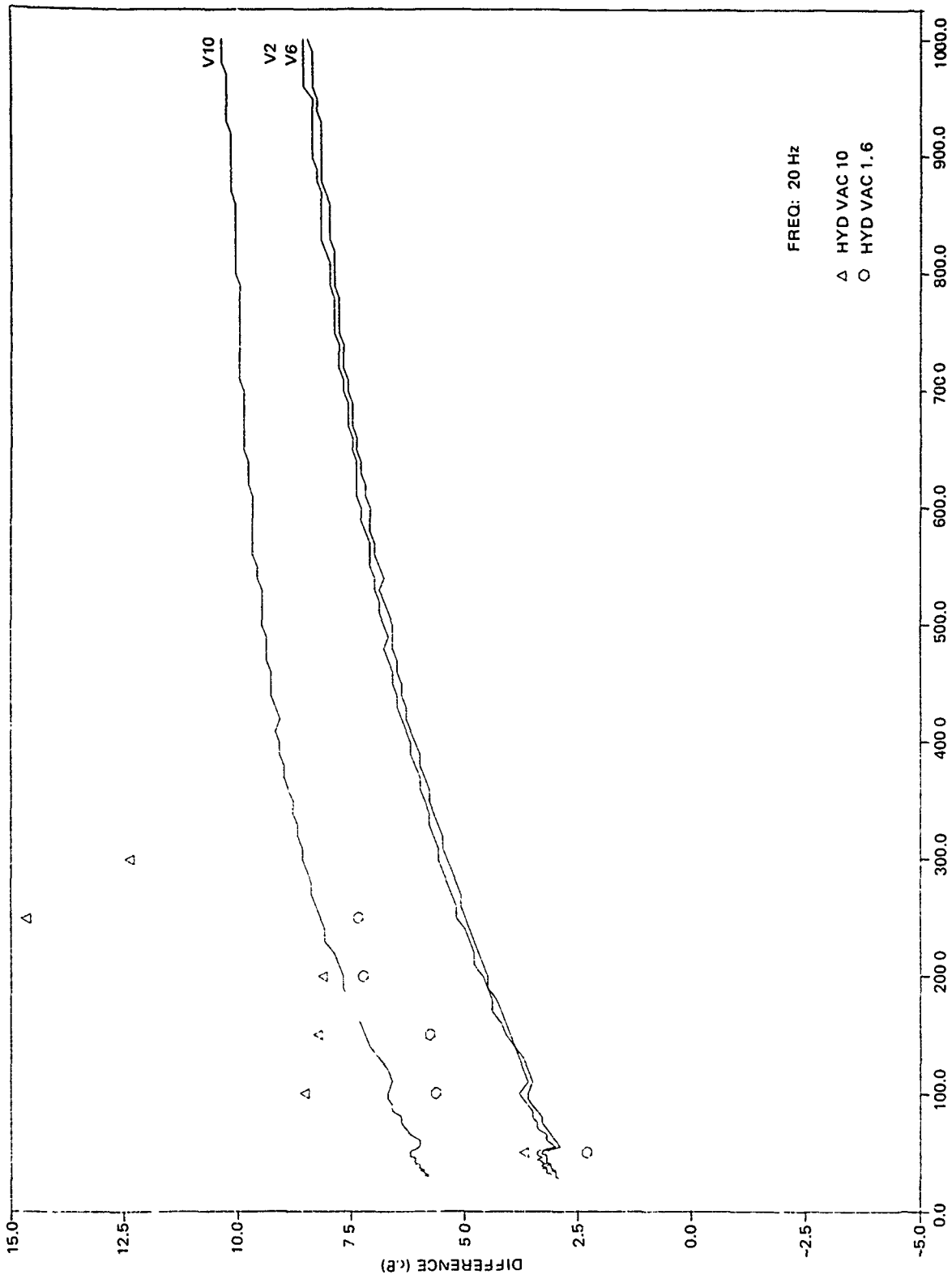

Figure 33. (C) Difference in propagation loss at 20 Hz between the 18-m SUS depth and the 91-m SUS depth as a function of range. The curves represent the normal mode results for the three ACODAC receivers. (C)

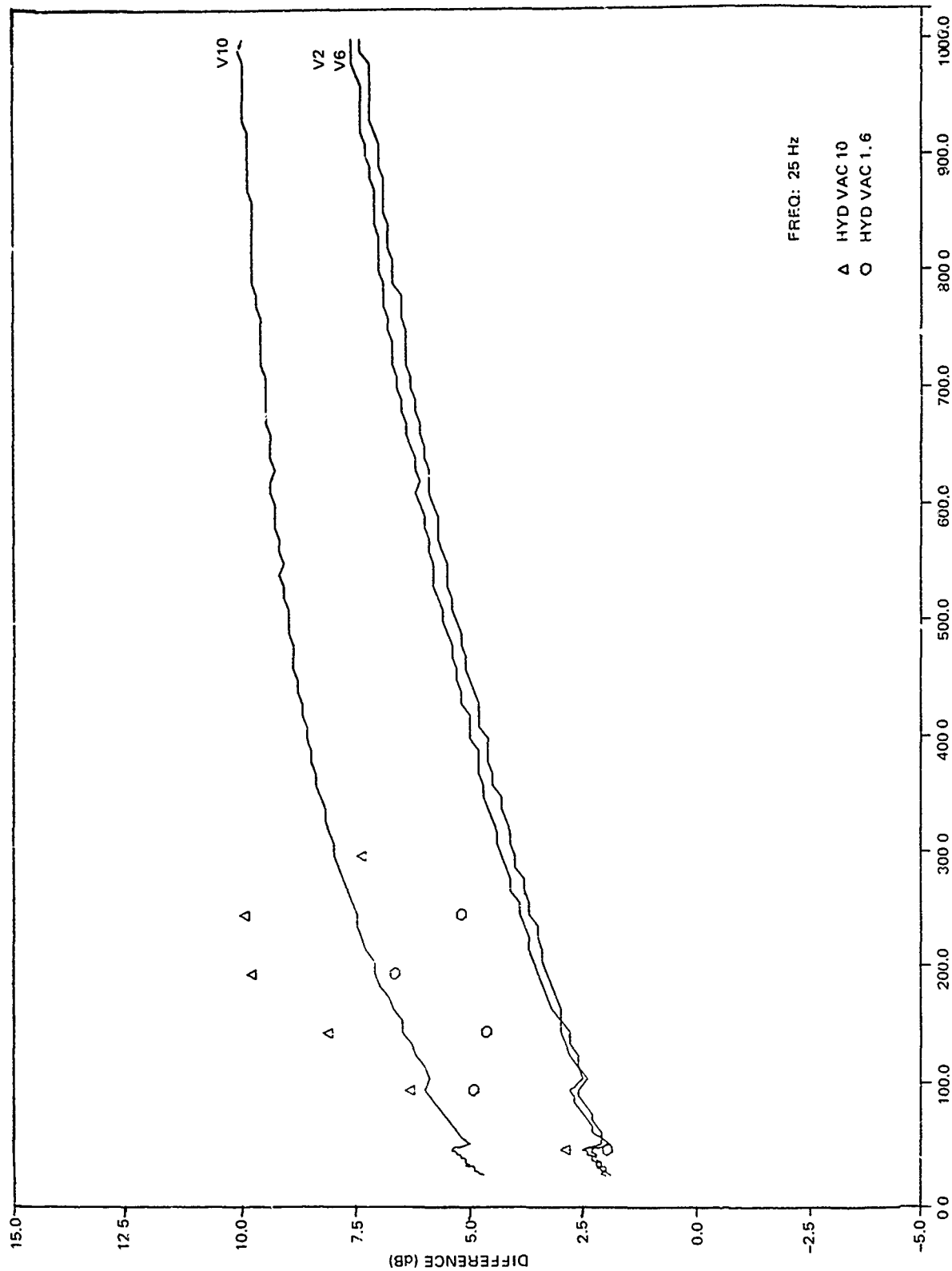

Figure 34. (C) Difference in propagation loss at 25 Hz between the 18-m SUS depth and the 91-m SUS depth as a function of range. The curves represent the normal mode results for the three ACODAC receivers. (C)

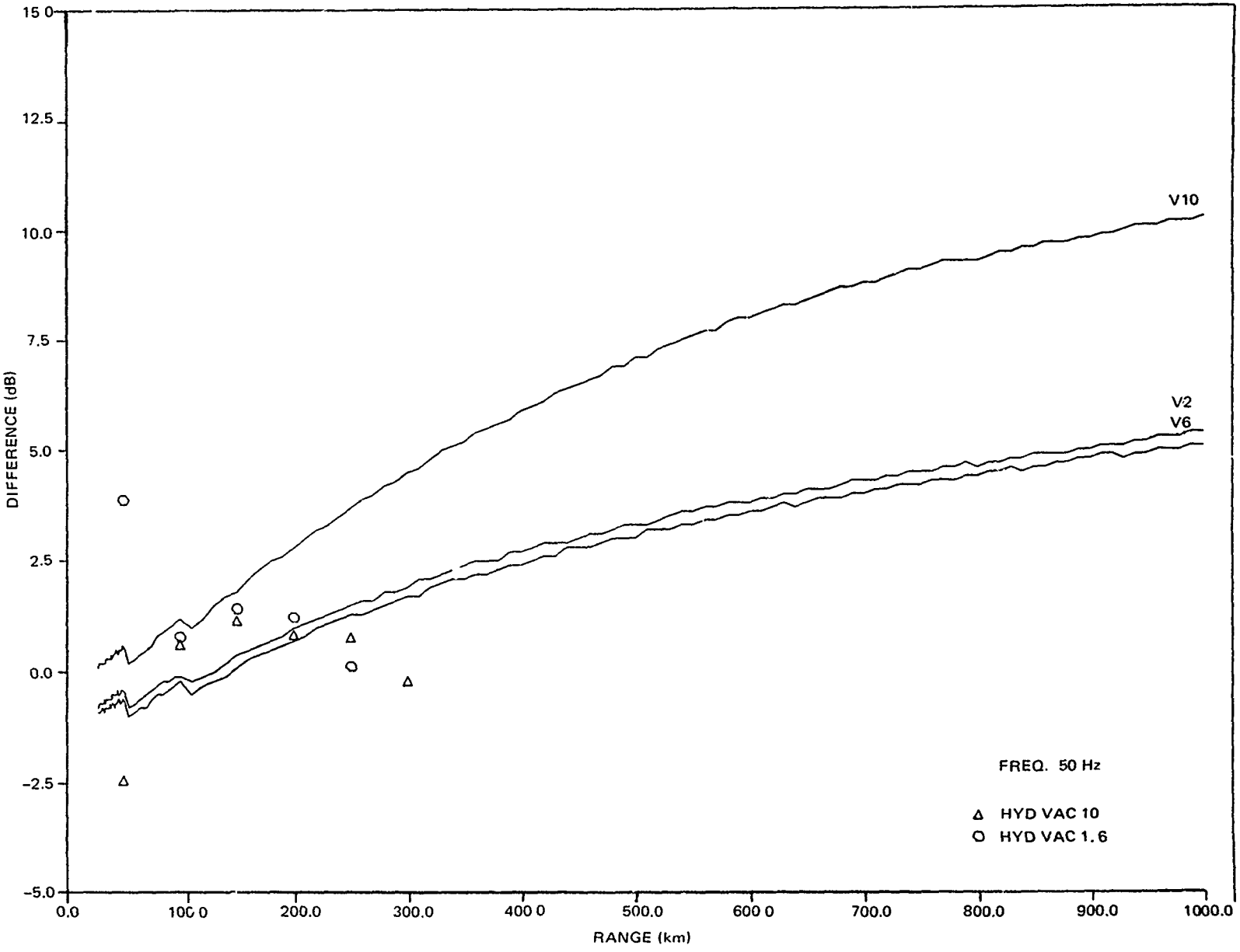

Figure 35. (C) Difference in propagation loss at 50 Hz between the 18-m SUS depth and the 91-m SUS depth as a function of range. The curves represent the normal mode results for the three ACODAC receivers. (C)

Table 14. (C) Average difference between the normal mode results of ACODAC 10 and the average of ACODACs 2 and 6 for both theory and experimental results. Also shown is the standard error for each case. (U)

Frequency (Hz)	Theory		Experimental	
	Average Diff	Standard Error	Average Diff	Standard Error
20	3.0	0.1	2.0	0.9
25	3.5	0.3	2.7	1.6
50	1.8	0.3	−0.2	0.2

of ACODACs 2 and 6 for ranges out to 250 km. Values of the standard error of this mean are also given as the second row of data for each frequency. The third column of table 14 is the experimental counterpart of the second column. In calculating these differences, the data points at 250 km in figure 33 and at 50 km in figure 35 were rejected for being too far out of line with the remaining data. Comparison between theory and experiment is fair at 20 and 25 Hz and poor at 50 Hz. The experimental data do show that the differences in propagation loss for the two source depths are indeed larger for receiver 10.

(C) The absolute values of the experimental data do not agree well with the theory. This is most likely due to relative errors in shot source levels. If the shot levels were adjusted according to table 13, the experimental values of figure 33 and 35 would be reduced by 3.2 and 0.5 dB, respectively. This adjustment does not markedly improve the agreement between theory and experiment. The necessity for rejecting overloaded data subjects the remaining data to a bias which is difficult to assess.

(C) Despite various difficulties, the data of figures 33 and 34, while not definitive, are certainly encouraging enough to recommend that the "notch" phenomenon be investigated further theoretically and that experiments be designed to specifically test it.

3.7 (U) QUESTIONABLE DATA SETS

(U) There were six data sets from Site 1 whose validity was questionable.

Event 1AP2 (U)

(U) The data set for this event was radically out of line (propagation loss was about 10 dB too high) with other data at Site 1A. A comparison with the WECo data report (ref 8) indicated that the original WECo data were correct, but that some error was introduced in preparing the data tapes which NOSC received from WECo. This data set was not included, therefore, in this report.

Event 1AP5 (U)

(U) The data set for this event at Site 1A was rejected as anomalous and not included in the analysis of this report.

Event 1BP2 (U)

(C) The data furnished to NOSC for this event at Site 1B gave an incorrect maximum range of 263 km, whereas the range should have been 131 km. This error was uncovered by noting that the propagation loss for the originally furnished data appeared much too low compared to that of other Site 1B events. The reason was that the ranges attributed to the data were too large by a factor of two After the ranges were corrected, the data fell into line with the other Site 1B data.

Event 1BS1, 1AS1, and 1AP7 (U)

(C) As previously discussed, the ACODAC data at 290 Hz at Site 1B appear suspect for three events and must be investigated further before being accepted as correct. The 140- and 290-Hz levels for the 91-m shots in event 1BS1 and the 140-Hz levels in event 1AP7 are definitely in error by about 2 dB. The 243 m shot data at 290 Hz for events 1BS1 and 1AS1 are possibly in error by about 2 dB. The 243-m shot data at 290 Hz for events 1BS1 and 1AS1 are possibly in error by about 1 dB. The 290-Hz data for event 1AP7 are possibly in error by about −1 dB.

3.8 (U) SITE 1 SUMMARY

(C) Site 1, which was occupied at two separate times during BEARING STAKE, was located at the mouth of the Gulf of Oman in the Oman Basin. Propagation losses were lowest along the floor of the basin in an east-west direction and somewhat higher losses occurred in the southern portion of the basin where the bottom shallows The largest measured losses occurred to the north of the site toward the continental rise.

(C) Minimum propagation losses at Site 1 over the range interval 50 to 250 km were 77.5 to 83.7 dB at 25 Hz, 82.5 to 89.8 dB at 140 Hz, and 82.6 to 92.6 dB at 290 Hz.

(C) At Site 1 average propagation losses were virtually independent of source depth for sources and receivers more than a few wavelengths away from the surface or bottom. An interference effect, producing a source-depth and frequency-dependent near-bottom propagation loss maximum ("notch"), was theoretically indicated and supported by the data. If confirmed, such a propagation loss depth dependence could be used to optimize SNR by selection of height off the bottom for near-bottom receivers.

(C) In the comparisons of propagation losses at Site 1 with the familiar Eleuthera reference curve, the propagation losses at 25 Hz were 6 to 12 dB less than those of the reference at ranges of 50 to 250 km. The propagation losses at 140 and 290 Hz were comparable to those of the reference at corresponding ranges.

(C) Good agreement was found between the experimental results and normal mode predictions of propagation loss for Site 1 at 25 and 50 Hz.

3.9 (U) RECOMMENDATIONS

(C) This section presents recommendations for additional processing of WECo BMA data which were recorded during BEARING STAKE but have not been processed. The basic WECo data collected at all sites consisted of analog tape recordings for eight receivers. However, the volume of data processed was generally limited to seven combinations of receiver depth and frequency for the SUS events and five to eight combinations for projector (CW) events. For example, the data processed for a typical SUS event consisted of 20, 50, 140, and 300 Hz for one receiver depth, and 50 Hz for three other depths. The typical CW event might consist of three receivers at 25 and 140 Hz and two receivers at 290 Hz, or four receivers at 25 Hz and two receivers at 140 and 290 Hz. For Site 1A as few as five combinations were processed and six or seven combinations were processed on occasion at other sites.

(C) At Site 4, two processing passes were made for most events. Four 7-combinations were processed for the SUS events, and one 8-combination and one 7-combination were processed for the CW events. The two processing passes at Site 4 were very helpful in exhibiting the complicated receiver depth-frequency dependence which was encountered at Site 4.

(C) With the exception of Site 4, at most only one-third of the available data was processed by WECo for CW events and an even smaller fraction for SUS events. Additional data should be processed to fill in gaps in existing processed data and to verify whether the existing data is erroneous or anomalous.

(C) At Site 1A, there were two suspended receivers used to collect data – receiver 1 about 500 m off the bottom and receiver 2 about 100 m off the bottom. For CW events, receiver 1 was processed at low frequencies while receiver 2 was not processed at all. For the SUS events, these two receivers were processed only at 50 Hz. Site 1A was the only site at which BMA receivers were suspended above a flat bottom. Hence, it is strongly recommended that for all CW events at Site 1A, an eight-channel data set be processed to include receiver 2 at 25, 140, and 290 Hz, receivers 1 and 8 at 140 and 290 Hz, and receiver 3 at 140 Hz.

(C) For all SUS events, it is recommended that WECo process a seven-channel data set to include receivers 1 and 2 at 20, 140, and 300 Hz and receiver 8 at 20 Hz. The low-frequency data for both CW and SUS events are particularly important because they could provide evidence for the propagation loss "notch" predicted by theory near the ocean bottom. The high-frequency data for receivers 1 and 2 are important because such data from suspended receivers were scarce for BEARING STAKE.

(C) The final recomendation for Site 1 is that NOSC be provided with a correct set of the already processed data for events 1AP2 and 1AP6. The data which NOSC was provided for event 1AP2 differed by as much as 10 dB from the corresponding data in the WECo data report, and data from event 1AP6 have never been provided to NOSC.

4.0 (U) SITE 2 ASSESSMENT

4.1 (U) INTRODUCTION

(C) Site 2 was located on a north-to-south extended ridge, called the Owen Fracture Zone, approximately 370.4 km (200 nmi) off the coast of the Arabian Peninsula. The crest of the ridge was at a depth of 1880 m and the bottom sloped downward to the Arabian Basin (4100-m depth) to the east and to a lesser depth (3200-m depth) to the west. Hydrophones of the bottom-mounted array (BMA) were positioned on the sides of the ridge so that various receiver depths were available. Figure 36 shows position and depth of the BMA hydrophones used to measure propagation loss.

(U) Figure 37 shows the direction of the various source runs that were made at the site by the source ship and aircraft SUS drops.

(C) A sound speed profile representative of the profiles that were taken at various ranges from the BMA at Site 2 is shown in figure 38. Site 2 had the highest surface sound speed of the five BEARING STAKE sites and was the most severely bottom-limited area for near-surface sources.

(C) A summary of the measured propagation loss data from the BMA at Site 2 from the CW and SUS runs is shown in table 15. The table shows which of the frequencies (at specified source depths) were received by one or more of the BMA hydrophones. The receiving hydrophone that was used to measure propagation loss at all the selected frequencies was hydrophone 3, which was at 3162-m depth.

(C) The key to propagation characteristics at Site 2 is intimately connected with the bathymetry at the site. The receivers were draped over the Owen ridge (see fig 36), which bounds the western edge of the Indus Fan. The close-range bathymetric profiles differ considerably for the various events because of the changing aspects of propagation paths to the ridge.

(U) In assessing the propagation losses in this section, the close range bathymetry for each event and its effect on propagation loss are discussed. The dependence of propagation loss on receiver depth, events conducted, range, and frequency at Site 2 is then assessed and conclusions drawn from the analyses are given.

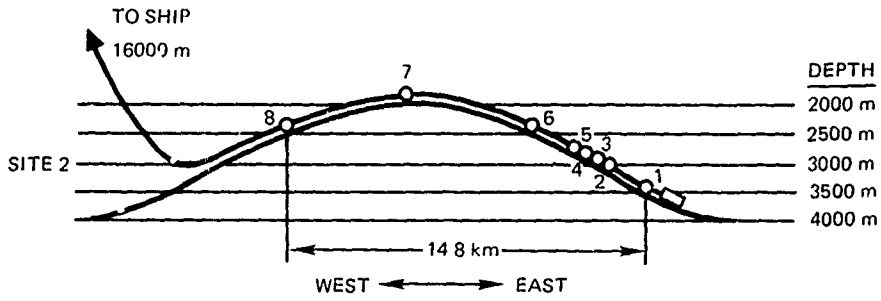

Figure 36 (U) Configuration of the BMA at Site 2. (U)

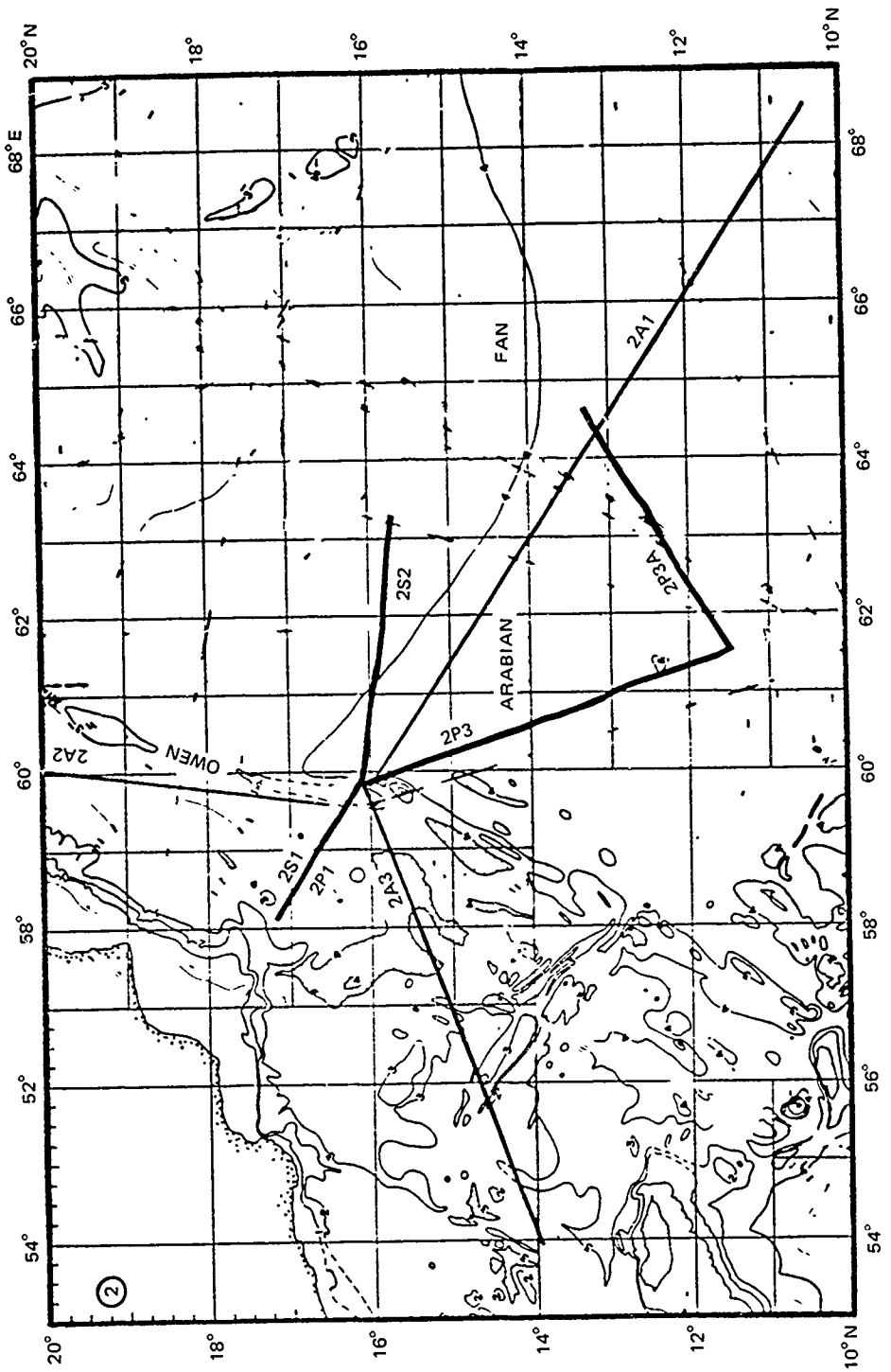

Figure 37. (C) Direction of the various events conducted at Site 2 by source ship and aircraft. (U)

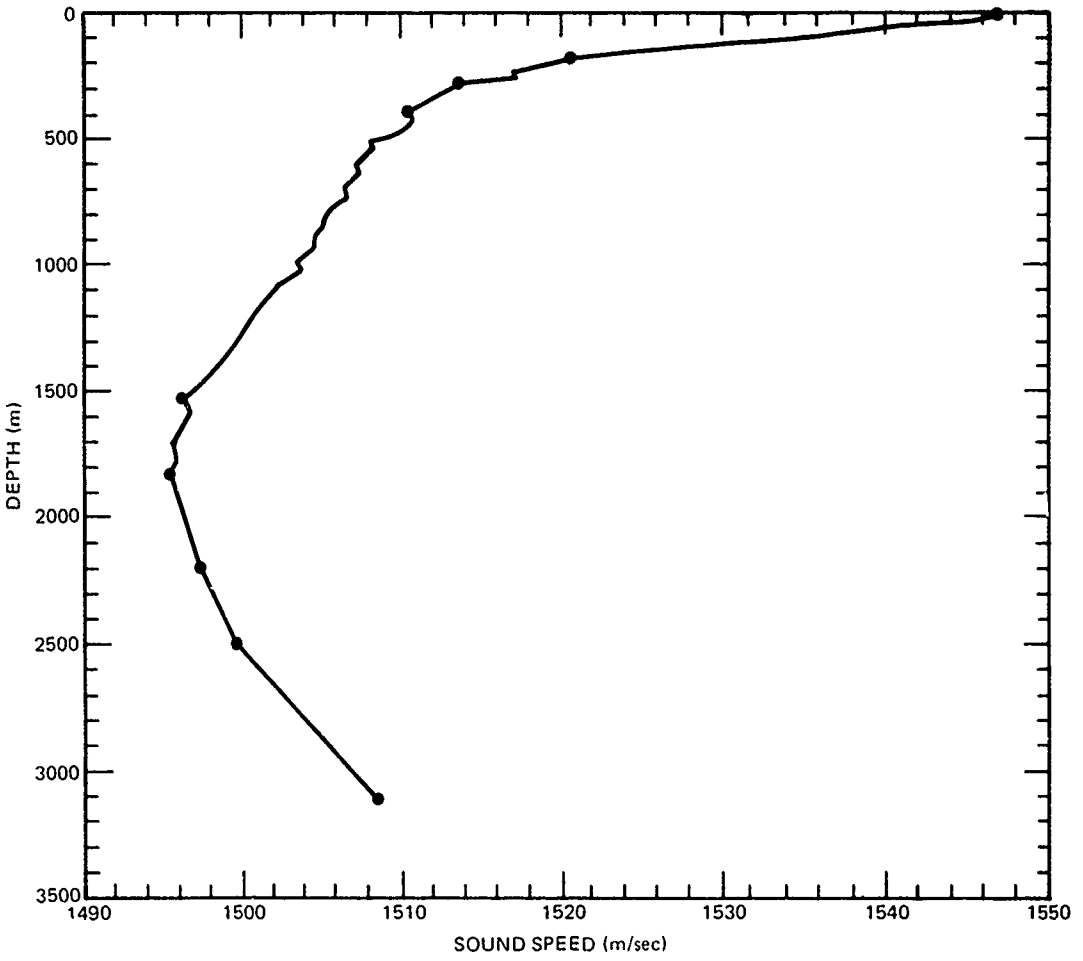

Figure 38 (U) Representative sound speed profile for Site 2. (U)

4.2 (U) CLOSE RANGE BATHYMETRY FOR EVENTS

(C) Figure 39 presents the close range bathymetry for event 2S2, which extended out over the Indus Fan in an easterly direction from the receivers. The direction of this event ran almost normal to the ridge. The eastern edge of the ridge is a steep scarp which intersects the Indus Fan at a depth of 4000 m. The slope of the scarp is about 16°. This event crossed the Indus Fan with a slight upslope of less than 0.5°. (For the long range bathymetry of this event, and others to follow, refer to appendix A.) The separation between BMA receivers 1 and 8 is about 13 km. The depths of the receivers are given in table 16.

Table 15. (C) Summary of the propagation loss data set from the BMA collected at Site 2 from the projector (P) and SUS runs. (U)

BMA Hydrophone No. / Depth (m)		1 / 3453	3 / 3162	6 / 2563	7 / 2111
Freq (Hz)	Source Depth (m)				
Run 2P1: 9-222 km					
25	88	X	X	X	X
140	18		X		
290	18		X		
Run 2P3: 544-9 km					
25	88	X	X	X	X
140	18		X		X
290	18		X		
*Run 251, 252, 2A1, 2A2, 2A3					
20			X		X
50			X		X
140			X		X
290			X		

These were SUS runs. SUS depths were 18, 91, and 243 m for ship runs (S) and only 18 and 91 m for aircraft runs (A).

*Run No	Range (km)
251	224-0
252	23-372
2A1	66-1093
2A2	837-24
2A3	676-41

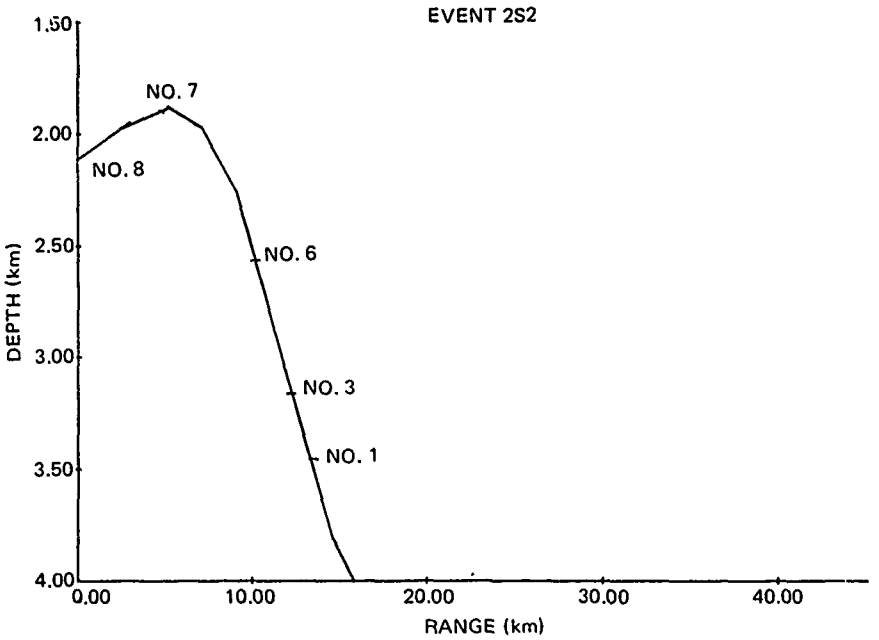

Figure 39. (U) Close range bathymetry for event 2S2. (U)

(U) Figure 40 shows the close range bathymetry for event 2A1. The bathymetry for this event was similar to that of event 2S2 – flat to long ranges with no obstructions.

(C) Figure 41 shows the close range bathymetry for event 2P3. The near range profiles change for each receiver because the event geometry was normal to the line of BMA receivers. (In events 2S2 and 2A1, the runs were almost parallel to the line of receivers.) The long range bathymetry is almost flat but crosses a minor feature at 375 km and a major feature at 450 km which rises 750 m above the fan floor.

(C) Figure 42 presents the close range bathymetry for events 2P1 and 2S1, which were almost perpendicular to the ridge and ran in a northwesterly direction. The maximum slope in this direction is about 4°. The deepest point along the event is 3700 m. There was a small ridge near the end of the event at a range of 210 km.

(C) Figure 43 presents the close range bathymetry for event 2A3, which is essentially the same for receivers 1, 3, and 5 but changes slightly for 7 and 8. The long range bathymetry drops to 4-km depth between 100 and 275 km and then crosses a jumble of prominent features which rise to about 2-km depth.

(C) Figure 44 shows the close range bathymetry for event 2A2, which proved to be too complicated to be of any value for modeling purposes. The event parallels the ridge and each close range bathymetric cut changes drastically with range. The long range bathymetry of this event shown in figure A-5, appendix A, is for receiver 7. The long range bathymetry is shown to be not as rugged for this event as for event 2A3 only because this event crosses regions where the general features of the area are not well established.

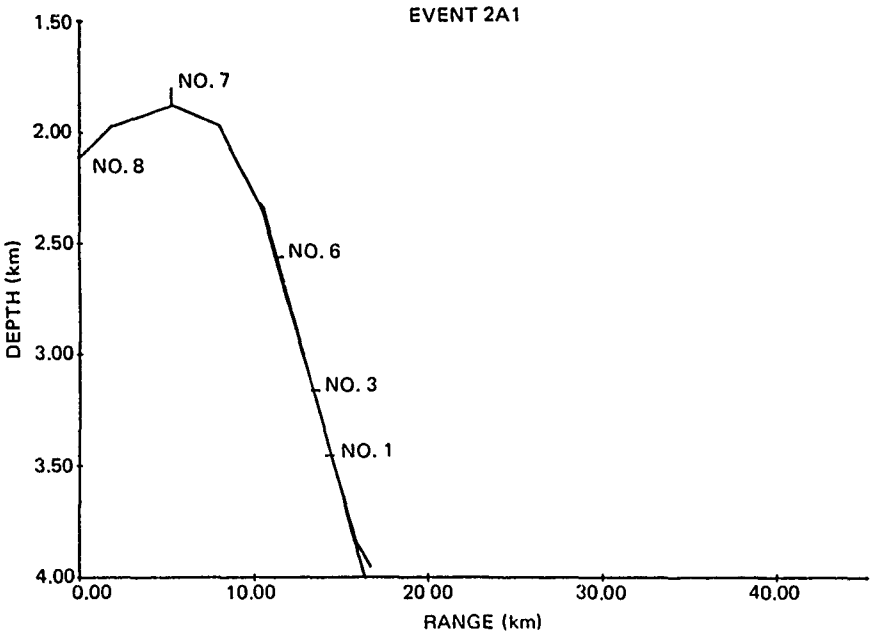

Figure 40. (U) Close range bathymetry for event 2A1. (U)

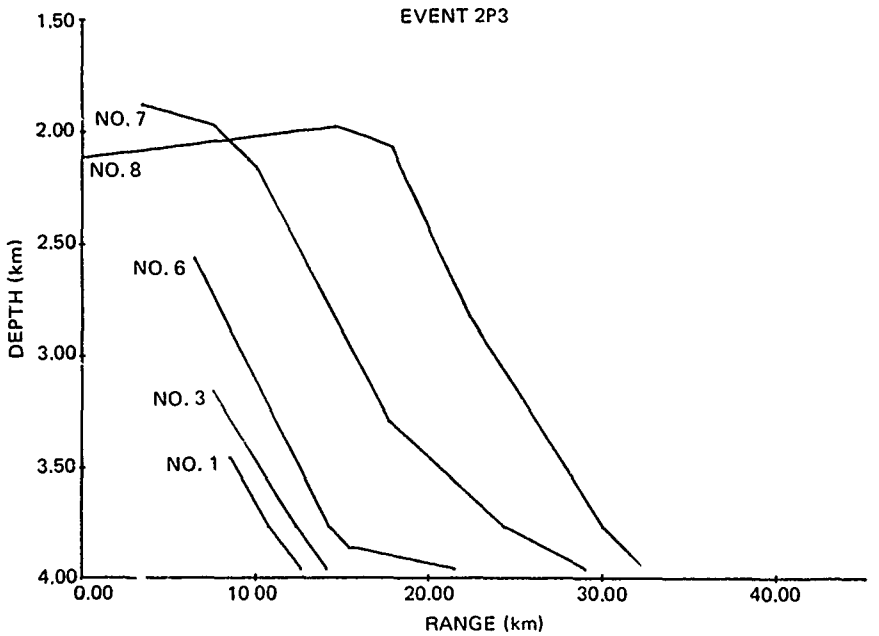

Figure 41. (U) Close range bathymetry for event 2P3. (U)

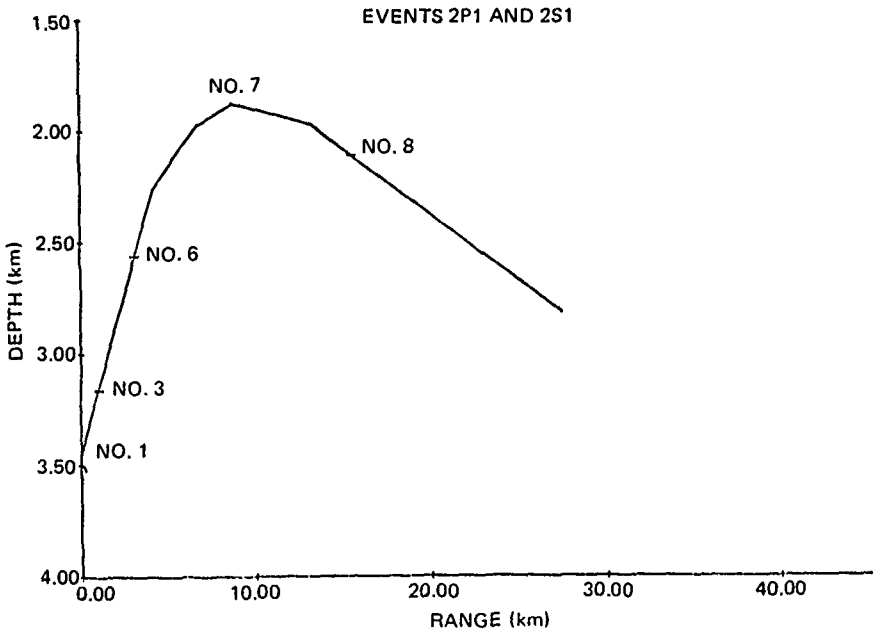

Figure 42. (U) Close range bathymetry for events 2P1 and 2S1. (U)

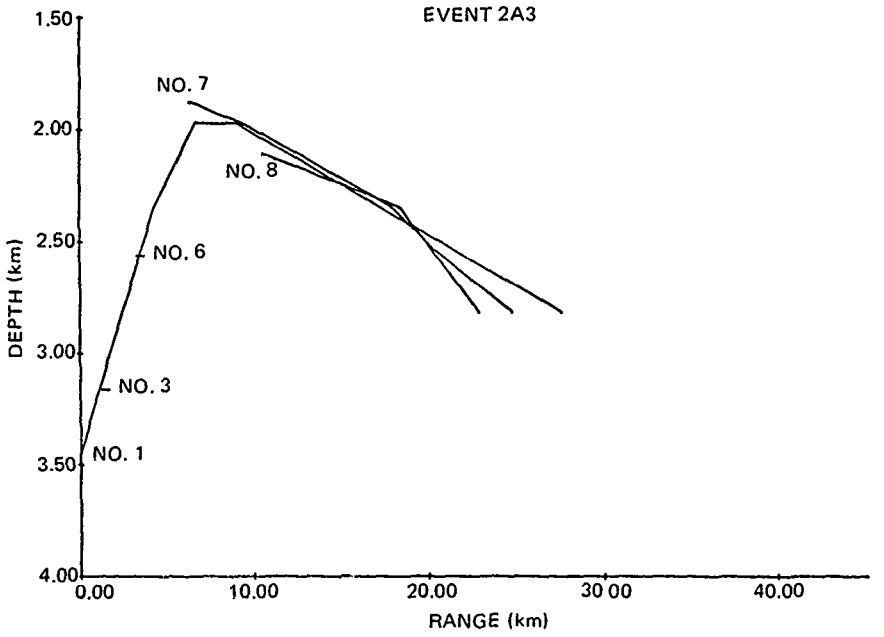

Figure 43. (U) Close range bathymetry for event 2A3. (U)

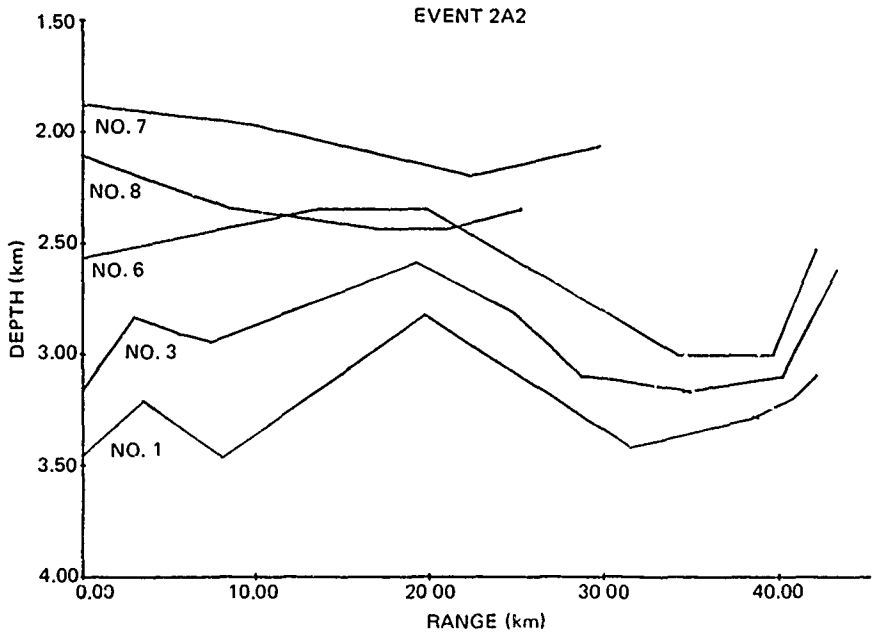

Figure 44. (U) Close range bathymetry for event 2A2. (U)

4.3 (U) DEPENDENCE ON RECEIVER DEPTH

(C) Receiver depth dependence for the CW and SUS events is given in tables 16 and 17, respectively. The results at 25 Hz for event 2P1 appear to be reasonable for propagation conditions from the westerly direction at Site 2. The lowest loss occurs at receiver 8 as expected, since the receiver is on the western slope of the Owen Ridge (see fig 36), facing the source. The propagation loss generally increases over the ridge and down the steep scarp. However, it is not clear why the loss should be higher for receiver 3 than for receiver 1, as receiver 1 is further down the scarp. The loss for receiver 7, which is on top of the ridge, is less than that for receiver 3 for the CW events as well as the SUS events, as shown in table 17 for events 2S1 and 2A3. Again, this is to be expected for propagation from west of the ridge.

(C) The results at 25 Hz for event 2P3 in table 16 appear reasonable for propagation from the southeast direction to the receivers. The propagation losses were, in general, larger for event 2P3 than for event 2P1 because 2P3 required longer propagation traverses up the slope of the ridge. It is not known at the present time why receivers 3 and 6 should have lower loss than 1. The results at 140 Hz for event 2P3 were as expected.

(C) The results for events 2S2 and 2A1 in table 17 are generally as expected for propagation up the scarp of the ridge. The losses for receiver 3 were less than for 7 in 11 out of 15 possible cases. However, it is somewhat puzzling why the differences at 140 Hz for event 2A1 are so much smaller than those for event 2S2 when it is considered that their bathymetric profiles are so similar (see fig 39 and 40).

(C) The results for event 2A2 in table 17 show that there is very little difference between the losses for receivers 3 and 7 This is probably related to the fact that the event ran parallel to the ridge and the propagation paths apparently do not favor one receiver over the other.

Table 16. (C) Propagation loss differences between the BMA receiver with lowest propagation loss and other BMA receivers for Site 2 CW events. (U)

BMA Receiver Number	Receiver Depth (m)	Propagation Loss Diff. (dB)			
		Event 2P1		Event 2P3	
		25Hz	140Hz	25Hz	140Hz
1	3454	5.0	—	0.8	—
3	3162	7.6	5.8	0	0
6	2563	1.4	—	0.5	—
7	1880	1.1	0	1.2	7.2
8	2112	0	—	1.5	—

Table 17. (C) Propagation loss differences between BMA receivers 3 and 7 for the SUS events at Site 2. Zero indicates the receiver with lowest loss. (U)

Event	BMA Receiver Number	20Hz			50Hz			140Hz		
		SUS Depth (m)			SUS Depth (m)			SUS Depth (m)		
		18	91	243	18	91	243	18	91	243
251	3	4.1	4.8	5.5	4.8	4.6	7.0	5.5	3.2	5.5
	7	0	0	0	0	0	0	0	0	0
2A2	3	0.6	2.0	—	0	0	—	0	0.1	—
	7	0	0	—	1.8	0.8	—	0.3	0	—
2A3	3	5.6	5.5	—	7.3	7.6	—	4.2	5.0	—
	7	0	0	—	0	0	—	0	0	—
252	3	0	0.2	0	3.3	0	0	0	0	0
	7	0.4	0	2.9	0	2.1	2.9	5.6	8.4	5.7
2A1	3	0	1.3	—	0	0	—	0.5	0	—
	7	0.2	0	—	3.9	4.8	—	0	1.3	—

4.4 (U) ERROR ANALYSIS OF DATA SETS

(U) This section is limited to Site 2. It illustrates how eight similar data sets were treated to detect and correct errors in two of them. Although this discussion concerns correcting a particularly critical data set, it illustrates a powerful technique which may be used to exploit similar experimental data sets which were collected on BEARING STAKE. This discussion is presented now rather than later, since the assessment of Site 2 data, which follows, considers the results of this error analysis in reaching conclusions. The results of this error analysis do not affect significantly the conclusions reached in the preceding section on Receiver Depth Dependence.

(C) In the analysis of the BEARING STAKE data, comparison of events with lowest propagation losses indicated that the 50-Hz data for event 2A1 at Site 2 for BMA receiver 3 for the 91-m shot depth were significantly in error. An indication that an error existed was found in examining figure 216 of the WECo data report (ref 8). The figure showed that the propagation losses at 20 and 50 Hz for event 2A1 were almost the same. This situation did not make any sense from a physical standpoint. It was also completely different from other comparisons of 20- and 50-Hz BEARING STAKE data, which show a significant difference.

(U) Since the error concerned event 2A1 at Site 2, a critical event, it was most important to correct the error before any further assessment of Site 2 was made. The approach to determining the error was based on comparisons with similar data. Events 2A1 and 2S1 were selected for comparison since they had very similar bathymetry and would have a similar behavior with respect to hydrophone depth and frequency. The data for six range bins from 100 to 300 km were used for this analysis. BMA receivers 3 and 7 at 20 and 50 Hz were used for each event; thus, eight data sets.

(C) The first step was to calculate the average difference in propagation loss for the 50- and 20-Hz data in the two events over the available range interval. Values obtained for events 2S2 and 2A1 for receiver 7 at 50 and 20 Hz were both 6.3 dB. Thus, there is verification that the four sets of receiver 7 data were consistent and that events 2S2 and 2A1 had a similar frequency dependence.

(C) The next step was to calculate the difference for receiver 3, at 50 and 20 Hz, for the same two events. Values obtained for events 2S2 and 2A1 were 4.2 and 0.3 dB, respectively. However, it was not clear at this juncture whether the data for 50 Hz, 20 Hz, or both were in error.

(C) In order to pinpoint the error, the average difference in propagation loss was calculated between receivers 7 and 3. The values obtained for events 2S1 were −0.5 and 1.7 dB for 20 and 50 Hz, respectively. Corresponding values for event 2A1 were −1.6 and 4.5 dB. Assuming that the values for event 2S1 are correct and the dependence on receiver depth is the same for the two events, it is seen that the propagation loss for receiver 3 should be decreased by 1.1 dB at 20 Hz and increased by 2.8 dB at 50 Hz.

(C) The correction for the 50-Hz data is the one of most interest in this report. The correction brings the Site 2 data into substantial agreement with the data from other sites. Several means were used to check the corrections for consistency. When the corrections are applied to the difference in propagation loss between 50 and 20 Hz for event 2A1, receiver 3,

the value 0.3 + 2.8 + 1.1 = 4.2 dB is obtained, which is indeed equal to the value for event 2S1. (This does not "prove" the corrections – it merely indicates that the arithmetic is correct.

(C) These corrections also tie in with some of the discrepancies of table 17 for event 2A1 for the 91-m shots. The value for receiver 3 becomes 0.2 dB at 20 Hz and the value for receiver 7 becomes 2.0 dB at 50 Hz. These corrected values are now in substantial agreement with their counterparts in event 2S2. It should be remembered that the corrections were derived by equating these results for a subset of the 2S2 and 2A1 data. Hence, this near equivalence means that the entire set of 2S2 and 2A1 data was brought into agreement by corrections based on the subset.

(C) There are, undoubtedly, other similar data sets which could be subjected to comparisons such as discussed herein. However, the scope of the present report limits such a detailed investigation to only the critical data sets.

4.5 (U) DEPENDENCE ON EVENTS

(C) Figures 45, 46, 47, and 48 show the propagation loss for the receiver with the lowest loss for all events conducted at Site 2. There were five receiver depths to select from for events 2P1 and 2P3 at 25 Hz. At 290 Hz, only one receiver depth was used for all events. In all other cases, processed data were available from two receiver depths for this analysis. The events which ran over the Indus Fan (2A1, 2S2, and 2P3) are given line symbols in the four figures, whereas the events which ran west of the Owen Ridge are given open symbols.

(C) Table 18 ranks the events according to increasing propagation loss at each frequency. The most significant feature of the table is the higher losses for those events conducted west of the ridge at 50, 140, and 300 Hz. This feature is also evident in figures 45, 46, 47, and 48, where the line symbols show less propagation loss than the open symbols. At 25 Hz, event 2P1 appears to be an exception in that it is an event conducted west of the ridge and yet has lower losses than events 2P3 and 2S2. This result suggests that the low-frequency bottom loss west of the ridge may not be a great deal larger than that east of the ridge. (Results from event 3A2 at Site 3 will support this conclusion later in this report.)

(C) A combination of circumstances complicated the overall ranking of the events at Site 2. Early in the data reduction stage of this assessment, WECo noted that there were problems with event 2S1. However, the analysis of the event at NOSC indicated that the 2S1 data were not seriously in error. In contrast, NOSC was convinced that the 2P1 data at 140 and 300 Hz were in error. (This belief is discussed in the next section on range and frequency dependence.) If the data for event 2P1 are disregarded, the overall ranking of the events is 2A1, 2S2, 2P3, 2S1, 2A3, and, finally, 2A2.

(C) The events conducted at Site 2 cannot be put into proper perspective without a comparison with the other BEARING STAKE sites. Although this comparison will be discussed in detail later, the results will be mentioned now. Consider, first, those events which ran west of the Owen Ridge – events 2A2 and 2A3. These events have higher propagation losses than the highest-loss event at any other site. Not only were the averaged propagation losses highest for event 2A2, it is clear from the SUS records that more values were below the noise level for this event than for any other BEARING STAKE event.

(C) Event 2S1 had higher losses than the highest-loss event at any site for 140 and 300 Hz. With the exception of one event, this is also true of event 2S1 for 20 and 50 Hz.

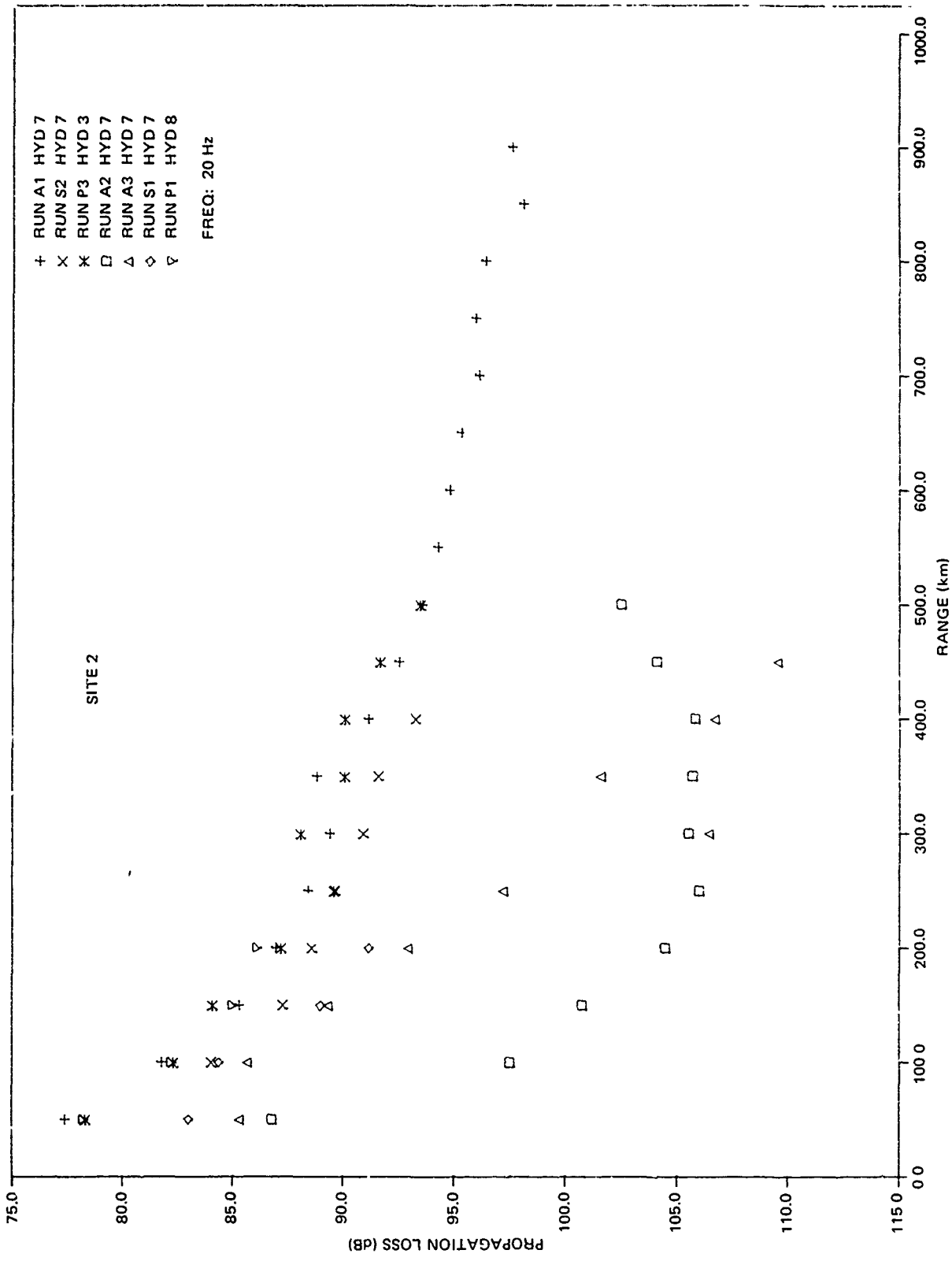

Figure 45. (C) Propagation loss at 20 Hz as a function of range for the receiver with the lowest propagation loss for events conducted at Site 2. (C)

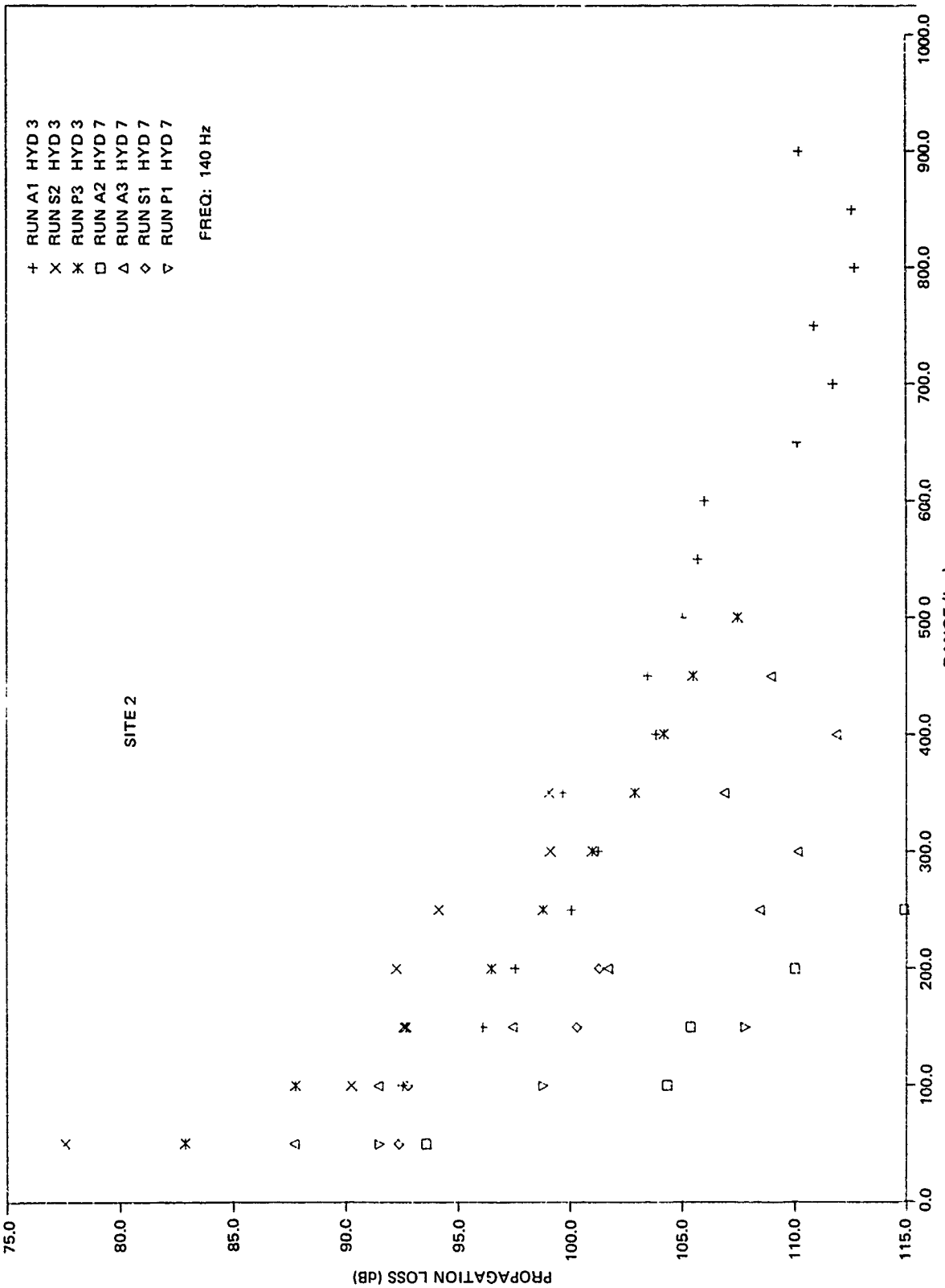

Figure 46. (C) Propagation loss at 140 Hz as a function of range for the receiver with the lowest propagation loss for events conducted at Site 2. (C)

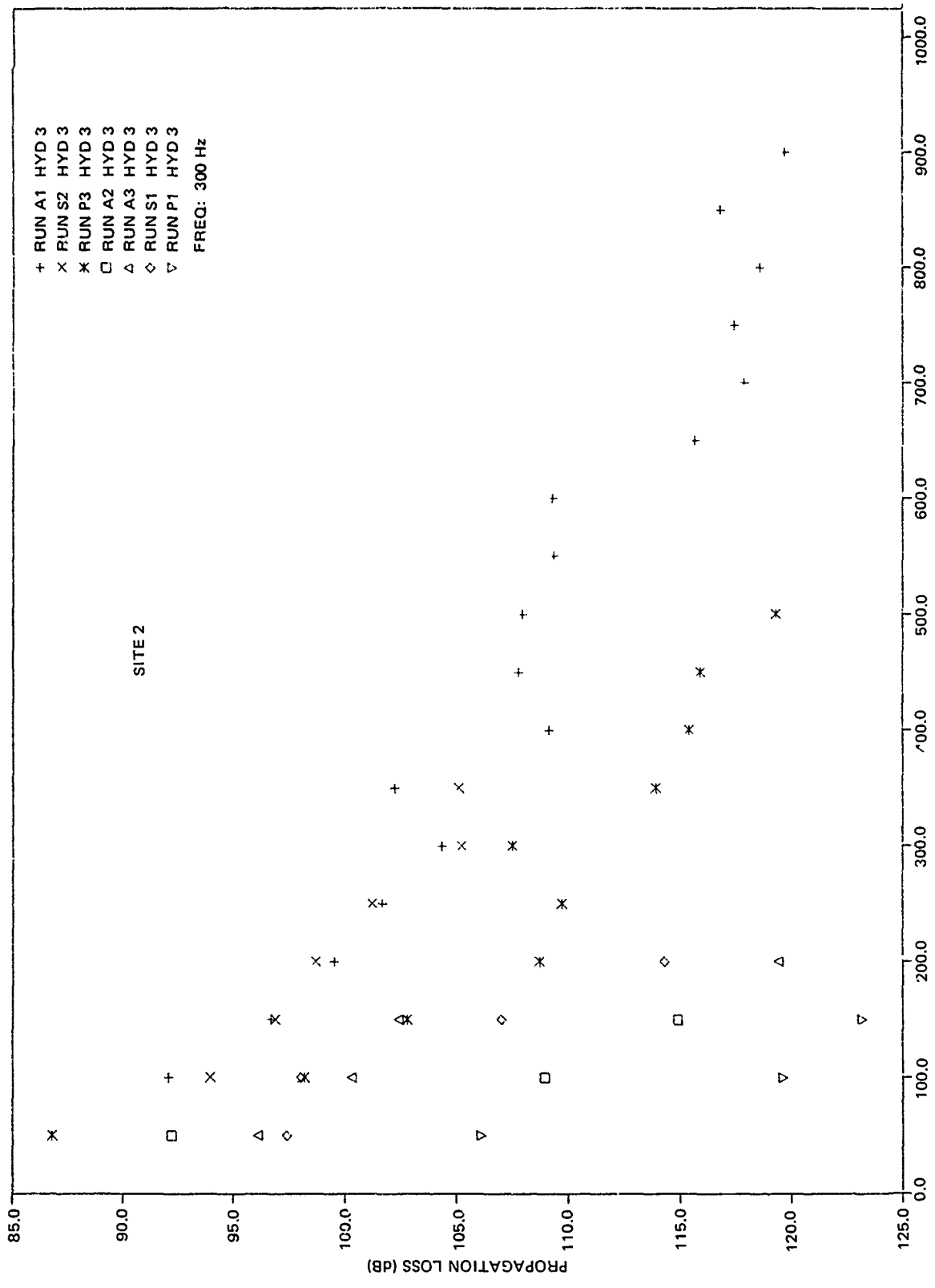

Figure 47. (C) Propagation loss at 300 Hz as a function of range for the receiver with the lowest propagation loss for events conducted at Site 2. (C)

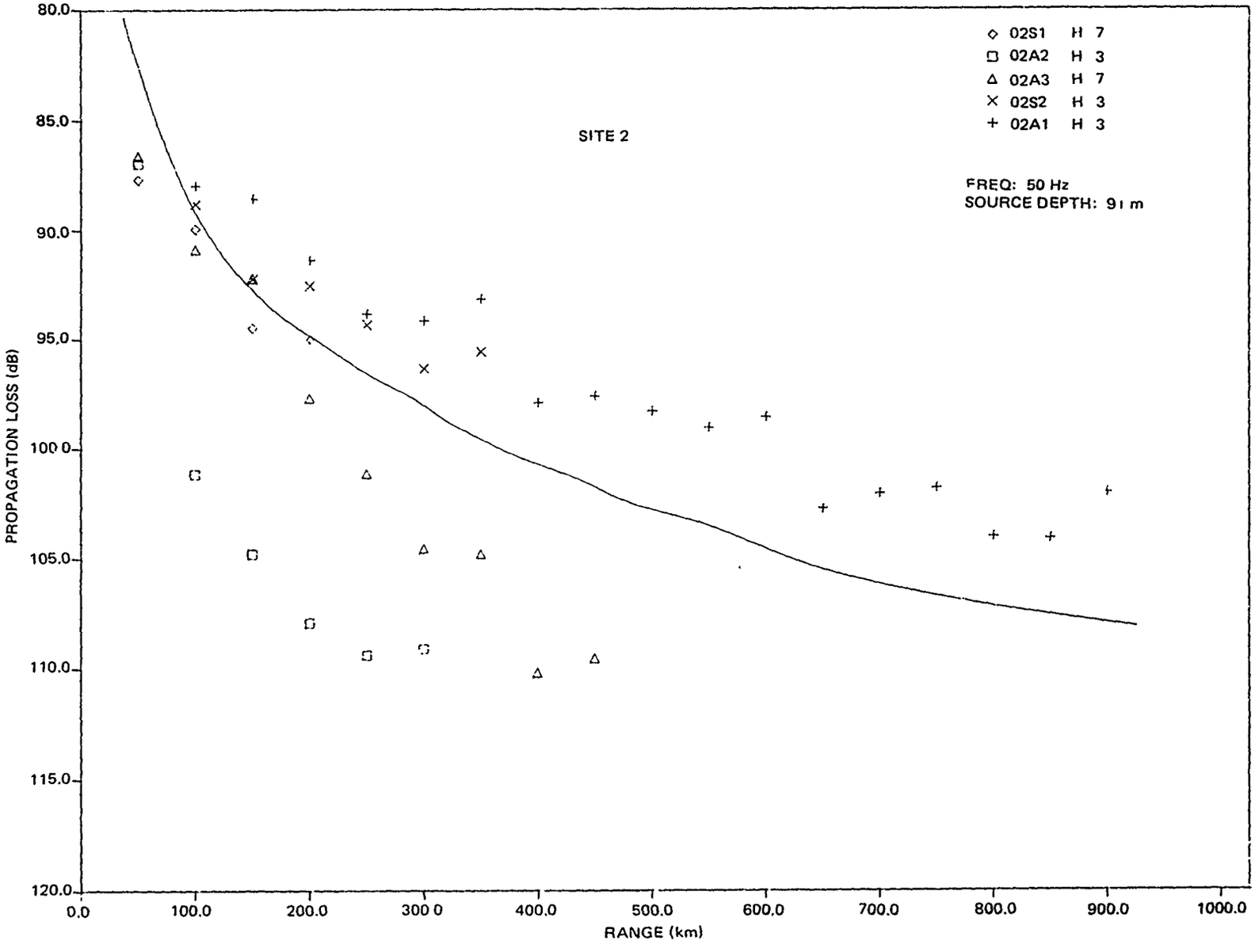

Figure 48. (C) Propagation loss at 50 Hz as a function of range for the receiver with the lowest propagation loss for SUS events conducted at Site 2. Also shown is the Eleuthera reference curve. (C)

CONFIDENTIAL

Table 18. (C) Ranking of events for Site 2. (U)

Rank	Events				Overall Ranking
	Low (20-40) Hz	140Hz	300Hz	50Hz	
1	2A1	2S2	2A1	2A1	2A1
2	2P1	2P3	2S2	2S2	2S2
3	2P3	2A1	2P3	2S1	2P3
4	2S2	2A3	2S1	2A3	2P1
5	2S1	2S1	2A3	2A2	2S1
6	2A3	2A2	2A2	—	2A3
7	2A2	2P1	2P1	—	2A2

High bottom loss contributed to the results for events 2S1, 2A2, and 2A3. In addition, event 2A3 had a very rugged long range bathymetry while event 2A2 had a very complicated short range bathymetry.

(C) Event 2P1, at 25 Hz, appears to be a rather good event. Of the total of 19 CW events for all the sites, event 2P1 had lower loss than 13.

(C) Although event 2P3 ran over the Indus Fan, it had high losses at 140 and 300 Hz. Of the 16 CW events at 290 to 300 Hz for BEARING STAKE, event 2P3 had higher losses than all but event 4P5 at Site 4. Of the 17 events at 140 Hz, event 2P3 had higher losses than all but event 4P5 at Site 4 and events 5P2 and 5P5 at Site 5. However, at 25 Hz, event 2P3 appears to be a fairly good CW event. Of the 17 CW events for all sites, event 2P3 had lower losses than 10.

(C) Based upon the comparisons discussed above, the overall conclusion that can be made with respect to Site 2 is that, of all the sites occupied in BEARING STAKE, this site suffered the most propagation loss.

4.6 (U) RANGE AND FREQUENCY DEPENDENCE

(C) To determine range and frequency dependence of the data at Site 2, the propagation loss for the events with lowest propagation loss at 20, 140, and 300 Hz was plotted as a function of range. Figure 49 shows the plotted results as well as the Eleuthera reference propagation loss curve for comparison purposes. The propagation loss values plotted in figure 49 are also given in table 19. The interesting feature of table 19 is that the events with the lowest propagation losses at the selected frequencies were SUS events rather than, as at the other four sites, CW events.

(C) The slope of the propagation losses at 20 and 140 Hz with range, as shown in figure 49, is comparable to the slope of the reference curve, whereas the slope of the 3000-Hz data is greater than that of the reference.

(C) The propagation losses at 20 Hz are as much as 10 dB below those of the reference beyond 250 m. The propagation losses for 140 Hz are generally less than those of the reference and the losses for 300 Hz are greater than those of the reference.

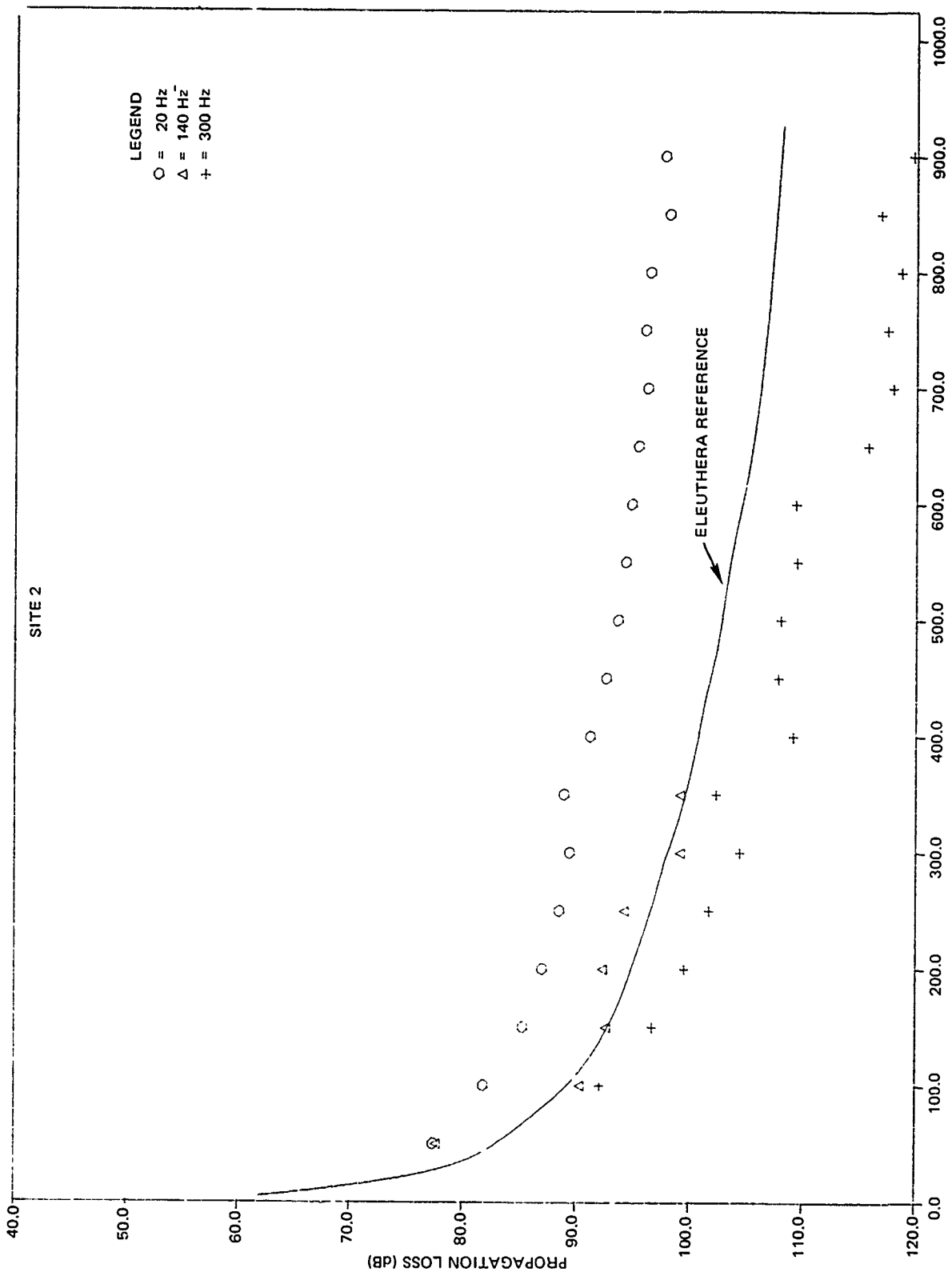

Figure 49. (C) Propagation loss at 20, 140, and 300 Hz as a function of range. Also shown is the Eleuthera reference curve. (C)

Table 19. (C) Propagation loss results of the best events at Site 2 for various frequencies. (U)

	Propagation Loss (dB)			
Range (km)	Event 2A1 20 Hz	Event 2S2 140 Hz	Event 2A1 300 Hz	Event 2A1* 50 Hz
100	81.8	96.3	92.1	87.9
150	85.3	92.6	96.7	88.5
200	87.0	92.3	99.5	91.4
250	88.5	94.2	101.7	93.8
300	89.4	99.1	104.4	94.1
350	88.9	99.1	102.3	93.2
400	91.2		109.1	97.9
450	92.6		107.8	97.6
500	93.6		108.0	98.3
550	94.3		109.4	99.0
600	94.8		109.3	98.6
650	95.4		115.7	102.7
700	96.2		117.9	102.1
750	96.0		117.4	101.8
800	96.4		118.6	104.0
850	98.1		116.8	104.1
900	97.7		119.7	102.0

*WECo values increased by 2.8 dB

(C) Propagation losses at 50 Hz as a function of range for the SUS event with the lowest propagation losses (event 2A1) are also listed in table 19 and plotted in figure 48 for comparison with the reference curve. The slope of the losses at 50 Hz is somewhat less than that of the reference, with losses ranging from 1 to 6 dB less than those of the reference.

(U) From figure 49 it is seen that propagation losses at Site 2 increase with increasing frequency and range.

4.7 (U) QUESTIONABLE DATA SETS

(C) The propagation losses for event 2P1 at Site 2 are incredibly high at 140 and 300 Hz. Events 2S1 and 2P1 essentially covered the same track, but the propagation loss differences for 140 and 300 Hz were 8 and 15.5 dB, respectively, between the two events; event 2P1 had the higher loss in each case. Moreover, event 2P1 losses were much higher than those of any other site. For example, the propagation loss for event 2P1 for 300 Hz at the 150-km range bin is 123 dB. Corresponding examples of the extreme losses at the same range bin are 93, 94, 98, 105, and 105 dB for Sites 1A, 1B, 3, 4, and 5, respectively. Thus, the event 2P1 data in question have 18 dB more loss than the data for any other CW event

at any site. Although the propagation losses for event 2P1 were expected to be high, a value of 18 dB is clearly excessive and, thus, questionable.

(C) Event 2P3 also had inexplicably high propagation losses for 140 and 300 Hz and should be regarded as questionable until further reprocessing by WECo.

4.8 (U) SITE 2 SUMMARY

(C) In summary, the propagation loss results measured for Site 2 indicate that this site had the highest losses of the five sites occupied. The minimum propagation losses measured at Site 2 for the range interval 100 to 900 km were 81.8 to 97.7 dB at 25 Hz, 87.9 to 102.0 dB at 50 Hz, and 92.1 to 119.7 dB at 300 Hz.

(C) The higher propagation losses for this bottom-limited site can be attributed to placement of the BMA receivers on the Owen Ridge. Propagation losses would have been lower if the receivers had been placed at the base of the ridge on the floor of the Indus Fan.

(U) Measured propagation losses to the west of the ridge were always larger than the losses to the east of the ridge.

(C) Comparisons of propagation losses at Site 2 with the Eleuthera reference curve show that the propagation losses at the lower frequencies (20 to 140 Hz) are less than those of the reference while the losses at 300 Hz are greater at comparable ranges.

4.9 (U) RECOMMENDATIONS FOR ADDITIONAL DATA PROCESSING

(C) One of the objectives of BEARING STAKE is to perform surveillance systems performance predictions based upon the results of the data collected at the various sites. To perform a system evaluation of Site 2, Bell Telephone Laboratories (BTL) selected BMA receiver 3 as the appropriate depth. Let us examine this choice from the standpoint of measured results.

(C) First, from tables 16 and 17, note that receiver 3 was not the best receiver for events 2P1, 2S1, and 2A3, and only the best in half of the cases for event 2A2. It is assumed, then, that BTL is not concerned with surveillance to the west of the Owen Ridge. Consider, next, the measured results for events 2P3, 2A1, and 2S2 which would be appropriate for surveillance to the east of Site 2. From table 16 it is seen that receiver 3 is indeed the best choice, by 0.5 dB, from five available receivers. Examination of the 10 available range bins on an individual basis shows that receivers 3 and 6 each had the lowest losses for four range bins and were the same in one range bin. (Receiver 8 was low for the remaining range bin.) This near-equal performance of receivers 3 and 6 strongly suggests that at low frequency (25 Hz), receiver 4 or 5 (4 and 5 were not processed) may be a better choice than receiver 3 or 6. At 290 Hz, receiver 3 was the only receiver processed.

(C) Therefore, on the basis of available data, receiver 3 is the best choice. However, there is still a good possibility that other receiver depths may be better. The possibility that receiver 4 or 5 may be better at 25 Hz has already been stated. Moreover, the dependence on receiver depth varies with frequency. Hence, there is skepticism that receiver 3 is the best receiver depth at 140 and 300 Hz.

(C) Although the assessment of Site 2 indicates that for best performance the receivers should be placed on the floor of the Indus Fan rather than anywhere on the ridge, it would still be of value to determine which was the optimum receiver available from the measurements. A complete set of measurements would also be of value in the evaluation of propagation conditions up a steep slope. For these reasons it is recommended that for event 3P3 data be processed for BMA receiver 5 at 25 Hz, receivers 1, 5, and 6 at 140 Hz, and receivers 1, 5, 6, and 7 at 300 Hz. For events 3A1 and 3S1 it is recommended that receiver 1 at 20, 50, 140, and 300 Hz and receiver 5 at 20, 50, and 140 Hz be processed.

(C) WECo did not process any data for event 3P3A at Site 2 because the event was designed for the ships towing the OAMS and LATA arrays. If data were recorded during this event, they should be processed. Such data would help to establish the boundary between bottom loss regimes on the Indus Fan. The data set to be processed would be the same as recommended for event 3P3.

5.0 (U) SITE 3 ASSESSMENT

5.1 (U) INTRODUCTION

(C) Site 3 was located in the middle of the Arabian Basin. The seafloor slopes gently to the south from the site depth of 3545 m. The configuration of the bottom-mounted array (BMA) to measure propagation loss is shown in figure 50. The directions of the nine propagation loss runs made at Site 3 are shown in figure 51. As can be seen from the figure, the measurements covered the Arabian Basin quite thoroughly. The runs to the north and northeast (3P1 and 3S1) encountered the shallow water of the Indus River fan-delta while runs 3A3 and 3A4 extended up to the continental rise of India.

(C) Figure 52 is a typical and representative sound speed profile of the measured profiles for the events conducted at Site 3. As can be seen from the profile, Site 3 was bottom limited throughout the operating area.

(C) Table 20 is a summary of the propagation loss data measured at Site 3 and analyzed for this report. The table shows, for each run at this site, the frequencies and the depths of both CW and SUS sources. Also shown are the depths of the receiving hydrophones of the BMA and the frequencies each hydrophone measured. The only hydrophone measuring all frequencies was hydrophone 6 which was at a depth of 3546 m.

(U) In this section, assessments are made on the effects on propagation loss at Site 3 of receiver depth, events conducted, range, and frequency.

5.2 (U) DEPENDENCE ON BMA RECEIVING HYDROPHONES

(C) Data were reduced for three BMA receivers mounted on the ocean floor. The range displacement between receivers 8 and 6 was about 550 m. The range displacement between receivers 1 and 6 was about 450 m. Corresponding depth displacements were 6 and 12 m. Comparisons of propagation loss were based on four CW events and a total of from 21 to 24 range bins. Receiver 8 had losses which were –0.5, 0.9, and –0.3 dB greater than those of receiver 6 at respective frequencies of 25, 140, and 290 Hz. Receiver 1 had losses which were 0.3 and 0.8 dB greater than those of receiver 6 at respective frequencies of 25 and 140 Hz. Student's t-test indicates that the two smallest absolute differences (0.3 dB) are not statistically significant whereas the larger differences are significant at better than the 95% level.

(C) Data were available for the two shot events, 3S1 and 3S2, at 50 Hz for four receivers mounted on the ocean floor. In addition to the receivers just discussed, data were available for receiver 2, which was located 380 m in range and 11 m in depth from receiver 6. Comparisons of propagation loss were made for data from 91- and 243-m depth shots for a total of 16 range bins. Receivers 8, 1, and 2 had losses which were, respectively, –0.2, 1.0, and 0.8 greater than those of receiver 6. The latter two differences are significant at better than the 95% level. It was noted, however, that receivers 1 and 2 were only about 70 m apart in range and 1 m apart in depth. The difference in loss between these two receivers was only 0.2 dB. This suggests that the larger differences in propagation loss for receiver 6 are indicative of real differences in the propagation environment for receivers 1 and 2.

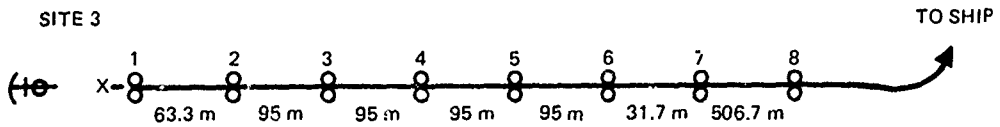

Figure 50. (U) Configuration of the BMA on the ocean floor at Site 3. (U)

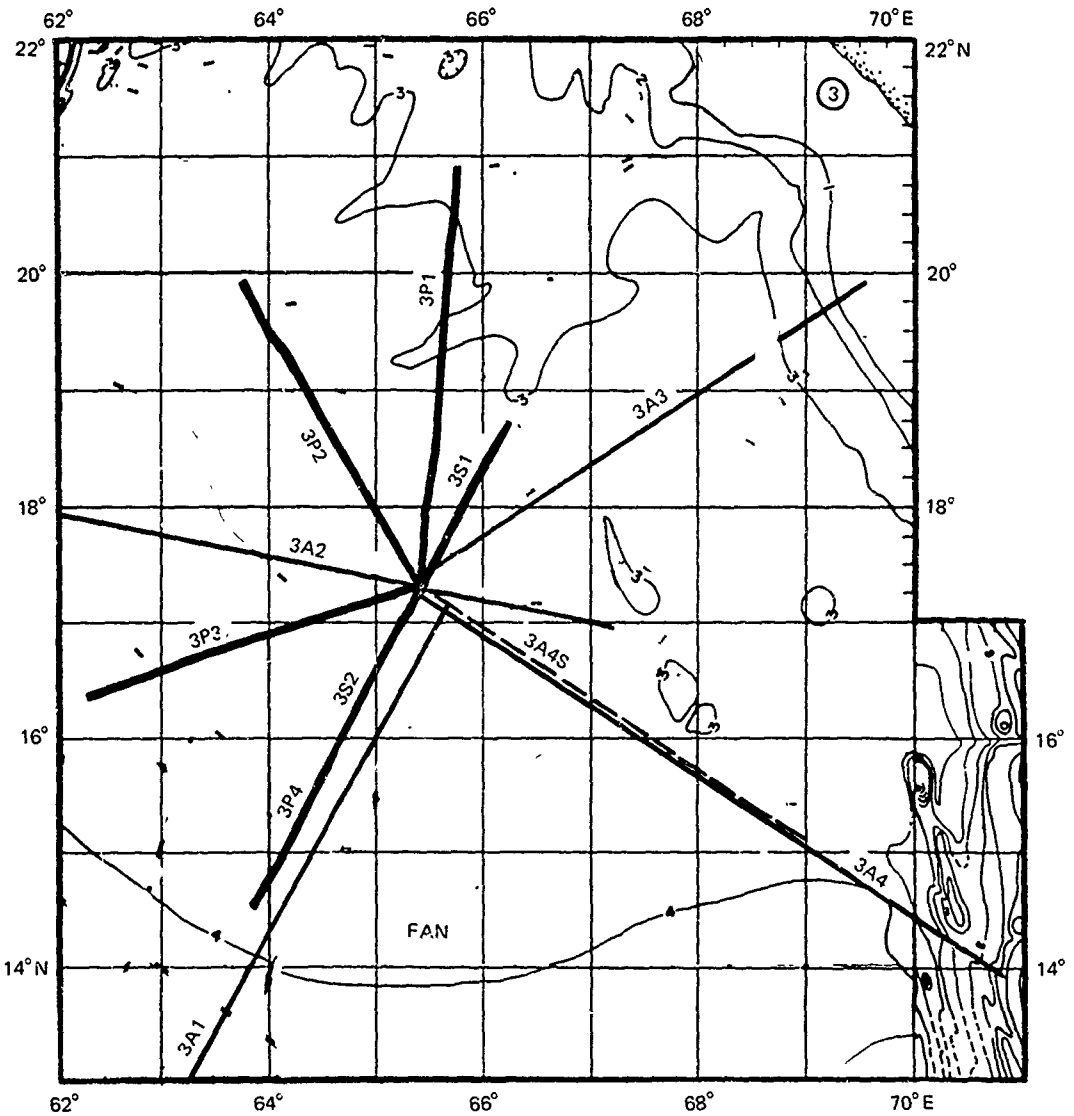

Figure 51. (C) Geometry of propagation loss runs conducted at Site 3 by source ship and aircraft. (U)

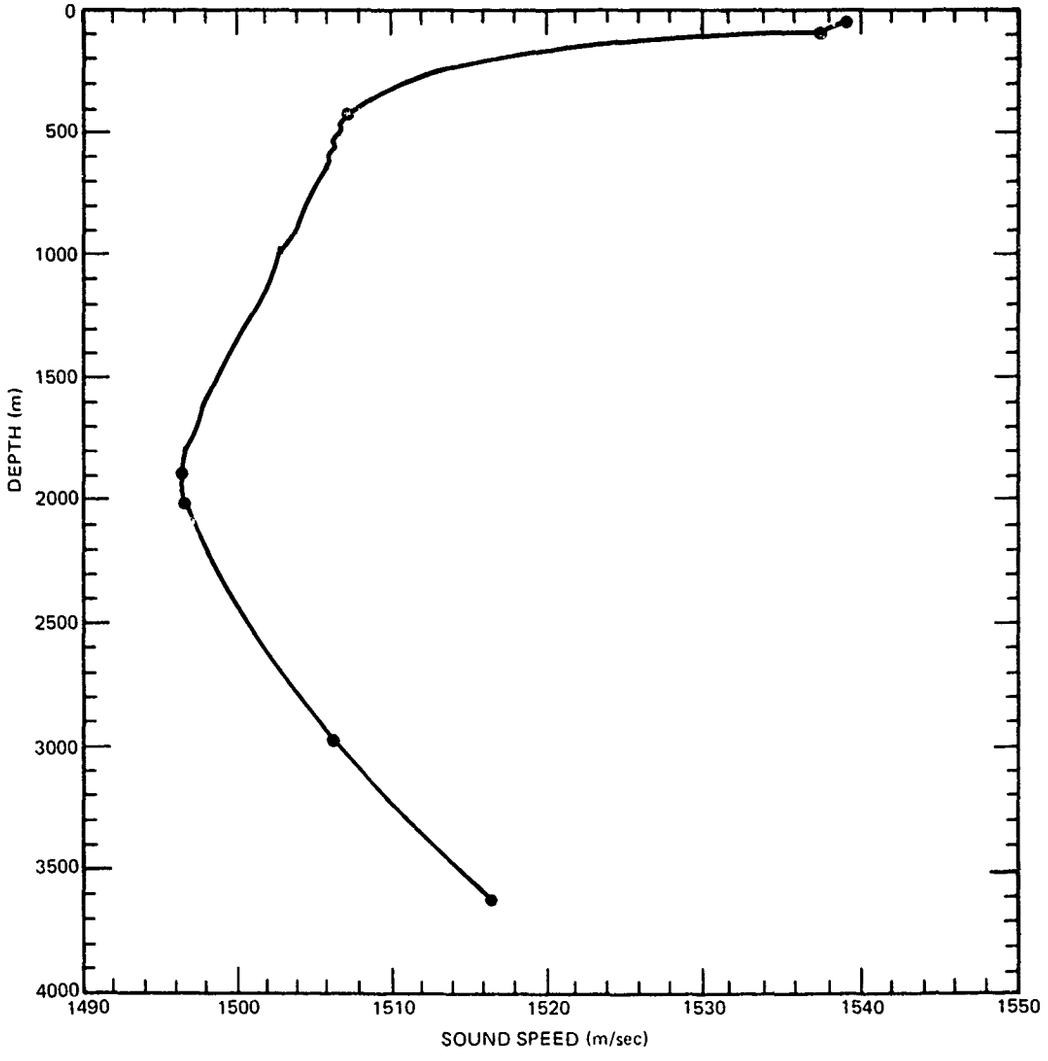

Figure 52. (U) Representative sound speed profile for Site 3. (U)

(U) Hence, it can be concluded that there was a statistical dependence on which BMA receiver was used at Site 3 to measure propagation loss in most cases.

5.3 (U) DEPENDENCE ON EVENTS

(C) Figures 53, 54, 55, and 56 present the propagation losses at 25, 140, 290, and 50 Hz, respectively, for all the events conducted at Site 3. Since all the receivers were on the ocean bottom, the propagation losses shown are averaged losses based on all the receivers that were processed.

Table 20. (C) Summary of the propagation loss data set from the BMA collected at Site 3 from the projector (P) and SUS runs. (U)

BMA Hydrophone No. / Depth (m)		1 / 3558	2 / 3556	6 / 3546	8 / 3539
Freq (Hz)	Source Depth (m)				
Run 3P1: 9-402 km					
25	82	X	X	X	
140	18	X	X	X	
290	18		X	X	
Run 3P2: 333-0 km					
36	81	X	X	X	
140	18	X	X	X	
290	18		X	X	
Run 3P3: 9-354 km					
42	84	X	X	X	
140	18			X	X
290	18			X	X
Run 3P4: 352-0 km					
25	77	X	X	X	
140	18	X	X	X	
290	18		X	X	
*Run 3S1, 3S2, 3A2, 3A3, 3A4					
20				X	
50		X	X	X	X
140				X	
290				X	

These were SUS runs. SUS depths were 18, 91, and 243 m for ship runs (S) and only 18 and 91 m for aircraft runs (A).

*Run No.	Range (km)
3S1	0-189
3S2	0-198
3A2	22-769
3A3	530-24
3A4	32-691

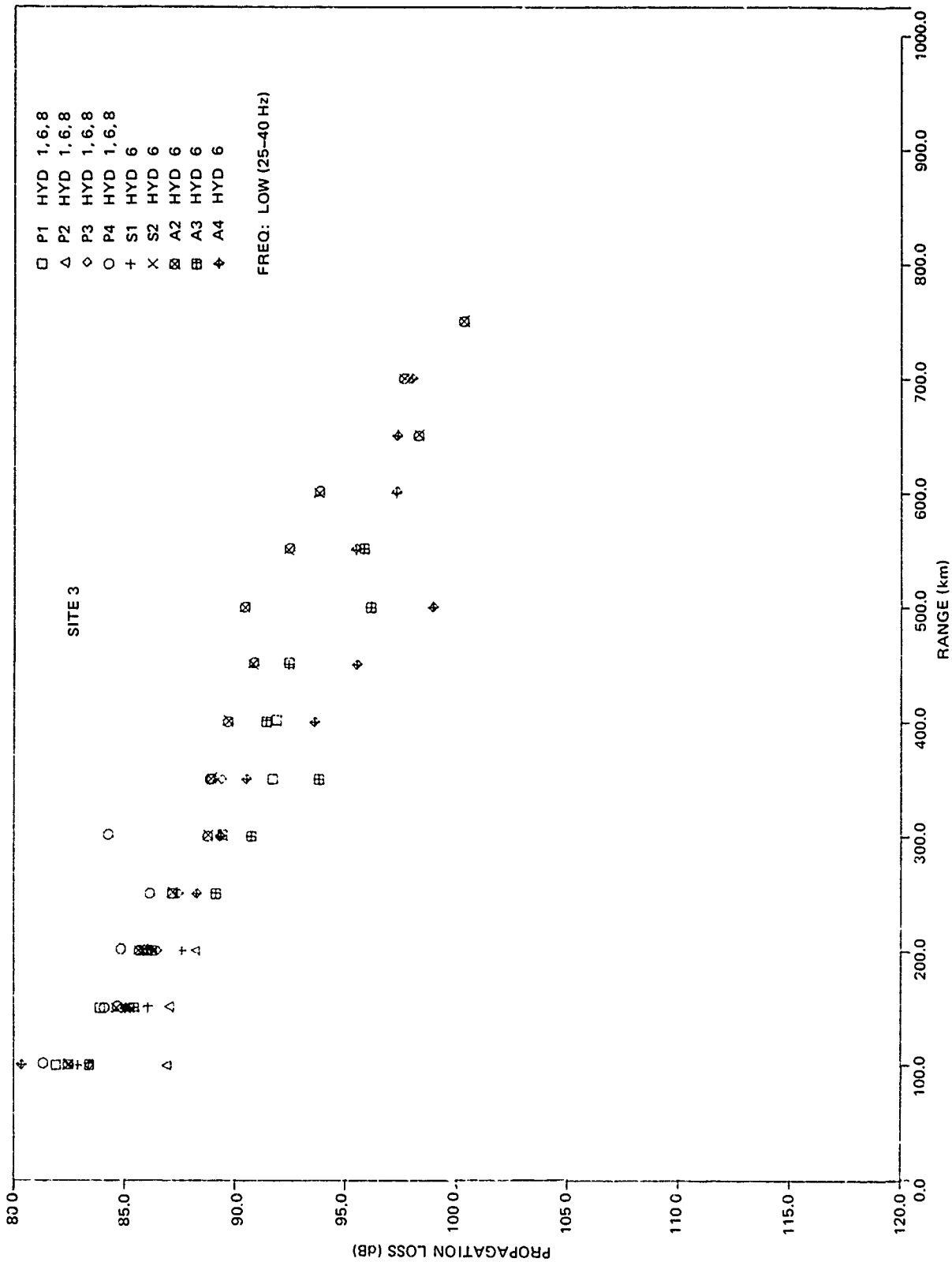

Figure 53. (C) Propagation loss at low frequency (20–40 Hz) as a function of range for all the events conducted at Site 3. (C)

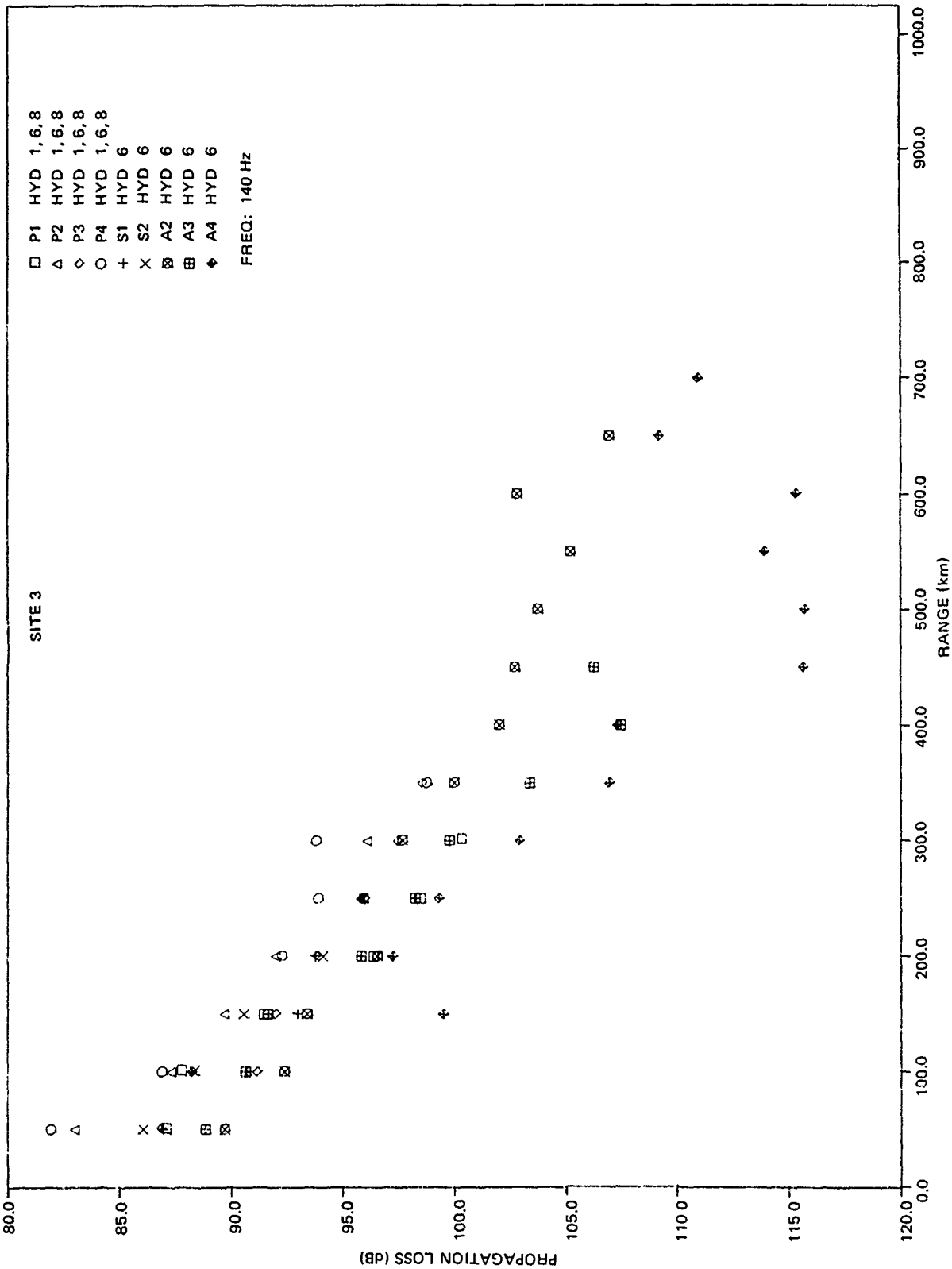

Figure 54. (C) Propagation loss at 140 Hz as a function of range for all the events conducted at Site 3. (C)

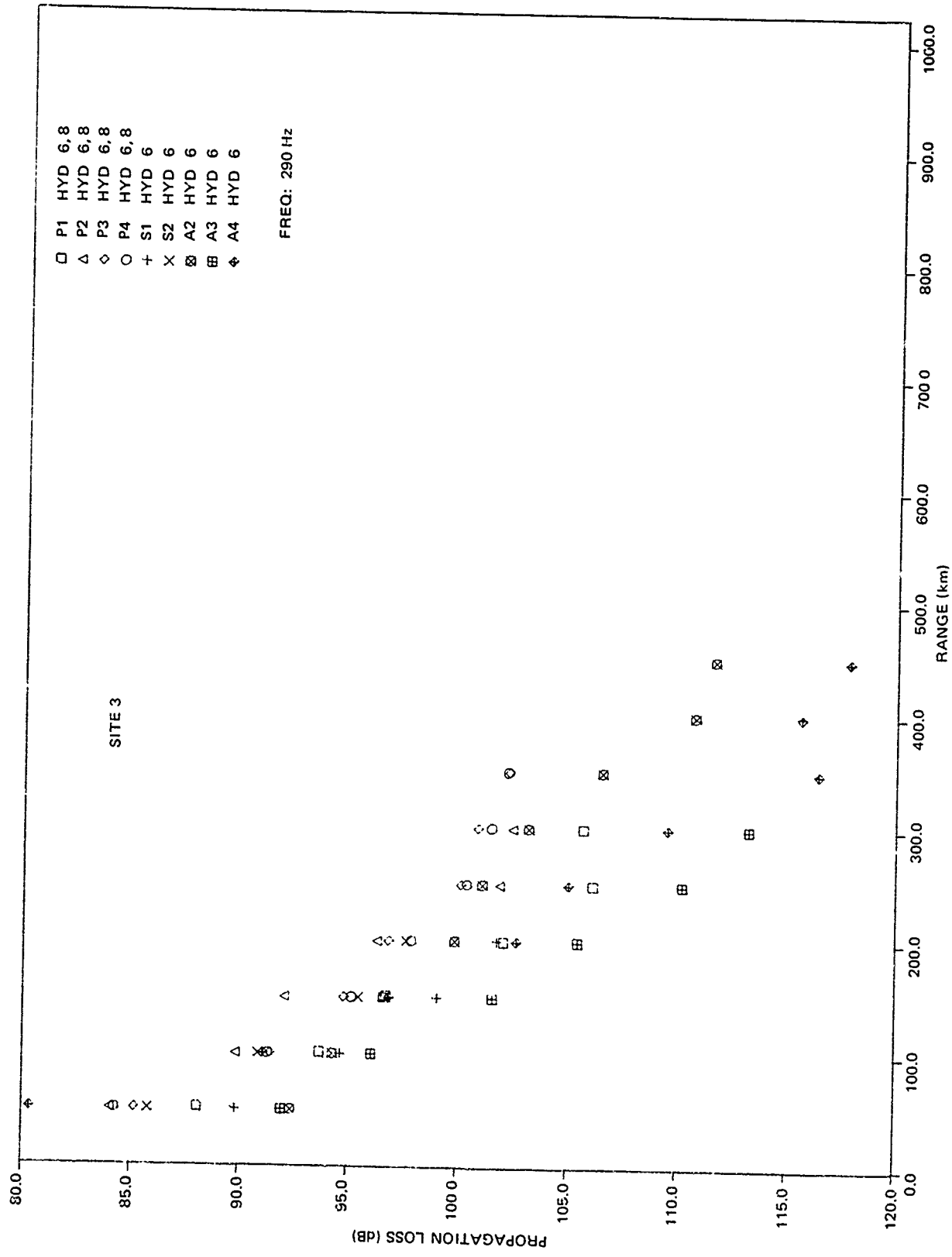

Figure 55. (C) Propagation loss at 290 Hz as a function of range for all the events conducted at Site 3. (C)

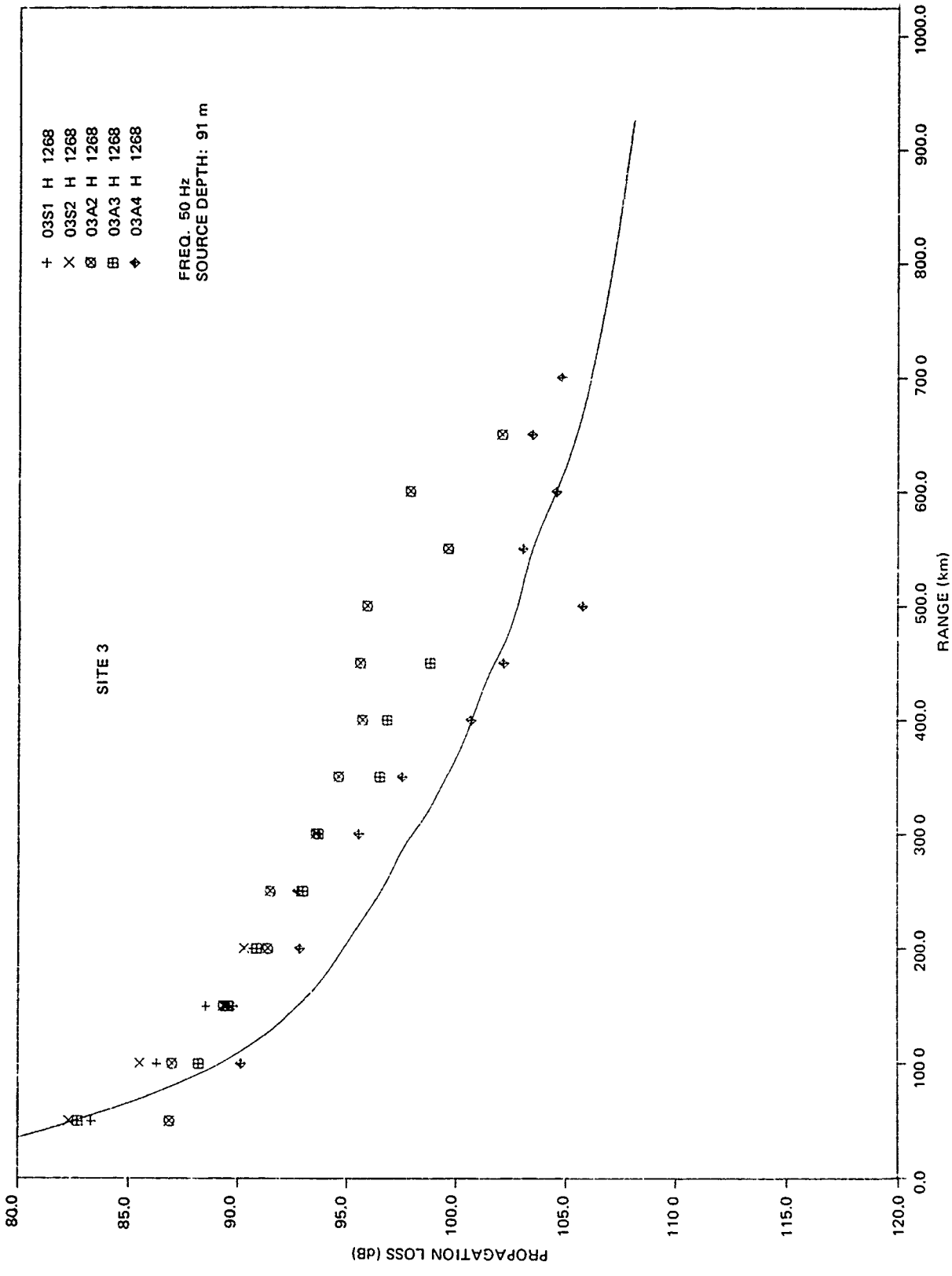

Figure 56. (C) Propagation loss at 50 Hz as a function of range for the SUS events conducted at Site 3. (C)

(C) Table 21 ranks the events according to increasing propagation loss. The rankings are not entirely consistent for each frequency listed. It should be pointed out here that the 25-Hz column of table 21 contains some events which processed the low-frequency data at 36 or 42 Hz instead of 25 Hz. The overall ranking of CW events appears to be 3P4, 3P2, 3P3, and 3P1. The low ranking of events 3P2 and 3P3 in the 25-Hz column is owing to the fact that they were conducted at 36 and 42 Hz, respectively, and had somewhat higher losses because of the higher frequencies. The overall ranking of the SUS events appears to be 3S2, 3A2, 3S1, 3A4, and 3A3.

Table 21. (C) Ranking of events at Site 3. (U)

Rank	Events			
	Low (20-40) Hz	140 Hz	290 Hz	50 Hz
1	3P4	3P4	3P2	3S2
2	3P1	3P2	3P3	3S1
3	3S2	3S2	3P4	3A2
4	3A2	3P1	3S2	3A3
5	3A4	3P3	3A2	3A3
6	3P3	3S1	3A4	
7	3S1	3A3	3P1	
8	3A3	3A2	3S1	
9	3P2	3A4	3A3	

(C) The nine radial events conducted at Site 3 afforded a unique opportunity to prepare contours of constant propagation loss for the site. In preparing the contours, the 91-m source depth data from the SUS events were adjusted to be comparable to the data of the CW events. On the basis of events 3P4 and 3S2, which were conducted along the same track, it was de ermined that the propagation loss for the 20-Hz SUS data should be increased by 1 dB to be comparable to the loss for the CW data at 25 Hz. Similar corrections for 140 and 290 Hz were 1.5- and 0.3-dB increase, respectively. Minor adjustments were also made to the 42-Hz data in event 3P3.

(C) Figures 57, 58, and 59 present propagation loss contours from 85 dB and up in 5 dB increments for 25, 140, and 290 Hz, respectively. Several conclusions are apparent from an examination of these contours. At the longer ranges, there is consistently less propagation loss in the directions of events 3A2, 3P3, and 3P4 as compared to events 3P1, 3A3, and 3A4. This is most apparent in the 85- and 90-dB contours at 25 Hz, the 100-dB contour at 140 Hz, and the 100–110-dB contour at 290 Hz. This conclusion is consistent with the overall ranking of events in table 21.

(C) Propagation in the direction of event 3P2 is somewhat ambiguous as there were no useful data available at low frequency because of a source failure. However, at the longest ranges tested, the losses for the event at 140 and 290 Hz fall between those of events 3A2 and 3P1.

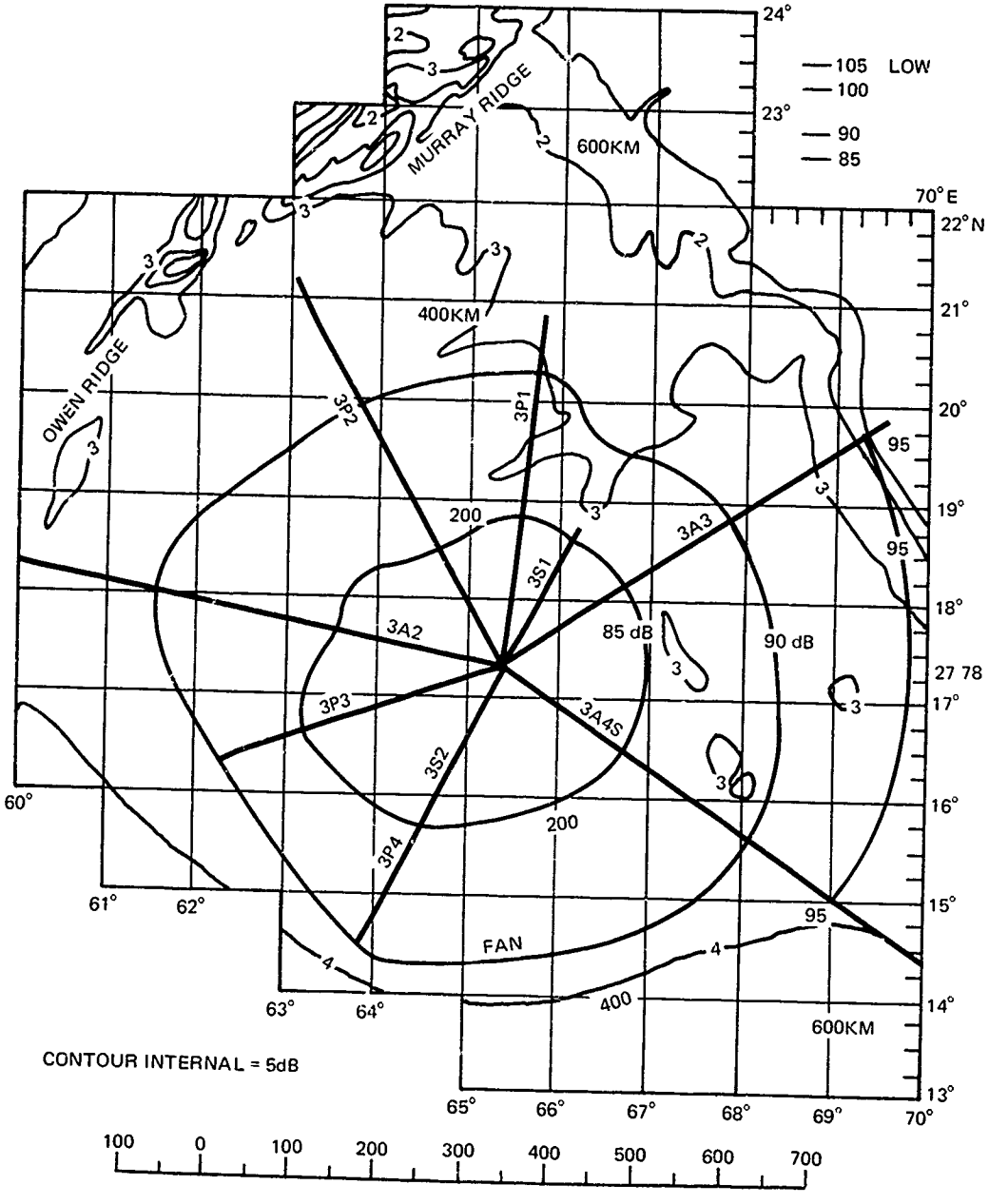

Figure 57. (C) Propagation loss contours at 25 Hz for Site 3. (C)

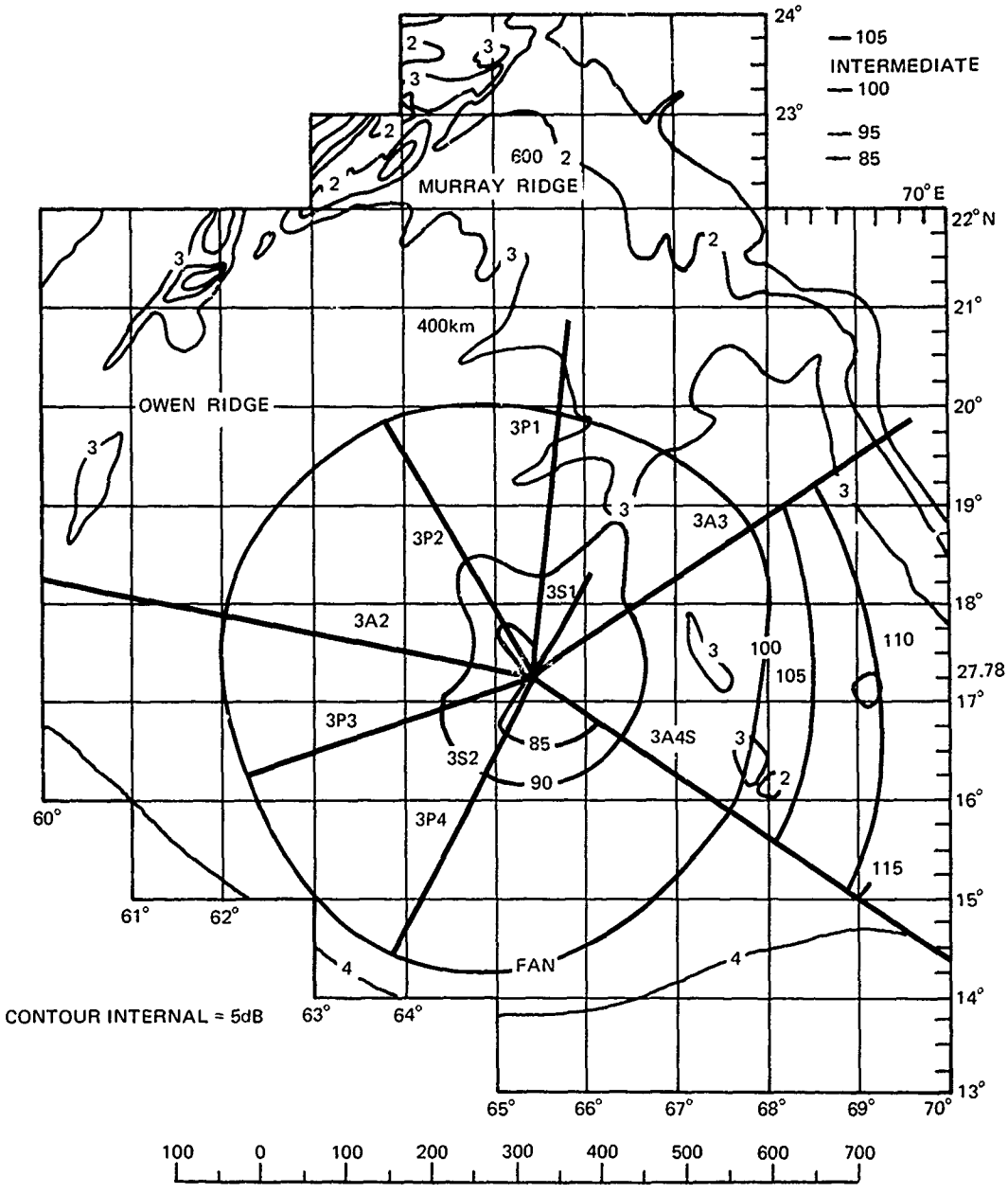

Figure 58. (C) Propagation loss contours at 140 Hz for Site 3. (C)

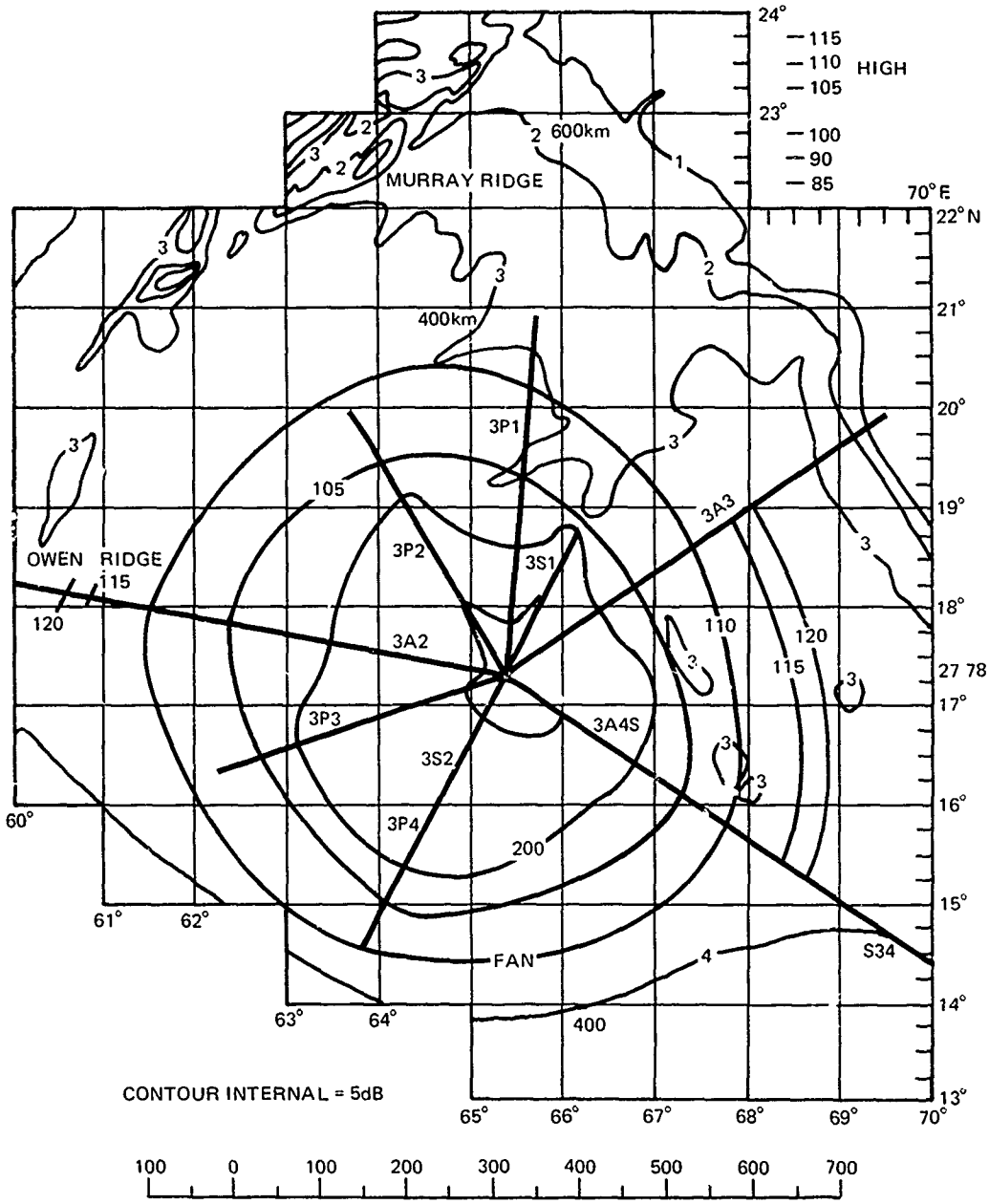

Figure 59. (C) Propagation loss contours at 290 Hz for Site 3. (C)

(C) Bathymetric profiles of the various events for Site 3 are shown in appendix A (fig A-7 to A-9). The better propagation in the directions of events 3A2, 3P3, and 3P4 as compared to events 3P1, 3A3, and 3A4 does not appear to correlate particularly well with the bathymetry, since the bottom slopes out to ranges of 350 km do not appear to be significantly different for all the events.

(C) In actuality, the propagation losses for events 3A1, 3A3, and 3A4 were somewhat higher than those shown in the closed contours in figures 57, 58, and 59 at long ranges. The data at long ranges were sparse and not too reliable, and some of the SUS signals were below the ambient noise level and could not be measured. Hence, the long range propagation loss data tend to be biased towards the low side.

(C) For event 3A4 the propagation loss increased rapidly between the ranges of 358 and 425 km at 140 Hz and 290 Hz. Also, at 25 Hz, the 95-dB loss contour occurred at a shorter range than one would anticipate on the basis of the 85- and 90-dB contour. The bathymetry for this event did not change markedly until 550 km.

(C) Event 3A4 exhibited rapid propagation loss increases at long ranges similar to those of event 3A4, but the 25-Hz data appeared to be as one would expect.

(C) The long range results of event 3A2 appear to confirm some previous conclusions reached in assessing Site 2 about propagation loss results west of the Owen Ridge. Event 3A2 intersects the ridge about 120 nmi north of Site 2. On the line of crossing, the ridge rises only about 400 m above the basin floor whereas the ridge at Site 2 rises about 2000 m. As seen in figure 57, at 25 Hz there appears to be no rapid increase in propagation loss west of the ridge. This indicates that (since Site 3 is bottom limited) at 25 Hz the bottom loss to the west of the ridge is not radically greater than that to the east. In contrast, at 140 Hz there is a very rapid increase in propagation loss to the west of the ridge, as seen in figure 58. In figure 59 no values are shown west of the ridge at 290 Hz for the event. However, the WECo data report (ref 8) indicated that there were high losses at 290 Hz to the west of the ridge which exceeded 125 dB and dropped below the noise threshold. Hence, the results of event 3A2 confirm the previous conclusion that the propagation to the west of the ridge suffers a relatively minor increase at 25 Hz and major increases at 140 and 290 Hz when compared to propagation east of the ridge.

5.4 (U) DEPENDENCE ON RANGE AND FREQUENCY

(C) The CW events with the lowest propagation loss at 25, 50, 140, and 290 Hz for Site 3 are compared to the Eleuthera reference in figure 60. The values plotted in the figure are given in table 22. Event 3P4 had the lowest propagation loss for 25 and 140 Hz while event 3P2 had the lowest for 290 Hz. However, event 3P4 had lower losses than event 3P2 for 290 Hz at ranges of 250 and 300 km, and is also plotted.

(C) The slopes of the propagation loss curves at 25 and 140 Hz in figure 60 appear to be somewhat less than that of the reference, whereas the slope for 290 Hz is slightly greater. Propagation losses at 25 and 140 Hz are, respectively, 5 to 14 dB and 1 to 4 dB less than those of the reference, and corresponding values at 290 Hz are from 0 to 4 dB greater than those of the reference.

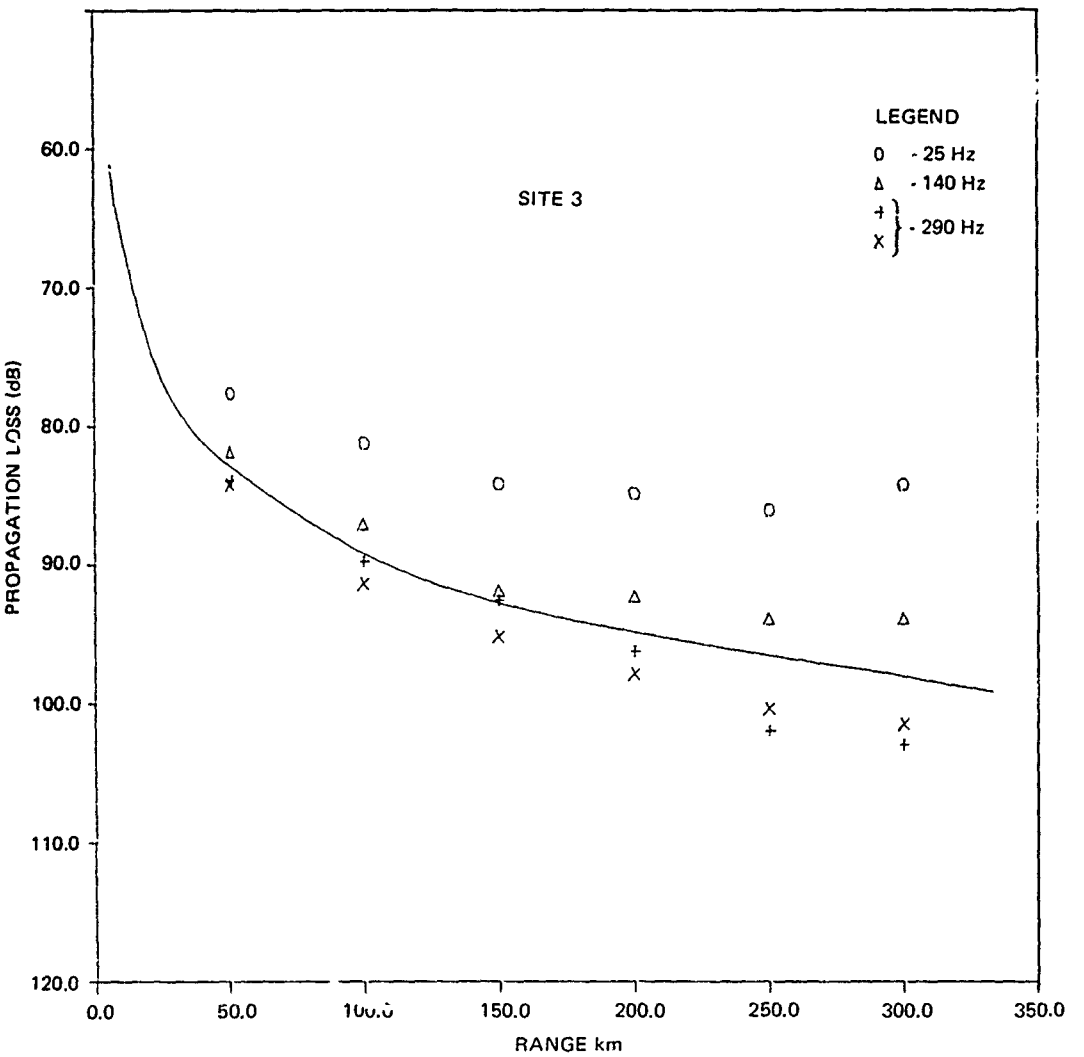

Figure 60. (C) Propagation loss for 25, 140, and 290 Hz as a function of range at Site 3. (C)

(C) The propagation losses at 50 Hz for the SUS event of lowest loss (3S1) are also given in table 22 but are plotted in figure 56 for comparison with the Eleuthera reference. As shown in figure 56, the propagation losses at 50 Hz range from 1 dB greater to 4 dB less than those of the reference.

Table 22. (C) Propagation losses for the best events at Site 3. (U)

Range (km)	Propagation Loss (dB) Event 3P4 25 Hz	Event 3P4 140 Hz	Event 3P2 290 Hz	Event 3P4 290 Hz	Event 3S2 50 Hz
50	77.7	81.9	84.0	84.3	82.3
100	81.3	87.1	89.8	91.4	85.5
150	84.2	91.9	92.6	95.2	89.5
200	84.9	92.3	96.3	97.9	90.3
250	86.1	93.9	102.0	100.4	—
300	84.3	93.9	103.0	101.5	—

5.5 (U) SITE 3 SUMMARY

(U) Site 3, which was located in the middle of the Arabian Basin, was a bottom-limited area. All receivers used at the site were mounted on the ocean floor. The propagation loss measurement results show that there is less propagation loss in the southwestern direction from the site towards the Indus Fan than to the east and north of the site.

(C) The minimum propagation losses measured at Site 3 for the range interval 50 to 300 km were 77.7 to 84.3 dB at 25 Hz, 81.9 to 93.9 dB at 140 Hz, and 84.0 to 101.5 dB at 290 Hz.

(C) In comparison with the Eleuthera reference curve, the propagation losses at Site 3 for 25 Hz ranged from 5 to 14 dB less than those of the reference for the range interval 50 to 300 km. At corresponding ranges, the propagation losses at 140 Hz were 1 to 4 dB less, and at 290 Hz, 0 to 4 dB greater.

5.6 (U) RECOMMENDATIONS FOR ADDITIONAL DATA PROCESSING

(U) The data reduction for event 3A1 at Site 3 was not completed by WECo because the aircraft was about 80 nmi off course at the end of the event. Despite this drawback, it is recommended that all the data for the event be processed since it is one of only two events in BEARING STAKE which penetrated into the Carlsberg Ridge, a high-bottom-loss region. The data will provide information which will aid in establishing the boundary between the bottom loss regimes of the Indus Fan.

(U) No other additional processing of the other events at Site 3 is recommended.

6.0 (U) SITE 4 ASSESSMENT

6.1 (U) INTRODUCTION

(C) Site 4 was located in the deep (5100 m) Somali Basin that lies between the Chain Ridge and the east coast of Africa. This site was chosen because long range propagation via refracted paths (convergence zone) was possible. This site was the only site of BEARING STAKE in which bottom-limited propagation conditions were not expected to prevail during the exercise. (Figure 61 shows the physical configuration of the BMA installed at the site on the western slope of the Chain Ridge.

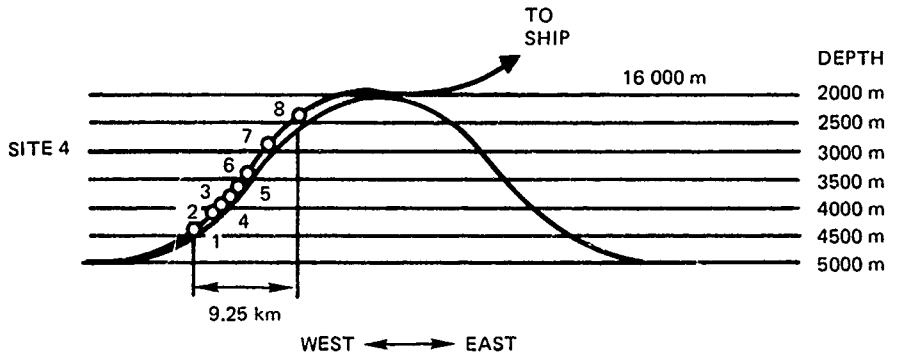

Figure 61. (U) Configuration of BMA at Site 4. (U)

(U) Propagation runs were made to north, west, and southwest of the site, as shown in figure 62. No runs were made to the east, as it was anticipated that the Chain Ridge would block any signals coming from that direction. As shown in the figure, the radial runs crossed the deep basin and terminated near the continental slope.

(C) The sound speed profiles measured at Site 4 were unusual in that they showed a considerable number of sound speed gradient reversals in the upper 1500 m. This irregularity is attributed to the interfringing of the Somali Basin water with the Red Sea water above 1000 m and Antarctic intermediate water from 1000 to 1500 m (ref 12 and 13). However, for the frequencies used during BEARING STAKE, these irregularities appeared to have little effect on the propagation loss results. A representative sound speed profile for Site 4 is shown in figure 63. The profile shows that even for this deep water site, acoustic propagation could be bottom limited for sources at shallow depths (< 500 m). Fortunately, the source depths used at the site included depths below 50 m, which allowed for convergence zone mode of propagation.

---

12. "The Sound Velocity Structure of the North Indian Ocean," NAVOCEANO TR 231, by D F. Fenner and D. C. Bucca, December 1972

13. "Sound-Speed Distribution in the Western Indian Ocean," NUC TP 502, by J. G. Colborn, 1976

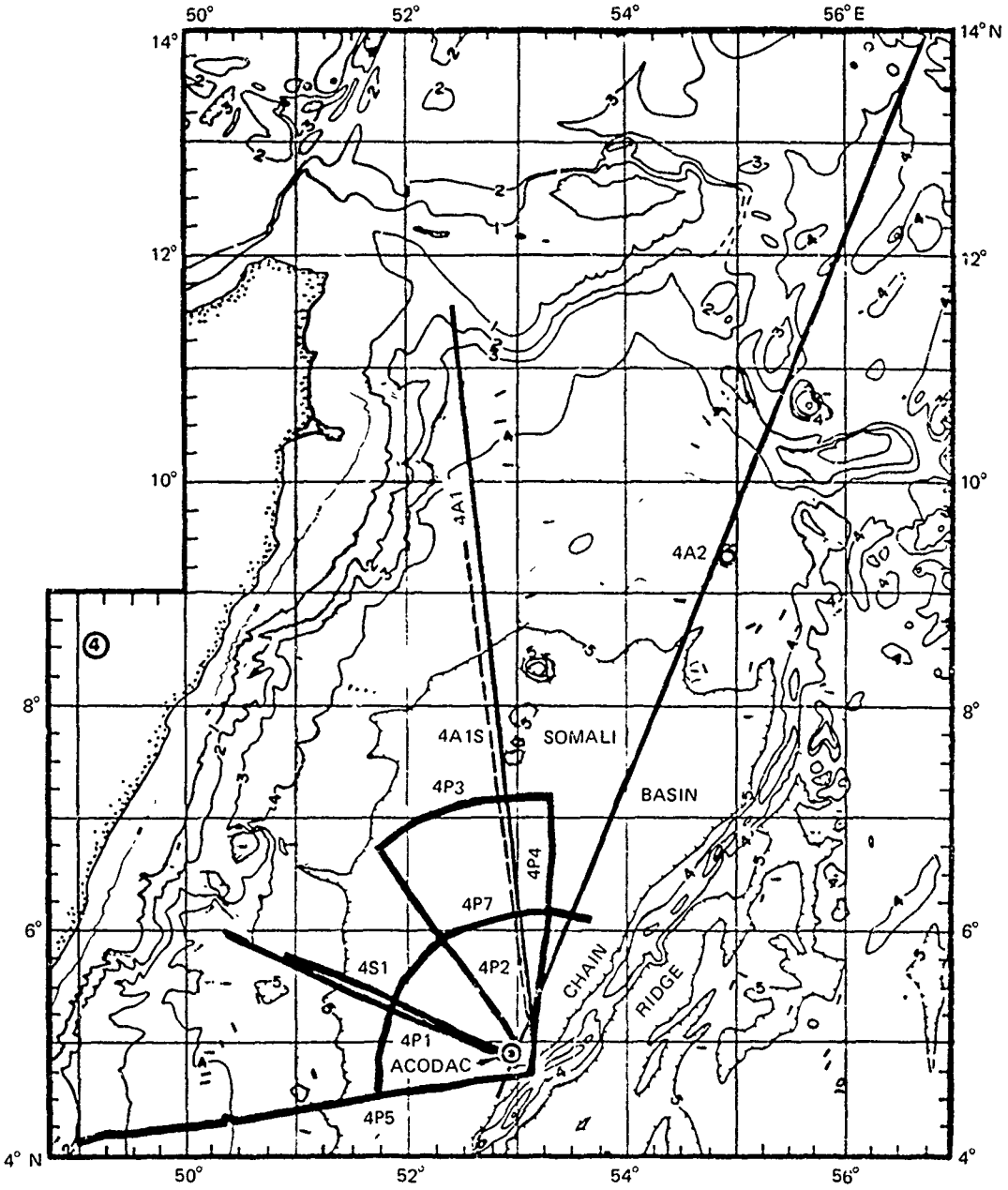

Figure 62. (C) Geometry of events conducted at Site 4 by source ship and aircraft. (U)

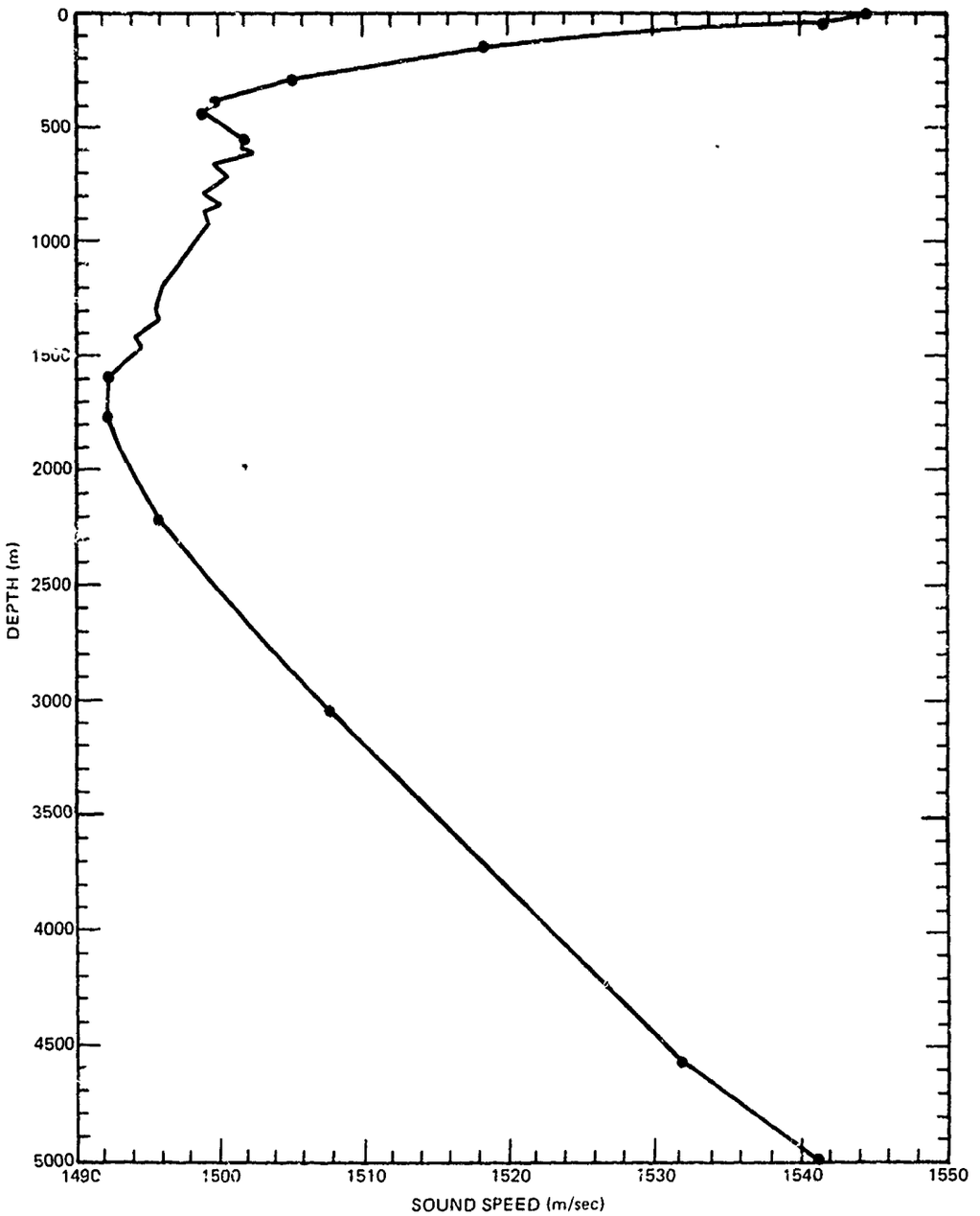

Figure 6.3. (U) Representative sound speed profile for Site 4. (U)

(U) Table 23 is a summary of the propagation loss data measured at Site 4. The table shows, for each run, the measured frequencies and their source depths, and the BMA receiver depths. The ACODAC was used at this site, and the depths of its receiving hydrophones are listed. The SUS source runs were recorded only by the BMA at the site. As can be seen from the summary table, the data for this site are quite extensive.

(U) In this section, the close range bathymetry to the receivers and their effect on propagation paths are discussed first. Then the effects on propagation loss at Site 4 of receiver depth, events conducted, range, frequency, and seasons are assessed and summarized.

6.2 (U) SITE 4 BATHYMETRY

(C) The bathymetric features and sound speed profiles measured at Site 4 played a prominent role in the acoustic propagation of the events conducted at the site. The events conducted at Site 4 and their tracks, as well as bathymetric features, were shown previously in figure 62. The BMA receivers at Site 4 were draped up the Chain Ridge which bounds the eastern edge of the Somali Basin. The ACODAC receivers were located about 25 km from the base of the Chain Ridge along the track of event 4P1. ACODAC receiver 13 was mounted on the floor of the basin with receivers 2, 5, and 9 suspended in the water column.

(C) Figure 64 shows the close range bathymetry for event 4P2. This event ran almost normal to the Chain Ridge. The bathymetric profile was the same for BMA receivers 1 to 7, and a slightly different profile applies to receiver 8, as shown. (The ridge was shallower than 3 km. However, since no events were conducted over the ridge, the bathymetry beyond receiver 8 is not shown. The slope of the ridge was about 15°. The maximum bottom depth in the Somali Basin was at the base of the Chain Ridge at 5110 m, where the BMA was located. For event 4P2, the bottom of the basin was essentially flat for the entire event.

(C) The close range bathymetry for events 4P1/4S1, 4P5, 4A1, 4P4, and 4A2 is shown in figures 65, 66, 67, 68, and 69, respectively. (The long range bathymetry of these events is shown in appendix A, fig A-10 and A-11.) Event 4P5 had the longest sloping bathymetry (0 to 20 km) at close range of all the events conducted at Site 4. For event 4P1/4S1, the basin bottom was flat out to 175 m, and the event crossed an obstruction which rose about 1 km above the basin floor at 320-km range. For event 4A1, the basin floor was flat out to 425 km and then sloped about 0.5 degree to 725 km. Beyond this range, the event had slopes as steep as 2.5 degrees. For event 4A2, the basin was flat out to 450 km and sloped 0.5 degree to 625 km. Beyond this range, the bathymetry was very rugged, with individual features rising to a depth of 3.2 km.

(C) The bottom depth where the ACODAC was located was 5106 m. The long range bathymetry for the ACODAC data is similar to that of the BMA data except, of course, the bathymetry starts at the basin floor rather than on the Chain Ridge for all the events, although, for event 4P5, the acoustic paths intercepted a seamount which rose some 1000 m above the basin floor. The seamount obstructed propagation to the ACODAC for the 250-km range bin but was not a significant feature for propagation paths to the BMA receivers.

Table 23. (C) Summary of the propagation loss data set from the BMA and ACODAC at Site 4 from projector (P) and SUS runs. (U)

BMA Hydrophone No.		1	3	6	7	8	ACODAC			
Depth (m)		4725	4486	4235	4078	3778	400	1916	5076	5106
Freq (Hz)	Source Depth (m)									
Run 4P1: 11-326 km										
25	91	X	X	X	X	X				
140	18	X	X	X	X	X	X	X	X	X
290	18	X	X	X	X	X	X	X	X	X
Run 4P2: 13-272 km										
25	91	X	X	X	X	X				
140	18	X	X	X	X	X				
290	18	X	X	X	X	X				
Run 4P3: Circular 272 km										
25	91	X	X	X	X	X				
140	18		X							
290	18		X							
Run 4P4: 279-11 km										
25	88	X	X	X	X	X				
140	18	X	X	X	X	X	X	X	X	X
290	18	X	X	X	X	X	X	X	X	X
Run 4P5: 13-295 km										
36	87	X	X	X	X	X				
140	18	X	X	X	X	X	X	X	X	X
290	18	X	X	X	X	X	X	X	X	X
Run 4P7: Circular 159 km										
36	91	X	X	X	X	X				
140	18		X							
290	18		X							
*Run 4S1, 4A1, 4A2										
20		X	X	X	X					
50		X	X	X	X	X				
140		X	X	X	X					
300			X							

These were SUS runs. SUS depths were 18, 91, and 243 m for ship runs (S) and only 18 and 91 m for aircraft runs (A).

*Run 4S1: 333-0 km, Run 4A1: 2-778 km, Run 4A2: 1100-2 km

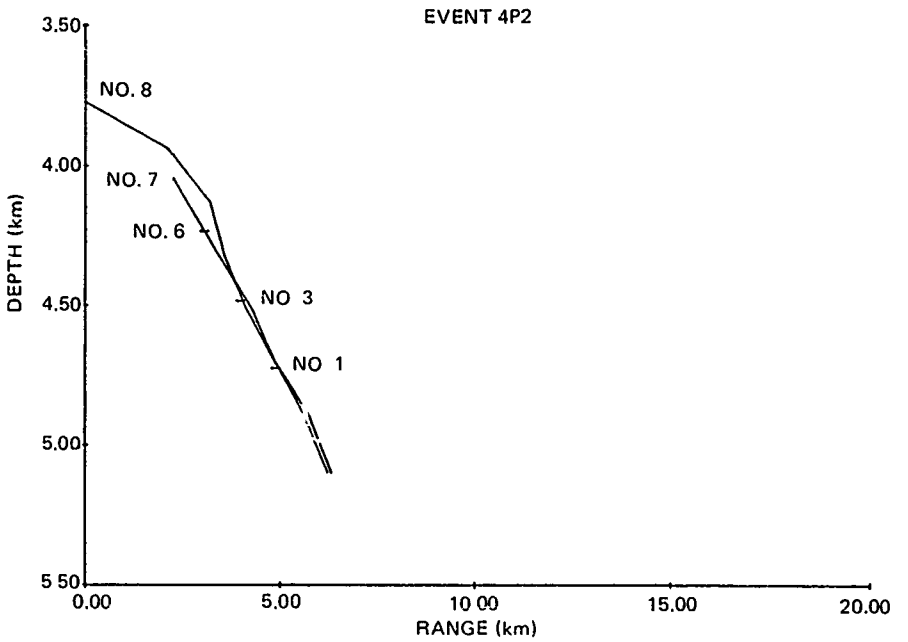

Figure 64. (U) Close range bathymetry for event 4P2. (U)

(C) The sound speed profiles at Site 4 required more consideration than at the other BEARING STAKE sites. Estimated values of the depth excess for various source depths and events are listed in table 24. The table was based upon a fixed bottom depth (5106 m) which was the value of ACODAC receiver 13 and the average sound speed as measured along the track of each event at critical depths. The 18-m source depth is appropriate for CW sources at 140 and 290 Hz and the 91-m source depth for low-frequency (20–42 Hz) CW sources. The depth excess entries under "0" source depth are based on the maximum near-surface sound speed and represent the depth excess for the lowest-angle ray which reaches the ocean surface. For event 4P5, the near-surface sound speed exceeds that at the basin bottom; hence, zero depth excess is noted.

6.3 (U) CONVERGENCE ZONE PROPAGATION LOSSES

(C) The nature of the acoustic propagation at Site 4 was radically different from that of the other sites. Whereas the other sites were bottom limited, the conditions at Site 4 made convergence zone propagation possible. Figure 70 shows propagation loss at 290 Hz from events 4P1 and 4P5 as well as the propagation loss predicted from the RAY WAVE and ASTRAL models Event 4P1, represented by the triangle symbols in the figure, had the lowest propagation loss at 290 Hz of all the events at Site 4 and was also the event with the greatest depth excess. Event 4P5, represented by the cross symbols, had the largest propagation loss at 290 Hz as recorded on BMA receiver 3. All the experimental propagation losses shown in figure 70 (and in this section on Site 4) were averaged in 2-km range

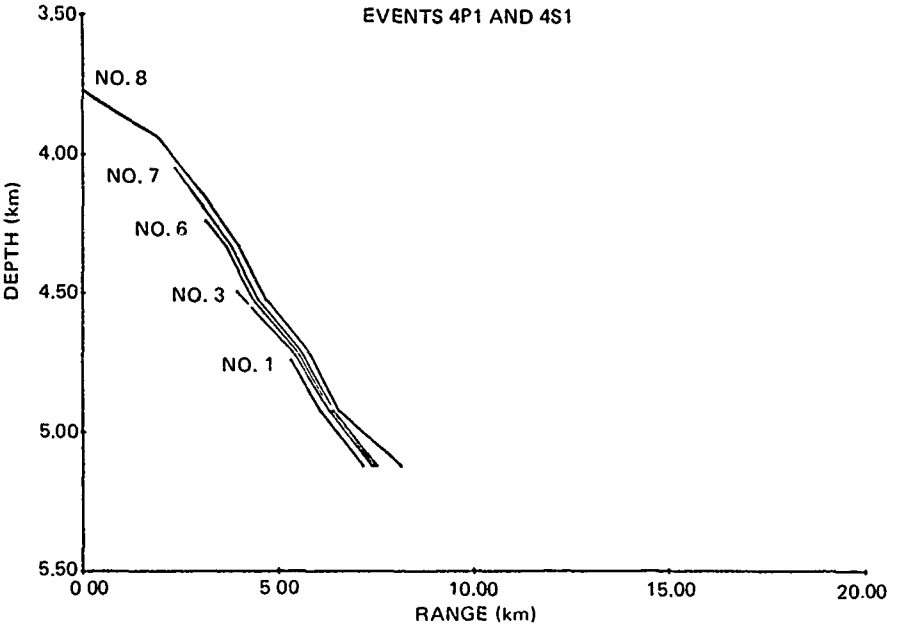

Figure 65. (U) Close range bathymetry for events 4P1 and 4S1. (U)

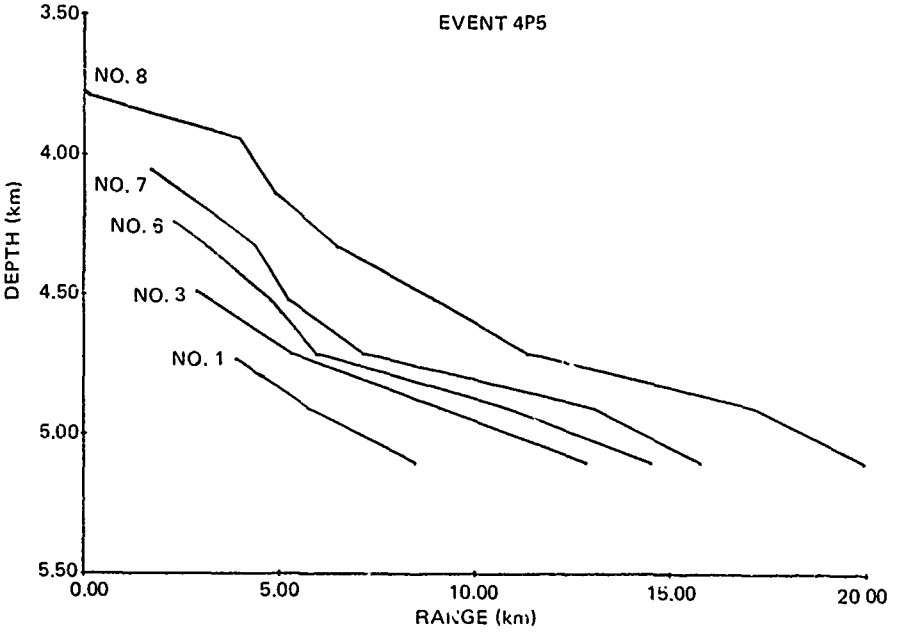

Figure 66. (U) Close range bathymetry for event 4P5. (U)

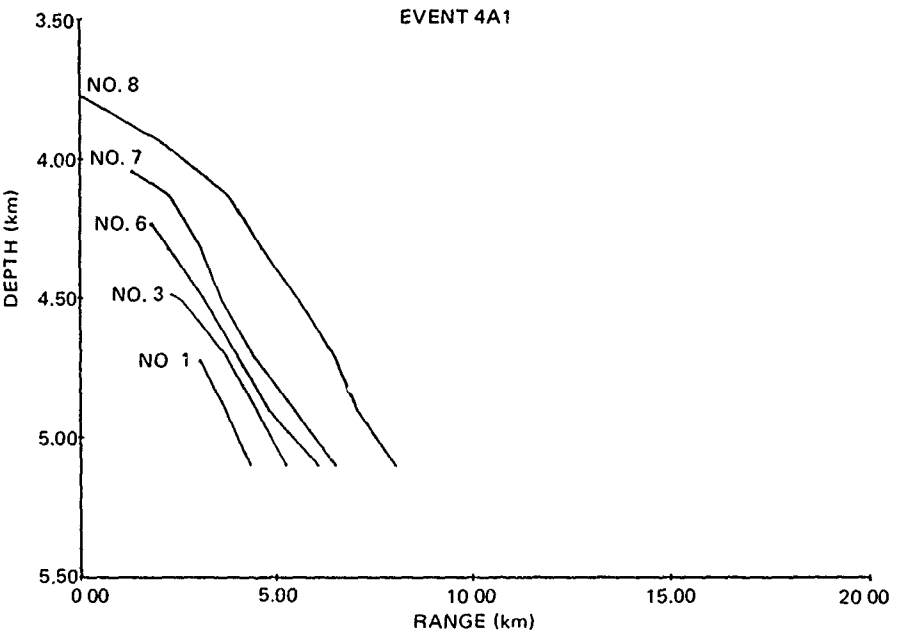

Figure 67. (U) Close range bathymetry for event 4A1. (U)

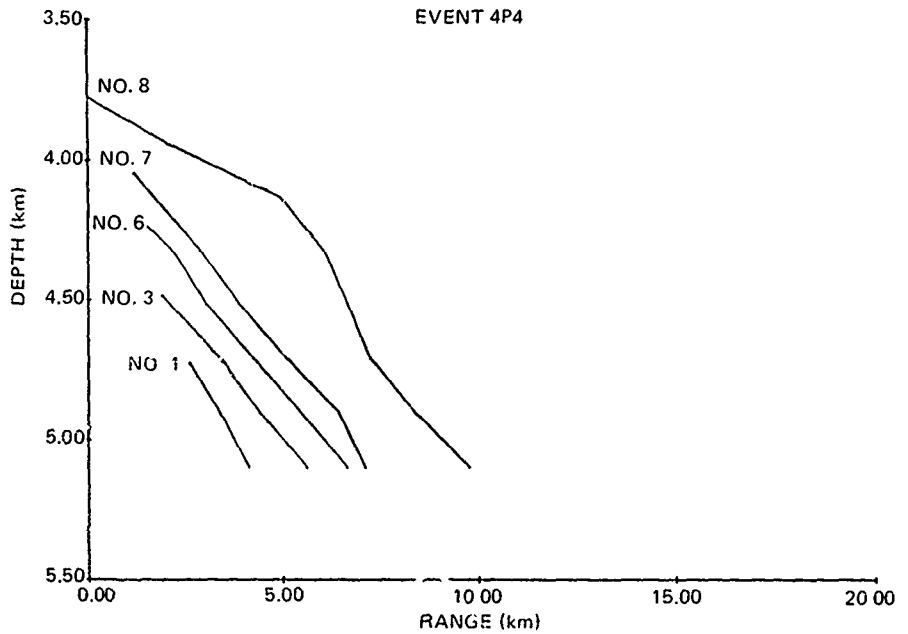

Figure 68. (U) Close range bathymetry for event 4P4. (U)

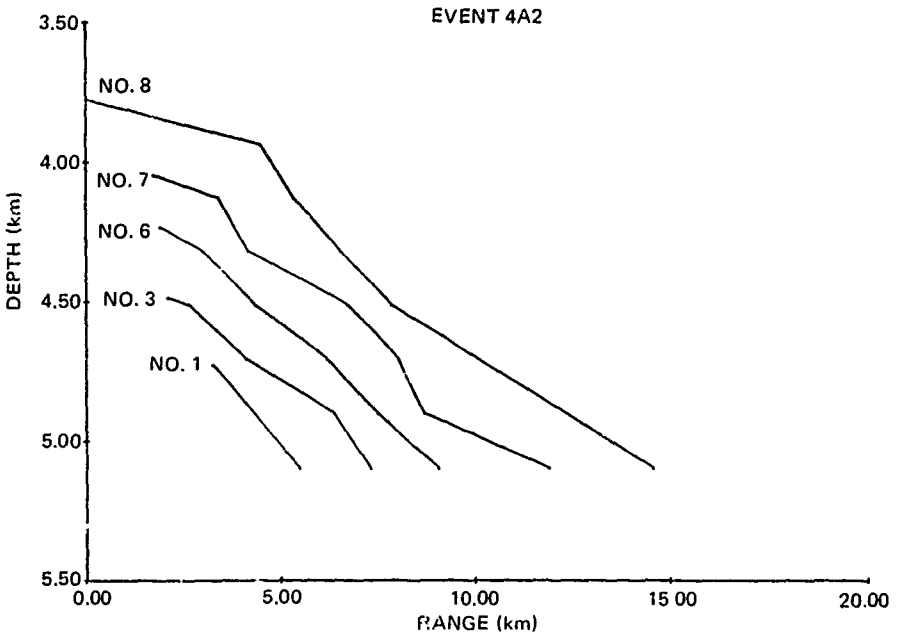

Figure 69. (U) Close range bathymetry for event 4A2. (U)

Table 24. (U) Depth excess in metres at Site 4 for various source depths and events. (U)

Event	Source Depth (m)		
	0	18	91
4P1	121	147	263
4S1	96	121	259
4P2	51	76	197
4P4	35	66	238
4S5	0	30	276

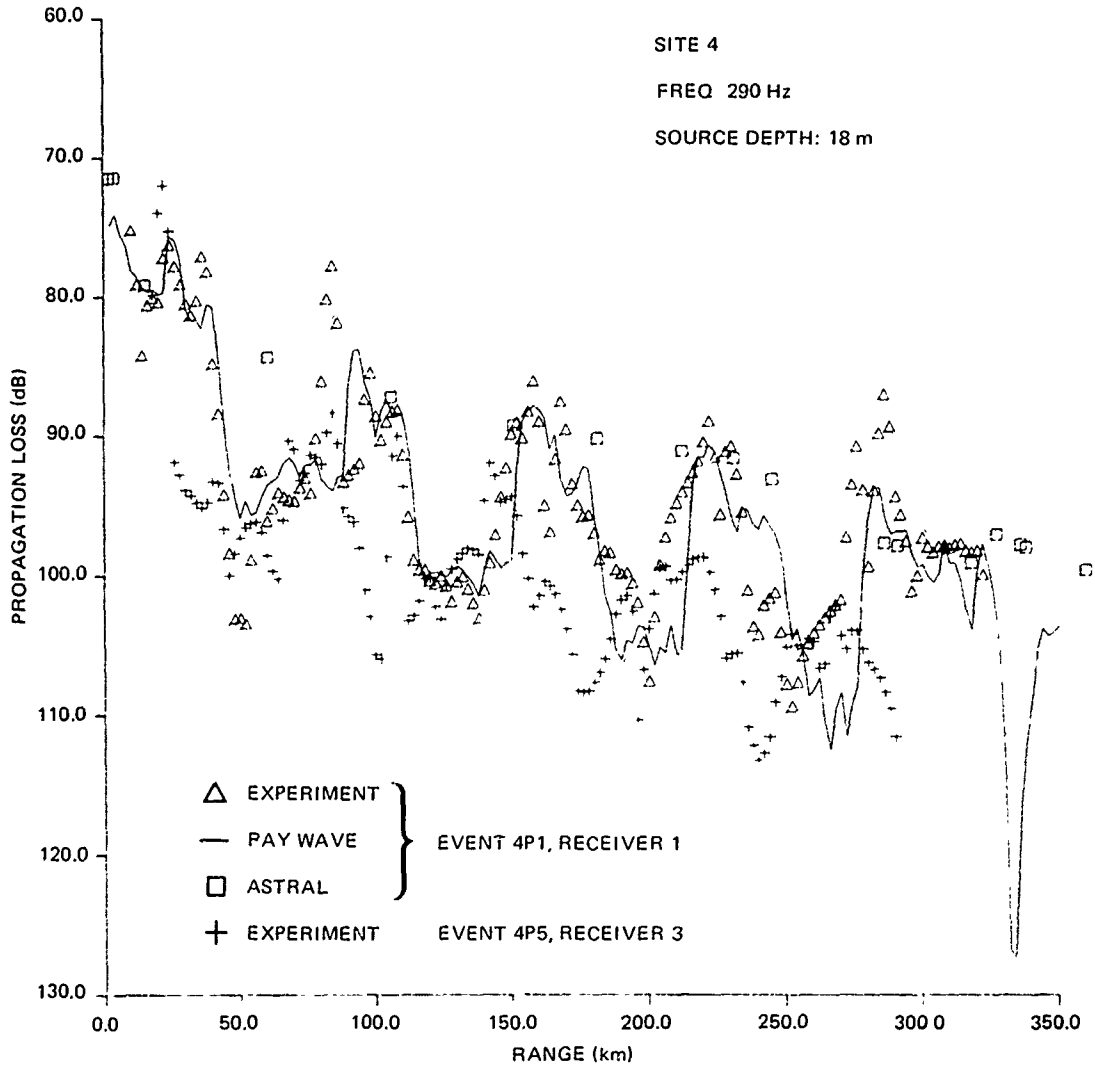

Figure 70. (C) Propagation loss at 290 Hz as a function of range for a source depth of 18 m at Site 4. Also shown are the corresponding propagation losses from the ASTRAL and RAY WAVE models. (C)

bins in order to show detailed structures of the propagation loss. The solid curve is the theoretical propagation loss as calculated by the RAY WAVE model and the square symbols are the corresponding results from the ASTRAL model.

(C) As can be seen from figure 70, the convergence zones rise 10 to 20 dB above the bottom-reflected propagation losses between the zones. Both the RAY WAVE and ASTRAL models agree reasonably well with the experimental results. The experimental results show a good correlation with the depth excess values shown in table 24, where event 4P5 has the least depth excess for a source at the surface and at 18-m depth. Although there are convergence zones for event 4P5, the losses are significantly higher than for event 4P1.

(C) Figure 71 shows the propagation loss at 25 Hz for the experimental data and theoretical models. Again, the ASTRAL and RAY WAVE models agree reasonably well with the experimental results. As can be seen in figure 71, in both experimental and theoretical results, there is little evidence of convergence zones. One possible explanation of this lack of definitive convergence zones at 25 Hz is that although the bottom loss at Site 4 is higher than at any of the other BEARING STAKE sites, the acoustic signals are still strong enough to fill in between the zones, thus masking the zones.

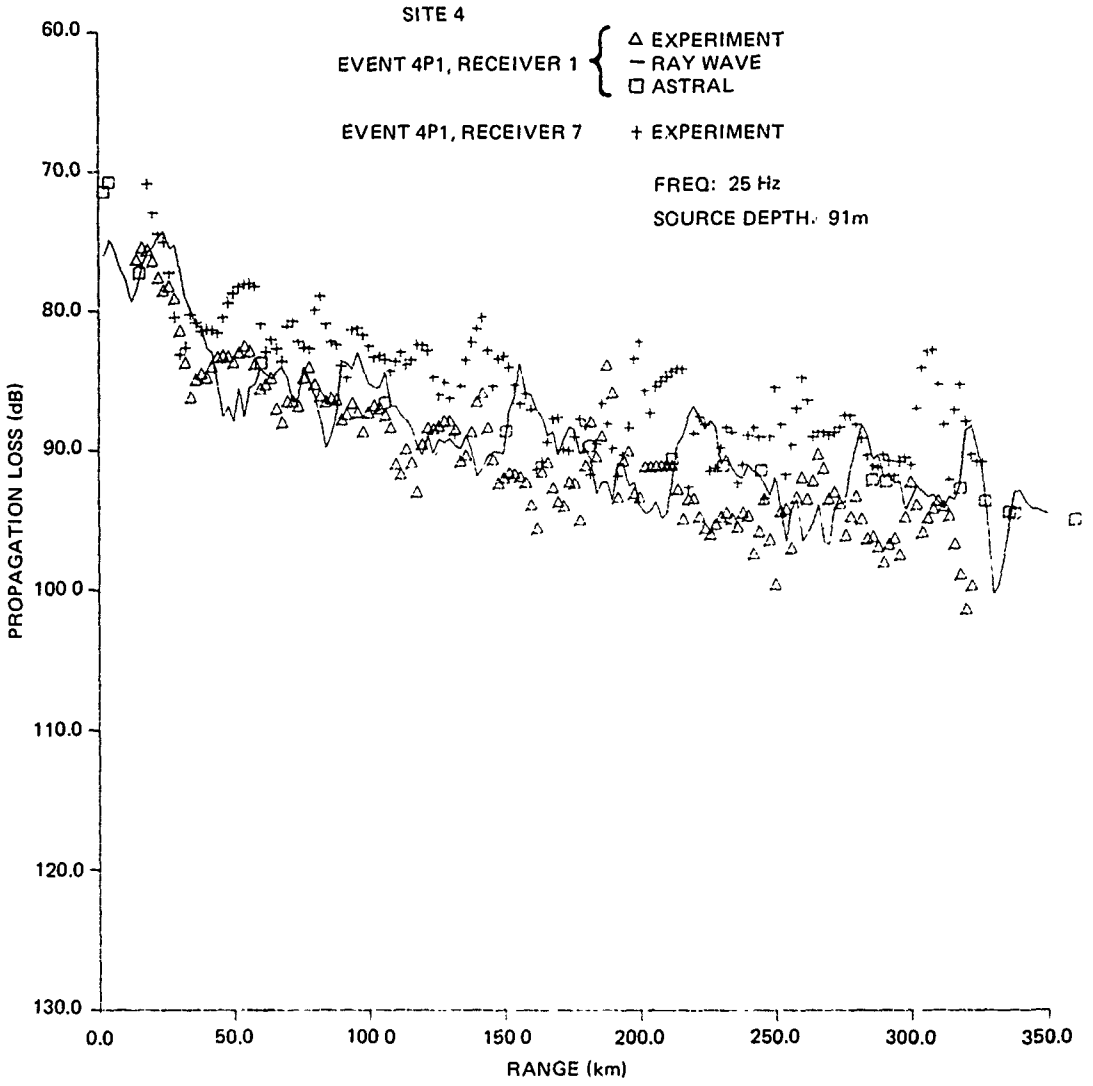

Figure 71. (C) Propagation loss at 25 Hz as a function of range for a source depth of 91 m at Site 4. Also shown are the corresponding propagation losses from the ASTRAL and RAY WAVE models. (C)

(C) However, on the basis of figure 71, it is suspected that convergence zone behavior at low frequency for small depth excess is quite complicated. For example, at 25 Hz the source depth was 91 m compared to 18 m for 290 Hz. Hence, there are more non-bottom-reflected paths available for 25 than 290 Hz. On this basis, one would expect the zones to be more pronounced at 25 Hz. This was not the case. Another example is that the receiver with the lowest propagation loss at 25 Hz for event 4P1 was receiver 7 (see fig 71) instead of receiver 1, which was the best receiver at 290 Hz. Whatever the reason, the only thing that can be said at present is that the behavior of the propagation loss is significantly different at 25 Hz from that at 290 Hz for Site 4. Present plans call for a normal mode investigation of this behavior.

(C) Figure 72 compares the experimental propagation loss results of the best receiver for event 4P4 at 39 Hz with those for event 4P5 at 36 Hz. Event 4P4 had the lowest propagation loss of all CW events at 39 Hz whereas event 4P5 had the highest propagation loss at 36 Hz. The propagation losses at 25 Hz for events 4P1 and 4P2 fell between the losses of the events in figure 72. The higher losses for event 4P5 are probably due to conditions of smaller depth excess and, in the case of events 4P1 and 4P2, to a higher bottom loss at 36 Hz. However, it is not too clear why, at 39 Hz, event 4P4 had less propagation loss, since it had less depth excess than event 4P1. A possible explanation for the low losses for event 4P4 is that, for some reason or other, the convergence zone structure was enhanced for the geometry and frequency of the event. Figure 72 exhibits some convergence zone-like structure for event 4P4.

6.4 (U) DEPENDENCE ON RECEIVER DEPTH

(C) Receiver depth dependence is given for the CW and SUS events at Site 4 in tables 25 and 26, respectively. Both BMA and ACODAC systems were used to receive data at the site. However, only the BMA results for the SUS events are shown in table 26 because the ACODAC data were overloaded and are not reliable.

(C) Nevertheless, the tables show that, in most cases, the receiver with the lowest propagation loss is either BMA receiver 1 or 7. In a few cases, BMA receiver 3 or 8 has the lowest propagation loss. The behavior of receiver 3 is quite similar to that of receiver 1, and receiver 8 is similar to receiver 7. This similarity substantiates the results of receivers 1 and 7 as "real" and not an artifact of calibration or processing procedures. In all but three cases (event 4P4 at 290 Hz and events 4A1 and 4A2 at 50 Hz), the losses for BMA receiver 6 are greater than for BMA receivers 3 and 7. Since receiver 6 is between receivers 3 and 7, the results of receiver 6 are strongly suspect. The most important comparisons are between BMA receivers 1 and 7 because they represent two possible choices for optimum receiver depth.

(C) Consider, first, events 4P1, 4P2, and 4P4 of table 25 and their propagation loss behavior at 140 and 290 Hz. Under convergence zone conditions, we would expect the minimum propagation loss to occur near the critical depth (or conjugate depth), which, according to table 24, is between 147 and 66 m off the ocean floor for the 18-m source depth. It is not surprising, then, at 140 and 290 Hz, the best BMA receiver depth was receiver 1. This receiver at 380 m off the ocean floor was nearest to the optimum receiver configuration. For events 4P1, 4P2, and 4P4 (table 25), BMA receiver 1 is from 2.4 to

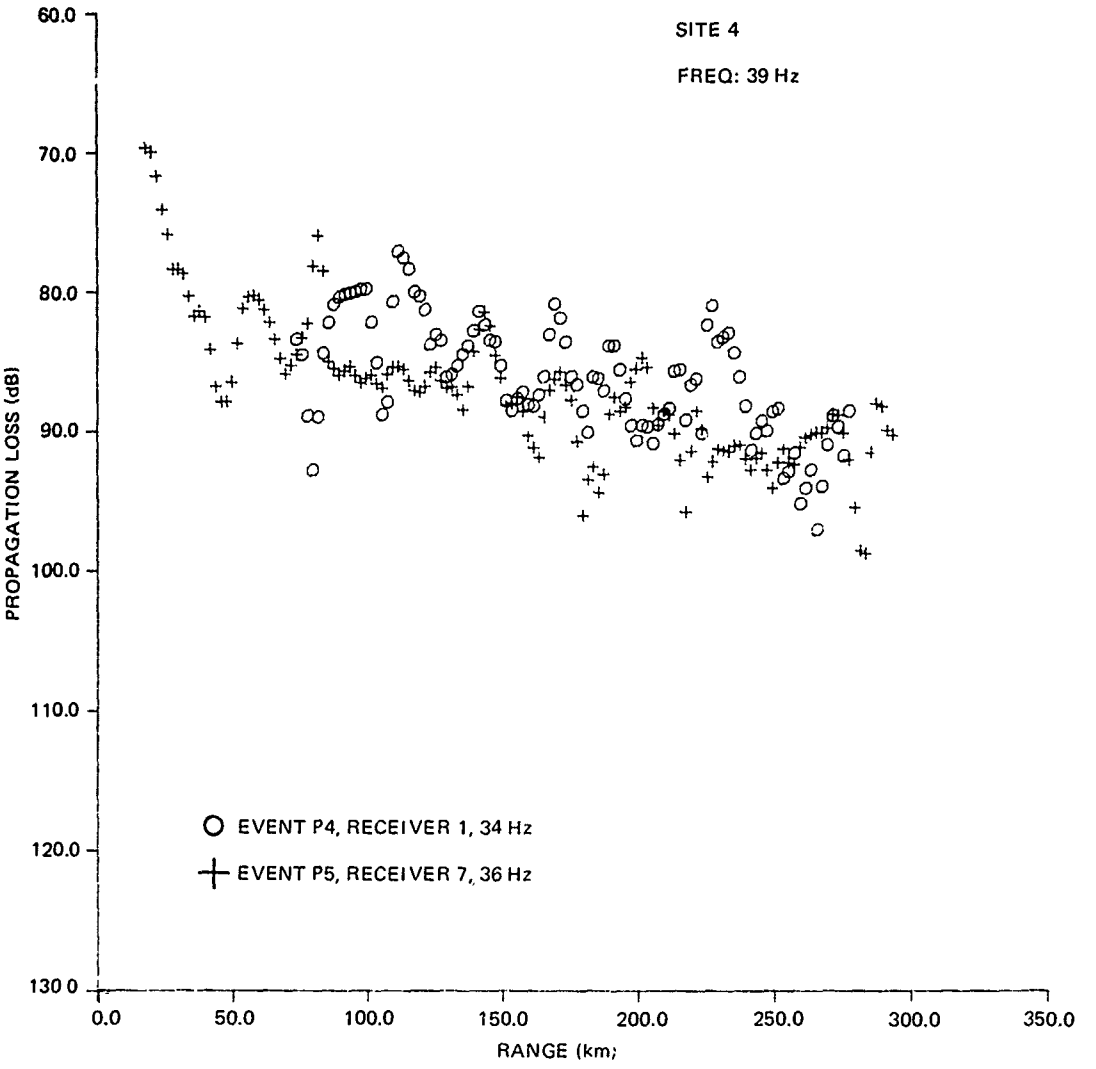

Figure 72. (C) Propagation loss at 39 Hz as a function of range at Site 4. (C)

7.9 dB better than BMA receiver 7 at 140 and 290 Hz. Furthermore, BMA receiver 1 is 9.7 to 14.2 dB better than ACODAC receiver 13, which was on the ocean floor. (This is not surprising – ACODAC receiver 13 was expected to have the highest losses because it is ensonified only by bottom bounce paths or, possibly, refracted paths.) Note that BMA receiver 1 has less propagation loss for these events than ACODAC receiver 9. Although receiver 9 was 30 m off the ocean floor and was closer to the critical depth excess of 66 m than BMA receiver 1, the higher loss at ACODAC receiver 9 was expected since it was below the critical depth.

Table 25. (C) Propagation loss differences between the receiver with lowest propagation loss and other receivers used at Site 4 CW events. (U)

Receiver Number		Receiver Depth (m)	Propagation Loss Differences (dB)											
			Event 4P1			Event 4P2			Event 4P4			Event 4P5		
			25Hz	140Hz	290Hz	25Hz	140Hz	290Hz	36Hz	140Hz	290Hz	39Hz	140Hz	290Hz
BMA	1	4726	4.8	0	0	3.3	0	0.1	0	0	0	6.3	3.5	0.6
	3	4486	4.5	0.8	0.9	4.8	1.5	0	5.6	2.8	3.3	5.3	0	0
	6	4236	12.2	5.5	8.1	5.9	7.0	3.8	6.9	7.4	5.5	8.8	7.8	3.7
	7	4048	0	2.4	5.4	0	5.9	3.0	1.9	6.8	7.9	0	3.7	2.2
	8	3778	1.0	3.3	8.5	0.8	5.9	5.0	1.0	6.1	7.6	0.3	3.7	2.3
ACODAC	2	400	4.1	5.1	6.1	4.3	8.3	3.8	5.3	8.5	6.4	4.1	5.2	2.2
	5	1916	4.3	4.3	7.5	4.0	8.1	5.5	5.5	8.2	7.5	3.7	5.1	3.6
	9	5076	0.5	1.7	8.0	1.4	4.7	6.6	2.0	5.2	9.1	−0.2	1.6	−0.1
	13	5106	1.7	10.8	12.0	1.7	14.2	9.7	2.5	13.0	12.4	0.3	11.3	4.7

Table 26. (C) Propagation loss differences between the receiver with the lowest loss and other receivers used at Site 4 SUS events. (U)

Event	BMA Receiver Number	20Hz Source Depth (m)			50Hz Source Depth (m)			140Hz Source Depth (m)		
		18	91	243	18	91	243	18	91	243
4S1	1	1.9	4.7	8.8	0.4	0.5	1.5	0	0	2.1
	3	1.0	4.4	6.7	3.0	3.0	3.4	0.7	0	1.3
	6	5.7	10.1	11.7	4.6	4.8	5.6	5.2	5.5	6.8
	7	0	0	0	0.7	0	0.5	1.4	0.2	0
	8	—	—	—	0	0.5	0	—	—	—
4A1	1	1.4	1.9		0	0		0	0	
	3	4.3	3.9		5.9	7.2		0.4	0	
	6	8.1	8.1		5.7	7.3		6.4	5.5	
	7	0	0		1.4	1.2		3.0	2.3	
	8	—	—		1.0	0.2		—	—	
4A2	1	1.2	0.1		0.8	0.7		0	0	
	3	7.1	4.3		9.2	8.7		2.7	2.8	
	6	5.5	7.0		4.7	7.3		3.6	3.7	
	7	0	0		1.4	2.7		1.8	1.6	
	8	—	—		0	0		—	—	

(C) Consider next, event 4P5, which had a critical depth excess of 30 m for an 18-m source depth. There are two important factors of this event that are clearly evident in table 25.

1. (C) ACODAC receiver 9 has the lowest propagation loss at 36 and 290 Hz, and is the second best at 140 Hz to BMA receiver 3.

2. (C) The small range of propagation loss differences at 290 Hz indicates that, under conditions of small critical depth excess, the dependence on receiver depth is not very significant. However, when the results of table 25 are taken as a whole and compared with the receiver depth dependence tables for Site 1B or Site 5, it is seen that the dependence on receiver depth is significantly more under convergence zone conditions than under bottom-limited conditions.

(C) The fact that the best receiver depth for event 4P5 at 290 Hz is ACODAC receiver 9 is of particular interest. This receiver was 30 m off the ocean bottom, which correlates well with the depth excess for the 18-m source shown in table 24 for event 4P5. As mentioned earlier, BMA receiver 1, the best receiver for the other CW event, was 380 m above the ocean floor. This is considerably more than the depth excess of table 24, which

varied between 147 and 30 m for the same events. The event 4P5 results strongly suggest that although BMA receiver 1 was generally the best receiver for events 4P1, 4P2, and 4P4 at 140 and 290 Hz, it was not at the optimum depth. It is believed that a receiver suspended perhaps 100 m off the bottom would have performed better than BMA receiver 1 because it would have been in the critical depth region.

(C) Consider now the dependence on receiver depth for the SUS events and frequencies of table 26 for Site 4. The highest frequency of the data from the SUS events that were processed for Site 4 was 140 Hz for the BMA receivers. For all the SUS events at 140 Hz for source depths of 18 and 91 m, BMA receiver 1 had the lowest propagation loss. Although the differences between receivers 1 and 7 of the SUS events were not as large as for the CW events, the results here substantiated the conclusion that receiver 1 was the best receiver at Site 4 for 140 and 290 Hz at the shallow source depths.

(C) In event 4S1 for the 243-m source depth at 140 Hz, receiver 7 had less propagation loss than receiver 1 by 2.1 dB. This result was not surprising since the conjugate depth for the 243-m source depth was approximately 3000 m, which is closer to the depths of receivers 7 and 8 than the depth of receiver 1. (This is also a possible explanation why receivers 7 and 8 have smaller losses than receiver 1 at 20 and 50 Hz for the 243-m source depth. However, it is not clear whether conjugate depth is the principal mechanism, since similar results hold for the 18- and 91-m source depths.)

(C) The analyses of the low-frequency (25 to 50 Hz) results show a significant contrast to the results at 140 and 290 Hz. Under convergence zone conditions, we would expect the minimum loss to occur near the conjugate or critical depth, which, according to table 24, was between 197 and 276 m off the ocean floor for the 91-m source depth of the CW events. We would also expect, then, that BMA receiver 1 would be the best receiver at these low frequencies and at the 18-m source depth. However, these expectations were not confirmed.

(C) BMA receiver 7 was the best receiver for events 4P1, 4P2, 4S1, 4A1, and 4A2 at 25 or 20 Hz. For the CW events (4P1, 4P2, and 4P5), receiver 7 had lower propagation losses, 3.3 to 6.3 dB, than receiver 1 for the 91-m source depth. Corresponding values for the SUS events ranged from 0.1 to 4.7 dB. The low value of 0.1 dB (event 4A2 in table 26) resulted because receiver 1 had lowest losses at the near ranges and receiver 7 at the longer ranges. Since event 4A2 had the most oblique close range bathymetry at Site 4, the results for the event suggest perhaps that the relative losses for receivers 1 and 7 depend on the bottom slope away from the receivers.

(C) At 50 Hz for the 18- and 91-m source depths (table 26) the propagation losses for receivers 1, 7, and 8 are comparable and within 1 dB of each other. For event 4A1, receiver 1 has the lowest loss whereas for events 4S1 and 4S2, receiver 7 or 8 has the lowest losses. The results of event 4P4 at 39 Hz also show that the three receivers are comparable. This indicates that, at the lower frequencies, the choice between receivers 1 and 7 is not clear-cut as it was for 140 and 290 Hz.

(C) Hence, this analysis of the low-frequency results at Site 4 suggests that the optimum receiver depth may be a very complicated function of frequency and that convergence zone propagation may not be effective at the low frequencies

(C) After the BEARING STAKE tests at sea and before the above analyses reported herein, Bell Telephone Laboratories (BTL), a participant in BEARING STAKE, recommended that a surveillance systems assessment be made at Site 4 utilizing data from BMA

receiver 7. This recommendation, no doubt, was based upon the smaller propagation loss for receiver 7 at 20 and 25 Hz. However, as has been shown in this report for event 4P4, the propagation loss for receiver 7 was 6.8 and 7.9 dB greater than the propagation loss for receiver 1 at 140 and 290 Hz, respectively. Moreover, the smaller losses for receiver 1 at 39 Hz for event 4P4, and the mixed results of the 50-Hz data, suggest that a strong case can be made for receiver 1 for a systems assessment. Also, in other seasons with greater depth excess conditions, the dependence on receiver depth may be quite different.

(C) The assessment of receiver depth dependence at Site 4 in this report is that the optimum receiver depth at the site is an open issue. Before an optimum depth at Site 4 can be selected, a much better understanding of the physical principles involved is necessary. This understanding can be obtained by a vigorous theoretical analysis, followed and verified by additional experimental measurements.

6.5 (U) DEPENDENCE ON EVENTS

(C) Propagation loss is presented as a function of range for the receivers with lowest losses for the radial events at Site 4 in figures 73, 74, 75, and 76. The CW events are plotted as open symbols, the SUS events as line symbols. The "arc" events are not included in the analysis because, under convergence zone conditions, slight changes in range can obscure azimuthal dependence.

(C) The ranking of the events according to increasing propagation loss is given in table 27. The ranking at 140 Hz is the same as at 25 and 50 Hz with the exception of event 4A2. The general pattern to the rankings is that the highest-rank event was conducted in a northerly direction from the site, and each descending-rank event approaches a westerly direction in a counterclockwise direction (see fig 62). In other words, the propagation loss to the north of Site 4 was found to be less than the losses to the west. There was very little difference in the maximum bottom depth, event to event, as they crossed the Somali Basin. However, the upward slope of the bottom was less in the northerly direction than in the westerly direction. Small but consistent differences in bottom depth could affect CW sources at 18-m depth for 290 Hz. However, it is difficult to imagine how these differences would affect the 91-m source depths since table 24 indicates a relatively large depth excess for a 91-m depth.

(C) At 290 Hz, the rankings of events 4P1 and 4P5 agree with the depth excesses of table 24. However, that is about the extent of agreement between tables 24 and 27. As noted in the optimum receiver depth discussion, there needs to be a better understanding of the physical principles of near-bottom-limited propagation before a satisfactory interpretation can be made of the ranking of events conducted at Site 4.

6.6 (U) DEPENDENCE ON RANGE AND FREQUENCY

(C) The propagation losses for the events with the lowest propagation losses at Site 4 for 25, 39, 140, and 290 Hz are compared to the Eleuthera reference in figure 77. The values plotted in figure 77 are given in table 28. First, note that despite the fact that there are strong convergence zones at 290 Hz, the curves of the propagation loss averages over the 50-km range bins are just as smooth as the curves presented previously for the

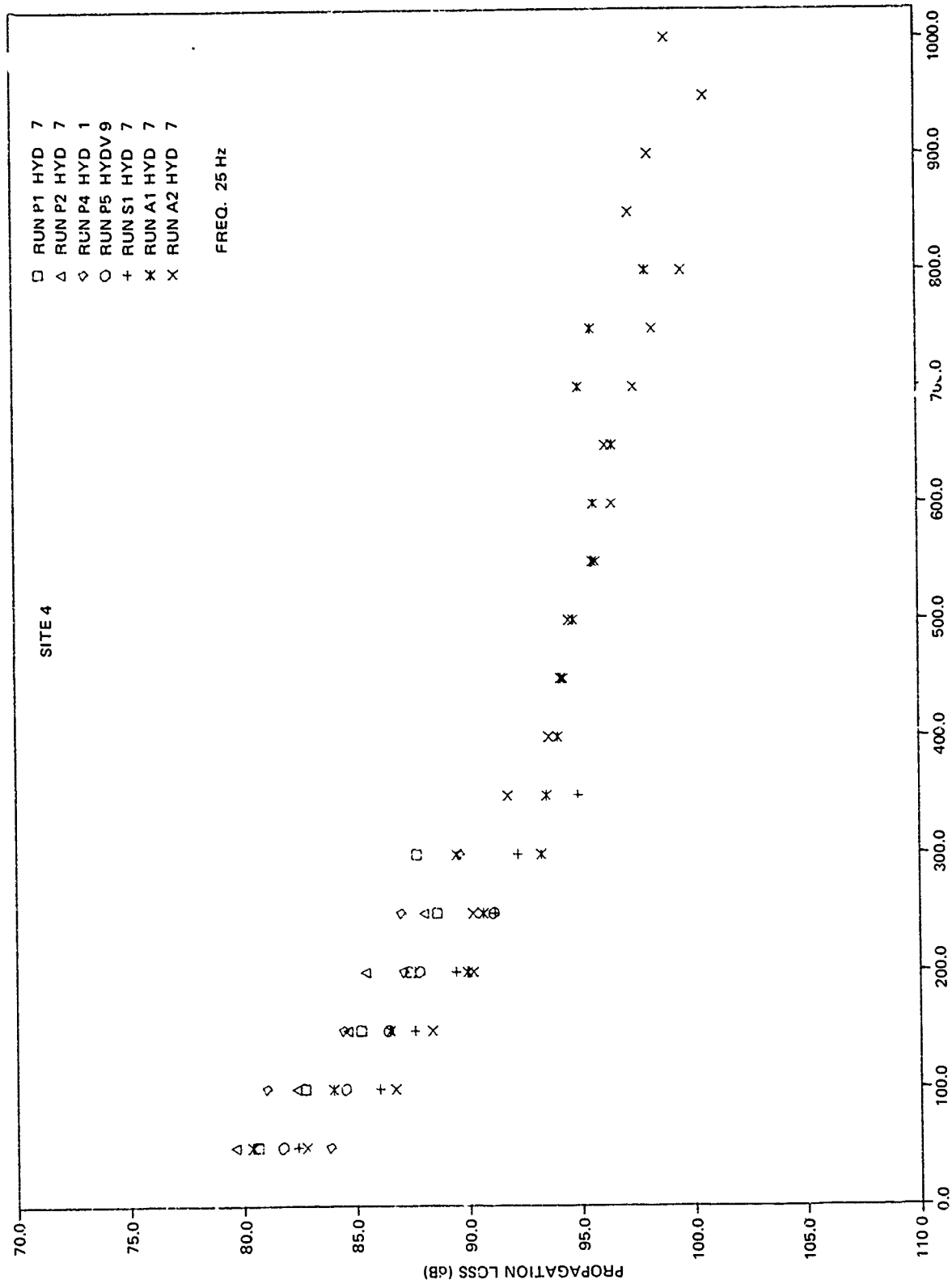

Figure 73. (C) Propagation loss at 25 Hz as a function of range for the events conducted at Site 4. (C)

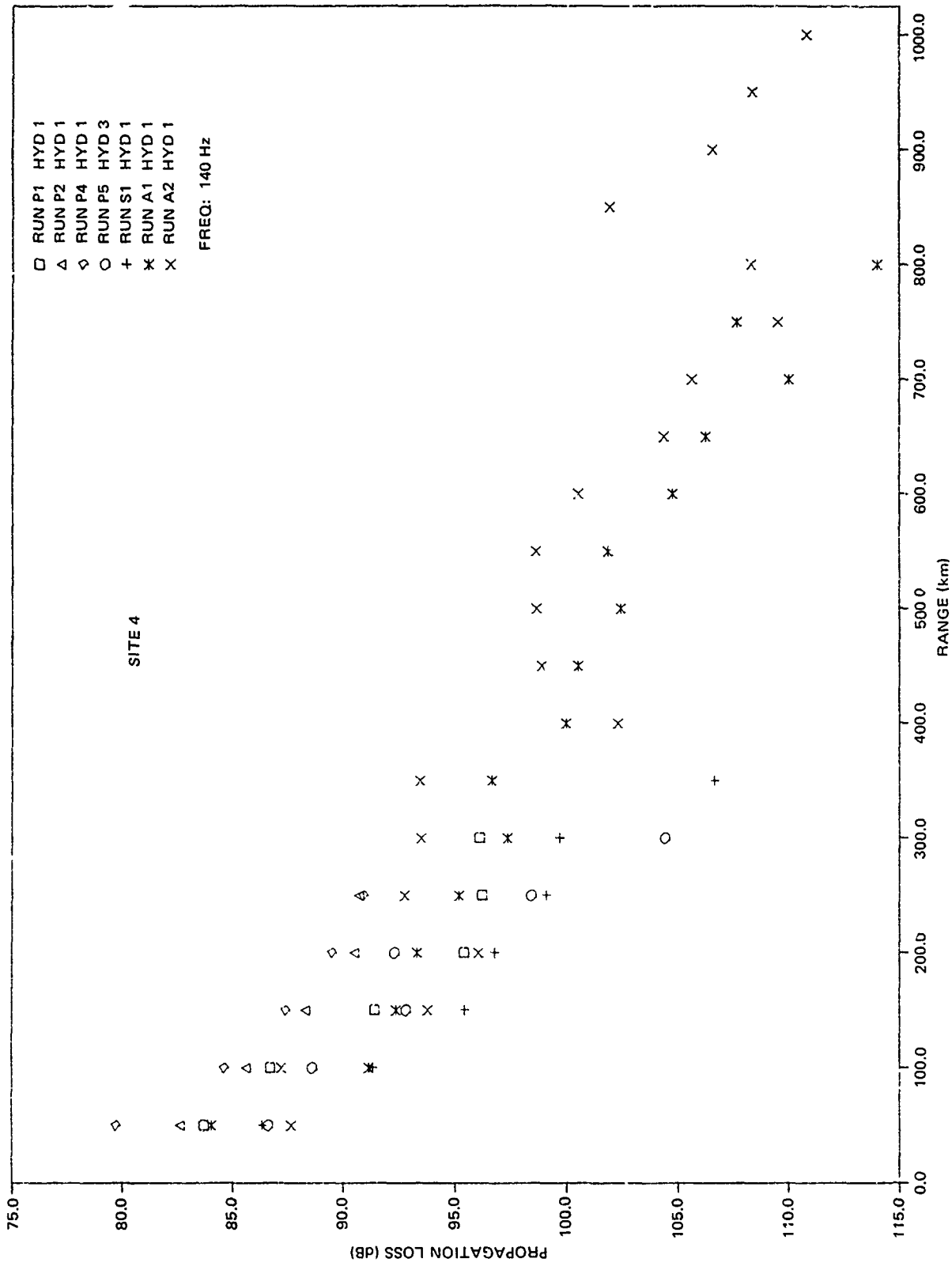

Figure 74. (C) Propagation loss at 140 Hz as a function of range for the events conducted at Site 4. (C)

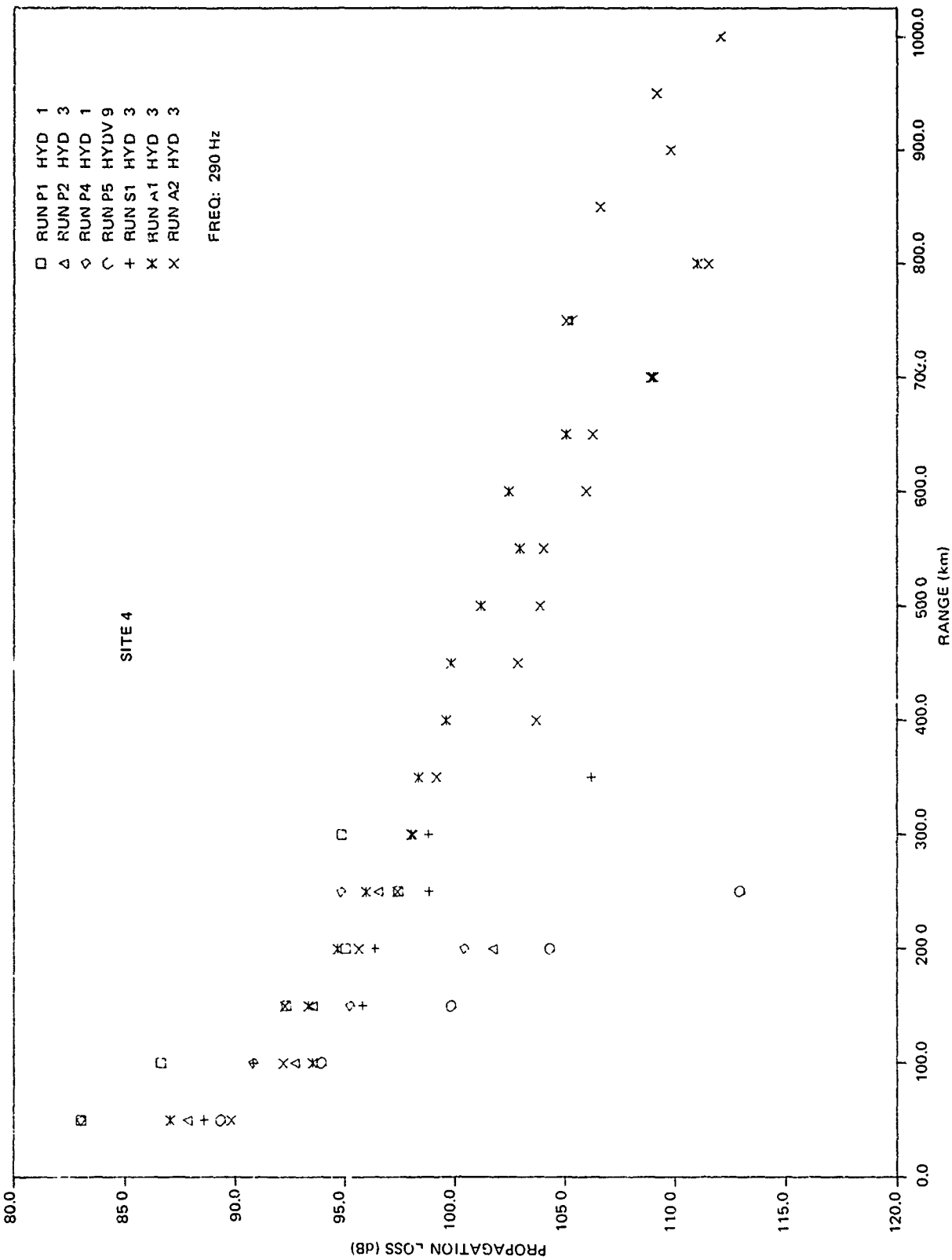

Figure 75. (C) Propagation loss at 290 Hz as a function of range for the events conducted at Site 4. (C)

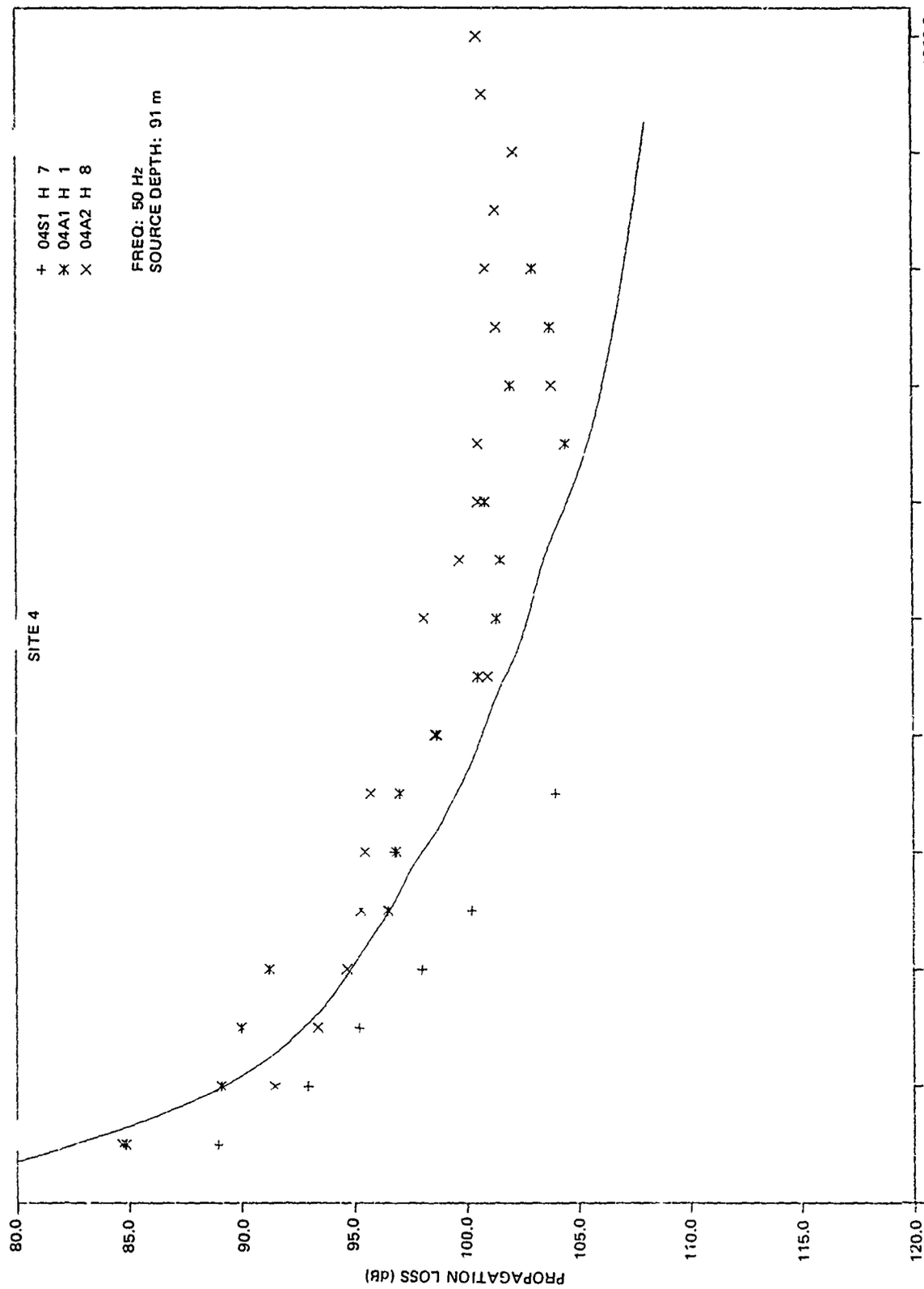

Figure 76. (C) Propagation loss at 50 Hz as a function of range for the events conducted at Site 4. (C)

Table 27. (C) Ranking of events at Site 4 according to propagation losses. (U)

Rank	Events				
	Low (20-40) Hz	140Hz	290Hz	50Hz	Overall Ranking
1	4P4	4P4	4P1	4A1	4P4
2	4P2	4P2	4P4	4A2	4P2
3	4P1	4P1	4A1	4S1	4P1
4	4A1	4A2	4A2	—	4A1
5	4P5	4A1	4P2	—	4A2
6	4S1	4P5	4S1	—	4S1
7	4A2	4S1	4P5	—	4P5

bottom-limited sites. Although the 50-km range-bin averages were devised to treat bottom-limited propagation losses, the same procedure worked well for the convergence zone conditions of Site 4. The reason it works is that each 50-km range bin contains the data from one convergence zone.

(C) The slopes of the propagation loss curves for 25 and 39 Hz shown in figure 77 are less than that of the reference curve. The propagation losses at long range for these low frequencies are about 10 dB less than those of the reference. At 140 Hz, the propagation losses are as much as 6 dB less than those of the reference; and at 290 Hz, the losses are generally equal to those of the reference.

(C) The SUS event with the lowest propagation loss at 50 Hz was event 4A1. The propagation loss curve is plotted in figure 76. The slope of the loss curve appears somewhat less than that of the reference. At short ranges, the 50-Hz loss is greater than the reference loss by as much as 2.5 dB and is about 6 dB less than the loss of the reference at the longer ranges.

6.7 (U) SEASONAL DEPENDENCE

(C) The analyses of the propagation loss data at Site 4 at the present time indicate that the results from the site may be strongly dependent on seasonal variations in the environment. The acoustic results for event 4P5 indicate that the near-surface sound speeds are critical. The sound speed at the ocean bottom (5106 m) was calculated to be 1543.7 m/s. The maximum near-surface sound speed for event 4P5 was calculated to be, on the average, the same value. Any increases in the near-surface sound speed will thus make the site bottom limited.

(C) In fact, Colborn's historical data (ref 13) appropriate for the Somali Basin indicate that the period March through May is the most likely period that the site will be bottom limited. In this time period, 7 of 21 sample cases had near-surface sound speeds

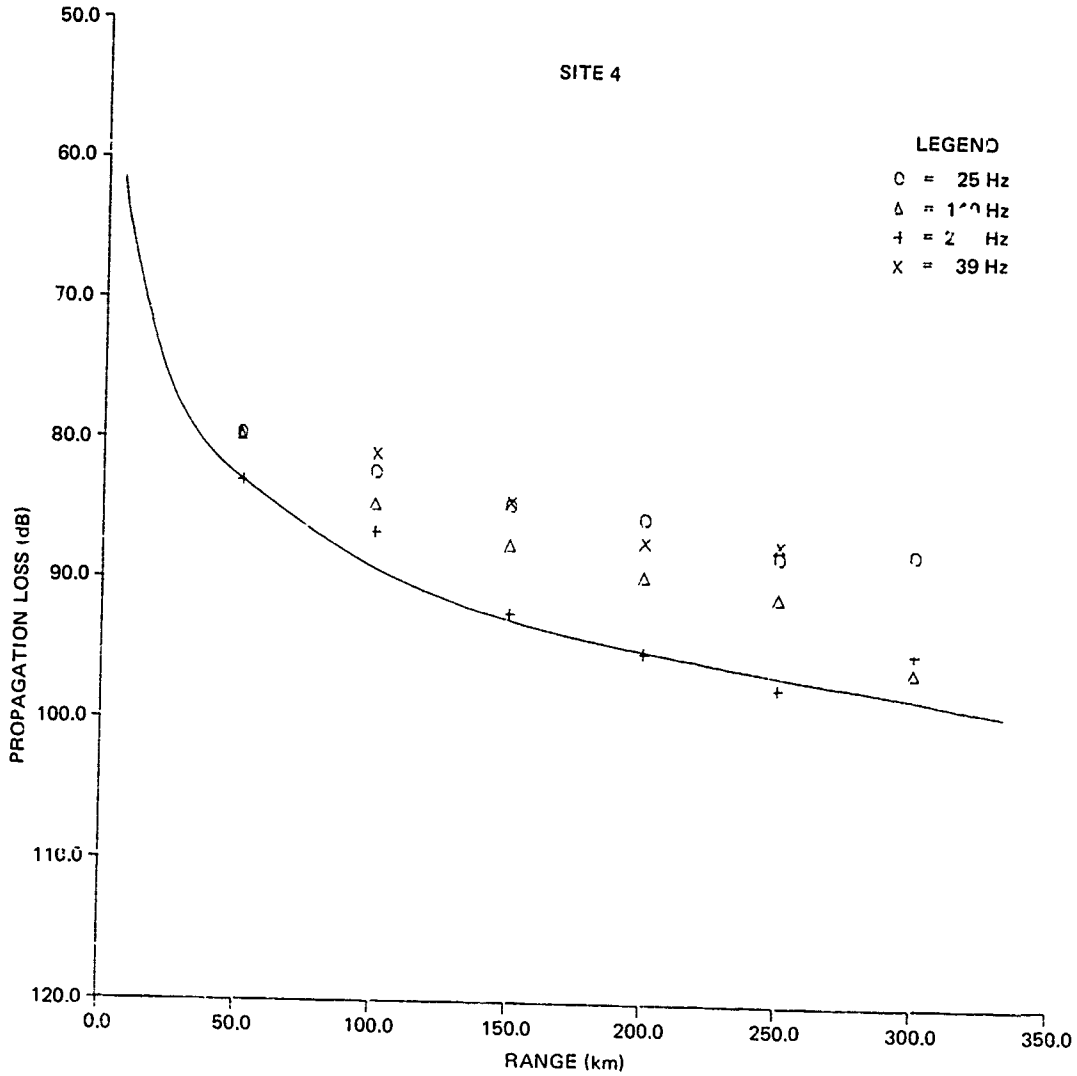

Figure 77. (C) Comparison of propagation loss at 25, 39, 140, and 290 Hz with the Eleuthera reference. (C)

which exceeded 1543.7 m/s. These 7 samples occurred between April 20 and May 17 and represented six different years. These data are in agreement with other studies of surface temperature which indicate maximum temperatures in April with higher temperatures in May than in March. Thus, propagation conditions at high frequencies (290 Hz) may be expected to be worse than those encountered in event 4P5 for the months of April and May, and better than those encountered in event 4P1 for the months of June through February. However, at low frequency (25 Hz) and perhaps at the intermediate frequency (140 Hz), we may expect that propagation conditions for April and May would not be significantly worse than those encountered during BEARING STAKE. Propagation at these frequencies could improve during conditions of large depth excess.

Table 28. (C) Propagation loss of the best events at Site 4 as a function of range and frequency. (U)

Range (km)	Propagation Loss (dB)				
	Event 4P2 (25 Hz)	Event 4P4 (140 Hz)	Event 4P1 (290 Hz)	Event 4P4 (39 Hz)	Event 4A1 (50 Hz)
50	79.6	79.7	83.0	—	84.8
100	88.3	84.6	86.6	81.0	89.1
150	84.6	87.4	92.3	84.4	90.0
200	85.4	89.5	95.0	87.1	91.2
250	88.0	90.9	97.4	87.2	96.5
300	87.7*	96.1*	94.8	—	96.9

*Event 4P1

(C) Good convergence zone propagation requires some minimal depth excess. It is most likely that this minimal depth excess generally increases with decreasing frequency. Thus, at low frequencies, convergence zones may play a larger role in propagation under conditions of large depth excess.

6.8 (U) QUESTIONABLE DATA SETS

(U) As pointed out in the discussion of tables 25 and 26, the propagation losses for BMA receiver 6 were excessively high. The calibration of this receiver could be in error or the receiver itself may have malfunctioned. It is also possible that the receiver was occluded by some small bathymetric feature.

(C) For BMA receiver 3, the propagation loss at 140 Hz at the range interval of 180 to 260 km appears to be about 10 dB too high. This questionable loss was discovered by noting that, for the range bin which includes these data, the difference between receivers 3 and 1 was 13 dB. If this value is excluded, the maximum loss at 140 Hz between the two receivers is 5.2 dB for the other range bins.

(C) The propagation losses for event 4S1 at all frequencies appear excessively high and should be re-examined. In figures 73 to 76, the losses for this event are inexplicably higher than for the other SUS events. Also a comparison of event 4S1 with event 4P1 shows differences which are 1.3, 1.4, and 2.8 dB higher, at respective frequencies of 20, 140, and 290 Hz, than the differences which are typical for this type of comparison at the other BEARING STAKE sites.

6.9 (U) SITE 4 SUMMARY

(C) Site 4, in the Somali Basin, the only BEARING STAKE site which was not bottom limited, exhibited convergence zone propagation behavior as expected. However, the convergence zones at the site were strongly frequency dependent. Prominent zones at

290 Hz appeared 15 dB above the bottom-reflected background. In contrast, there was very little evidence of convergence zones at 25 Hz.

(C) Propagation conditions at Site 4 may be seasonally dependent. The BEARING STAKE measurements at the site were made in March, which was near the predicted month (April) of maximum near-surface temperature and, thus, minimal depth excess. For other seasons, the depth excess will increase and a strong dependence of propagation loss on season is predicted. This is in contrast to the other strongly bottom-limited sites of BEARING STAKE, at which the seasonal dependence of propagation loss will be minimal.

(C) Nevertheless, the propagation losses to the north of Site 4 were found to be less than the losses to the west of the site. The minimum propagation loss over the range interval 50 to 300 km was 79.6 to 87.7 dB for 25 Hz, 79.7 to 96.1 dB for 140 Hz, and 83.0 to 94.8 dB for 290 Hz.

(C) The propagation losses at Site 4 for 25, 50, 140, and 290 Hz were less than those of the Eleuthera reference at corresponding ranges.

(C) At Site 4, the two receivers with lowest propagation loss results were receivers 1 and 7, located on the Chain Ridge about 400 and 1050 m, respectively, above the floor of the Somali Basin. At 140 and 290 Hz, receiver 1 had less propagation loss than receiver 7 by as much as 7 dB. This was as expected and is related to the critical depth of convergence zone propagation. However, at 25 Hz, receiver 7 had propagation losses which were as much as 5 dB less than those of receiver 1. The physical explanation for this result is not known and attempts to model the result have not been successful. The experimental results suggest a complicated dependence on receiver depth and frequency.

6.10 (U) RECOMMENDATIONS FOR ADDITIONAL DATA PROCESSING

(C) Additional data processing is required to establish the complicated frequency-receiver depth dependence in which BMA receiver 1 is best at 140 and 290 Hz while receiver 7 is best at 25 and 50 Hz. It is recommended that, for all the CW events at Site 4, additional data processing include BMA receivers 2, 4, and 5 at all frequencies. For SUS event 4S1, all receivers should be processed; i.e., receivers 1–8 at frequencies of 20, 35, 50, 75, and 100 Hz. These data sets will be analyzed and compared, and then a determination will be made whether additional receiver-frequency combinations are necessary.

(C) During event 4P5, the CW source was turned off at 0400, 19 March, at a range of 295 km. Both BMA and ACODAC data were processed to this point. Transmissions were resumed at 1500, 19 March, at a range of 485 km. If these latter data were recorded, they should be processed for both BMA and ACODAC systems. This portion of event 4P5 is the only CW event in BEARING STAKE in which there was substantial shoaling of the bottom along the track of the event. Event 4P5 started over a bottom depth of about 5100 m and ended over a bottom depth of about 1800 m.

7.0 (U) SITE 5 ASSESSMENT

7.1 (U) INTRODUCTION

(C) Site 5 was located on the northern edge of the Carlsberg Ridge south of the Suez Canal-Orient shipping lanes. It was located on the flat top of a low rise (500-m elevation above the seafloor) in 4500 m of water. Sediments from the Arabian deep sea fan edge up to the flanks of the ridge in this area, which gives the impression that the bottom is highlighted by elongated ridges. In actuality, they are partially buried ridges. It was atop one of these topographic highs that the BMA was positioned. Figure 78 shows the configuration of the BMA at the site.

(U) Figure 79 shows the propagation runs conducted at Site 5. The runs to the north and northeast were made over a smooth bottom which sloped gently upward to the northeast. The remaining runs (5P3 and 5P5) were made over rough bottoms associated with the Carlsberg Ridge proper.

(C) Sound speed profiles taken along the various tracks of each run at Site 5 indicated that acoustic propagation would be severely bottom limited throughout the operating area. Figure 80 is representative of the sound speed profiles that were measured at the site. The profile shows the presence of a depressed surface duct at 30–50-m depth, and sound speed minimums at 450- and 1768-m depths.

(U) Table 29 summarizes the extent of the acoustic data set, measured by the bottom-mounted array (BMA), used in this report to assess propagation loss at Site 5. Shown are the source frequencies and depths, and the depths of the receiving hydrophones.

(U) The discussions to follow in this section include the effects of the bathymetry close to the receivers and the effects on propagation loss of receiver depth, events conducted, range, and frequency. The results are then assessed and summarized.

7.2 (U) BATHYMETRIC FEATURES

(C) The bathymetry at Site 5 played a prominent role in the acoustic propagation conditions at the site. The events conducted at the site were shown previously in figure 79 and the configuration of the BMA receivers in figure 78. BMA receivers 3 and 5 were located about 10 m from the top of a small conical hill rising about 700 m above the south end of the Indus Fan. Receiver 2 was buoyed up about 380 m above the hill, while receiver 1 was buoyed up about 600 m above the hill.

(U) The close range bathymetry for events 5P1, 5S1, 5A1, 5A3, 5P2, 5A2, and 5P5 is shown in figures 81 through 87, respectively. Figures 81, 82, 83, and 84 (events 5P1, 5S1, 5A1, 5A3) show the conical hill with its peak at zero range. There were no obstructions at close range for these events. The long range bathymetry (see appendix A, fig A12 and A13) for the same events shows a very gentle slope with no obstructions.

(C) Figures 85 and 86 (events 5P2 and 5A2) show significant obstructions which rise about 500 and 600 m above the basin floor. The long range bathymetry for event 5P2 was flat beyond 40 km. However, the long range bathymetry for event 5A2 shows a minor obstruction at 280-km range and a major obstruction at 650-km range where the event crosses the Owen Ridge (appendix A, fig A-12).

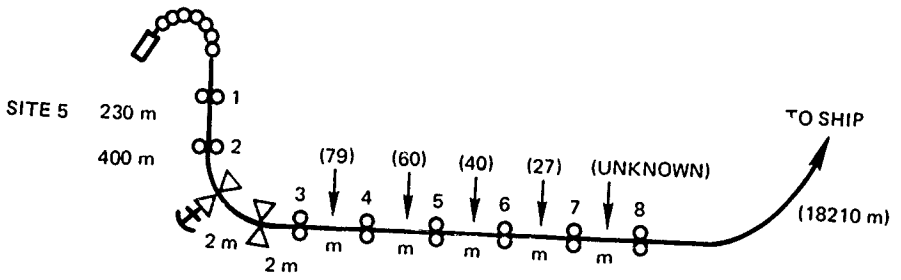

Figure 78. (U) Geometry of the BMA at Site 5. (U)

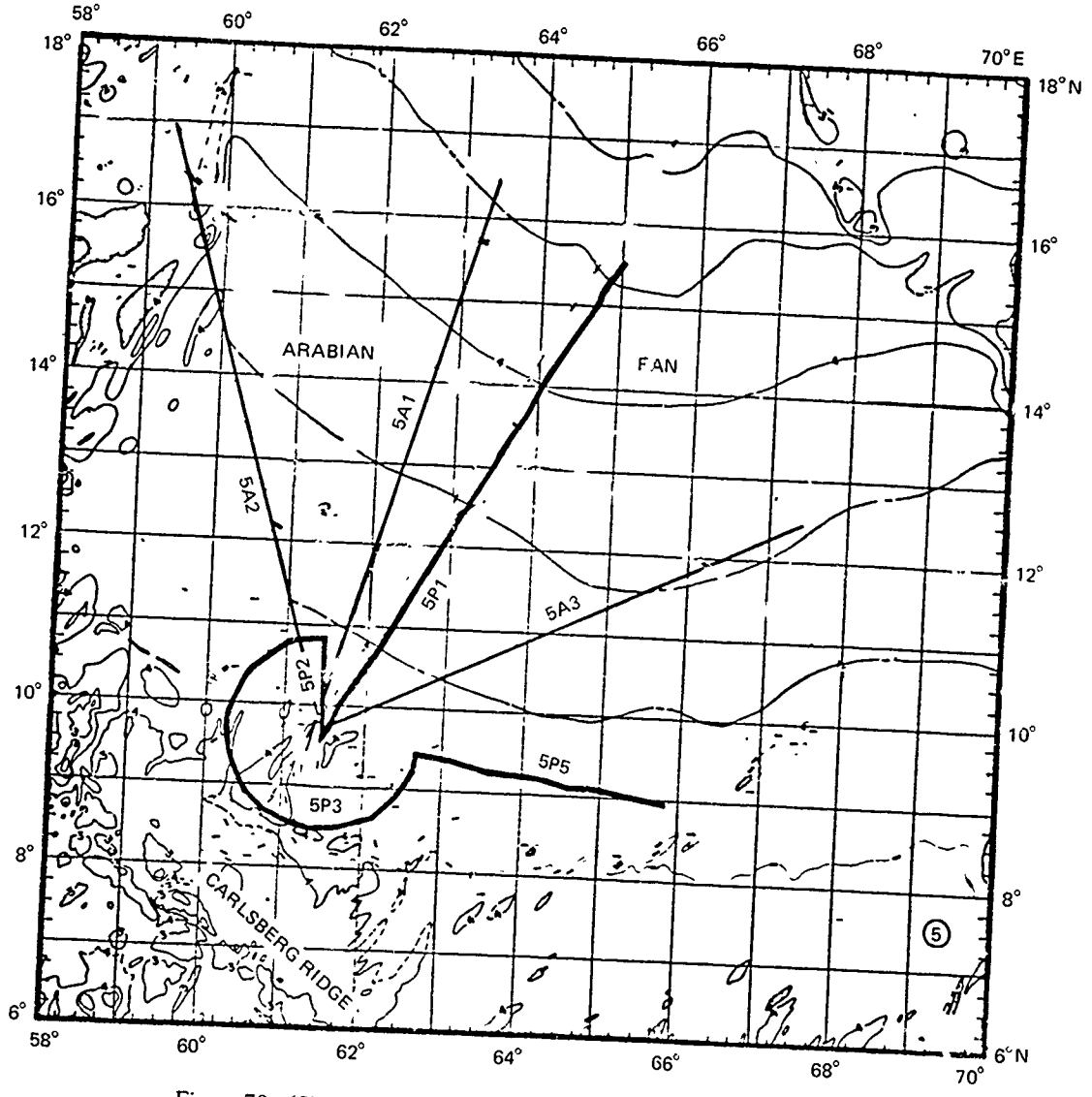

Figure 79. (C) Track of propagation loss runs conducted at Site 5 by the source ship and aircraft. (U)

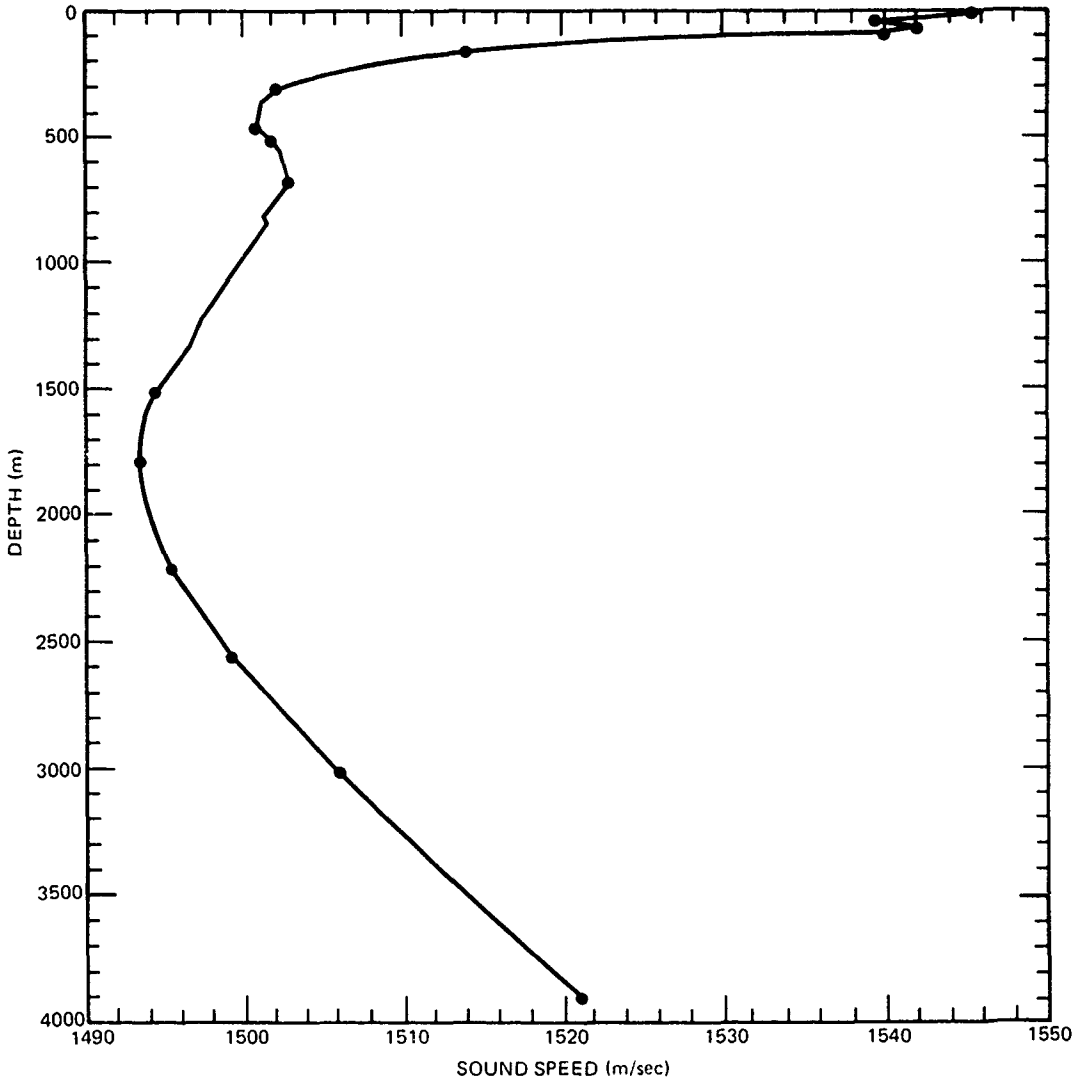

Figure 80. (U) Representative sound speed profile for Site 5. (U)

(C) In figure 87, the close range bathymetry for the propagation paths of event 5P5 shows a major obstruction rising about 1 km above the basin floor. At longer ranges, there was a minor obstruction centered at 150 km from the receivers. The range limits of event 5P5 were from 131 to 407 km so most of the event itself was over a flat bottom with the propagation paths crossing over the major obstruction and on to the receivers.

7.3 (U) DEPENDENCE ON RECEIVER DEPTH

(C) The receiver depth dependence for the CW and SUS events at Site 5 is given in tables 30 and 31. Consider, first, the low-frequency data at 22 to 50 Hz shown in the tables.

Table 29. (C) Summary of the propagation loss data set from the BMA collected at Site 5 from the projector (P) and SUS runs. (U)

BMA Hydrophone No. Depth (m)		1 3243	2 3468	3 3865	4	5 3844	6	7	8
Freq (Hz)	Source Depth (m)								
Run 5P1: 759 to - 12 km									
22	77	X				X			
140	18	X				X			
290	18	X				X			
Run 5P2: −9 to 131 km									
36	91	X	X	X		X			
140	18	X				X			
290	18	X				X			
Run 5P5: 130 to 409 km									
36	91	X	X	X		X			
140	18	X				X			
290	18	X				X			
Run 5P3: Circular 131 km									
36	91	X	X	X		X			
140	18	X				X			
290	18	X				X			
*Run 5S1, 5A1, 5A2, 5A3									
20						X			
50		X	X	X		X			
140						X			
300						X			

These were SUS runs. SUS depths were 18, 91, and 243 m for ship runs (S) and only 18 and 91m for aircraft runs (A).

*Run No	Range (km)
5S1	0 to 446
5A1	1 to 779
5A2	854 to 14 (closing)
5A3	0 to 714

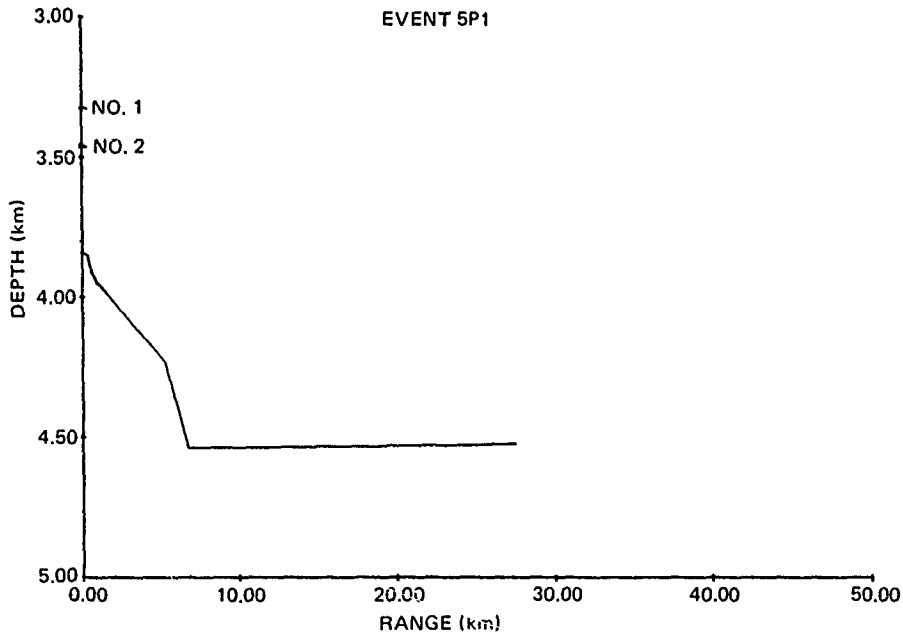

Figure 81. (U) Close range bathymetry for event 5P1. (U)

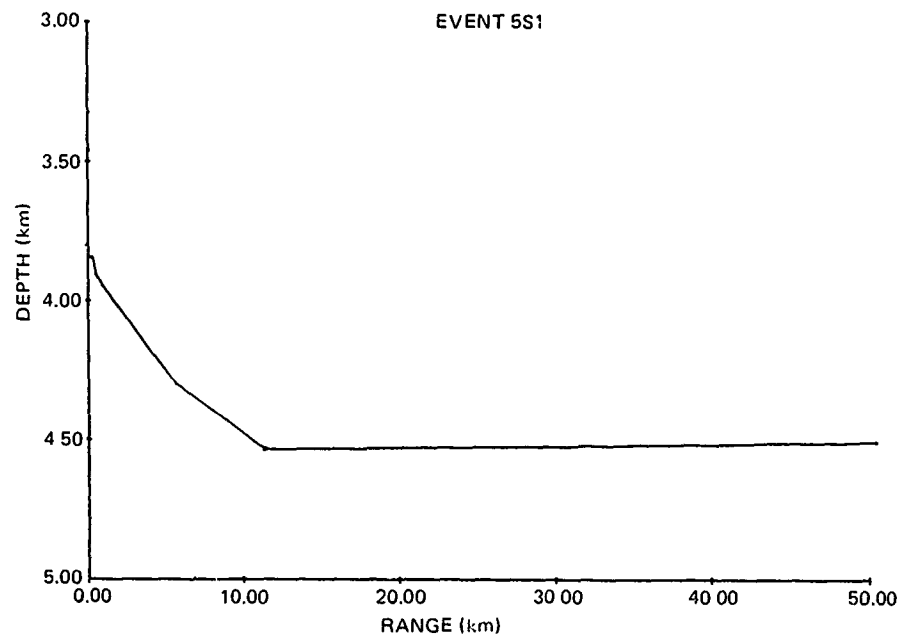

Figure 82. (U) Close range bathymetry for event 5S1. (U)

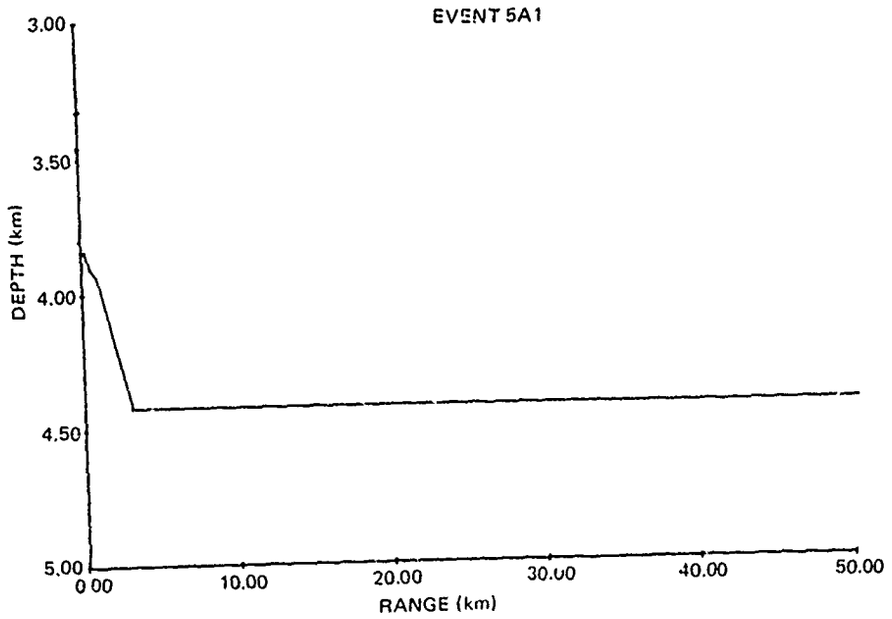

Figure 83. (U) Close range bathymetry for event 5A1. (U)

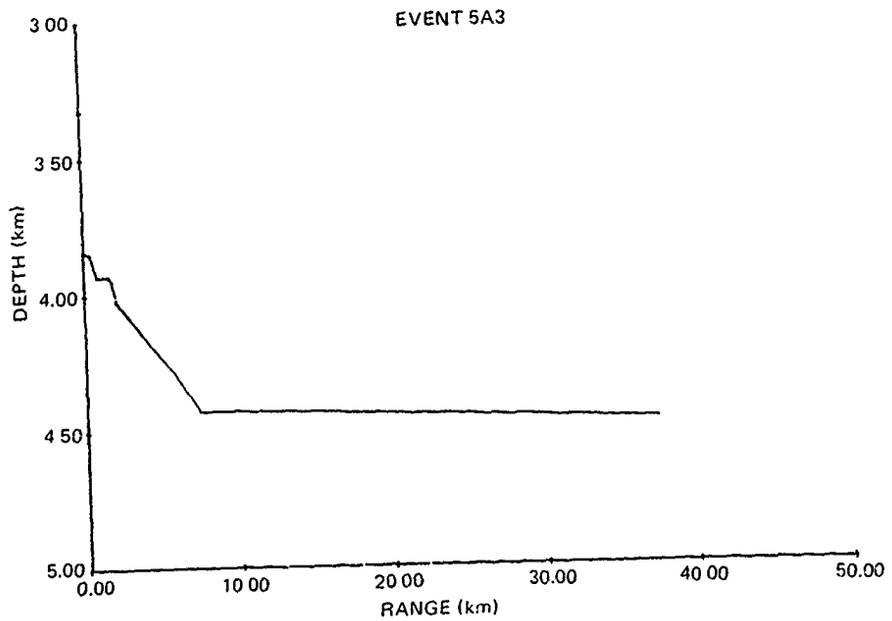

Figure 84. (U) Close range bathymetry for event 5A3. (U)

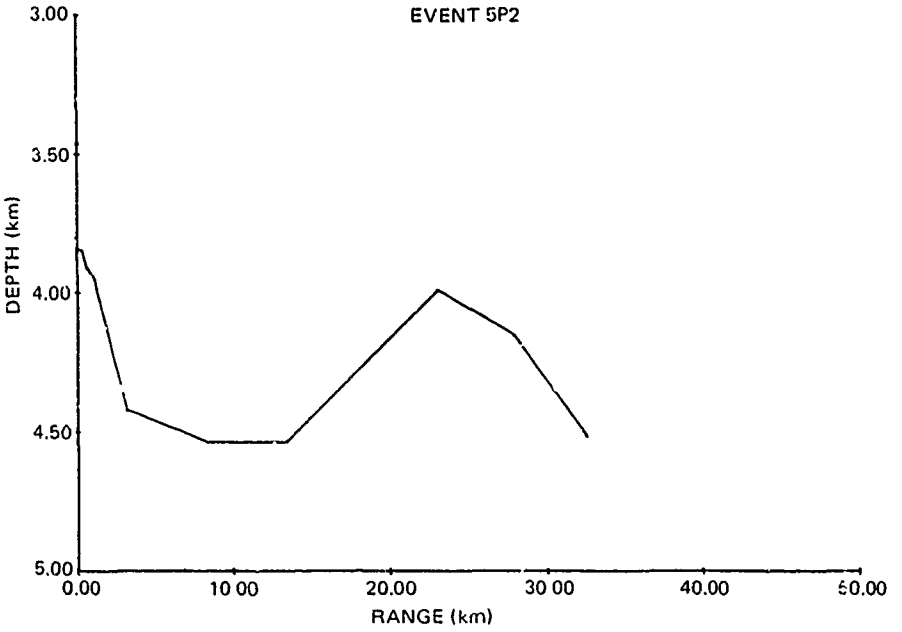

Figure 85. (U) Close range bathymetry for event 5P2. (U)

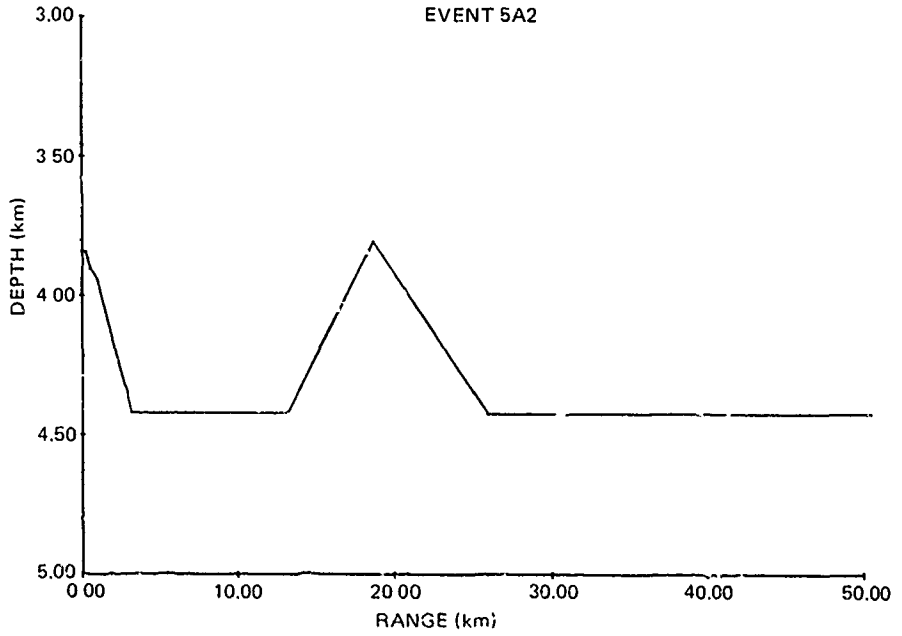

Figure 86. (U) Close range bathymetry for event 5A2. (U)

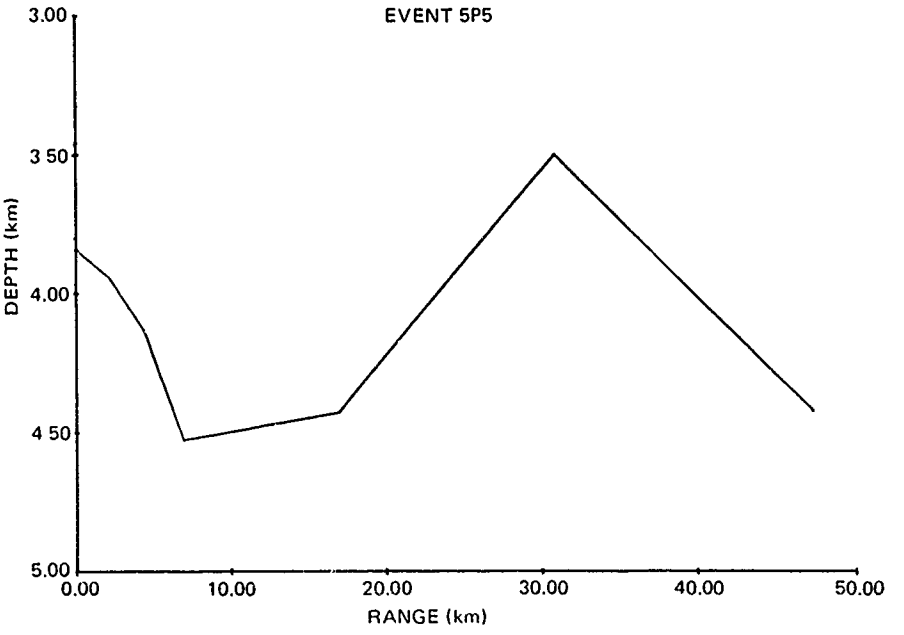

Figure 87. (U) Close range bathymetry for event 5P5. (U)

The bottomed receivers (receivers 3 and 5) always have less propagation loss than the suspended receivers (1 and 2). Moreover, there is no significant difference in the propagation loss between receivers 1 and 2. If all the low-frequency data are combined for each receiver, receiver 1 has an average propagation loss of 0.1 dB less than that for receiver 2. On the average, receiver 3 has 1.4 dB less propagation loss than receiver 5, and receiver 1 has 1.2 dB more loss than receiver 5.

(C) Unfortunately, only two receiver depths were processed at 140 and 290 Hz; namely, receivers 1 and 5. The results of the propagation loss differences at these frequencies and receivers are somewhat mixed, as can be seen in table 30. By averaging the propagation loss at 290 Hz for each receiver for all the events, the propagation loss for receiver 1 is only 0.1 dB less than the loss for receiver 5. However, receiver 5 may have been a poor receiver since it had 1.4 dB more loss than receiver 3 at the lower frequencies. It would be informative to know how receiver 3 would have behaved if compared to receiver 1 at 140 and 290 Hz. (The differences between receivers 1 and 5 may be a moot subject, since there is strong evidence suggesting that a receiver placed on the bottom of the Indus Fan will outperform any suspended receiver above the conical hill.)

7.4 (U) DEPENDENCE ON EVENTS

(C) The propagation losses for the receiver with the lowest loss for all the events conducted at Site 5 are plotted as a function of range, at four frequencies, in figures 88, 89, 90, and 91. Events in which there was no obstructing bathymetry at close range are shown as open symbols, events with obstructing bathymetry as line symbols. As expected, those

Table 30. (C) Propagation loss differences between the BMA receiver with the lowest propagation loss and other BMA receivers for Site 5 CW events. (U)

BMA Rcvr. No	Rcvr. Depth (m)	Propagation Loss Difference (dB)											
		Event 5P1			Event 5P2			Event 5P5			Event 5P3		
		22 Hz	140 Hz	290 Hz	36 Hz	140 Hz	290 Hz	36 Hz	140 Hz	290 Hz	36 Hz	140 Hz	290 Hz
1	3243	1.8	0	0	2.7	0	0	0.7	0	0.9	1.3	1.0	0.3
2	3468	–	–	–	2.5	–	–	1.7	–	–	2.2	–	–
3	3865	–	–	–	0	–	–	0	–	–	1.4	–	–
5	3844	0	2.8	1.0	0.7	2.8	0.6	0.8	0.1	0	0	0	0

CONFIDENTIAL

Table 31. (C) Propagation loss differences between the BMA receiver with the lowest propagation loss and other BMA receivers for Site 5 SUS events at 50 Hz. (C)

BMA Rcvr. No	Rcvr. Depth (m)	Propagation Loss Differences (dB)								
		Event 5S1			Event 5A1		Event 5A2		Event 5A3	
		Source Depth (m)								
		18	91	243	18	91	18	91	18	91
1	3243	1.7	2.8	2.4	1.8	3.5	3.4	3.0	5.8	3.3
2	3468	2.7	2.7	2.6	1.5	3.7	3.2	2.8	4.7	3.2
3	3865	0	0	0	0	0	0	0	0	0
5	3844	1.1	2.6	2.8	0.2	2.2	1.6	2.3	2.5	1.3

events with no obstructions suffer less propagation loss, as can be observed from the figures. In figures 88, 89, and 90, the vertical lines with arrows at a range of 131 km span the minimum and maximum propagation loss for ten 30° bearing bins from event 5P3, which was an "arc" event.

(C) Table 32 ranks the radial events according to increasing propagation loss at the frequencies listed. The ranking of events is identical at 50, 140, and 290 Hz. The ranking at 25 Hz is slightly different from the higher-frequency ranking, in that event 5A3 moves up two positions and events 5S1 and 5A1 drop back one. The higher ranking of event 5A3 at 25 Hz indicates that the track of the event probably had the lowest propagation loss of the SUS events. However, at the higher frequencies, event 5A3 showed higher losses at the longer ranges (greater than 300 km) then events 5S1 and 5A1 and thus ranked lower at the high frequencies.

(C) The three lowest-rank events (events 5P2, 5A2, and 5P5) all had close range bathymetric obstructions. The behavior of event 5A2 was somewhat complicated in that it had less propagation loss at all frequencies at 250-km range than events 5A1 and 5A3. However, beyond 400 km it had higher losses and, thus, overall had to be ranked lower. These higher losses at long range for event 5A2 appear to be consistent with the high losses for event 2P3 at Site 2, which paralleled event 5A2.

(C) Event 5P5 crossed over a severe obstruction (see fig 87) and is the lowest event in ranking. The slope of the propagation loss curve of event 5P5, as seen in figures 88, 89, and 90, is comparable to that for events 5P1 and 5A3. If the propagation losses of event 5P5 are subtracted from those of event 5P1 and averaged over six 50-km range bins common to the two events, values of 8.4, 8.9, and 8.4 dB are obtained for 25, 140, and 290 Hz, respectively. Thus, the propagation loss appears to undergo an increase in loss of about 8.5 dB in passing over the aforementioned bathymetric obstruction.

(C) The values for event 5P3 (the arc event at 131-km range) were consistent with the results from other radial events at Site 5. The propagation losses of this event span the results shown for events 5PP, 5P2, and 5A2 in figure 90, as expected, since these three events are included in the arc of event 5P3.

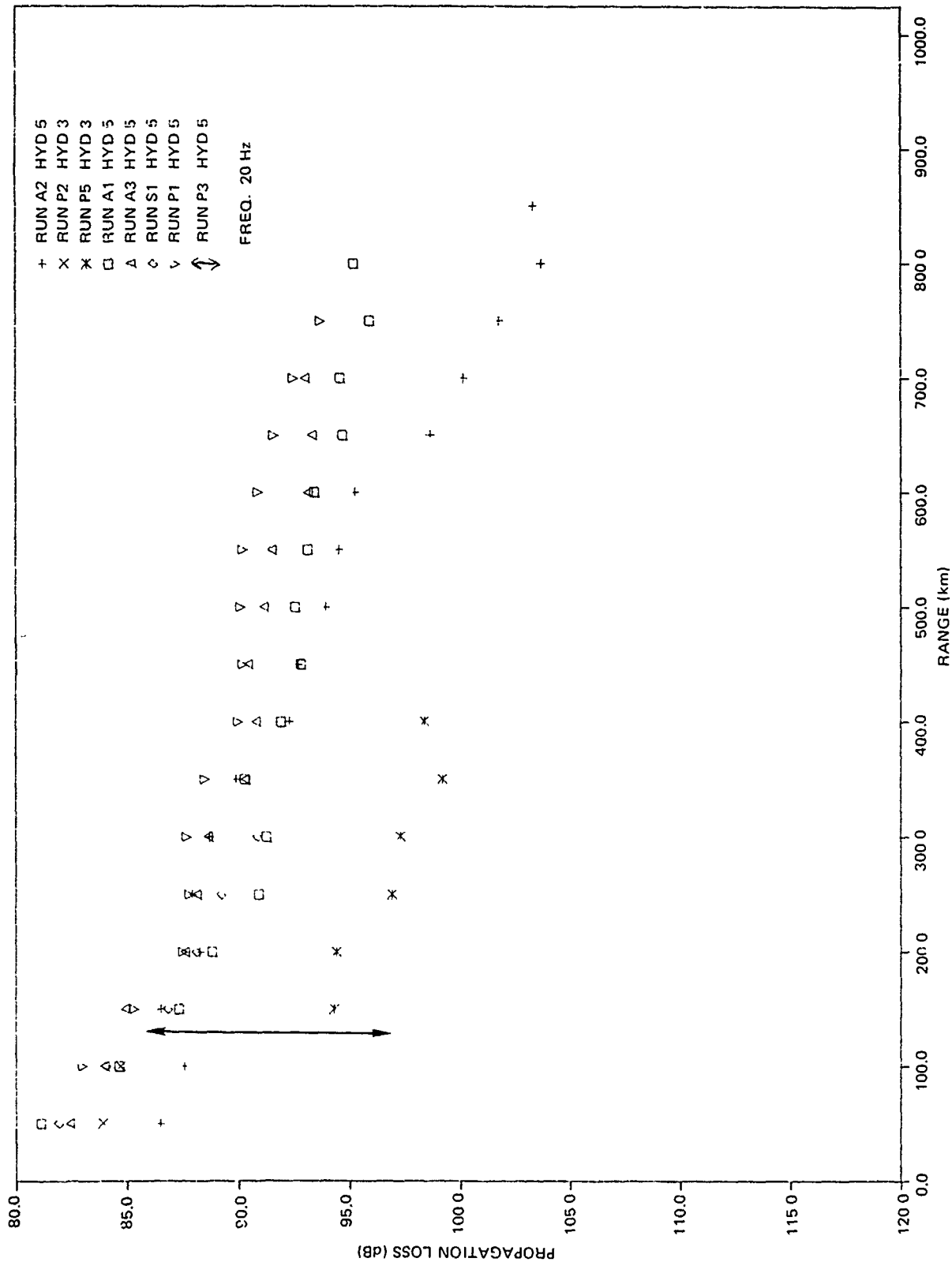

Figure 88. (C) Propagation loss at 20 Hz as a function of range for the events conducted at Site 5. (C)

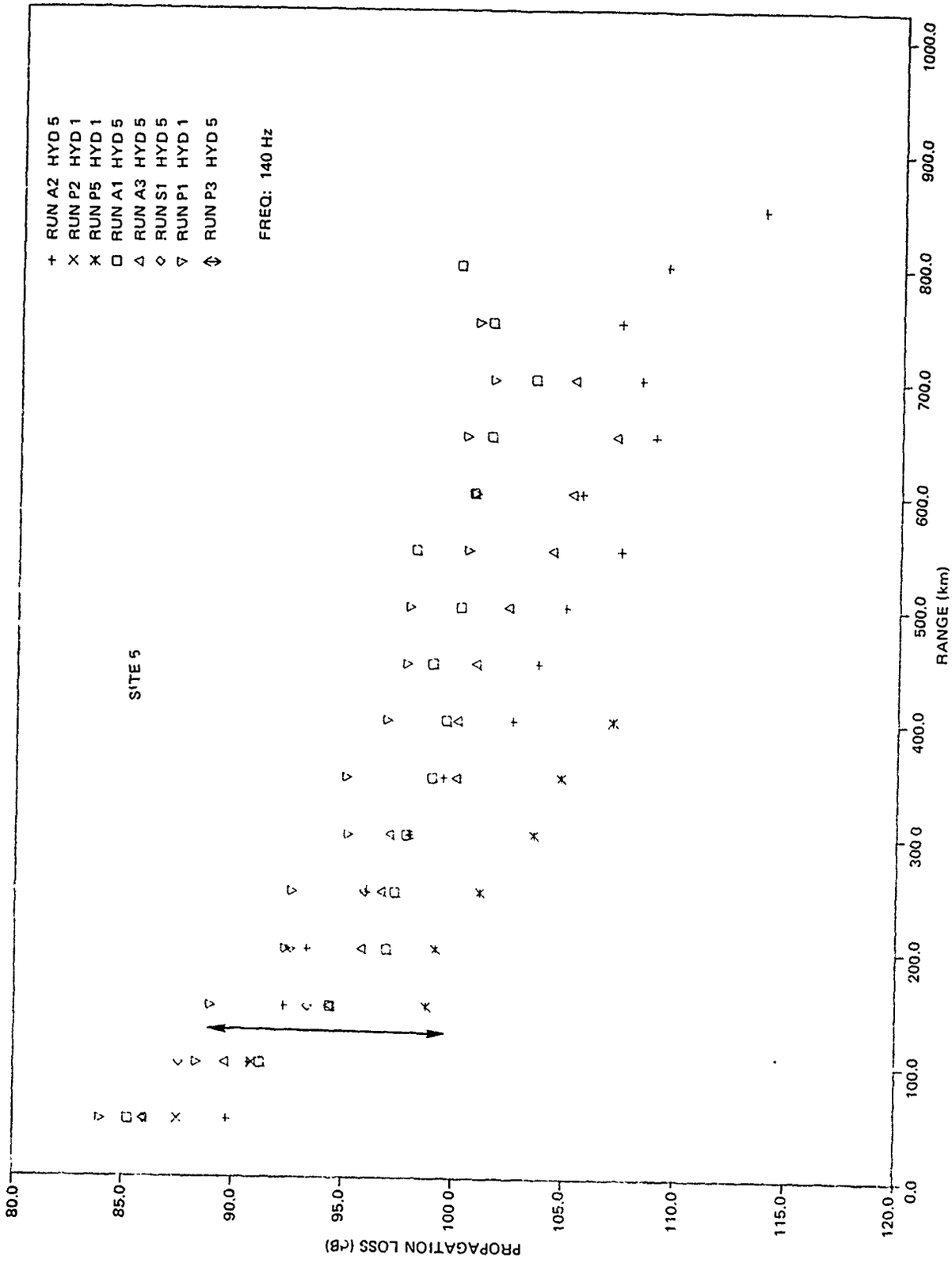

Figure 89. (C) Propagation loss at 140 Hz as a function of range for the events conducted at Site 5. (C)

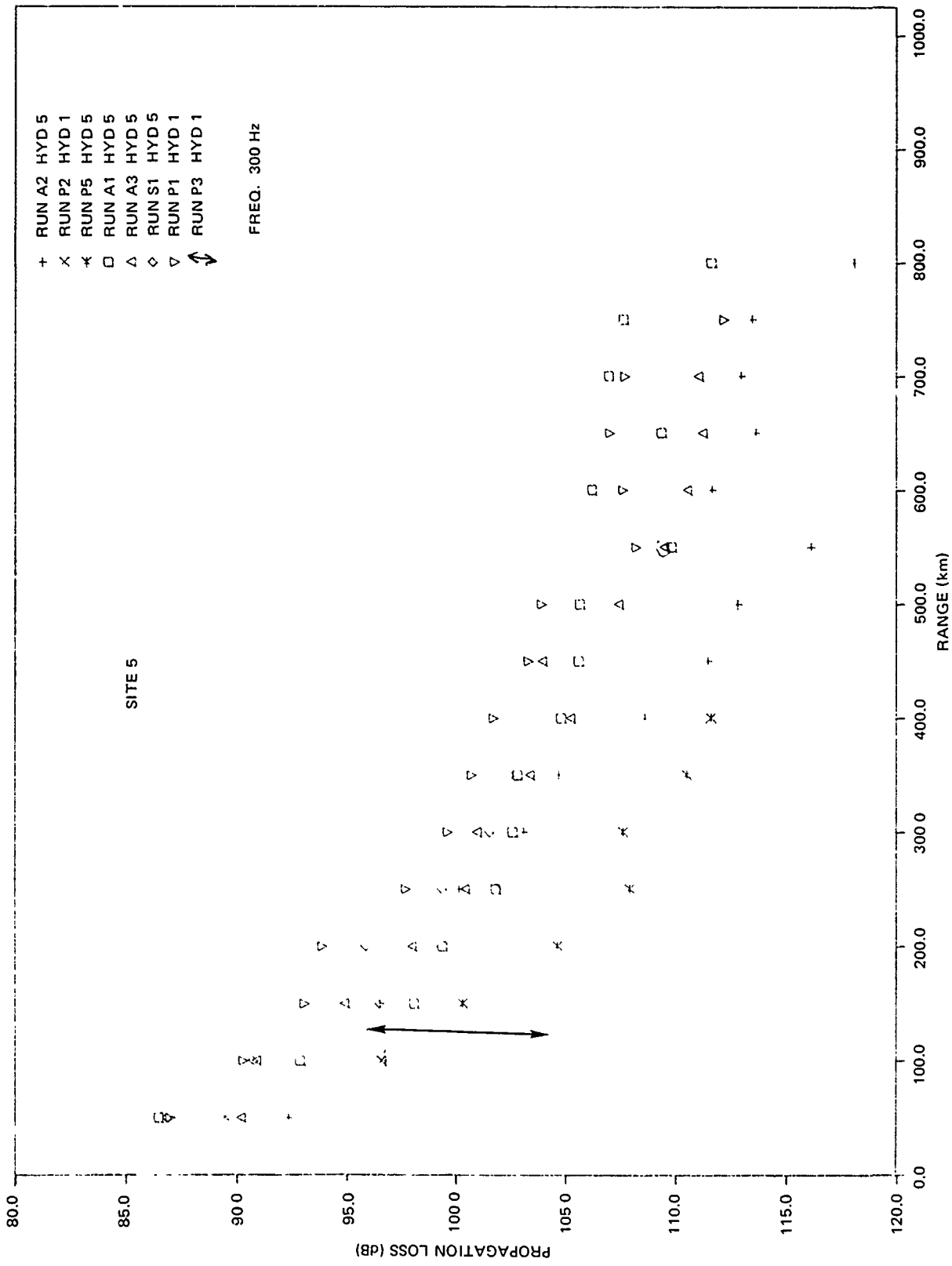

Figure 90. (C) Propagation loss at 290 Hz as a function of range for events conducted at Site 5. (C)

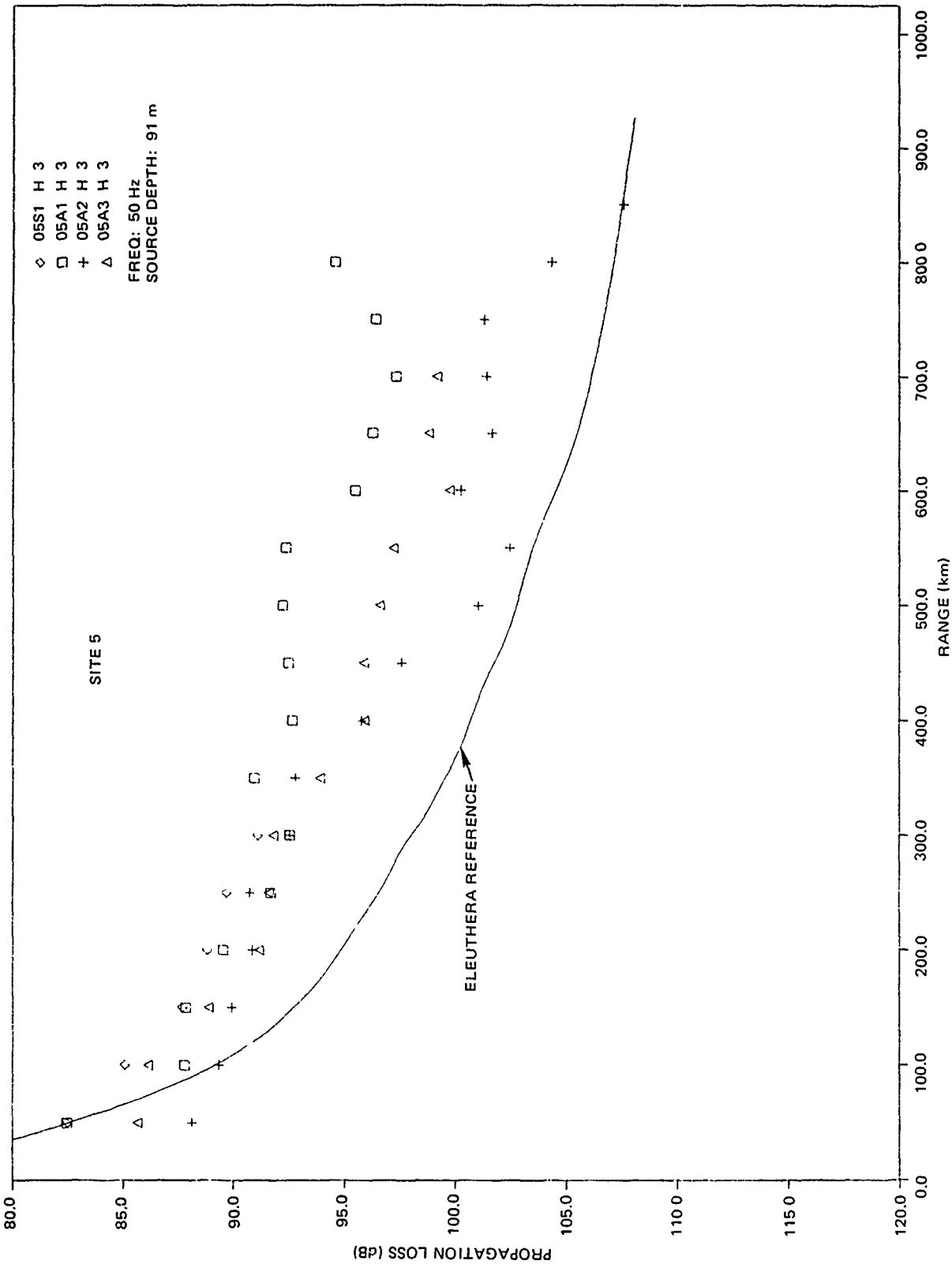

Figure 91. (C) Propagation loss at 50 Hz as a function of range for events conducted at Site 5. (C)

Table 32. (C) Ranking of events for Site 5. (U)

Rank	Events			
	Low (20-25) Hz	140 Hz	290 Hz	50 Hz
1	5P1	5P1	5P1	5S1
2	5A3	5S1	5S1	5A1
3	5S1	5A1	5A1	5A2
4	5A1	5A3	5A3	5A3
5	5P2	5P2	5P2	
6	5A2	5A2	5A2	
7	5P5	5P5	5P5	

7.5 (U) DEPENDENCE ON RANGE AND FREQUENCY

(C) The propagation losses for event 5P1 which had the lowest propagation loss at 22, 140, and 290 Hz for Site 5 are plotted and compared to those of the Eleuthera reference in figure 92. Table 33 lists the propagation loss values which are plotted in figure 92 as a function of range. The slope of the 22-Hz propagation loss curve is less than the slope of the reference with losses at long range being as much as 13 dB less than those of the reference. The 140-Hz propagation loss curve is about the same as that of the reference but has losses, at long range, about 6 dB less than those of the reference. At 290 Hz the slope of the propagation loss curve is comparable to the slope of the reference from 100 to 500 km, their losses being within 1 dB of each other. However, the experimental losses beyond 500 km are about 3 dB greater.

(C) Propagation losses at 50 Hz for the SUS event with lowest propagation loss (event 5S1) are also listed in table 33. This event is plotted in figure 91 along with the reference. The slope of the losses from event 5S1 is less than the slope of the reference, with loss values ranging from 1 to 7 dB less than those of the reference

(C) As shown in table 33, the propagation losses over the range interval 50 to 750 km for the best events range from 79.0 to 93.7 dB for 22 Hz, 84.0 to 100.9 dB for 140 Hz, and 87.0 to 112.2 dB for 290 Hz. Results for 50 Hz over the range interval 50–300 km are 82.4 to 91.1 dB.

7.6 (U) SITE 5 SUMMARY

(C) At Site 5, receivers were mounted near the top of a small conical hill rising 700 m above the southern end of the Indus Fan. Two other receivers were buoyed up 380 and 600 m above the hill. Differences in propagation loss between the various receivers were typically 1 to 3 dB. The measured results indicated that the minimum propagation losses occurred to the northeast of the site towards the Arabian Fan and that slightly higher

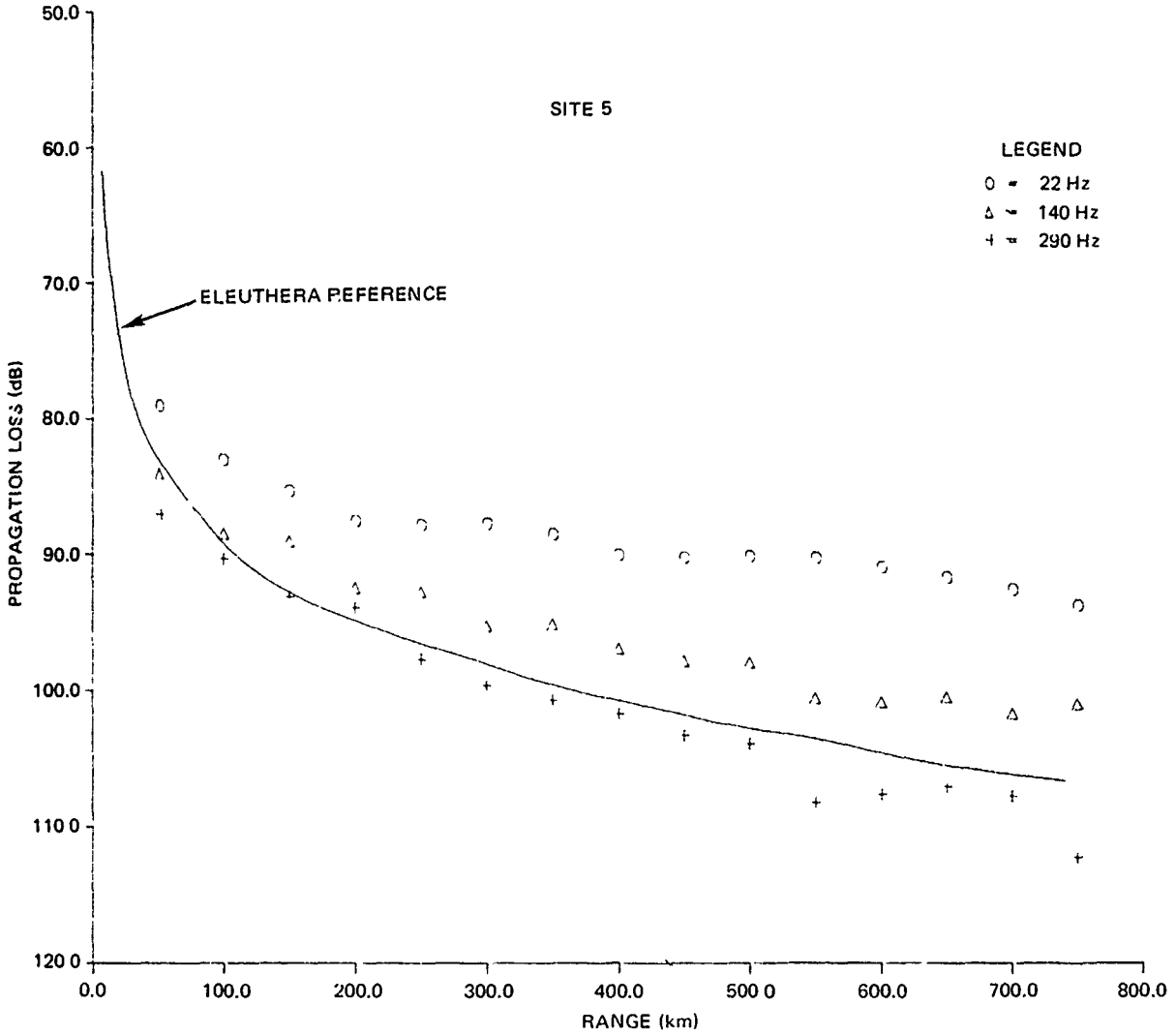

Figure 92. (C) Comparison of propagation loss at 22, 140, and 290 Hz for Site 5 with the Eleuthera reference curve. (C)

losses occurred to the north and east directions from the site. Theoretical computations, however, suggest that lower propagation losses at the site would have occurred if the receivers had been mounted at the base of the hill (on the floor of the Indus Fan) rather than atop the hill.

(C) The minimum propagation losses over the range interval 50 to 750 km from Site 5 were 79.0 to 93.7 dB at 22 Hz, 84.0 to 100.9 dB at 140 Hz, and 87.0 to 112.2 dB at 290 Hz. At 50 Hz for the range interval 50–300 km, the minimum propagation loss was 82.4 to 91.1 dB. There were significantly higher losses for events conducted over seamounts extending out of the fan and to the south in the Carlsberg Ridge region.

Table 33. (C) Propagation loss of best event at Site 5 as a function of range and frequency. (U)

Range (km)	Propagation Loss (dB)			
	Event 5P1 22 Hz	Event 5P1 140 Hz	Event 5P1 290 Hz	Event 5S1 50 Hz
50	79.0	84.0	87.0	82.4
100	83.0	88.4	90.3	85.1
150	85.3	89.0	93.1	87.7
200	87.5	92.4	93.9	88.8
250	87.8	92.7	97.7	89.7
300	87.7	95.2	99.6	91.1
350	88.5	95.1	100.7	—
400	90.0	96.9	101.7	—
450	90.2	97.8	103.3	—
500	90.1	97.9	103.9	—
550	90.2	100.5	108.2	—
600	90.9	100.8	107.6	—
650	91.6	100.4	107.0	—
700	92.5	101.6	107.7	—
750	93.7	100.9	112.2	—

(C) In general, the propagation losses at the low frequencies (20 to 25 Hz) and 140 Hz were always less than those of the Eleuthera reference curve at comparable ranges. At 290 Hz, the propagation losses were equal to or greater than those of the Eleuthera reference.

7.7 (U) RECOMMENDATIONS FOR ADDITIONAL DATA PROCESSING

(C) BMA receivers 5 and 3 were bottom mounted on a conical hill about 125 m apart in range and about 21 m apart in depth, receiver 3 being deeper. In five of the seven events conducted at Site 5, BMA receiver 5 was the only bottom-mounted receiver that was processed at the frequencies above 36 Hz. However, for events 5P2 and 5P5 at 36 Hz, the propagation loss for receiver 3 was about 1 dB less than that of receiver 5. Moreover, for some of the SUS events at the low frequency, receiver 3 on the average had 1.4 dB less loss than receiver 5. These results suggest that perhaps receiver 5 may not be representative of the bottom-mounted receivers at Site 5. Since the present BEARING STAKE results at Site 5 rely heavily on receiver 5, it is important to establish firmly whether or not receiver 5

is representative of the bottom-mounted receivers. Therefore, it is recommended that the data from BMA receiver 3 be processed at all frequencies and compared with receiver 5 results to resolve the problem.

(C) The processing of data from suspended BMA receiver 2 was limited to the low frequencies for all the events at Site 5 except event 5P1. For event 5P1, no data from receiver 2 were processed at all. Additional data from receiver 2 are necessary to verify that receiver 1 is typical of suspended receivers. Events 5P1 and 5P2 indicate a complicated frequency-receiver relationship in which bottom-mounted receiver 5 had less propagation loss than suspended receiver 1 at 22 and 36 Hz but greater losses at 140 and 290 Hz.

(C) To resolve these problems and to effectively evaluate the effects of local bathymetry on event 5P3, it is recommended that additional data sets for events 5P1 and 5P3 be processed which include receivers 1, 2, 3, 6, and 8 at all frequencies. Further processing of events 5P2, 5P5, and 5S1 may be recommended, depending on the analyses of the augmented data for events 5P1 and 5P3.

8.0 (U) OVERALL PROPAGATION LOSS ASSESSMENT

(U) Based upon the assessments made in this report on the five sites occupied during BEARING STAKE, the overall propagation loss characteristics of the Northwest Indian Ocean can now be assessed. Figure 93 shows the composite of all the propagation loss measurement events and the area covered by the tracks for each event. As can be seen from the figure, BEARING STAKE measurements covered the Northwest Indian Ocean extensively in all directions. Some of the acoustic runs at each site overlapped into other sites and provided a common basis for comparisons between sites.

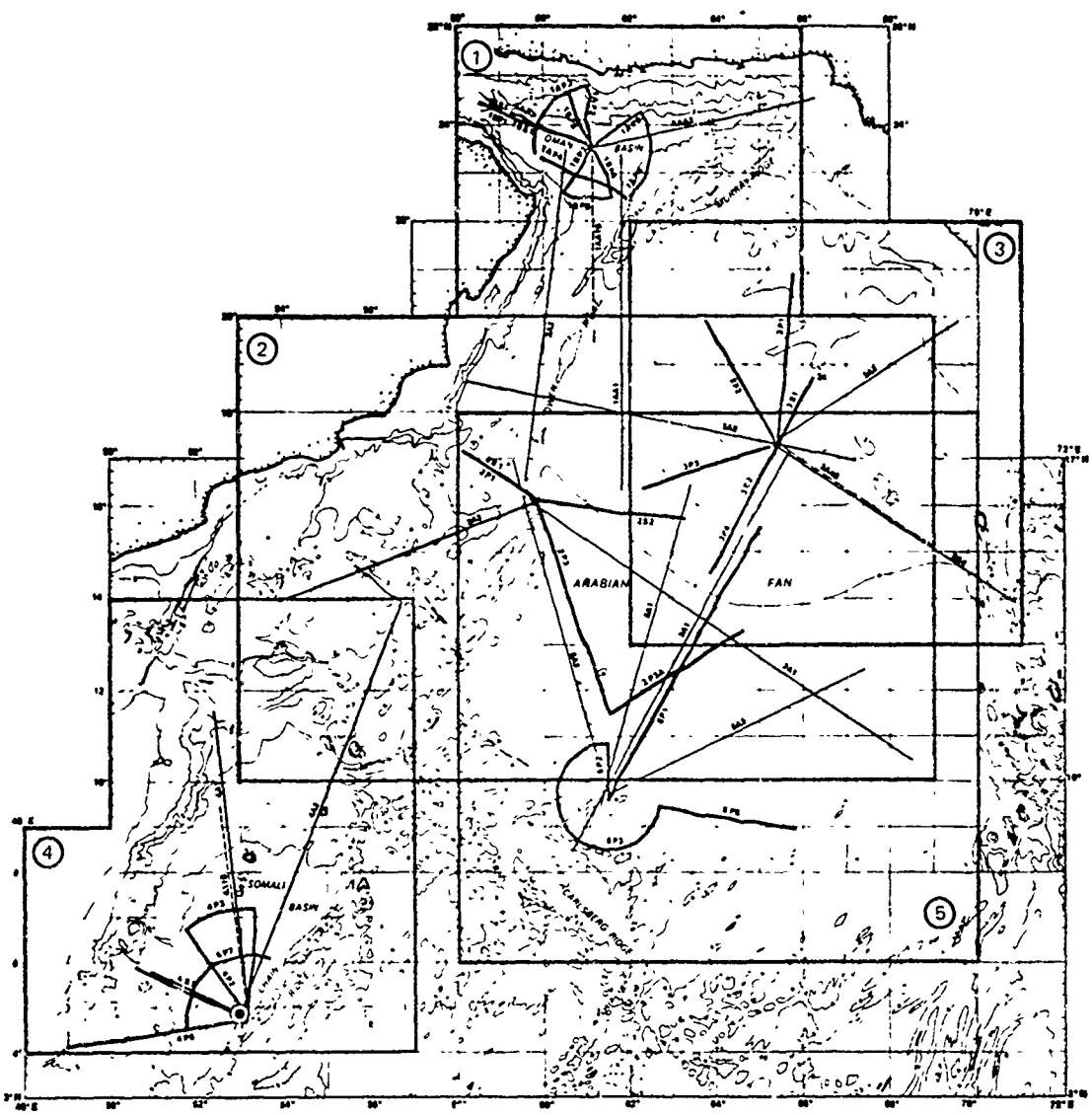

Figure 93. (C) Composite of all propagation loss runs conducted at all five sites during BEARING STAKE. (U)

(U) The discussions in this section assess the propagation loss in terms of bottom loss regions, source depth dependence, bathymetric effects, propagation loss comparisons between sites, and comparisons with the Eleuthera reference loss curve. Surveillance site selection considerations and an assessment of propagation loss models are also presented.

8.1 (U) ACOUSTIC DETERMINATION OF BOTTOM LOSS REGIONS

(U) For surveillance systems assessment of the BEARING STAKE operating area, it is necessary for investigators to know the propagation loss due to the ocean bottom of the operating area. For this purpose, bottom loss results based upon experimental data from BEARING STAKE were determined by the Applied Research Laboratory, University of Texas (ARL/UT), and reported in reference 7. For modeling purposes, the bottom losses were divided into bottom loss regions as shown in figure 94. Each 1° square contains a number from 1 to 6 associated with the level of bottom losses encountered. The number "1" denotes the region with lowest loss; "6" denotes the region with highest loss. This section of this report demonstrates how the acoustic propagation results were used to establish the boundaries between bottom loss regions numbers 1 and 2.

(C) The acoustic event which initiated the investigation into dividing the BEARING STAKE operating area into bottom loss regions was event 2P3 at Site 2. Figure 95 shows experimental propagation loss in 2-km range bins for event 2P3 at 290 Hz along with the results of propagation losses calculated by the ASTRAL model (represented by the open circles) based upon Site 3 bottom losses. A discrepancy was noted between the experimental data and ASTRAL at long ranges. Since there were no pronounced changes in the bathymetry or sound speed profiles along the track of the event, the possibility of different bottom loss regions became apparent. This possibility was strengthened by the fact that the bottom losses measured at Site 5 at the southern end of the Indus Fan were significantly lower than those measured at Site 3, which was in the northern portion of the fan. It was also noted that by overlaying various data plots, similar to figure 2, from Sites 2, 3, and 5, a rough boundary dividing the Indus Fan into two bottom loss regions could be established. Subsequently, these data were subjected to a more complete and vigorous analysis.

(C) The initial step was to establish a typical propagation loss slope (loss vs range) for event 5P1 at Site 5. The 50-km range-bin data for this event are shown in figure 96. Line "A" in the figure is a linear least-square fit of the 290-Hz data for receiver 5 over the range interval from 100 to 600 km. Line "B" is the corresponding fit to the 140-Hz data for receiver 1. (The low-frequency (20–50 Hz) data were not used in this analysis because the bottom loss is so small at the low frequencies that slope differences are indistinguishable.)

(C) The 50-km range-bin data for event 2P3 at Site 2 were then plotted as shown in figure 97. Comparison of figure 97 with figure 96 shows that line "A" has the same slope in both figures. Note that, with the exception of the data point at 300 km, line "A' in figure 97 is an excellent fit to the experimental data. (The slope of the line is the important factor in this discussion, not the absolute loss value.) Line "B" of figure 97 also compares favorably with figure 96, indicating that the slopes at long ranges in event 2P3 and 5P1 are essentially the same.

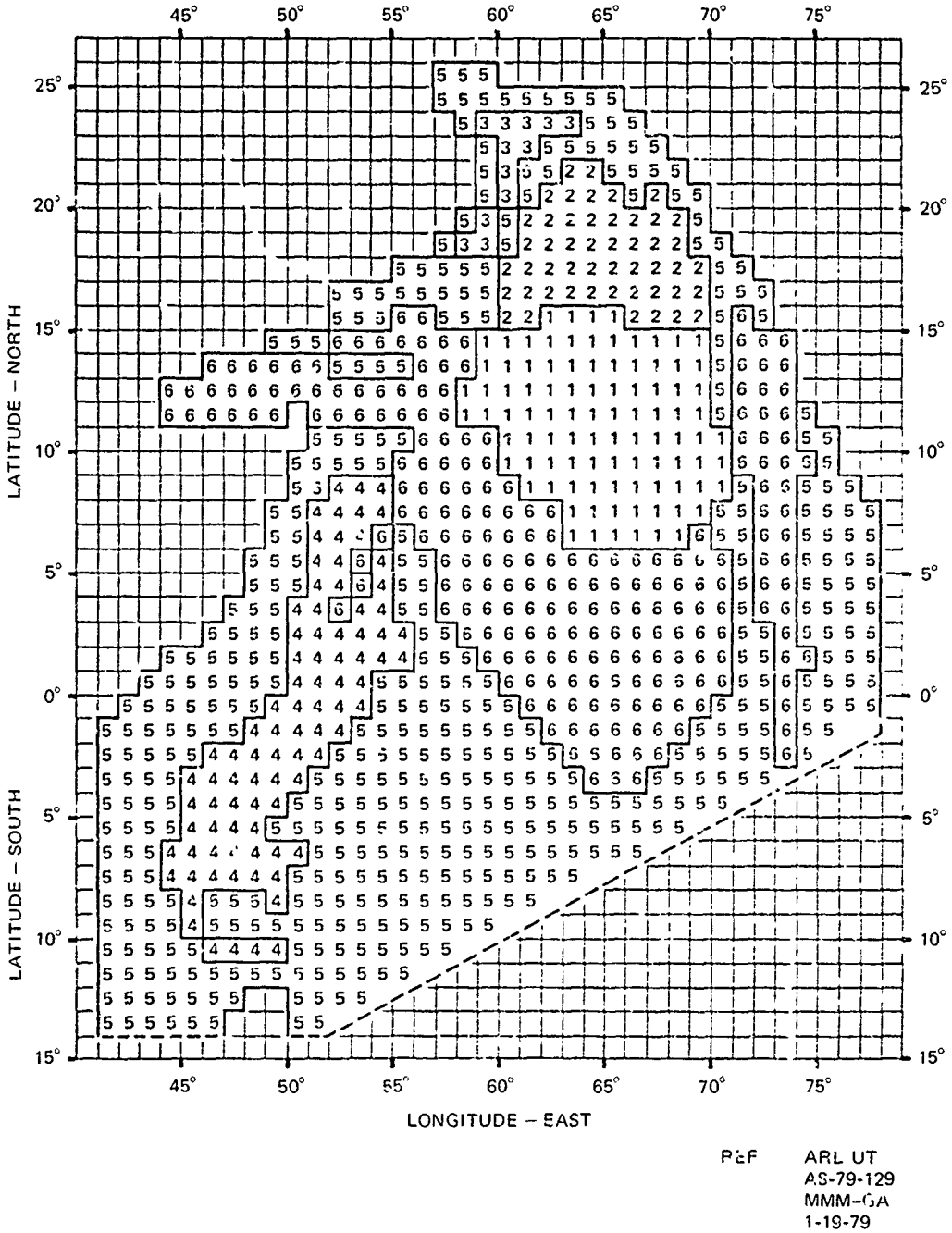

Figure 94. (U) BEARING STAKE bottom loss regions. (U)

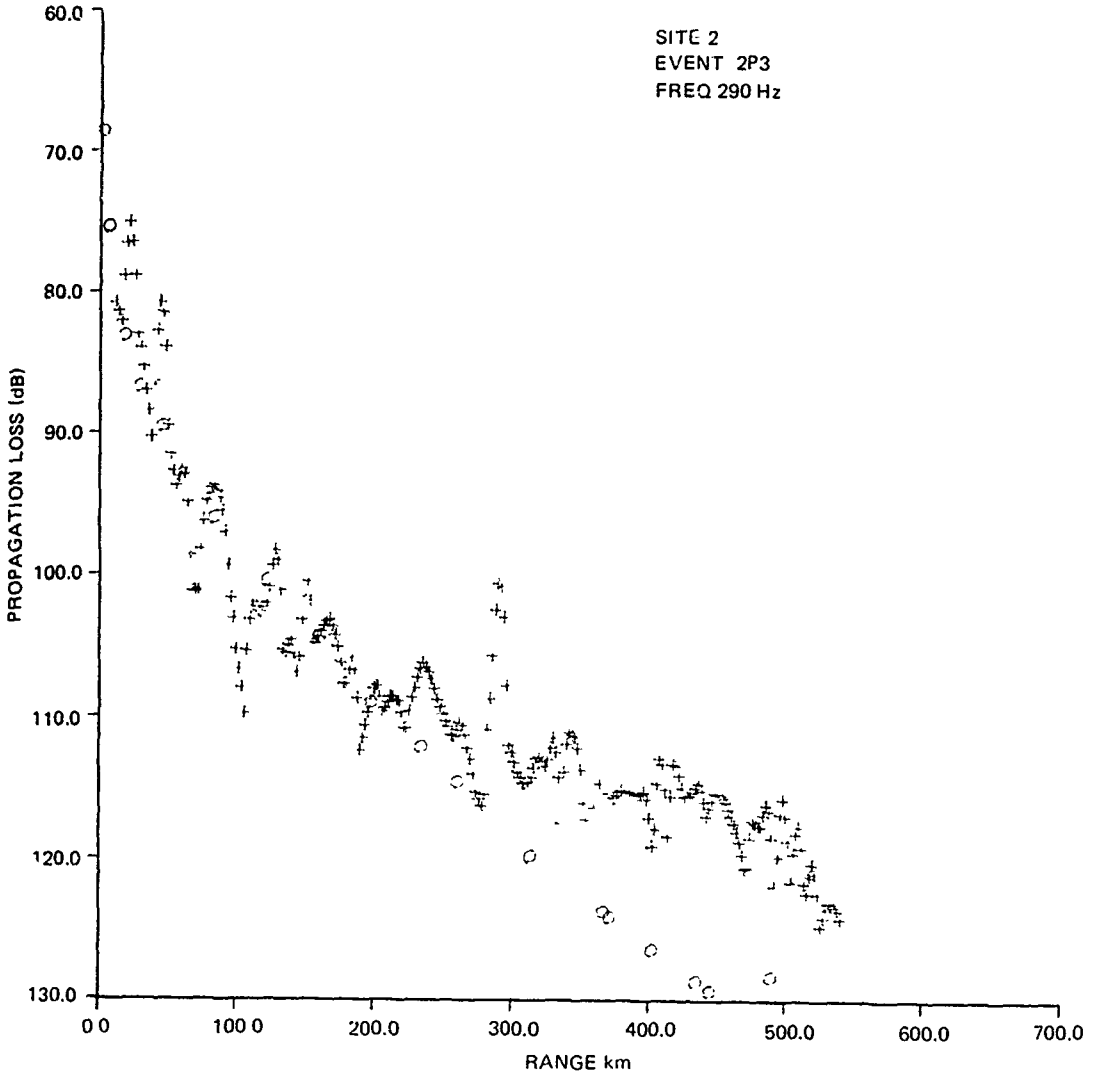

Figure 95. (C) Propagation loss at 290 Hz as a function of range for event 2P3. (C)

(C) The next step was to establish a typical loss slope for the short range data in figure 97. Lines "C" and "D" are visual fits to the data at 140 and 290 Hz, respectively. Lines "A" and "C" or "B" and "D" intersect at a range of about 175 km. This, then, established a boundary point along the track of event 2P3 between bottom loss regions.

(C) A similar analysis was performed for all the other Site 2 events. For example, the individual SUS propagation losses for event 2S2, receiver 7, for 140 Hz at 91-m source depth are shown in figure 98. The slopes of the experimental data at long and close range (lines "B" and "E") intersect at a range of about 100 km. For event 2A1 (fig 99) the slopes of the long and close range intersect at a range of about 200 km. In all cases, line "B" refers to the same slope as shown in figure 96

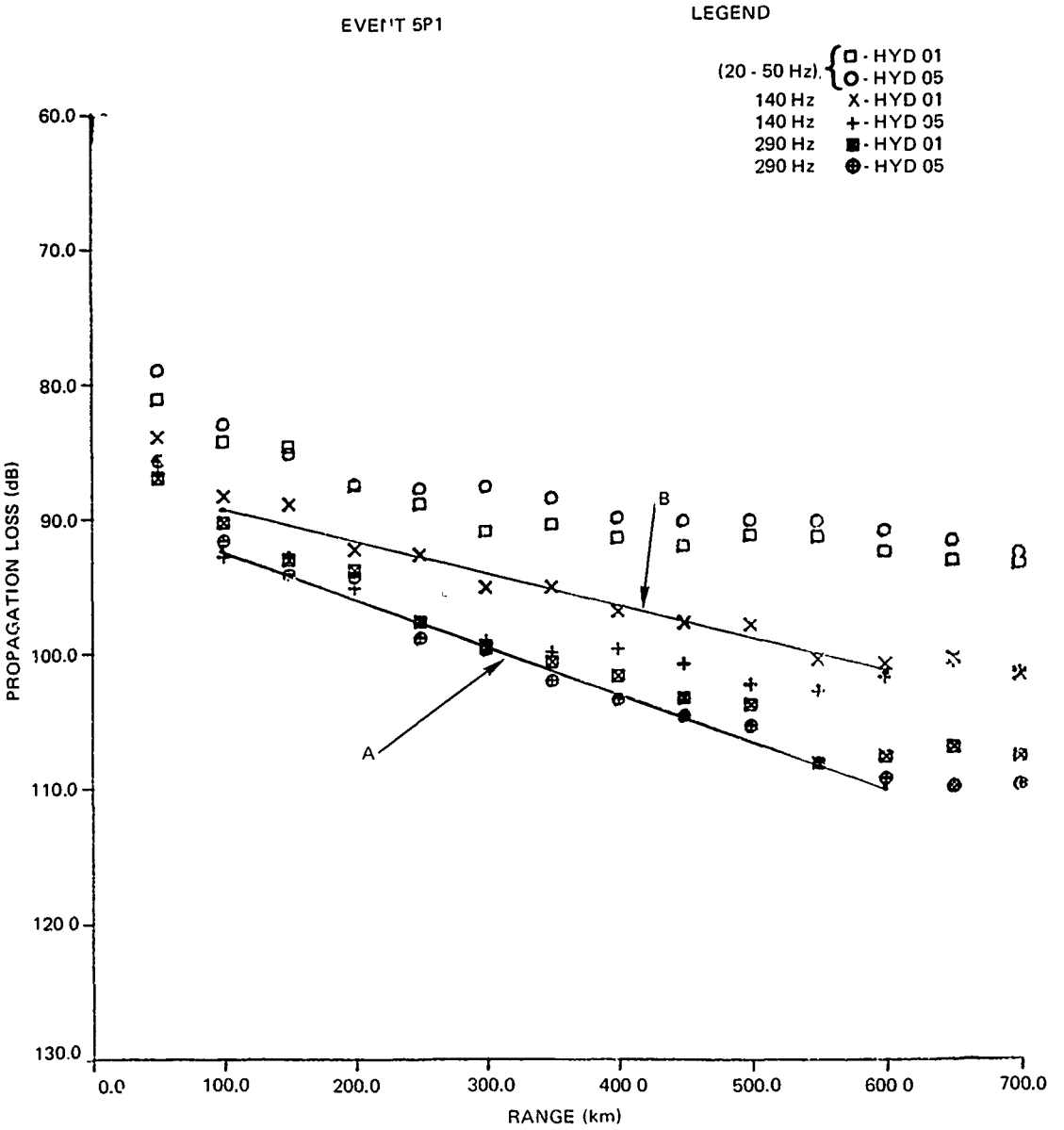

Figure 96. (C) Establishment of propagation loss slope for event 5P1 to determine bottom loss region boundary. (U)

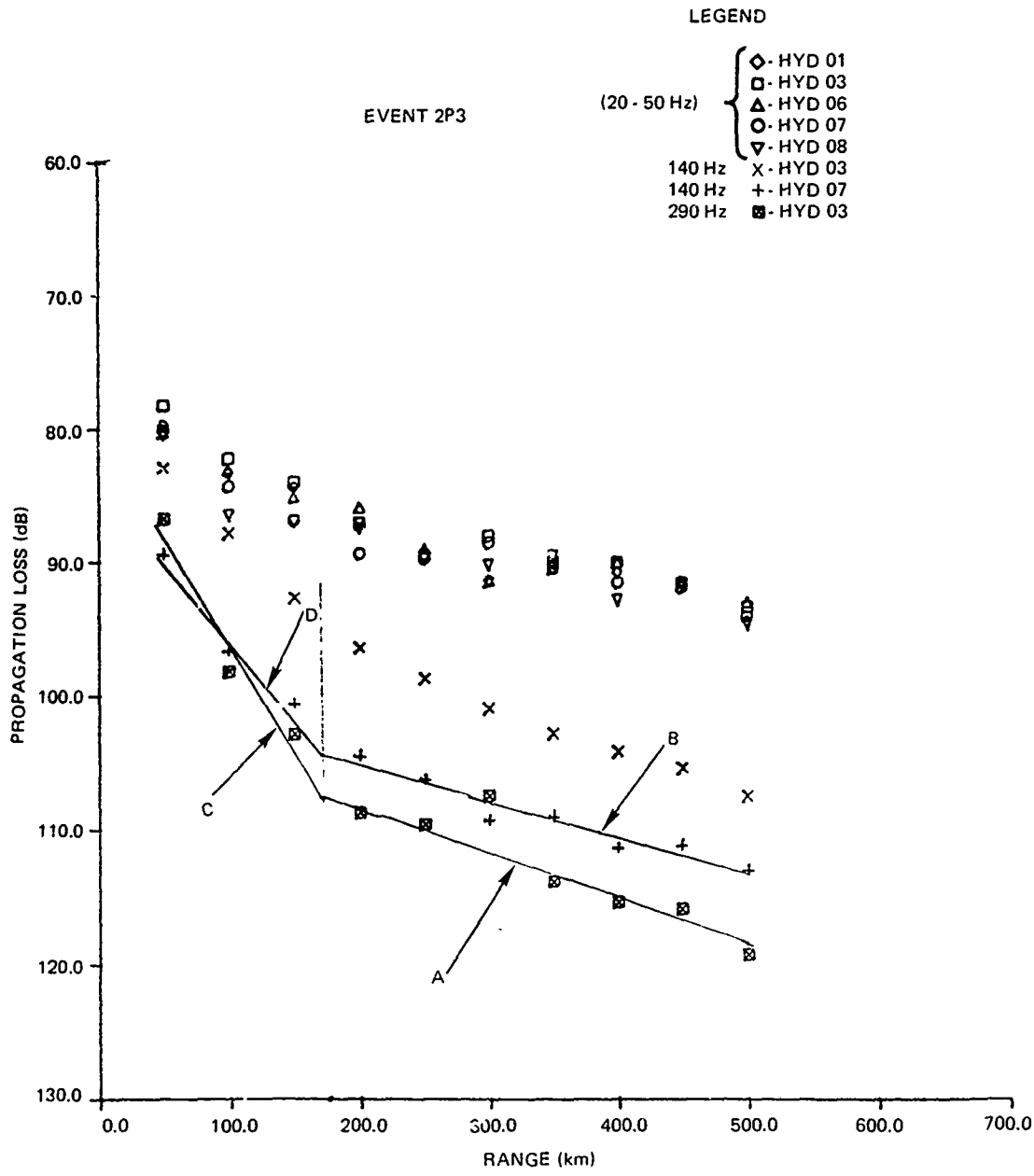

Figure 97. (C) Establishment of propagation loss slopes for event 2P3 to determine bottom loss region boundary. (U)

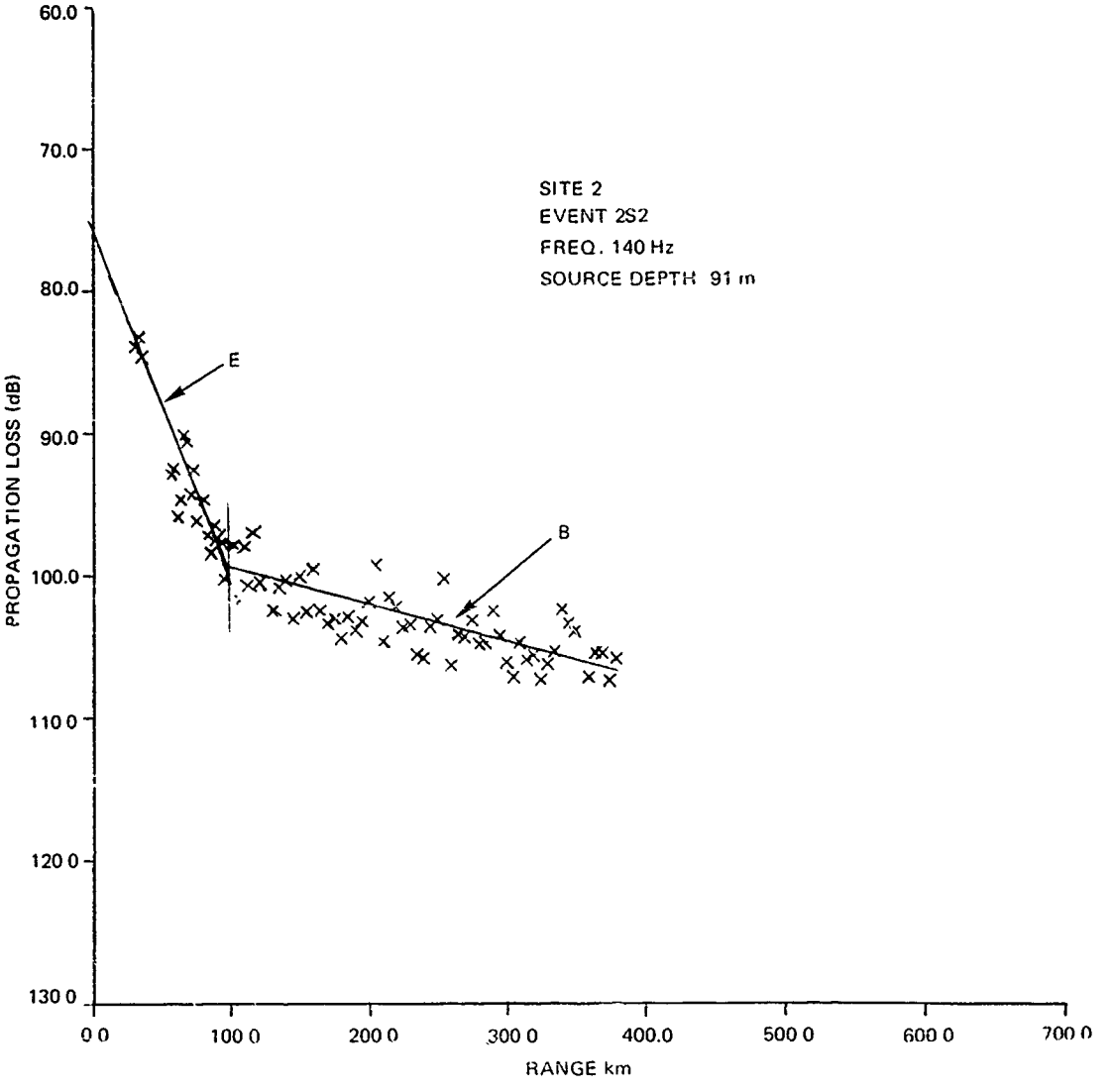

Figure 98. (C) Example of bottom loss region boundary determination for event 2S2. (U)

(U) The range to the intersection of the lines for long and close range was then plotted along the track of each event analyzed. Since it has been shown that the slope of the long range data is the same, the intersection represents the line, or boundary, dividing different bottom loss regions.

(U) The boundaries of the various bottom loss regions as shown in figure 94 should suffice at the present time for surveillance systems assessment model inputs. It should be pointed out, however, that the boundaries were based upon the analyses of the acoustic data available at the present time. The recommendations as set forth in each of the individual site assessments may (or may not) influence the boundaries as shown. However, it is expected that if changes are required, the boundaries will not move more than 1° in any particular direction.

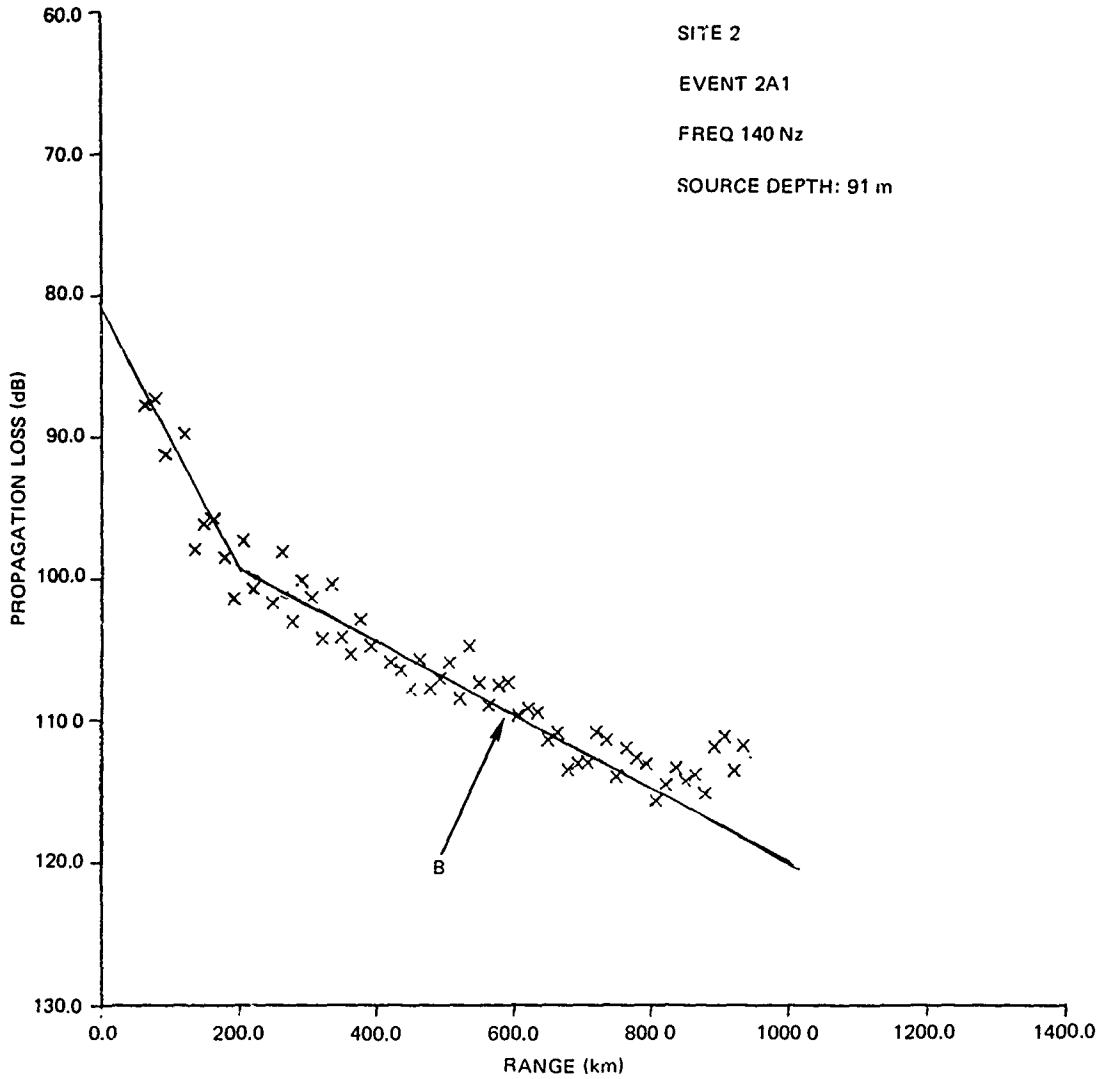

Figure 99. (C) Example of bottom loss region boundary determination for event 2A1. (U)

8.2 (U) SOURCE DEPTH DEPENDENCE

(C) During the BEARING STAKE exercise, a significant volume of data was collected to investigate the dependence of propagation loss on source depth. For this purpose, the explosive source events were planned so that a series of charges was detonated at different depths, but esentially at the same range, from an aircraft or a ship. The aircraft deployed SUS charges were limited to 18- and 91-m detonation depths while the ship-deployed charges were detonated at 18, 91, and 243 m.

(C) The propagation losses from the SUS charges as a function of range were calculated by investigators at WECo from the BMA for 20, 50, 140, and 300 Hz. The following

discussion of source depth dependence is presented in terms of frequency and range as well as bathymetric features whenever applicable.

(C) The overall behavior of propagation loss as a function of source depth is typified by the two plots shown in figure 100. The data are from hydrophone 1, run S1 at Site 4. The bottom depth over this run was constant (5 km) out to 280 km. The plots show the propagation loss at 20 and 140 Hz for source depths of 18, 91, and 243 m. (Plots exemplified in figure 100 were also generated for 50 and 300 Hz.) From figure 100 (upper half) it can be seen that, at 20 Hz, the 18-m source depth suffers significantly more propagation loss than the other source depths. This loss at 20 Hz at 18 m increases from about 4 dB at 50 km to 10 dB at 250 km, whereas the losses at 20 Hz from the sources at 91 and 243 m show little difference between them.

(C) For 140 Hz, figure 100 (lower half) shows that there is very little difference in propagation loss between the source depths of 18, 91, and 243 m.

(C) The other two frequencies, 50 and 300 Hz, exhibited source depth characteristics similar to those shown for 140 Hz in figure 100. The trend observed for 20 Hz at 18-m depth was not noticeable at 50 Hz for the same source depth.

(C) In order to analyze source depth effects in more detail, the differences in propagation loss between the 91-m source depth and the 18- and 243-m source depths as a function of frequency and range are shown in figures 101 and 102. In figure 101 the differences correspond to 18- and 91-m source depths and are given at frequencies between 20 and 300 Hz. Equivalent plots relating to 91- and 243-m differences are shown in figure 102. These figures include all available data from all sites and runs which do not have major bathymetric changes. The class including bathymetric effects will be discussed later.

(C) The general trends of figure 102 are also clear in figure 101. Negative values of propagation loss difference here indicate that the 18- or 243-m source depth has greater loss than the 91-m. The range dependence of this difference is also clear from figure 101(a) at 20 Hz and to a small extent at 50 Hz. The two higher frequencies have no significant range dependence.

(C) In all the cases shown in figure 101, there is a systematic negative average to the difference data which diminishes slightly as the frequency increases. The higher propagation loss from an 18-m source depth (for all frequencies shown, except 20 Hz) when compared with the losses from a 91-m source depth can be attributed to a change in the ray paths between transmission families with source depth. That is, the shallower source (18 m) will have fewer rays which vertex above the ocean bottom, thus suffering more bottom loss than the 91-m source depth.

(C) The propagation loss differences between the 91- and 243-m source depths shown in figure 102 are consistent with the results of table 1B (section 2.2.3), which showed a slight negative difference for 50 Hz of 2 to 3 dB from the other frequencies. As previously mentioned, the normal mode results predicted slightly lower losses for a 91-m source at 20 and 50 Hz. It is difficult to determine whether the experimental results of figure 102 are "real" or merely indicate incorrect SUS source levels as a function of depth and frequency.

(C) The most noticeable feature in this analysis, although not entirely unexpected, is the higher propagation loss at 20 Hz for the shallow source at 18 m. This higher loss is due to the acoustic effects of surface decoupling associated with low-frequency sources at shallow depths reported in reference 10. As can be seen from figure 101(a), surface

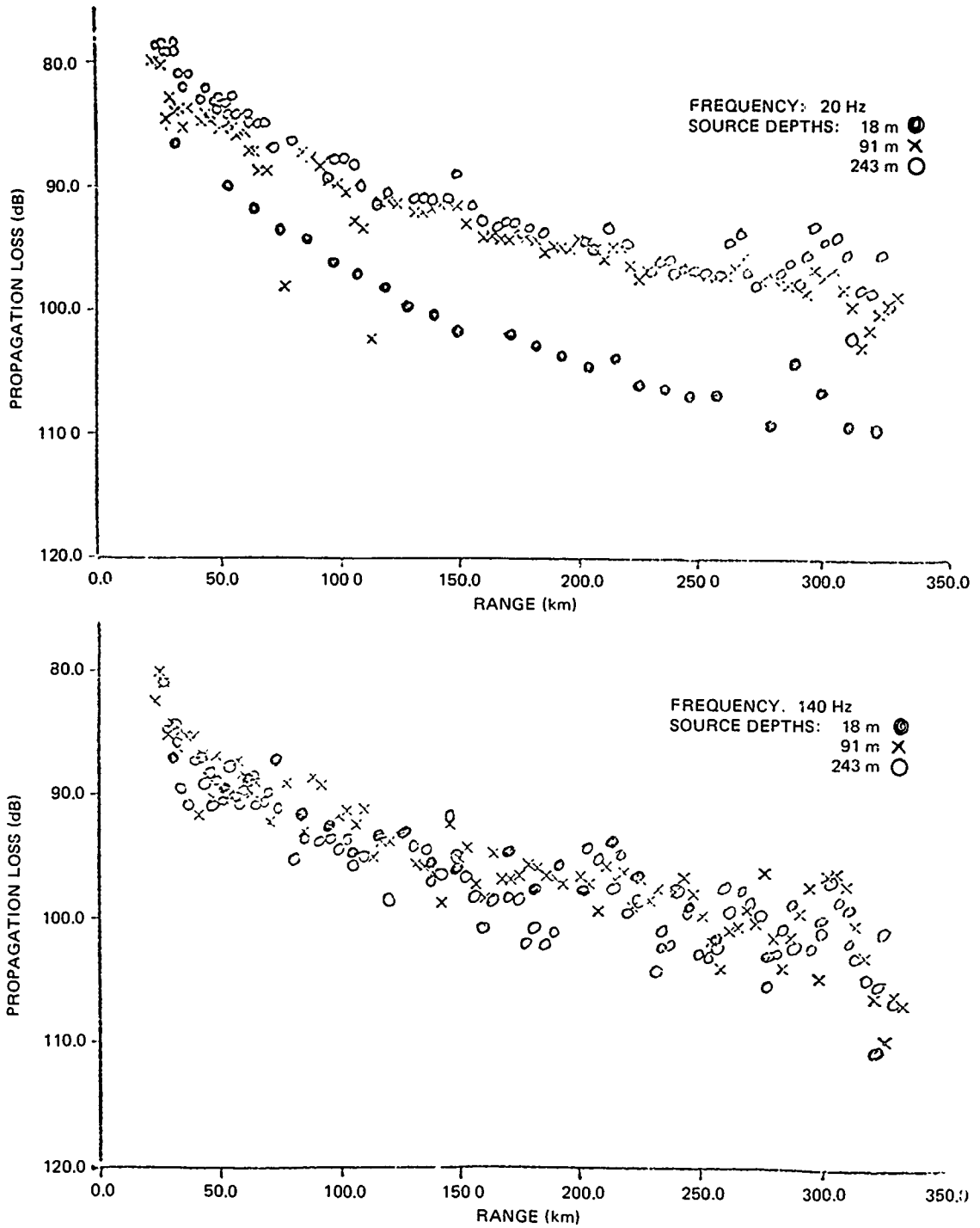

Figure 100. (C) Examples of propagation loss as a function of source depth and frequency. (U)

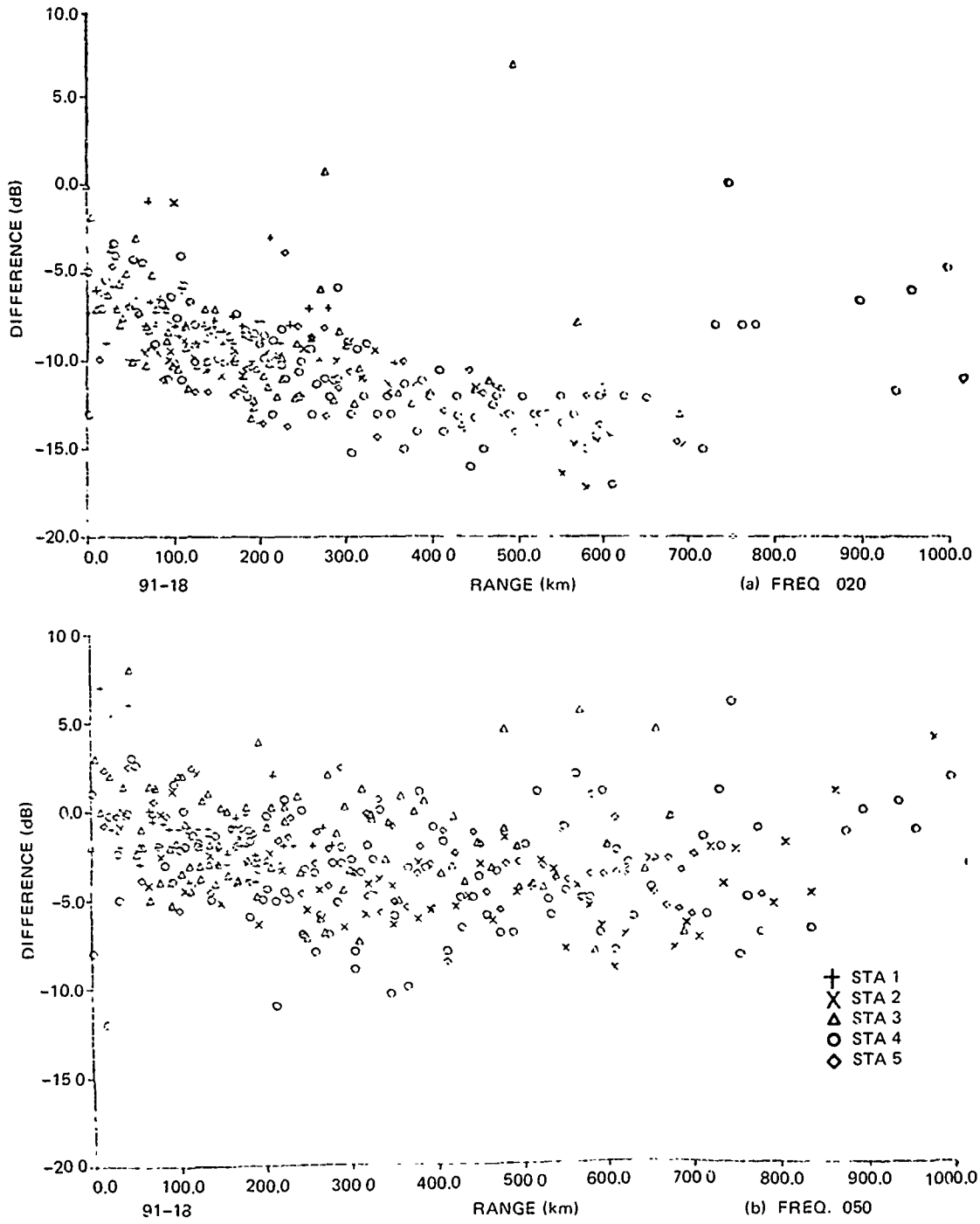

Figure 101. (C) Difference in propagation loss at 91-m and 18-m source depths as a function of range and frequency. (U)

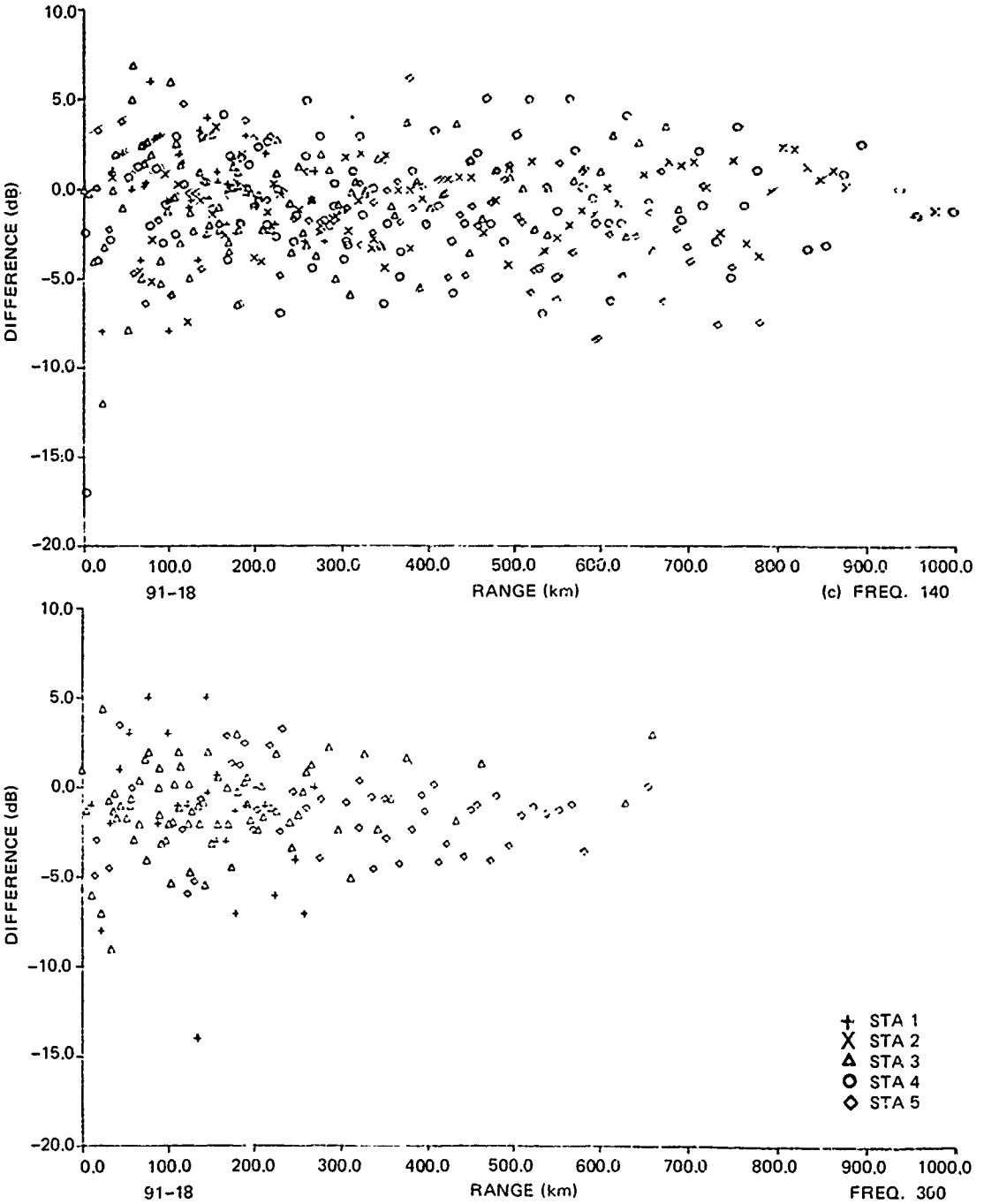

Figure 101. (C) (Continued). (U)

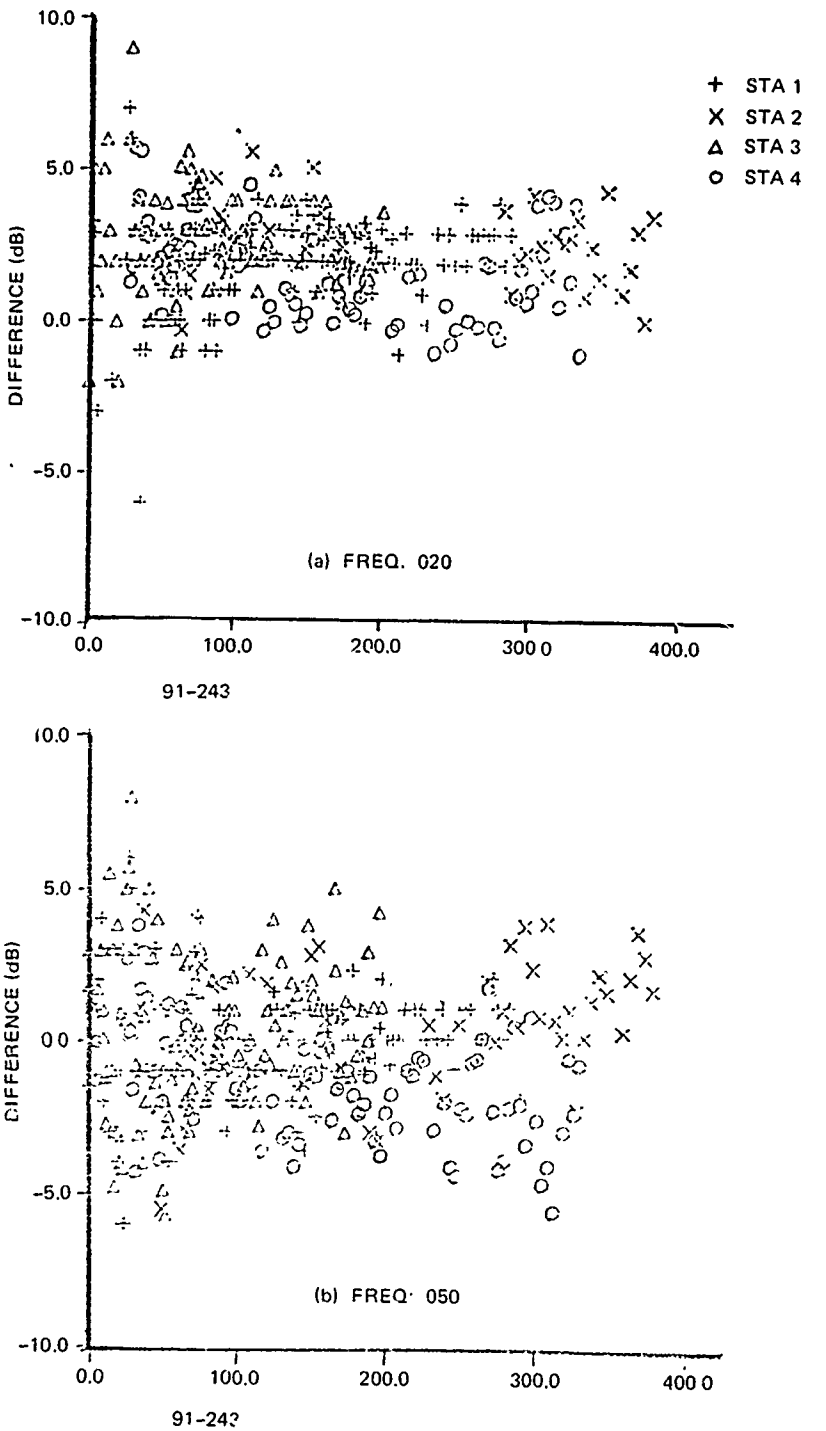

Figure 102. (C) Difference in propagation loss at 91-m and 243-m source depths as a function of range and frequency. (U)

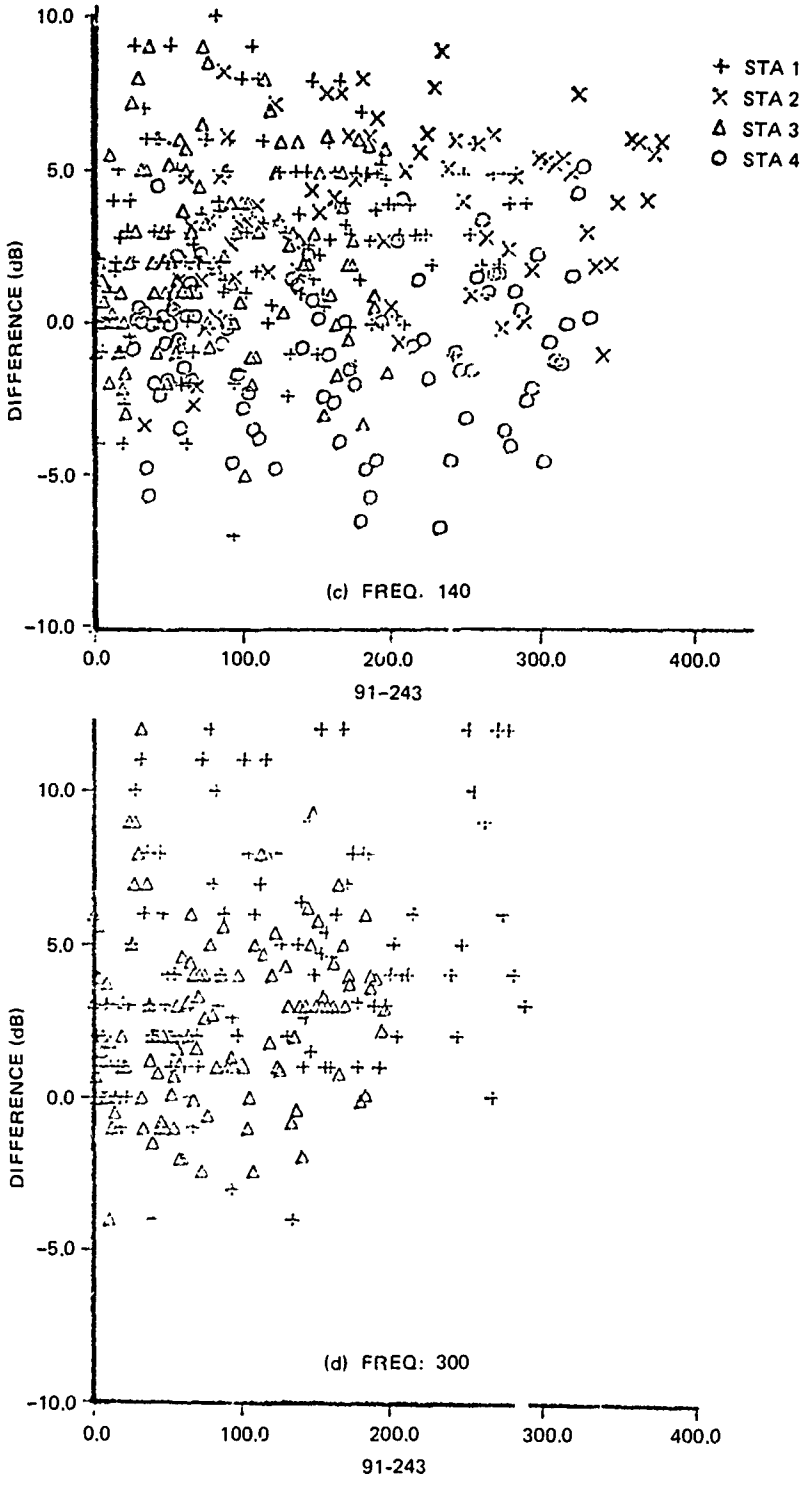

Figure 102. (C) (Continued). (U)

decoupling occurred at all five sites of BEARING STAKE at 20 Hz when the source depth was 18 m as indicated by the large loss differences at all ranges between the 91- and 18-m source depths.

(C) Briefly, surface decoupling is conceptually an interference effect involving an acoustic source and its surface images. In the simplest case (when sound rays are straight lines near the ocean surface) surface decoupling is equivalent to dipole radiation from a source. That is, the source may be regarded as having a vertical directional pattern with a directivity function proportional to the grazing angle (θ_S) at the surface. Under these conditions, rays with small surface grazing angles will suffer greater losses than rays with higher grazing angles. A sketch of the equivalent vertical source directivity is shown in figure 103. At high frequencies, or source depths greater than a few wavelengths, there is no dipole directivity and the curve "no decoupling loss" applies. As the frequency decreases below about 50 Hz and the source depth becomes shallower than 100 m, the directivity becomes apparent. The curves labeled "moderate" and "high" decoupling loss relate to this trend.

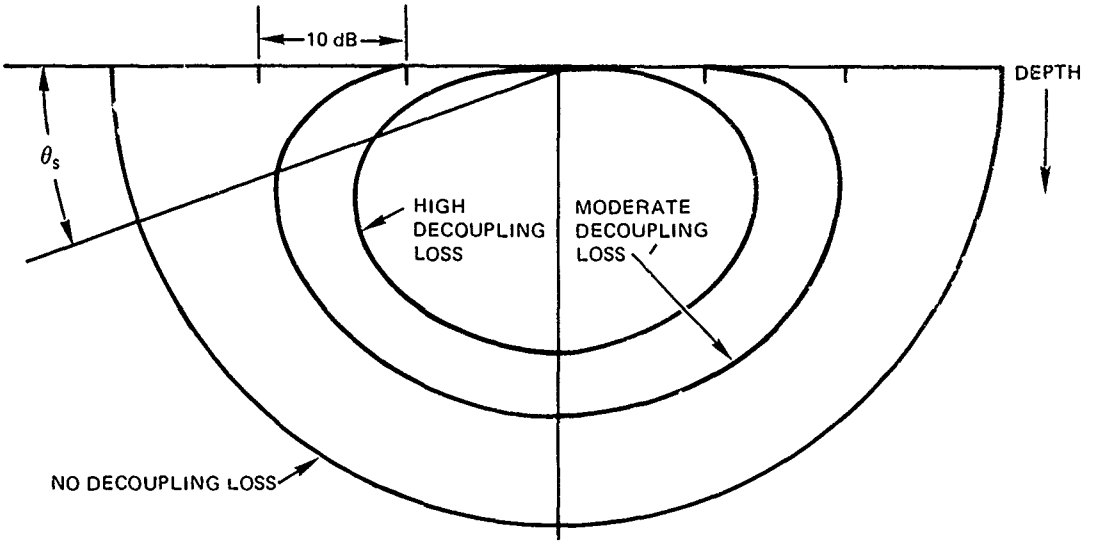

Figure 103. (U) Surface decoupling loss concepts. (U)

(C) Figure 104 shows surface decoupling loss as a function of surface grazing angle (θ_S) for source depths of 6, 18, and 91 m. As the surface angle decreases, the decoupling loss increases as shown. Decoupling loss is greatest for small surface angles and for shallow source depths. The figure also shows that at 91 m surface decoupling loss is practically nil.

8.2.1 (U) Bathymetric Effects

(C) The results and conclusions discussed thus far with respect to the dependence of propagation loss on source depth were based on data from areas in which the bathymetry was fairly uniform. In those instances in which major bathymetric features were encountered along the propagation path, the only propagation loss assessment affected was for 20 Hz at

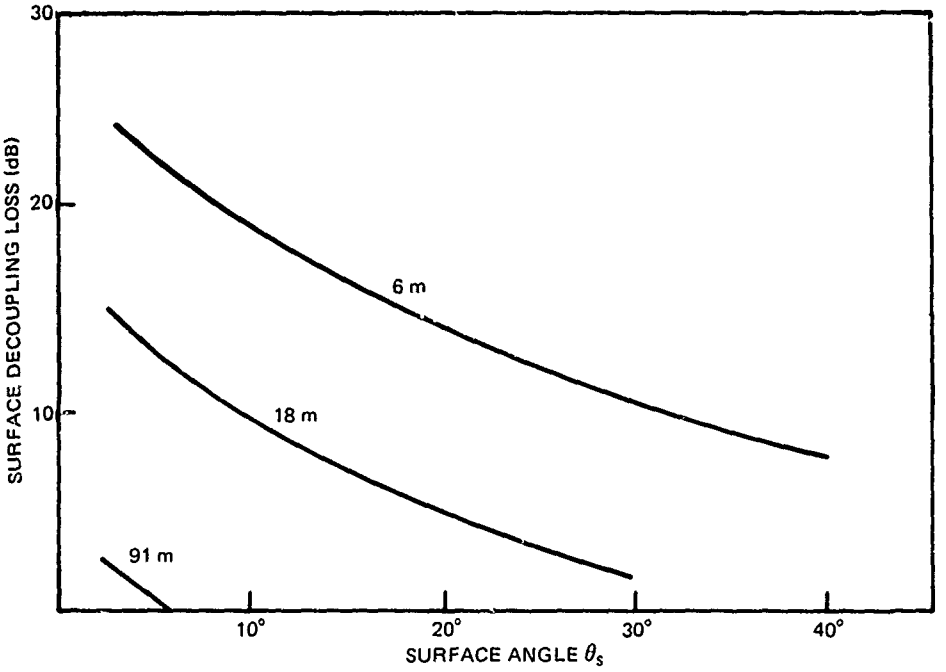

Figure 104. (U) Surface decoupling loss as a function of surface angle for 20 Hz for source depths of 6, 18, and 91 m. (U)

the 18-m source depth. A typical example of the effect of a bathymetric feature on propagation loss is shown in figure 105. The propagation loss curves shown in figure 105(a) are for 20 Hz at source depths of 18 and 91 m at Site 4. The range-dependent increased propagation loss from an 18-m source at 20 Hz is once more apparent out to 700 km (compare with fig 100). However, when the sloping bottom was encountered, the propagation loss at 20 Hz decreased significantly. This effect is known as upslope enhancement or "megaphone effect." It is also clear from figure 105 that the 91-m source depth at 20 Hz did not experience any significant enhancement.

(C) Corresponding propagation loss curves at 140 Hz for 18- and 91-m source depths are shown in figure 105. At this frequency (and also at 300 Hz) no enhancement effects are apparent in either source depth case.

(C) Another example of the enhancement effect is afforded by data from Site 1A and shown in figure 106. The propagation loss run passed over a seamount at a range of 250 km. As shown in figure 106(a), the propagation loss data at 20 Hz for 18 m are enhanced, whereas the 91-m source depth data are unaffected. At 140 Hz (fig 106(b)), neither source depth is affected by the bathymetric feature.

8.2.2 (U) Summary

(C) In summary, the variation of propagation loss due to changing source depths was most pronounced at the low frequency (20 Hz) and at the shallow source depth (18 m).

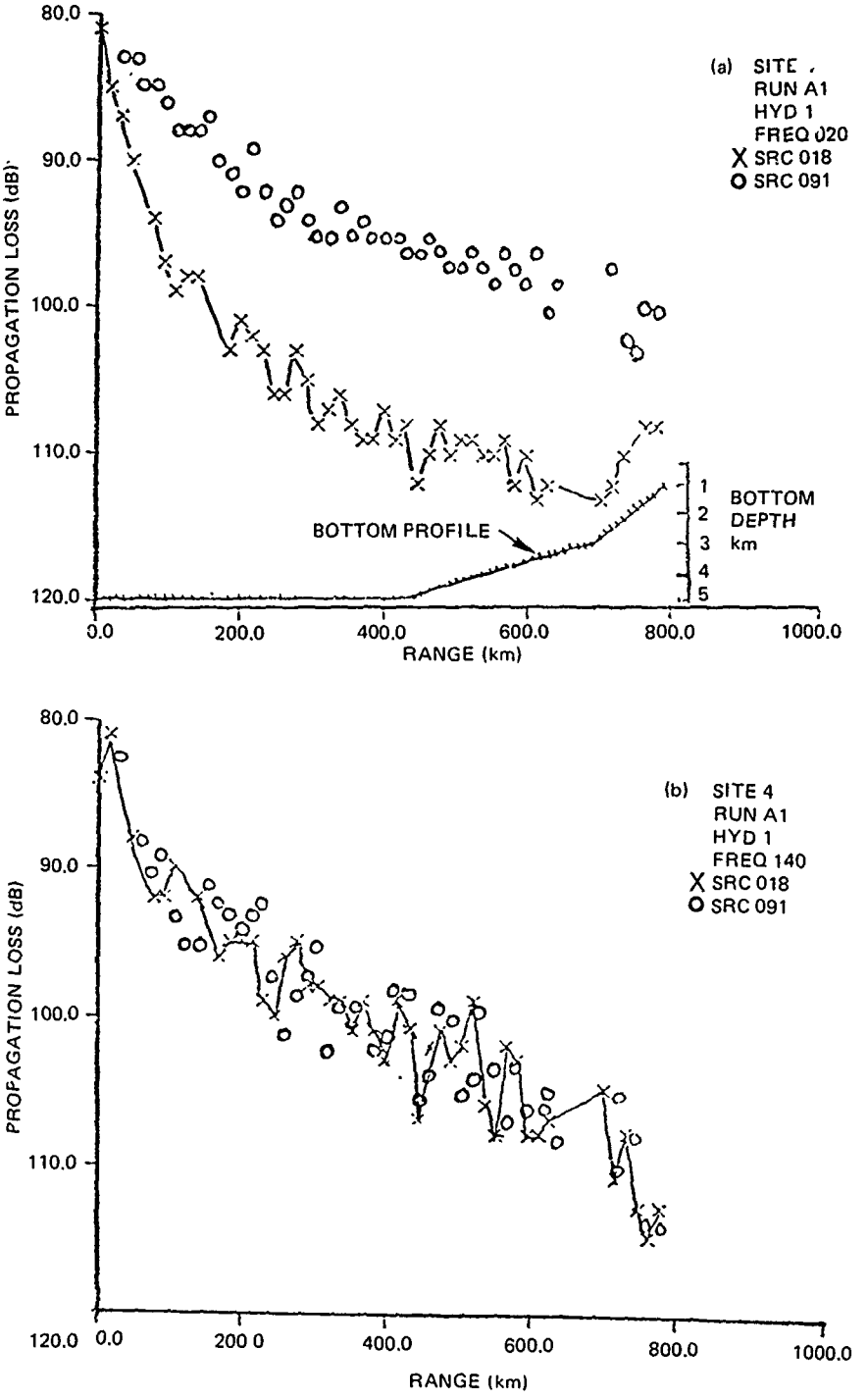

Figure 105. (C) Upslope enhancement at two frequencies and two source depths, Site 4, event 4A1. (U)

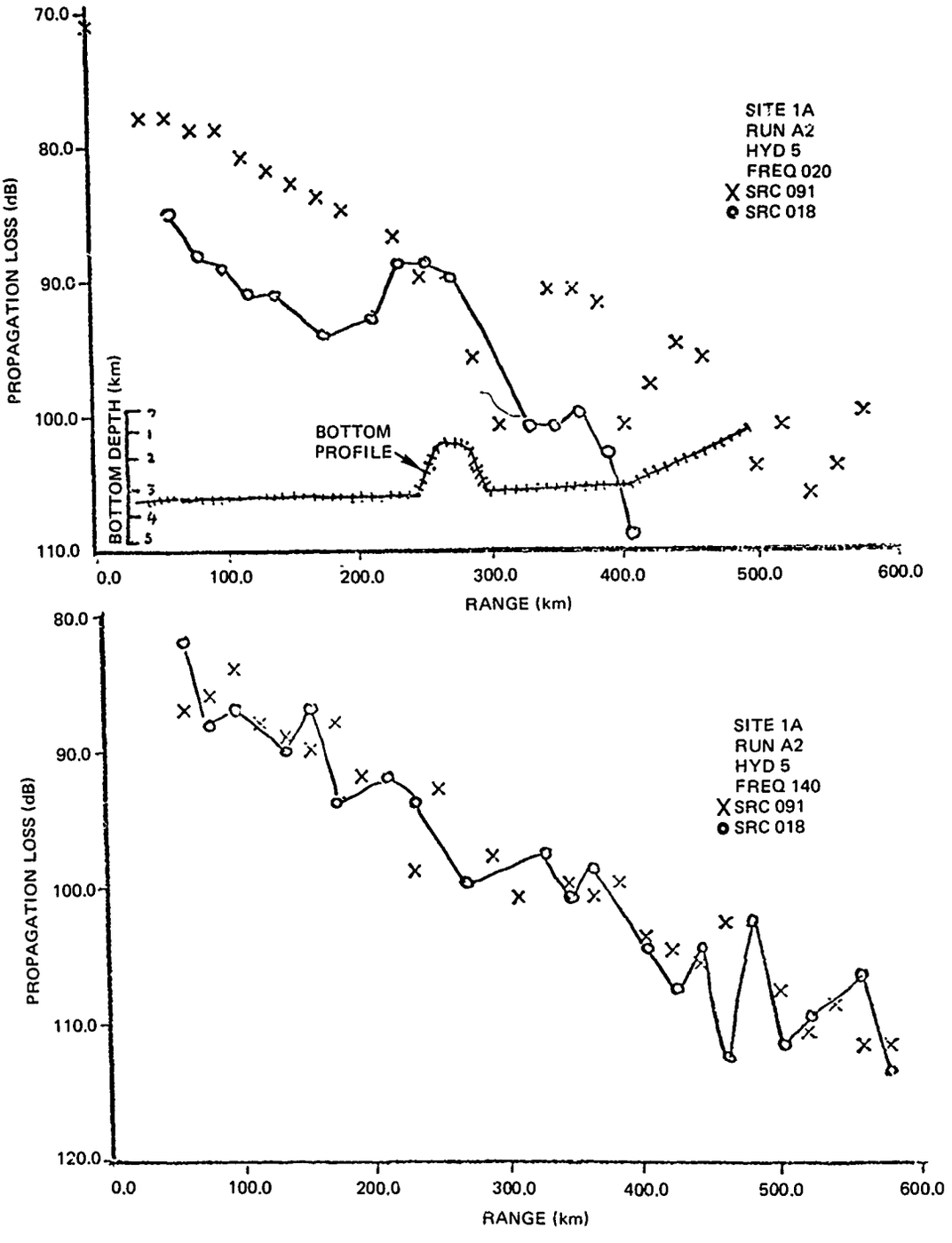

Figure 106. (C) Upslope enhancement over a seamount at Site 1A. (U)

At 20 Hz, a source at 18 m suffered approximately 10-dB more loss at 250-km ranges than a source at 91 m. This additional loss was range dependent and did not change significantly from site to site during BEARING STAKE. The higher loss at 20 Hz is attributed to surface decoupling effects.

(C) At 50 Hz the additional loss associated with the 20-Hz, 18-m source depth was negligible. At the upper two frequencies (140 and 300 Hz) there was no source depth dependence. There were no major differences in losses from sources at 91- and 243-m depths for all the frequencies examined.

(C) The propagation losses for 20 Hz at 18-m source depth are reduced in magnitude at ranges which coincide with major bathymetric features over the transmission path. This "enhancement" did not affect the losses for the other higher frequencies at 18 m nor for all the frequencies at the deeper source depths examined.

8.3 (U) PROPAGATION LOSS COMPARISONS BETWEEN SITES

(U) This section compares the propagation loss results for the five BEARING STAKE sites. The comparisons are discussed in two parts. The first part compares the sites on the basis of attenuation coefficients as derived from bottom loss tables and sound speed profiles. The second part compares the propagation losses of the events, first with the lowest loss at each site and then with the highest loss at each site.

8.3.1 (U) Attenuation Coefficient Analyses

(C) To determine the bottom attenuation coefficients, the bottom loss in 5° bottom grazing angle increments was divided by the range as calculated by ray theory for the corresponding grazing angle for each site. The values for the bottom losses at the various grazing angles were obtained from the bottom loss tables provided by ARL/UT in reference 7. The ray theory ranges were based upon representative sound speed profiles by Fenner (ref 10) for each particular site. Thus, the quotient, obtained by dividing the bottom loss by range, takes into account bottom loss, sound speed, and bottom depth, and is the attenuation coefficient due to bottom loss. These coefficients for each site are plotted as dB/100 km as a function of bottom grazing angle for frequencies of 25, 50, 140, and 290 Hz in figures 107, 108, 109, and 110, respectively. Values of the coefficients were plotted at 5° bottom grazing angle increments. Also noted in each figure along with the site is the bottom loss region number as discussed in the previous section of this report. Site 2 covered two different loss regions (2 and 5) and Site 5 also covered two loss regions (1 and 6). Hence, there are, at times, seven sites plotted in the figures instead of the five as mentioned.

(C) In analyzing the coefficients in the four figures we notice immediately that at all frequencies the highest coefficient in each case agrees with the site conditions of highest bottom loss regions; that is, Site 5 (region 6), Site 2 (region 5), and Site 4 (region 4). These differ enough from the other conditions that they are readily distinguishable in the data.

(C) The attenuation coefficients of the four remaining "sites" are not easily explained and must be examined in more detail. There are several subtle effects of bottom

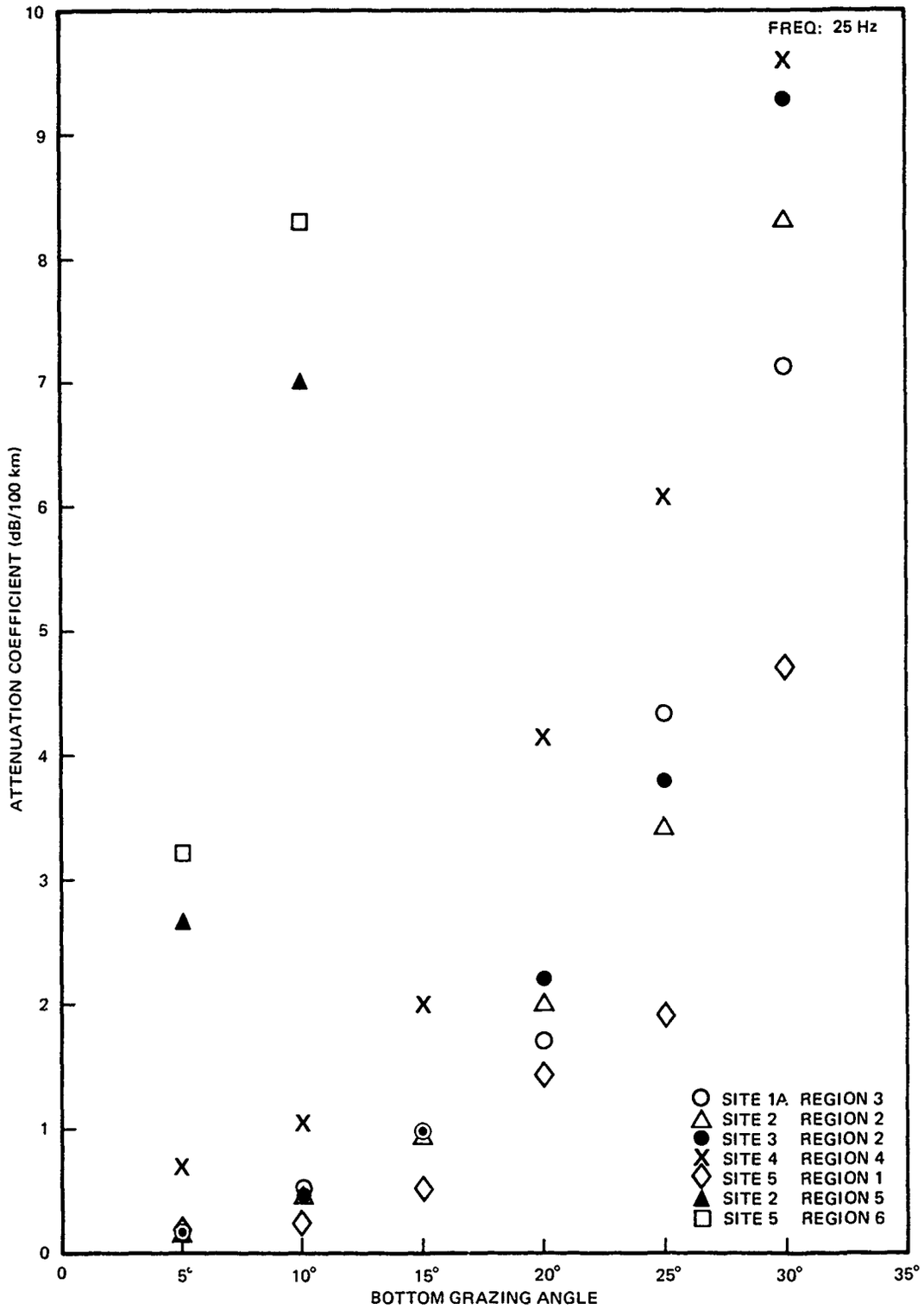

Figure 107. (C) Attenuation coefficients as a function of grazing angle for BEARING STAKE sites at 25 Hz. (C)

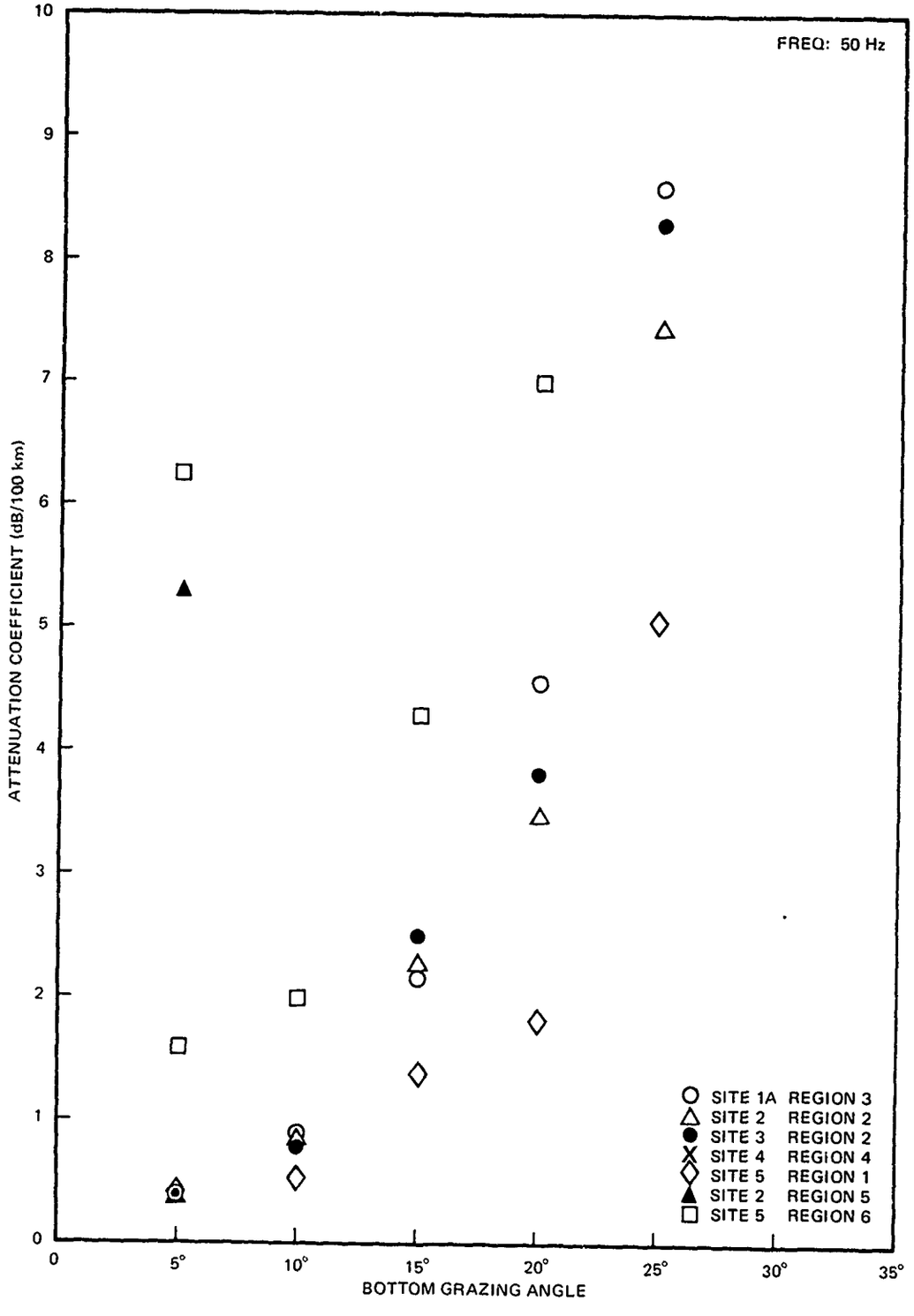

Figure 108. (C) Attenuation coefficients as a function of grazing angle for BEARING STAKE sites at 50 Hz. (C)

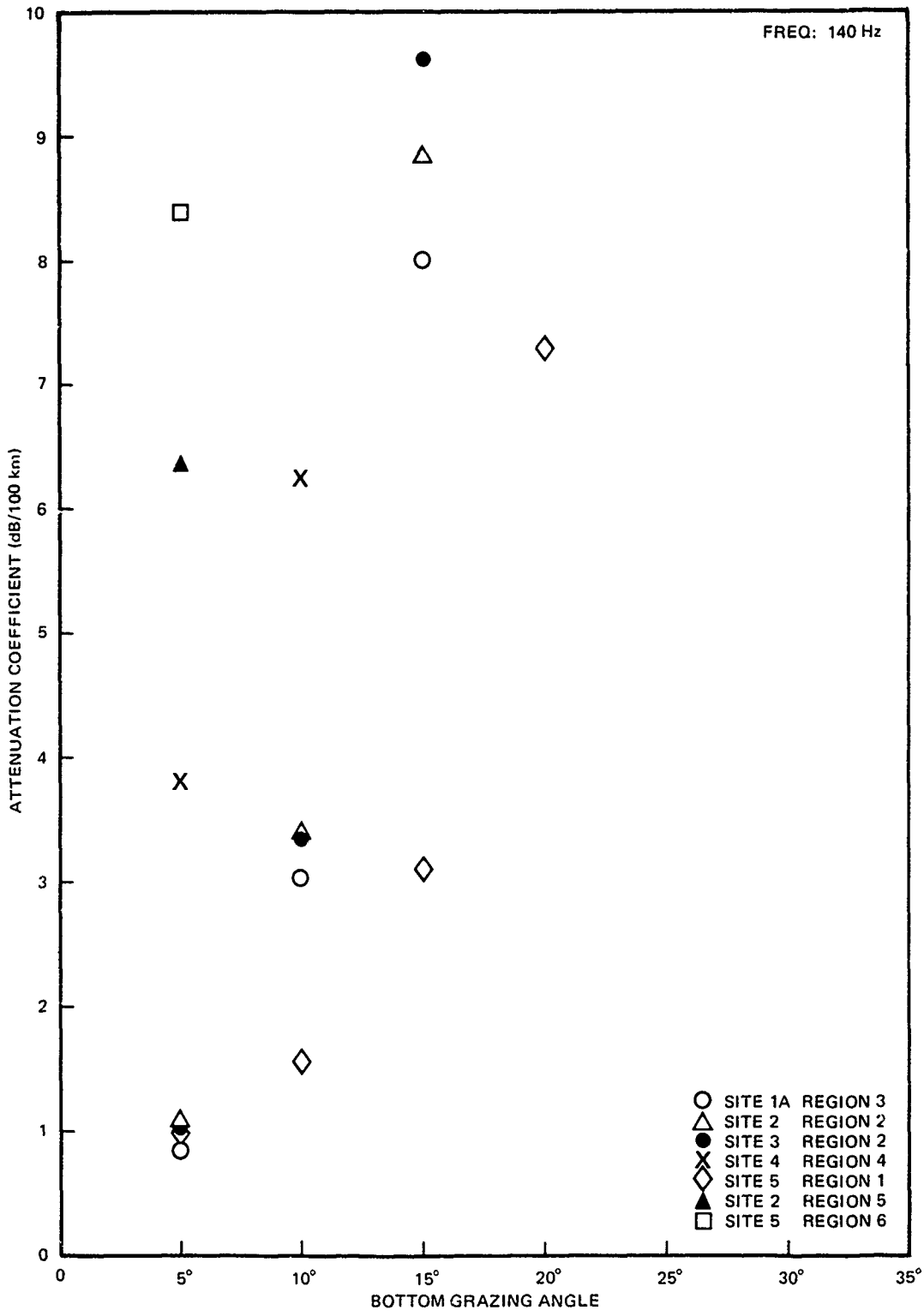

Figure 109. (C) Attenuation coefficients as a function of grazing angle for BEARING STAKE sites at 140 Hz. (C)

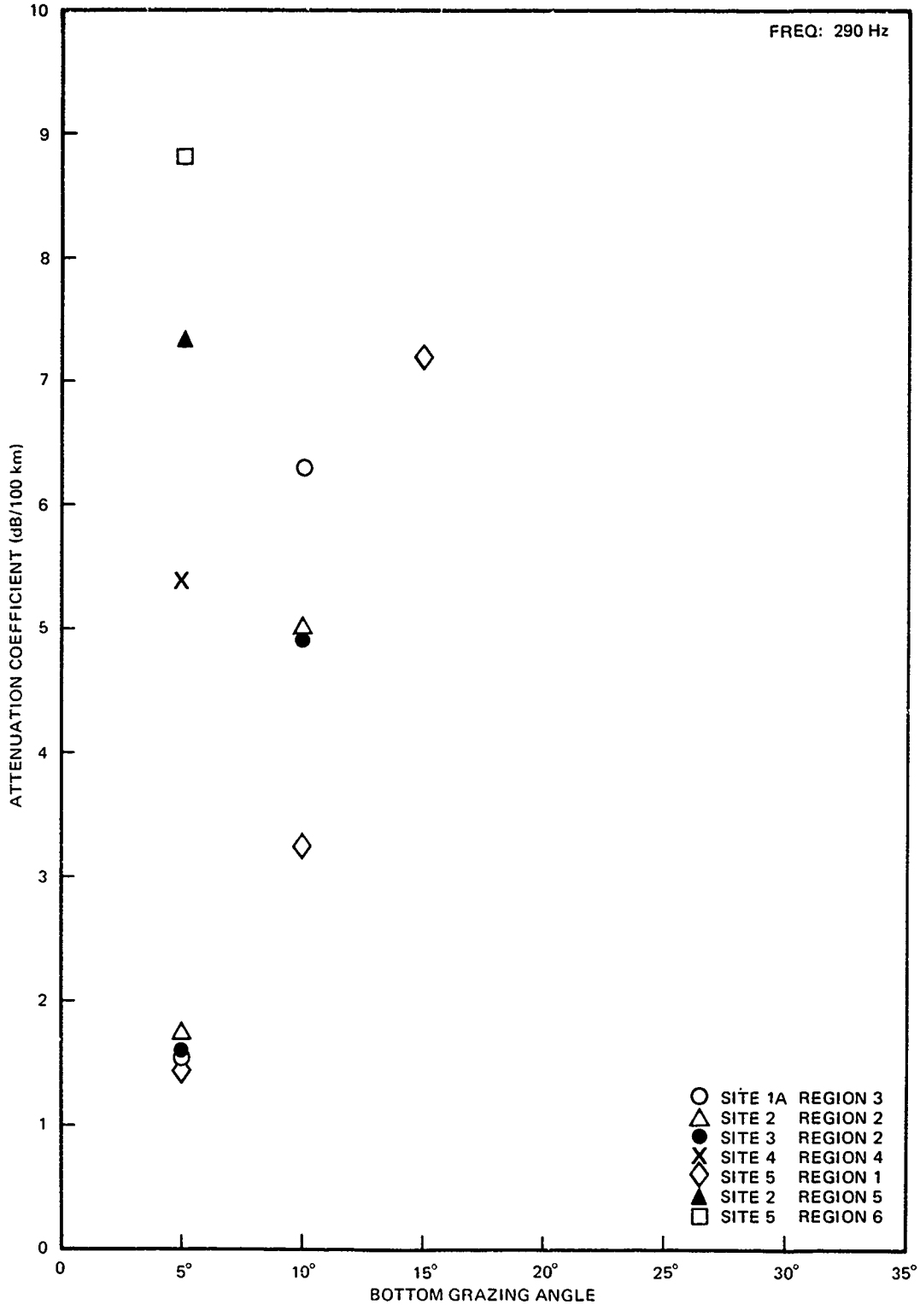

Figure 110. (C) Attenuation coefficients as a function of grazing angle for BEARING STAKE sites at 290 Hz. (C)

grazing angles on the attenuation coefficients which are not apparent from just a glance at figures 107 to 110. These effects are best illustrated in table 34, which lists the attenuation coefficients for the 0° ray at the standard source depths of 18 and 91 m. The first column lists the source depth. The second column indicates the site, and the third column indicates the type of bottom loss region. The fourth column presents the grazing angle at the bottom for the 0° ray from the source. The fifth column presents the range (loop length) of the ray. The remaining columns indicate the attenuation coefficient at the various frequencies as calculated by dividing the bottom loss at the corresponding grazing angle (column 4) by the range.

Table 34. (C) Attenuation coefficients for the 0° ray at source depths of 18 and 91 m at BEARING STAKE sites. (U)

Source Depth (m)	Site	Bottom Loss Region	Bottom Angle (Degrees)	Range (km)	Attenuation dB/100 km			
					25 Hz	50 Hz	140 Hz	290 Hz
18	1A	3	8.6	41.1	0.34	0.66	2.04	4.13
	1B	3	9.1	39.3	0.38	0.71	2.24	4.16
	2	2	9.3	38.7	0.41	0.73	2.11	4.15
	3	2	9.7	38.4	0.42	0.75	2.34	4.42
	4	4	0.6	63.0	0.06	0.63	0.33	0.54
	5	1	5.8	47.5	0.19	0.42	1.01	1.45
91	1A	3	7.1	41.5	0.27	0.58	1.54	3.80
	1B	3	7.1	44.0	0.25	0.55	1.45	3.70
	2	2	6.7	43.7	0.25	0.53	1.46	2.51
	3	2	8.1	25.9	0.36	0.72	2.11	4.05

(C) Simply stated, an analysis of table 34 shows that at very long ranges the lowest angles will dominate, and at short ranges the higher angles will dominate and larger attenuation coefficients will apply. Despite this simplification, the numbers in table 34 give some indication of the relative propagation loss for the various sites. (This analysis is not applicable to Site 4 because of convergence zone conditions. Site 4 is included in table 34 only for completeness.)

(C) Site 5 has significantly smaller coefficients than those of Sites 1, 2, and 3 for three distinct reasons. First, the bottom loss is smaller for any given grazing angle; second, the bottom grazing angle is smaller; and third, the ray loop length is longer.

(C) Sites 1A and 1B have very similar characteristics even though the site was occupied at different times of the exercise. The differences between the two are not readily distinguishable from the data. However, from table 34, the attenuation coefficients for Site 1A are slightly smaller because of smaller grazing angles and longer loop lengths.

(U) The attenuation coefficient calculations for Sites 2 and 3 were based on the same bottom loss region type. Site 2 has lower coefficients than Site 3 because the bottom grazing angles are smaller and the ray loop length is longer.

(U) Although the bottom losses of regions 2 and 3 bottom loss types are similar at low grazing angles, the grazing angles are smaller and ray loop lengths are longer for a region 3 type. Thus, the attenuation coefficients for Site 1 are generally smaller than those for Sites 2 and 3.

8.3.2 (U) Comparison of Propagation Losses

(C) This discussion on the comparison of the propagation loss at the various BEARING STAKE sites is based upon the event at each site that had the lowest measured propagation loss. Figures 111, 112, 113, and 114 show the propagation loss for these events at 25, 140, 290, and 50 Hz respectively. Also plotted on the figures is the Eleuthera reference propagation loss curve, which is included only for purposes of comparison.

(C) The most surprising feature in the comparison of the propagation losses between the five sites is the small spread in the data for the frequencies concerned. Indeed, the spread in the data for the various events at a given site, as reported in the individual site assessment sections, is generally larger than the spread for all the sites based upon the event with lowest loss. For example, the data spread in figures 111, 112, and 113 is smaller than that of their counterparts for Sites 1 and 3.

(C) The results plotted in figures 111, 112, 113, and 114 are summarized in table 35, which arithmetically averaged the propagation loss for the six 50-km range bins from 50 to 300 km for each site and each frequency. The values in table 35 are a measure of the average propagation loss over the range interval from 25 to 325 km, since the values include all the raw data over the interval. It should be noted that the results for Sites 1B, 3, 4, and 5 at 25, 140, and 290 Hz are all from CW events. All the 50-Hz results were derived from SUS events at all the sites. Table 35 also shows two sets of values for Site 2. The first set of values is based upon SUS events only, since the events at Site 2 with the lowest propagation losses at the indicated frequencies were SUS events. However, in order to compare Site 2 results with the CW results of the other sites, an adjustment was required. Hence, the second set of results (denoted by the asterisk) for Site 2 includes an adjustment to the SUS values by the median difference between SUS and CW events as previously discussed in the Site 2 assessment. These adjusted values are used in this comparison of Site 2 values with the CW values from other sites.

(C) The interesting feature about table 35 is not the magnitude of the propagation losses at each site but the various differences between the losses at each site. Table 36 presents the propagation loss differences between sites at the selected frequencies. The differences are referenced to the site with the lowest propagation loss as shown in table 35. Note that the propagation loss differences between Site 1B and Site 3 in table 36 are 0.2, 0.7, 0.0, and 1.4 dB for 25, 140, 290, and 50 Hz, respectively. This result agrees very well with the previous analyses of attenuation coefficients, which indicated that the propagation at Site 1B would be slightly better than that at Site 3.

(C) Table 37 shows the difference in propagation loss between 25 Hz and the higher frequencies. The differences may be regarded as the increase in attenuation due to absorption

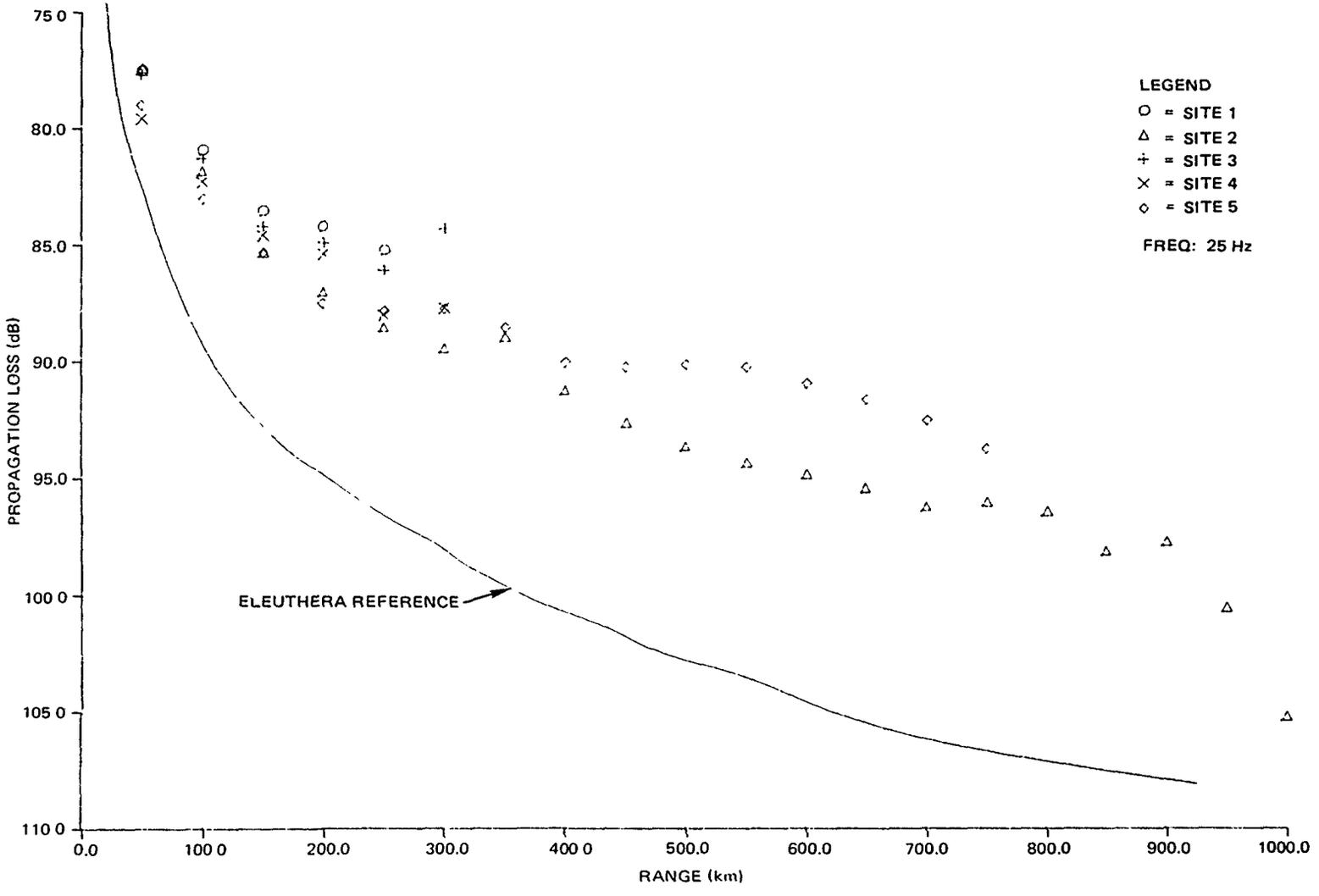

Figure 111. (C) Comparison of propagation loss at 25 Hz for each site with the Eleuthera reference curve. (C)

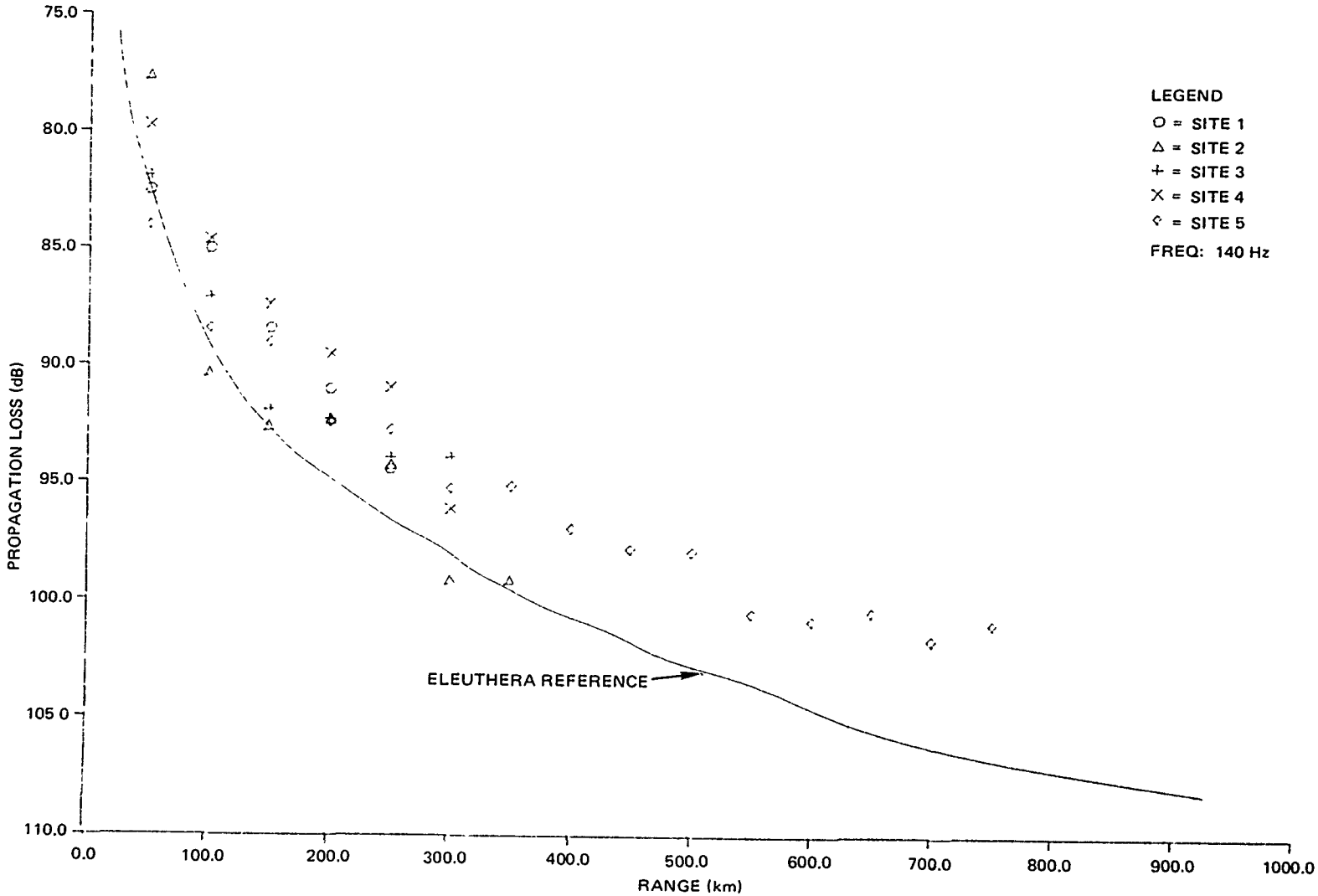

Figure 112. (C) Comparison of propagation loss at 140 Hz for each site with the Eleuthera reference curve. (C)

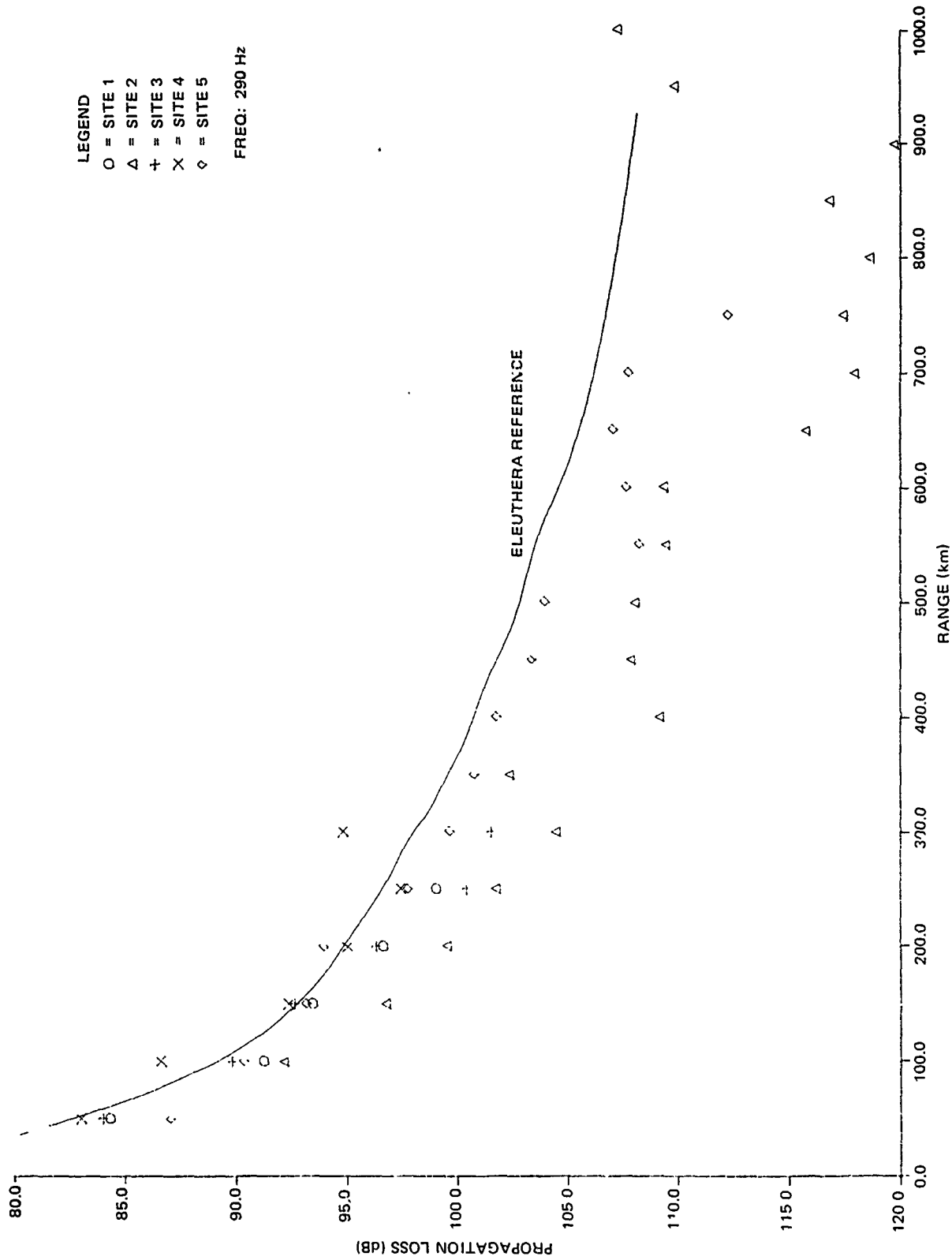

Figure 113. (C) Comparison of propagation loss at 290 Hz for each site with the Eleuthera reference curve. (C)

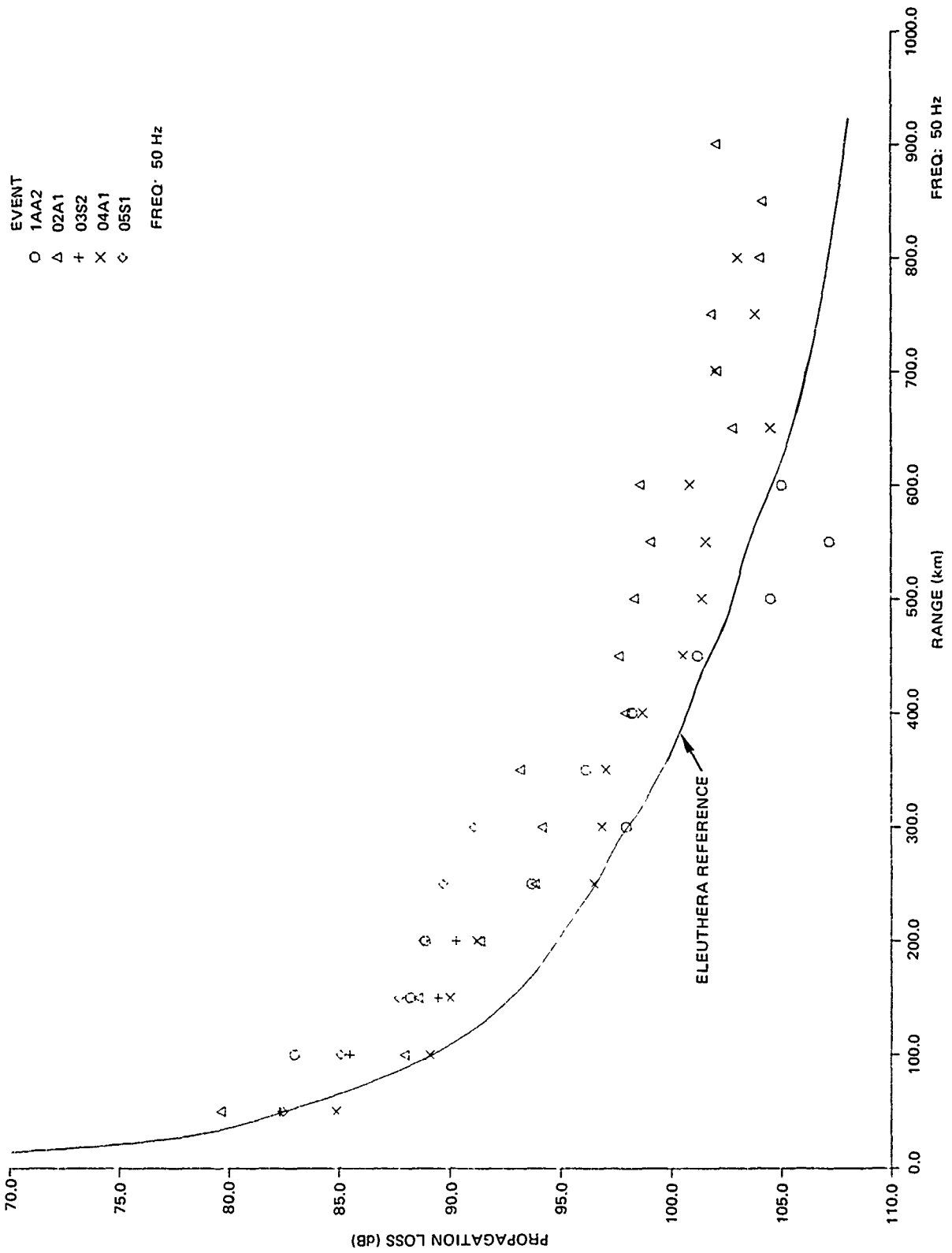

Figure 114. (C) Comparison of propagation loss at 50 Hz for each site with the Eleuthera reference curve. (C)

Table 35. (C) Average propagation losses for the best event at each site for the 25–325-km range interval. (U)

Site	Event Type	Propagation Loss (dB)			
		25 Hz	140 Hz	290 Hz	50 Hz
1B	CW	82.9	89.5	94.1	87.4
2	SUS	85.3	92.3	97.0	89.8
2*	CW	83.9	91.2	95.0	—
3	CW	83.1	90.2	94.1	88.8
4	CW	84.6	89.5	91.5	91.4
5	CW	85.0	90.3	93.6	87.5

*Adjusted to CW values for this site.

Table 36. (C) Propagation loss differences between the site with the lowest propagation loss and the other given sites for the various frequencies. (U)

Site	Propagation Loss Difference (dB)			
	25 Hz	140 Hz	290 Hz	50 Hz
1B	0	0	2.6	0
2	2.4	2.8	5.5	2.4
2*	1.0	1.7	3.5	—
3	0.2	0.7	2.6	1.4
4	1.7	0	0	4.0
5	2.1	0.8	2.1	0.1

*Adjusted to CW values.

and higher bottom losses for a nominal range of 175 km. Note that the difference values for Site 2 are very similar to those for Site 1B and Site 3. This suggests that the attenuation characteristics across the Indus Fan near Site 2 are comparable to those of Site 3 and Site 1B. Thus, the assignment of a number "2" to the bottom loss region at Site 2 appears reasonable.

(C) Note also in table 37 the smaller differences for Site 5 as compared to Site 1B, 2, or 3. This is in good agreement with previous analyses which indicated that Site 5 should have a significantly smaller bottom attenuation than the other bottom-limited sites.

(C) In table 37, Site 4 shows the smallest values for 140 and 290 Hz. This results because the principal propagation paths at these frequencies are by convergence zone and therefore do not suffer bottom losses. However, at 50 Hz, Site 4 has the highest value of the sites. This suggests that the principal propagation path at 50 Hz is by bottom bounce,

Table 37. (C) Propagation loss difference between 25 Hz and 140, 290, and 50 Hz for each site, based on the propagation loss of the best event at each site. (C)

Site	Propagation Loss Difference (dB)			
	25 Hz	140 Hz	290 Hz	50 Hz
1B	0	6.6	11.2	4.5
2	0	7.0	11.7	4.5
2*	0	7.3	11.1	—
3	0	7.1	11.0	5.7
4	0	4.9	6.9	6.8
5	0	5.3	8.6	2.5

*Adjusted to CW values.

with the higher value resulting from higher bottom attenuation losses than experienced by the other sites.

(C) One critical question arises from this analysis of the propagation loss differences between sites. If the bottom loss is lowest at Site 5, as concluded, why does table 35 show that Site 5 has higher propagation loss than Sites 1B and 3 at 25 and 140 Hz? Moreover, figures 112 and 113 showed that Site 5 has the highest propagation loss of all the sites at ranges of 50 and 100 km for 140 Hz and at a range of 50 km for 290 Hz. After a reexamination of the data, it was hypothesized that the reason for this higher loss was that the receivers at Site 5 were mounted on a small conical hill (discussed previously in the Site Analysis section of this report). This hill is part of the Carlsberg Ridge, which has a number "6" bottom loss region designation. At least half of the acoustic arrivals at Site 5 must reflect at least once off this hill with high loss. Thus, it was estimated that the propagation loss would be increased by about 3 dB. This hypothesis was tested by utilizing the ASTRAL propagation loss model. The model compared the propagation loss for a receiver mounted on the hill with those for a receiver, north of the hill, on the floor of the Indus Fan. The propagation losses, beyond the direct field, for frequencies of 25, 140, and 29 Hz were, respectively, about 2, 3, and 3 dB greater for the receiver mounted on the hill. Thus, if the propagation losses for Site 5 in table 35 are reduced by these amounts, Site 5 is comparable to Sites 1B and 3 at 25 Hz and superior at 140 and 290 Hz. No ASTRAL run was made at 50 Hz, but a 2.5-dB correction would be a fair estimate. This would make Site 5 superior to Sites 1B and 3 at 50 Hz as well.

(C) A similar comparison of ASTRAL runs was made for Site 2. There the receivers were mounted on a scarp which had been rated a number "5" bottom loss region. The propagation losses predicted by the ASTRAL model for 25, 140, and 290 Hz were about 1, 4, and 4 dB, respectively, greater for the receivers on the scarp as compared to receivers mounted on the floor of the Indus Fan at the foot of the scarp. Thus, the higher losses for Site 2 as shown in table 35 are no doubt due to receiver placement on the scarp.

(C) Up to now, very little has been said about Site 4 as related to table 35. At 25 and 50 Hz, the propagation loss for Site 4 is higher than that for Sites 1B and 3, and would also be higher than that for Sites 5 and 2 if the adjustments just discussed above for the placement of receivers were made for Sites 5 and 2. The Site 4 results in table 35 are in agreement with other features of Site 4; i.e., at 25 and 50 Hz, the propagation appears to be bottom bounce rather than convergence zone and the bottom losses are significantly higher at Site 4 than at Sites 1B, 3, and 5. At the higher frequencies of 140 and 290 Hz at which convergence zones dominate, the similarity of the results of Site 4 to those of the other sites is fortuitous. It is certainly not the intent here to leave the general impression that acoustic propagation in bottom-limited areas is comparable "on the average" to that under convergence zone conditions. This appears to be true for BEARING STAKE only because of the low bottom loss at the bottom-limited sites and the marginal convergence zones for small depth excesses.

(U) At the other extreme, comparisons of the events with the highest propagation loss at each site were made to determine their impact on the overall propagation loss assessment for BEARING STAKE.

(C) The event at each site with the highest propagation loss, and the Eleuthera reference loss curve, are plotted for 20, 140, 290, and 50 Hz in figures 115, 116, 117, and 118, respectively. Note that there are five events plotted for Site 2 at 20, 140, and 290 Hz. The reason for plotting these five events was that in the initial comparisons for this analysis it became apparent that all the Site 2 events conducted west of the Owen Ridge (events 2A2, 2A3, 2S1, and 2P1) should be included (as well as event 2P3, which ran across the Indus Fan) in order to make this analysis more complete.

(C) The events for Sites 1, 3, 4, and 5 are indicated in the figures by open symbols, the Site 2 events by line symbols. The interesting feature about the results is that for 20 Hz (fig 115) and 50 Hz (fig 118), the propagation losses for all the sites, except Site 2, are generally less than those of the Eleuthera reference curve, especially at long ranges. It must be remembered that these results are from the events with highest loss at each site. At 140 and 290 Hz, all the results fall below the reference curve.

(C) Table 38 ranks the events of this analysis in order of increasing propagation loss at the selected frequencies. (The rankings are relative to the longest ranges at which data were available because the short range data often are not representative of the bathymetric conditions along the track.)

(C) The most significant feature of table 38 is the fact that the four highest-loss events at 140 and 290 Hz are all Site 2 events conducted west of the Owen Ridge. Under the low and 50-Hz column, two of the Site 2 events have the highest losses. The main reason that the Site 2 events are generally worse than any other BEARING STAKE event is that the propagation paths at Site 2 involve high-bottom-loss types. Events 2P1 and 2S1 were conducted over a type "5" bottom loss region. Event 2A3 was conducted over type "5" and "6" regions. Event 2A2 was conducted mostly over a type "5" region. The highest-loss events at the other four sites sometimes involved high-loss regions for only a portion of the events. Hence, the principal difference between Site 2 events and the events for the other sites is that the Site 2 events were conducted entirely over high-bottom-loss regions.

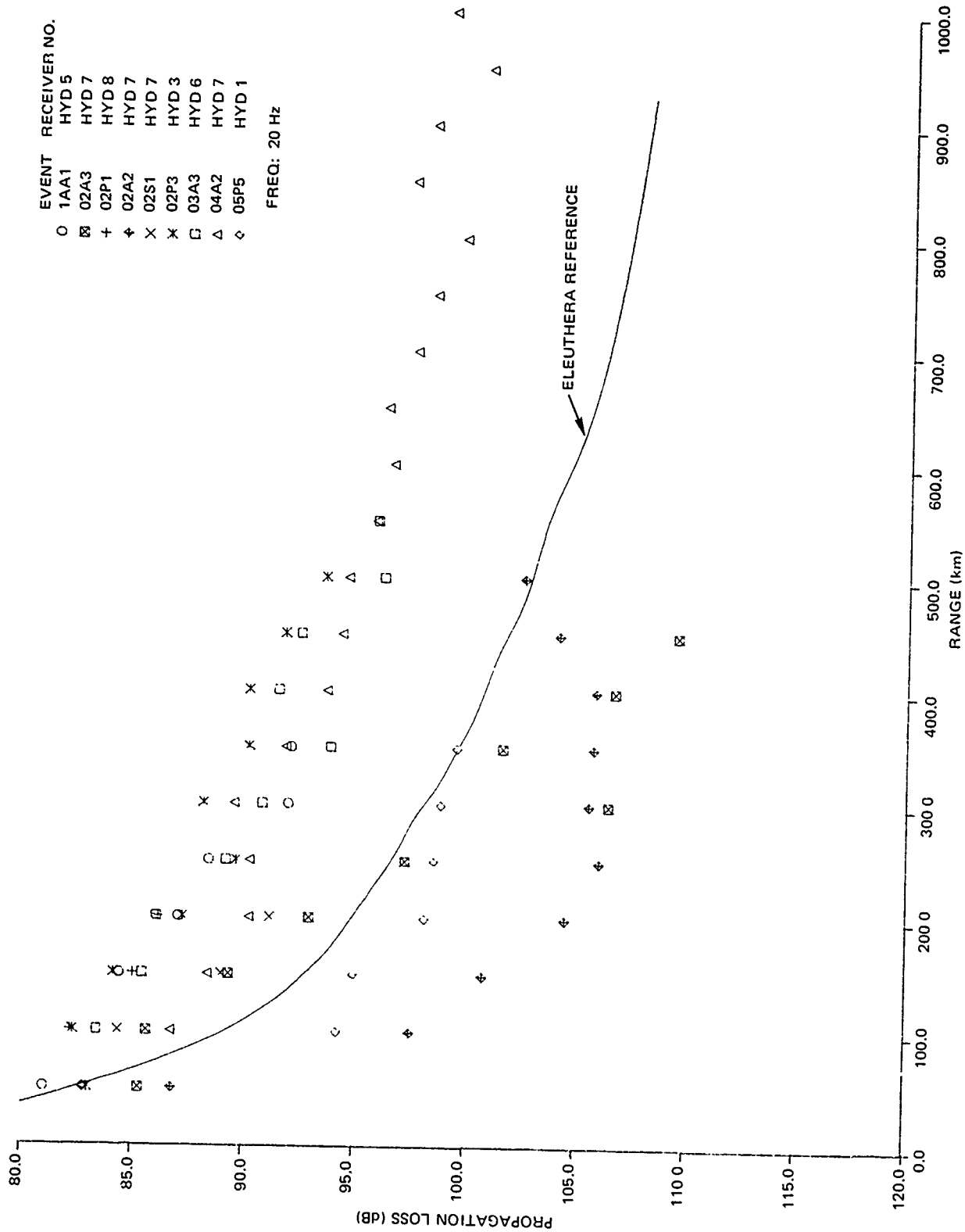

Figure 115. (C) Comparison of propagation loss at 20 Hz, from the events at each site which had the highest propagation loss, with the Eleuthera reference. (C)

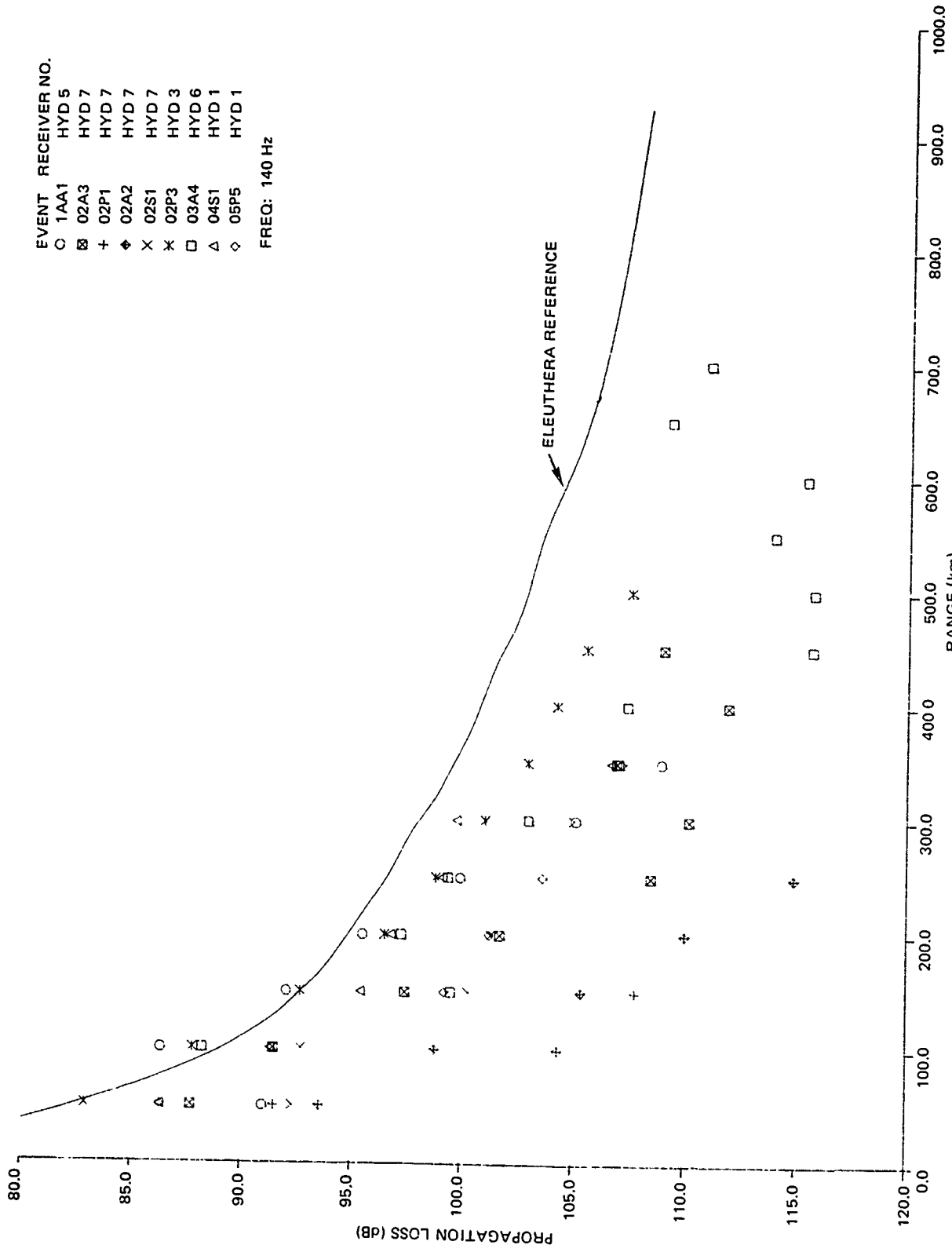

Figure 116. (C) Comparison of propagation loss at 140 Hz, from the events at each site which had the highest propagation loss, with the Eleuthera reference. (C)

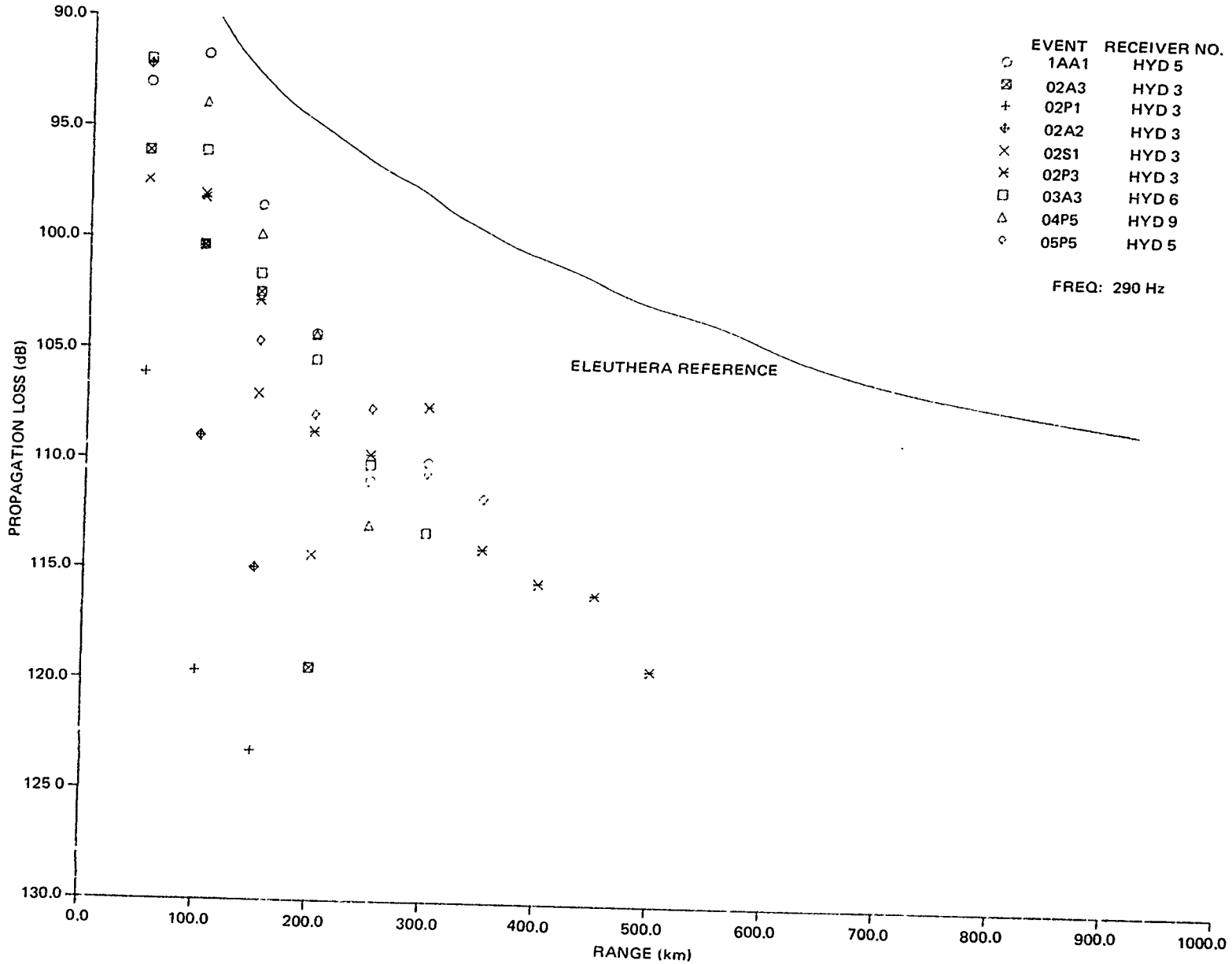

Figure 117. (C) Comparison of propagation loss at 290 Hz, from the events at each site which had the highest propagation loss, with the Eleuthera reference. (C)

CONFIDENTIAL

CONFIDENTIAL

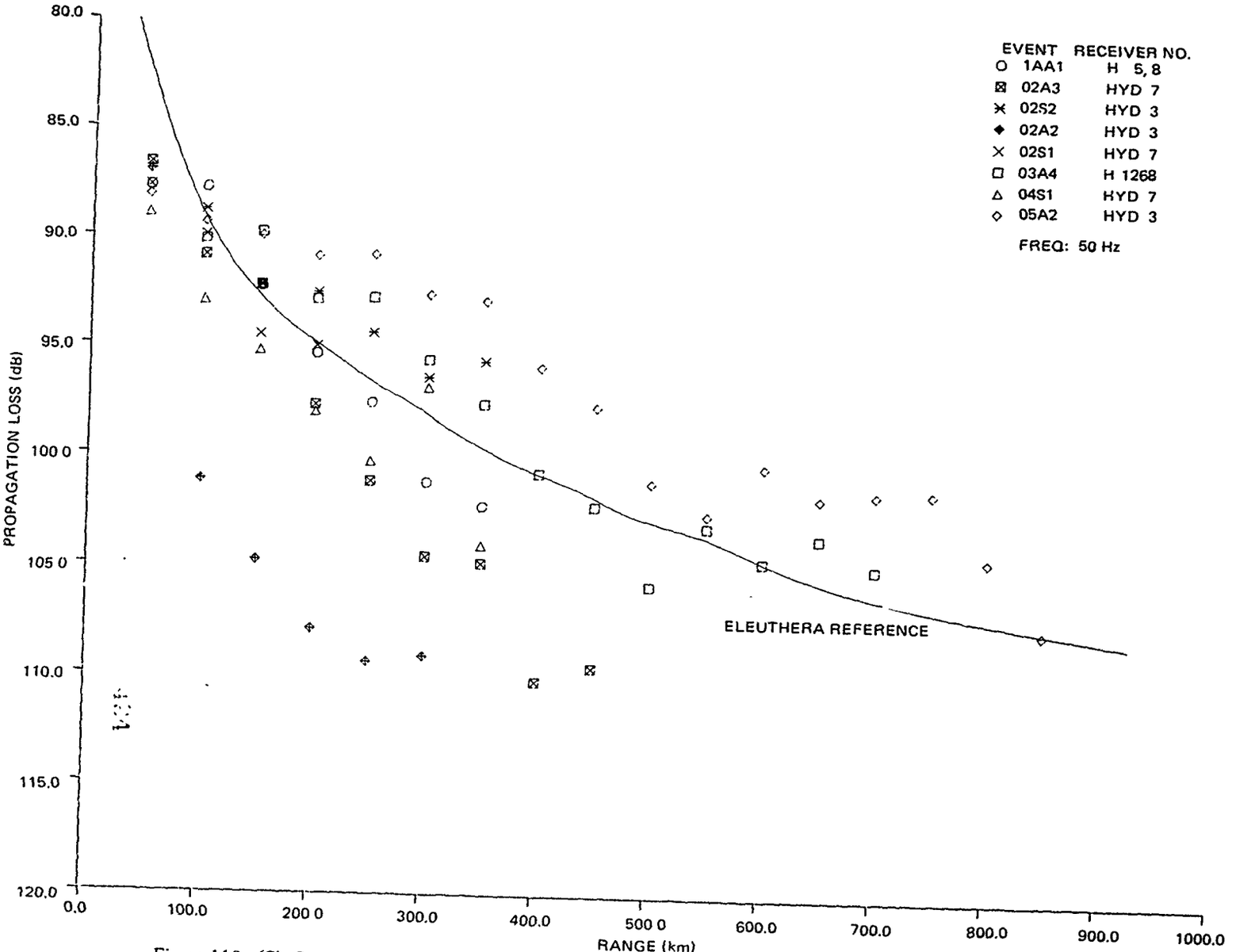

Figure 118. (C) Comparison of propagation loss at 50 Hz, from the events at each site which had the highest propagation loss, with the Eleuthera reference. (C)

CONFIDENTIAL

Table 38. (C) Ranking of various events which had exceptionally high propagation losses. (U)

Rank	Events				Overall Ranking
	Low (20-25) Hz	140 Hz	290 Hz	50 Hz	
1	2P1	4S1	5P5	5A2	2P3
2	2P3	2P3	2P3	2S2	5P5
3	4A2	5P5	1AA1	3A4	3A4
4	3A3	3A4	3A3	1AA1	3A3
5	1AA1	1AA1	4P5	2S1	1AA1
6	2S1	2A3	2S1	4S1	2S1
7	5P5	2S1	2A3	2A3	2A3
8	2A2	2A2	2A2	2A2	2A2
9	2A3	2P1	2P1	—	2P1

(C) The remaining events of table 38 are now discussed on a site-by-site basis. Of these remaining events, event 1AA1 had the highest overall propagation losses at all frequencies. This event was conducted over a severe obstruction with portions of the event in a type "5" region. The events with the next highest overall losses appear to be events 3A3 and 3A4. There were no bathymetric obstructions along the paths of these two events, but at long ranges the events appear to have passed from a type "1" loss region to a type "5" region.

(C) Event 5P5 shows up at all three CW frequencies in table 38. This event displays relative losses which range from very high at 25 Hz to low at 290 Hz. This is the event which crossed over a seamount projecting out of the Indus Fan with, presumably, a type "6" loss region.

(C) The ranking of the Site 4 events is somewhat mixed as shown in table 38. Since Site 4 involves convergence zone propagation, it is difficult to place it in context with the bottom-limited sites. Note, however, the relatively low ranking of event 4P5 at 290 Hz. This event was bottom limited and the ranking of it is indicative of the high bottom losses at Site 4 at the high frequencies.

(C) Finally, the best of the events with high losses were events 2P3 and 2S2. This was not surprising since these events were conducted over the Indus Fan, which has a region "1" bottom loss designation. However, as discussed earlier in the Site 2 assessment section of this report, event 2P3 was a relatively poor CW event at 140 and 290 Hz.

8.4 (U) SELECTION OF SURVEILLANCE SITES ON THE INDUS FAN

(C) The present procedure of selecting surveillance sites mounted up on the ridges bounding a basin does not appear to be the best choice for a bottom-limited basin with low bottom loss. As previously discussed, the experimental data at Sites 2 and 5, as well as the

special ASTRAL runs, strongly suggest that surveillance arrays should be placed on the low-loss Indus Fan rather than above the floor on high-loss hills or scarps. Furthermore, the normal mode model studies and experimental measurements of Site 1B suggest that an improvement of several dB in SNR might be achieved with the optimum placement of surveillance arrays about 20 to 30 m off the bottom (depending on the low frequency of primary interest). The placement of surveillance arrays on the periphery of the Indus Fan should be re-examined. Once the hypothesized advantage of mounting receivers on ridges has been eliminated, it is not clear that configurations on the periphery of the basin are superior to other configurations distributed throughout a basin.

8.5 (U) ELEUTHERA REFERENCE COMPARISONS

(C) Acoustic propagation conditions in the Northwest Indian Ocean were exceptionally good during the BEARING STAKE exercise time period. This feature is best illustrated by comparison of the BEARING STAKE propagation loss curves (based on the longest run at each site and the receiver depth with the lowest loss) with the Eleuthera reference propagation loss curve as shown previously in figures 111, 112, and 113. The comparisons were made with the propagation losses as measured from the CW source runs. Although shot data from the aircraft runs went to longer ranges, the data were too sparse for reliable numerical comparison.

(C) At low frequency (25 Hz), averaged experimental propagation loss was less than that of the Eleuthera reference for all available ranges at Sites 1B, 2, 3, 4, and 5. At the maximum available ranges for each of the respective sites, the propagation loss was 13, 11, 11, 11, and 12 dB less than that of the reference at the corresponding range. For 25 Hz, the slopes of the measured propagation loss curves were generally less than that of the reference.

(C) At 140 Hz, the slopes of the experimental loss curves were comparable to that of the reference for Sites 1B, 3, 4, and 5. The experimental losses were respectively 1–5, 2–6, 0–4, and 0–6 dB less than those of the reference. The behavior of the 140-Hz comparison for Site 2 was a little more complicated. At Site 2, the slope of the experimental loss curve was comparable to that of the reference for the range intervals of 50 to 150 km and 300 to 500 km; for the range interval of 150 to 300 km, the slope was greater. The experimental losses were less than 1 dB smaller for the 50–150-km range interval and 2 dB greater for the 300–500-km range interval than those of the reference for the same intervals.

(C) At 290 Hz, the slopes of the experimental loss curves were comparable to that of the reference for Sites 1B, 3, and 4. The experimental losses were, respectively, 1–3 dB more, 0–3 dB more, and 0–4 dB less than those of the reference. At Site 5, the experimental losses were comparable to those of the reference from 150 to 500 km but increased to about 3 dB from 500 to 750 km. At Site 2, the experimental loss curve was comparable to that of the reference from 200 to 500 km but the experimental losses were greater by 10 dB.

(C) From the above comparisons, it can be concluded that acoustic propagation losses are smaller at 25 and 140 Hz in the Northwest Indian Ocean than those of the Eleuthera reference at comparable ranges and that at 290 Hz, for the most part, the losses will be equal to or greater by about 3 dB than those of the reference.

8.6 (U) PROPAGATION LOSS MODEL ASSESSMENT

(U) Three propagation loss prediction models were exercised and their results were compared with the results from BEARING STAKE. The models were (1) RAY WAVE, developed at NOSC; and (2) ASTRAL and (3) FACT, both developed by C. Spofford, who is currently with Systems Application, Inc (SAI). The purpose of the discussion to follow (and of this report) is not to discuss the merits of each of the models exercised nor to say which one is superior to the others, but rather to assess the results of each model to determine which one can predict, nearly, the actual propagation losses as measured during BEARING STAKE.

(C) Initial comparisons of the three propagation models, RAY WAVE, FACT, and ASTRAL, with the WECo low-frequency (25 Hz) data measured by the BMA at three sites all showed a consistent discrepancy. The experimental propagation losses were about 6 dB less for each at Sites 1B, 3, and 5. These differences were attributed to four separate factors, each of which may reduce the discrepancy between experiment and theory by 1 or 2 dB.

(C) The first factor was a decrease in the bottom loss used in the models at low frequency. The initial comparison used, as model inputs, the bottom loss measured by ARL from shot data at Sites 1B, 3, and 5. In response to the aforementioned discrepancy, ARL re-examined these measured losses and concluded that as a set the initial losses at low frequency were not reliable and were too high. (ARL has recently prepared new values of bottom loss based on a theoretical model of the bottom forced to fit with measured acoustic data at high frequencies and extrapolated down to low frequency.)

(C) The second factor was the result of two observations made during the course of analyzing the data at Site 1B.

1. (C) The NOSC normal mode model was exercised with the data from Site 1B and the latest sub-bottom structure as provided by ARL. The propagation loss results from this model were only 2.5 dB greater than the WECo data as opposed to the 6-dB discrepancy shown by the previously mentioned three models. The better prediction performance of the normal mode model was attributed to the fact that it sums up the acoustic energy coherently rather than incoherently as the other models do. (The model depth structure at the site showed a near-bottom maximum, with amplitudes dropping off several decibels away from the bottom. This strongly suggested that the upgoing and downgoing arrivals are nearly in phase rather than 90° out of phase, the relationship inherent in incoherent addition.)

2. (C) The normal mode model results were used to generate a table of bottom losses and the results were then used as inputs to the RAY WAVE model. The propagation loss results for this RAY WAVE model were found to be about 1.5 dB greater than those of the normal mode model. The implication here is that the 1.5 dB can be attributed to the difference between incoherent addition (RAY WAVE) and coherent addition (normal mode).

(U) As a result of this factor, SAI has proceeded to modify the original ASTRAL model by taking into account the phase of arrivals refracting in the sub-bottom layers.

(U) The third factor is a possible increase in the low-frequency source levels used to reduce experimental data to propagation loss. A limited comparison between the result of a theoretical analysis and a measurement of the direct field propagation at short horizontal ranges suggests that the source levels were underestimated.

(C) The fourth factor is the possibility that the WECo data processing procedure results in a systematic biasing of propagation loss to the low side. This possibility is suggested by a comparison, although limited, of WECo data with ACODAC data. The indications of the comparison were that WECo results at 25 Hz were about 1.5 dB lower than ACODAC results.

(C) If the above factors are proved valid, the discrepancy between the experimental data results and model results will be eliminated. It should be noted here that factors 1 and 2 are corrections to model inputs or models which are still being exercised; hence, their results are not included in this assessment report. In contrast, factors 3 and 4 represent corrections to the experimental data. Further examination of these two factors will have to be completed before any recommendations can be made as to probable adjustments to the data set. Then the entire problem of the discrepancy between theory and experiment will be re-examined by using the adjusted experimental data and model calculations incorporating factors 1 and 2.

(U) Notwithstanding, initial comparison of the results of the ASTRAL model for propagation loss with experimental results, and with the results of the RAY WAVE and FACT models, indicates that ASTRAL is well suited for the prediction of mean propagation losses in an environment such as BEARING STAKE. Undoubtedly, there will be some "tweaking" of the ASTRAL model as special situations are uncovered which require minor adjustments. Indeed such tweaking has already taken place as a result of the initial comparison. Since the outputs of ASTRAL are mean propagation losses, some independent model of the fluctuation due to multipath effects will be a necessary adjunct to ASTRAL for systems performance evaluation.

8.7 (U) RECOMMENDATIONS FOR ADDITIONAL MEASUREMENTS

(U) Although the acoustic measurements made during BEARING STAKE provide to the surveillance community heretofore unavailable data for propagation loss analyses, the results of this propagation loss assessment report indicate that additional acoustic measurements should be made in the BEARING STAKE area. These additional measurements are set forth as a series of recommendations in this section. These recommendations differ from those presented in the individual site assessment sections of this report in that these are for new measurements, whereas the other recommendations were for additional processing of existing data.

(C) The following additional acoustic measurements in the Northwest Indian Ocean are recommended:

1. (C) Propagation measurements using CW sources should be made across the Chain Ridge, which bounds the Somali Basin to the east; across the Carlsberg Ridge, which bounds the Indus Fan to the south; across the Owen Ridge, which bounds the Indus Fan to the west; and across the Murray Ridge, which separates the Gulf of Oman from the Indus Fan. For a variety of reasons, good quantitative data over these bathymetric features were not obtained in BEARING STAKE. The chief purpose of these recommended measurements is to obtain propagation data necessary for the modeling of distant shipping noise which propagates over these bathymetric features.

2. (C) Detailed propagation loss measurements should be made to evaluate the slope enhancement of shipping noise. The shots from aircraft events on BEARING STAKE were too sparse for effective evaluation. High-density shot runs, with a ship, and/or CW events are recommended. Some events should be conducted with low-frequency CW sources at 6-m depth to properly simulate the source depths of shipping noise.

3. (C) Measurements should be made in several locations on the Indus Fan to verify the existence of the notch of higher propagation loss which theory predicts to be somewhat off the ocean floor. A string of receivers spaced at 10-m intervals above the ocean floor should be utilized. Propagation from simultaneous shallow and deep low-frequency CW sources should be measured. The sites tested should include a site at which measurements of noise could be compared on the various receivers. This location should be far from shipping lanes. Desirable locations would be on the fan near Site 2 and near Site 5. These measurements are needed to verify model results indicating that such receivers will perform better than those deployed on the Owen Ridge at Site 2 or on the conical hill at Site 5.

4. (C) Additional experiments on the Indus Fan should be designed to determine whether the fan can be modeled adequately by two bottom loss regimes and if so to locate the boundaries of these regimes.

5. (C) Possible advantages should be considered to the distribution of surveillance sites throughout a bottom-limited basin, such as the Indus Fan, as opposed to the current scheme of locating such sites on the periphery of the basin.

6. (C) Critical decisions as to a surveillance site configuration in the Somali Basin should be held in abeyance until the complicated dependence of propagation loss on frequency, receiver depth, and depth excess is understood more precisely. This understanding will come only with a rigorous theoretical investigation for a variety of seasons followed by experimental verification.

9.0 (U) OVERALL CONCLUSIONS

(C) This propagation loss assessment report of the BEARING STAKE exercise conducted in the Northwest Indian Ocean will provide the undersea surveillance community with heretofore unavailable propagation loss measurement results from this strategic area. It is hoped that the information and results from this report will provide designers of undersea surveillance systems with the inputs required to make improved assessments of surveillance system options for the Indian Ocean.

(C) The intent of this report has been to assess the nature of propagation loss in the Northwest Indian Ocean on the basis of the BEARING STAKE exercise. However, such an assessment cannot be totally separated from discussions of data analysis or theoretical studies made during the course of the assessment. Hence, the overall conclusions of this section include remarks about the exercise and analysis in addition to those concerning the propagation loss.

Propagation Loss (U)

(C) Although the Northwest Indian Ocean is acoustically bottom limited, propagation losses were unexpectedly low for all the BEARING STAKE sites. The good propagation conditions can be attributed to low bottom losses, which were measured to be much lower than predicted prior to the exercise.

(C) Comparisons of the event of lowest propagation loss at each site with the familiar Eleuthera reference show that for 25 Hz the measured losses at all available ranges for all the sites were less than those of the reference by as much as 13 dB. For 140 Hz, for all sites except Site 2, the losses were less than the losses of the reference by as much as 6 dB. Site 2 values varied from 1 dB smaller at short ranges to 2 dB larger at ranges beyond 300 km, when compared to the values of the reference. For 290 Hz, the losses were greater than the losses of the reference by up to 3 dB for Sites 1B and 3, and up to 9 dB for Site 2. At Site 4, the losses were less than the losses of the reference by up to 4 dB; and at Site 5, the losses were comparable to those of the reference at short ranges and exceeded them by 3 dB at ranges beyond 550 km.

(C) Propagation losses, averaged over the range interval from 25 to 325 km, for the event of lowest propagation loss at each site ranged from a minimum of 82.9 dB at 25 Hz for Site 1B to a maximum of 97.0 dB at 290 Hz for Site 2. The ranking, in order of increasing propagation loss, of the BEARING STAKE sites at 25 Hz is 1B, 3, 2, 4, and 5. At 290 Hz, the ranking is Site 4, 5, 1B, 3, and 2. The low propagation losses for Site 4 at 290 Hz represent convergence zone propagation, which is markedly better than bottom-limited propagation at the higher frequency.

(C) The propagation loss at Sites 5 and 2 was significantly increased by the placement of the receivers on high-loss bathymetric features. A better placement would have been on the low-loss floor of the Indus Fan. This conclusion was initially deduced from the experimental results at 25 Hz, in which the propagation loss was highest for Site 5 although the bottom attenuation coefficients at the site were lowest of all the sites. The result was also verified by theoretical computations in which the propagation loss for Sites 5 and 2 was 2 to 4 dB less for receiver placement on the floor of the Indus Fan than for their actual placement

on the Carlsberg and Owen Ridges, respectively. Thus, from the standpoint of propagation loss, the placement of surveillance receivers on the high-loss ridges bounding a low-loss bottom-limited basin is not an optimal choice.

(C) There was a definite dependence of propagation loss on the various azimuthal directions (events) at each of the five sites. Indeed, the spread in the data at Site 3, which was the most homogeneous of all the sites, was larger than the spread of data in the "best event" data for all sites. At Site 1B, the lowest propagation losses occurred for the two events conducted along the major axis of the Oman Basin. At Site 2, the losses were markedly greater for events conducted to the east of the Owen Ridge than for events to the west across the Indus Fan. At Site 3, the losses were somewhat higher to the northeast than in other directions. At Site 4, the losses were less for events conducted towards the north than for events to the south and west. At Site 5, the losses were strongly correlated with bathymetric obstructions to the northeast, east, and south of the site, with significantly higher losses for obstructed events than for events with no obstructions.

(C) Examination of the events with exceptionally high propagation loss indicated that they were generally associated with propagation over prominent bathymetric features with high bottom loss. The events which resulted in the highest propagation losses for all the sites were the four events at the site which traversed the regime east of the Owen Ridge. The event with the highest losses at Site 1A was the event which crossed over the Murray Ridge.

(C) Site 4 in the Somali Basin was the only BEARING STAKE site which was not bottom limited. The depth excess varied with event and fell between no excess for sources near the surface to a maximum value of 276 m for the 91-m source depth. The convergence zones were strongly frequency dependent. Prominent zones at 290 Hz appeared 15 dB above the bottom-reflected background. In contrast, there was little evidence of convergence zones at 25 Hz. The measurements were made in the month of March, which is near the predicted month (April) of maximum near-surface temperatures. For other seasons, the depth excess will increase and a strong dependence of propagation loss on season is predicted. This is in contrast to the other strongly bottom-limited sites of BEARING STAKE at which seasonal dependence of propagation loss will be minimal.

(C) The raw propagation loss data in BEARING STAKE are characterized by an extreme variability with range, and displayed little evidence of definitive structure except for the convergence zone propagation at Site 4. Normal mode computations for Site 1B successfully modeled this behavior, which appears to be typical of propagation involving large numbers of multipaths in a low-bottom-loss regime. The normal mode theory predicts that a 10-dB fade in propagation loss, at 25 Hz, occurs on the average every 1.4 km in range. This is at least more often than mode theory predicts for convergence zone propagation in the deep Atlantic or Pacific. These results suggest that arrays may experience more problems with beamforming in the Indian Ocean than in the Atlantic or Pacific.

Source/Receiver Depth Dependence (U)

(C) A significant dependence on source depth as a function of frequency was observed for propagation losses in the BEARING STAKE measurement results. At 20 Hz for a range of 50 km, the propagation loss for an 18-m SUS source depth was 4 dB greater than

for a 91-m SUS source depth. The corresponding value at 250 km was 10 dB. There were no such differences between the 18-m and 91-m SUS depths at 50, 140, and 300 Hz. This result can be explained in terms of surface decoupling loss. At 20 Hz, the 18-m source depth suffers additional losses due to destructive interference of rays near the ocean surface. This surface decoupling effect is smallest at short range, at which the dominant arrivals at the receiver have steep angles. However, the effect increases with increasing range as the steep-angle arrivals are "stripped" off by bottom reflection losses.

(C) Normal mode theoretical calculations made for Site 1B to determine an optimum source depth which would be typical for bottom-mounted receivers in a bottom-limited environment show that the source depth with minimum propagation loss below the sound channel axis is at the ocean bottom. Above the sound channel axis, the optimum source depth is at the surface decoupling depth. This latter depth at Site 1B was 45 m at 25 Hz. The normal mode theory predicted propagation losses between 45-m and 91-m source depths to be from 0.5 to 1.0 dB and about 1.0 dB between 45-m and 243-m source depths. Thus, the dependence on source depth is minimal below the surface decoupling depth according to theory.

(C) Experimental results for Site 1B were in substantial agreement with normal mode theory results with respect to the dependence of propagation loss on range and receiver depth. The normal mode calculations indicate that under bottom-limited conditions, the dependence of propagation loss on receiver depth is less than 5 dB for receivers below the near-surface region. At Site 1B, minimum propagation losses occurred at the ocean bottom for receivers below the sound channel axis and at the source depth for receivers above it.

(C) On the basis of the normal mode calculations for Site 1B, it can be concluded that in a low-loss, bottom-limited environment, a receiver located off the bottom (about 30 m) will have a 3-dB improvement in SNR over a receiver located on the bottom. This critical depth depends upon frequency but is independent of source depth.

(C) At Site 4, the two receivers with lowest propagation loss results were receivers 1 and 7, located on the Chain Ridge about 400 and 1050 m, respectively, above the floor of the Somali Basin. At 140 and 290 Hz, receiver 1 had less propagation losses than receiver 7 by as much as 7 dB. This was as expected and is related to the critical depth of convergence zone propagation. However, at 25 Hz, receiver 7 had propagation losses which were as much as 5 dB less than those of receiver 1. The physical explanation for this result is not known and attempts to model the result have not been successful. The experimental results suggest a complicated dependence on receiver depth and frequency. This dependence can only be established by a rigorous theoretical analysis and verified by additional experimental measurements.

(C) A significant decrease in propagation loss (~ 7 dB) was observed during two BEARING STAKE events. This decrease, commonly referred to as slope enhancement, occurred at Site 1A for event 1AA2 as the event progressed over the continental rise toward India, and at Site 4 for event 4A1 as the event progressed over the continental rise associated with the Horn of Africa. The enhancement occurred only for the 18-m source depth at 20 Hz. It did not occur at 50, 140, or 300 Hz or at any frequencies for the 91-m source depth. This phenomenon can be explained by the surface decoupling effect. Although surface decoupling increases the propagation loss for an 18-m source at 20 Hz, the losses are diminished when the source transits a sloping bottom because the acoustic propagation is dominated by steeper ray paths which have a smaller decoupling loss.

Bottom Loss (U)

(C) Bottom attenuation coefficients were obtained by comparing the propagation loss for various frequencies at each site. The ranking of the sites in order of lowest bottom loss coefficients was Site 5, 1B, 2, 3, and 4. Although the highest coefficient was for Site 4, the result only applies to low frequencies (25 and 50 Hz), at which convergence zone propagation did not occur as expected. This ranking of the sites is in general agreement with the independent measurement results of bottom loss for BEARING STAKE by ARL/UT.

(U) Propagation loss results were used to divide the Indus Fan into two different bottom loss regions – a northern region characterized by the bottom losses measured at Site 3 and a southern region characterized by the bottom losses measured at Site 5. The boundaries between these regions were determined by noting the location (or absence) of significant changes in the slope of the curves of the experimental propagation loss as a function of range.

Propagation Loss Model Assessment (U)

(C) Comparisons of three propagation loss models (ASTRAL, RAY WAVE, FACT) with the BEARING STAKE experimental data and results indicate that the ASTRAL model is well suited for the prediction of mean propagation loss in a bottom-limited environment. However, a minor modification to the ASTRAL model will have to be performed. Comparison of normal mode results for Site 1B with results of the RAY WAVE and ASTRAL propagation loss models yielded normal mode propagation losses which were 1.5 dB smaller. This result has been attributed to the incoherent addition of arrivals in the RAY WAVE and ASTRAL models. The normal mode standing wave patterns indicate that the upgoing and downgoing waves near the ocean bottom add coherently to produce a propagation loss which is about 1.5 dB less than that of random addition. The ASTRAL model will be modified to reflect this change.

Data Quality (U)

(U) The major portion of the propagation loss data collected on the BEARING STAKE exercise was found to be reliable, consistent, and valid. However, there were a few data sets at each site which were in error and regarded with suspicion. These data sets have been identified as questionable in this report and were not used to influence the conclusions of this assessment.

(U) Comparisons of propagation losses for receivers located near each other on the nearly flat bottom at Sites 1 (1A and 1B) and 3 indicate that the WECo data processing is remarkably consistent. Of 18 independent evaluations, 50% differed by no more than 0.3 dB, 75% by no more than 0.8 dB, and 100% by no more than 1.0 dB. This comparison also demonstrates that the process of averaging the pressure squared (p^2) over 50-km bins is very robust in that it effectively averages out the variability in the raw propagation data.

(C) A comparison of ACODAC and BMA data, measured under similar conditions at Site 1B, yielded ACODAC propagation losses which were 1.5, 2.6, and 4.6 dB higher than the corresponding BMA counterparts for frequencies of 25, 140, and 290 Hz. These differences are statistically significant and suggest some systematic processing or calibration errors in the data.

(C) Consistent propagation loss differences between the experimental CW data and the theoretical results of the normal mode, RAY WAVE, FACT, and ASTRAL models suggest that the source levels used to calculate experimental propagation losses are 1 to 2 dB too low.

(C) The median difference between the propagation losses for source depths of 91 and 243 m of the ship SUS events from all the sites were 2.7, –0.4, 1.9, and 2.8 dB, respectively, for 20, 50, 140, and 300 Hz. The negative value at 50 Hz compared to the positive values at the other frequencies provides strong evidence that some of the SUS source levels are in error. Comparisons of Site 1 experimental data with normal mode theory suggest that the 91- and 243-m SUS depth source levels used to determine propagation losses were 1.4 and 4.3 dB too low at 20 Hz and 2.3 and 1.6 dB too high at 50 Hz. (The accuracy of SUS source levels at 140 and 300 Hz was not investigated in this report.)

(C) A measure of the variance of the raw CW data was established by calculating the standard deviation (SD) of the propagation loss data about their mean value for the 50-km range bins. For Sites 1A, 1B, 2, and 3, the SD was found to be independent of frequency and site. The typical SD value was 5.3 dB, which was based on 374 independent determinations. This value is lower than the 5.6-dB value obtained from the theory of random vectors and the 5.8-dB value obtained from the normal mode model for Site 1B. This difference between experiment and theory is probably due to smoothing factors in the WECo data processing system. The SD for Site 5 was also independent of frequency but was significantly lower at 4.6 dB. The reason for the low value at Site 5 is not known, but the result was confirmed by the SD of the SUS data for Site 5, which was also significantly lower than that of the SUS data for Sites 1A, 1B, 2, and 3. The SD for Site 4 CW data was 5.2, 5.8, and 6.7 dB at 23, 140, and 290 Hz, respectively. The higher SD at 140 and 290 Hz can be attributed to convergence zone propagation which increased the SD in the 50-km range bins.

Summary (U)

(C) On the basis of the propagation loss results and the assessments of them contained in this report, we can conclude that acoustic propagation loss in the Northwest Indian Ocean will not adversely affect the performance of surveillance array systems operating in the area. How well a system will perform in the area will depend on other acoustic parameters such as signal coherence, noise background, and processing techniques.

(C) The BEARING STAKE exercise was successful in terms of collecting, analyzing, and interpreting acoustic data. The lesson learned from this exercise is that an acoustic measurement program such as BEARING STAKE should be conducted in ocean areas in which the deployment of surveillance systems is being considered. Although theoretical models have been developed to predict the propagation losses for surveillance systems in specified locations, these predictions are only as good as the environmental acoustic inputs to the models. This assessment of BEARING STAKE results shows that the propagation losses predicted for the Northwest Indian Ocean were significantly greater than those measured.

10.0 (U) REFERENCES

1. "Acoustic Survey Program: Planning Document (U)," S-2105-76, Naval Undersea Center, 15 June 1976. (SECRET)

2. "Technical Specifications for Project BEARING STAKE Acoustic Survey (U)," TS 196-76, Western Electric Company, 18 November 1976. (SECRET)

3. "Supplements to Technical Specifications for BEARING STAKE (U)," 00S-4061-76 Naval Undersea Center, 17 December 1976. (SECRET)

4. "BEARING STAKE Data Analysis Plan (U)," 00S-1055-77, Naval Ocean Systems Center, May 1977. (SECRET)

5. "BEARING STAKE Exercise: Preliminary Results (U)," by the Principal Scientific Investigators, Naval Ocean Systems Center TR 169, 31 October 1978. (CONFIDENTIAL)

6. "BEARING STAKE – Vertical ACODAC Acoustic Measurements Data Report (U)," ARL-TR-78-8, Applied Research Laboratories, The University of Texas at Austin, 15 February 1978. (CONFIDENTIAL)

7. "Analysis of Acoustic Bottom Interaction in BEARING STAKE (U)," by S. K. Mitchell, K. C. Focke, J. J. Lemmon, and M. M. McSwain, ARL-TR-78-52, November 1978. (CONFIDENTIAL)

8. "Project BEARING STAKE Transmission Loss, Omnidirectional Ambient Noise from Bottomed Arrays (U)," by J. T. Osborne, Western Electric Company, Greensborough, North Carolina, 5 May 1978. (CONFIDENTIAL)

9. "Statistics of Sound Propagation in the Ocean," by Ira Dyer, J. Acoustic Soc. Amer., vol. 48, no. 1 (part 2), p. 337–345, July 1970

10. "BEARING STAKE Exercise: Sound Speed and Other Environmental Variability (U)," by D. F. Fenner and W. J. Cronin, Jr., NORDA Report 18, September 1978. (CONFIDENTIAL)

11. "Low Frequency Propagation Effects for Source or Receiver Near the Ocean Surface (U)," by M. A. Pedersen, D. F. Gordon, and D. White, NUC TP 488, September 1975

12. "The Sound Velocity Structure of the North Indian Ocean," NAVOCEANO TR 231, by L. F. Fenner and D. C. Bucca, December 1972

13. "Sound-Speed Distribution in the Western Indian Ocean," NUC TP 502, by J. G. Colborn, 1976

14. Naval Ocean Systems Center TR 393, "Underwater Sound Propagation Loss Program: Computation By Normal Modes For Layered Oceans and Sediments," by D. F. Gordon (in publication) (see appendix B)

15. Gordon, D. F., and Floyd, E. R., "Acoustic Propagation Effects in Beamforming of Long Arrays (U)," JUA (USN) vol. 29, January 1979. (see appendix B) (CONFIDENTIAL)

16. Gordon, D. F., "Multipath Interference Nulls In Long Range, Low-Frequency, Acoustic Propagation By Normal Modes," article submitted to JASA (see appendix B)

APPENDIX A: BATHYMETRIC PROFILES FOR BEARING STAKE ACOUSTIC RUNS (U)

(U) This appendix contains reconstructed and smoothed bathymetric and navigation profiles for the ship and aircraft acoustic source runs for each of the five BEARING STAKE test sites. The data for these reconstructions were supplied to NOSC by NORDA (Code 341) and NAVOCEANO.

(U) The vertical scale has been exaggerated by the amount indicated on each profile. For example, a vertical exaggeration of 25 ("VE = 25X") means that if 1 inch on the vertical scale represents 1 km of depth, then 1 inch on the horizontal scale represents 25 km of range. Also included on each bathymetric profile is a true slope inset which shows various slopes plotted for the exaggeration of the profile.

(U) Bathymetric profile reconstruction was straightforward in those cases in which the source run was essentially a straight line passing over, or very near, the receivers. However, for those cases in which the source run was not in line with the receiver, the reconstruction was a little more complicated. In one case (aircraft source run 1A1) the flight line passed approximately 35 nautical miles to the east of the receiver. A further complication was the fact that the flight line diagonally crossed the Murray Ridge-Owen Ridge complex. In such a situation, each source SUS shot propagated over a unique path to the receiver. The reconstruction of this run was simplified by considering only those shots which propagated across the ridge, and by grouping the shots and then constructing a representative bathymetric profile for each group. Figure A-1 shows the results of this reconstruction.

(U) The bathymetric profiles in this appendix were used in propagation loss modeling analyses for BEARING STAKE.

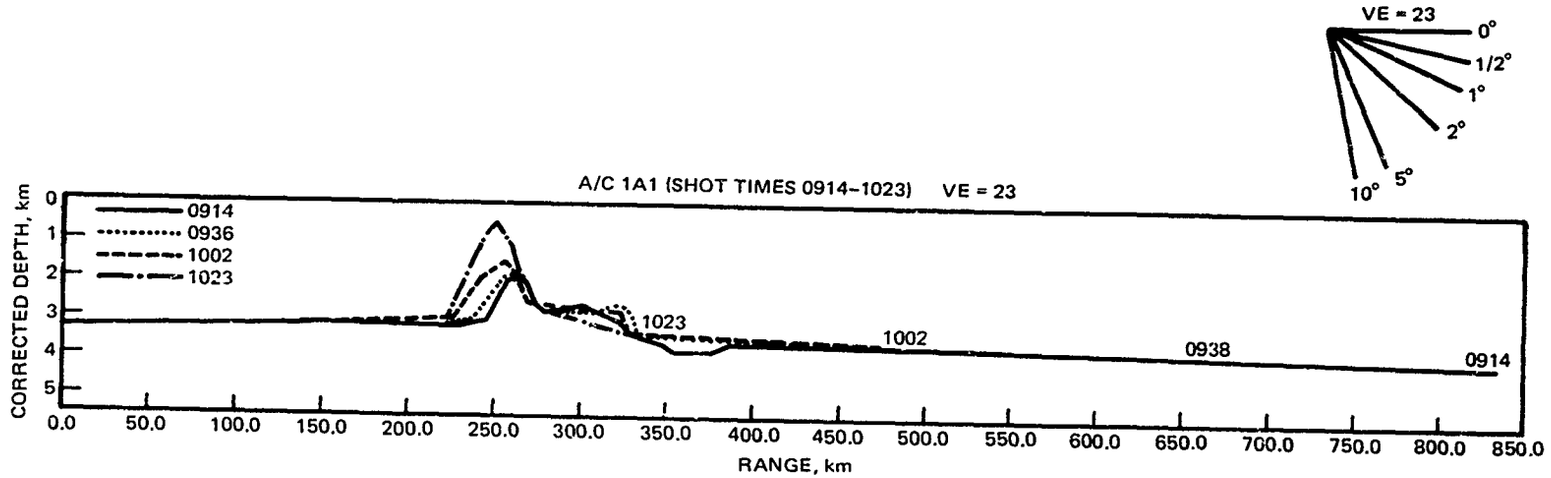

Figure A-1. (U) Long range bathymetry for event 1AA1. (U)

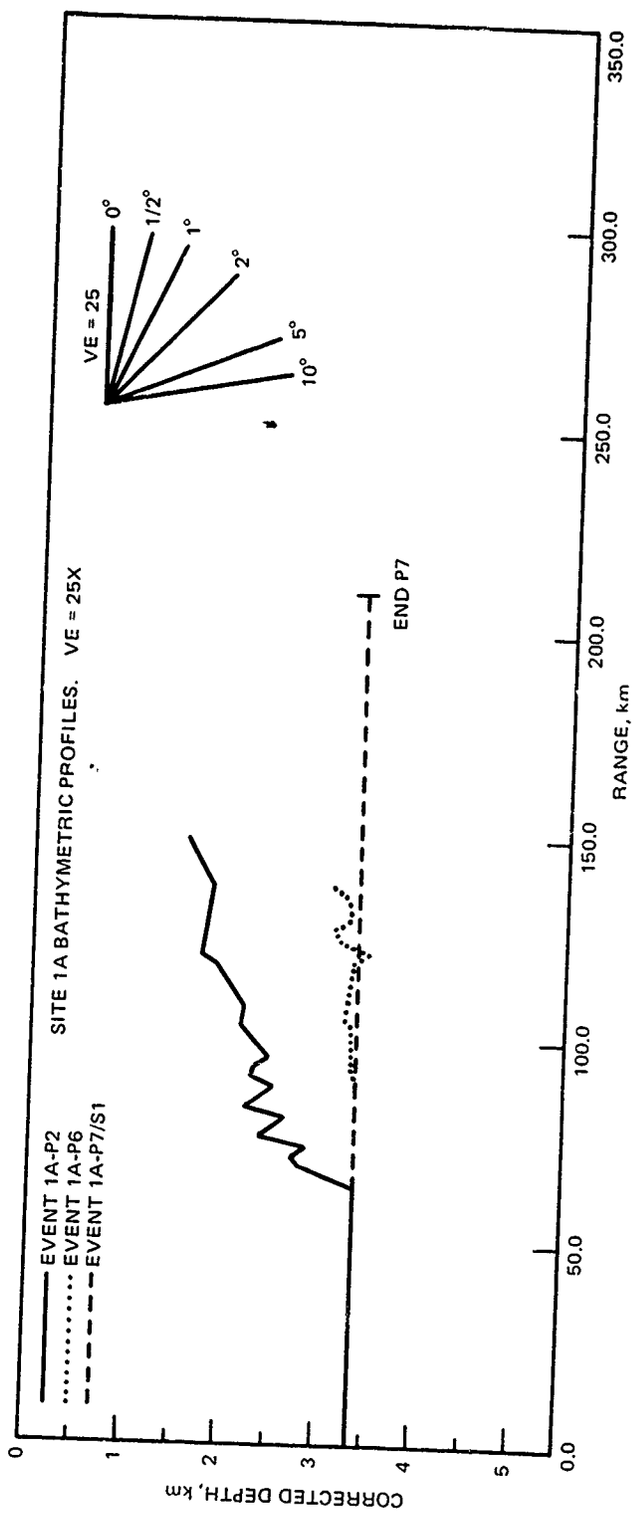

Figure A-2. (U) Long range bathymetry for events 1AP2, 1AP6, 1AP7, and 1AS1. (U)

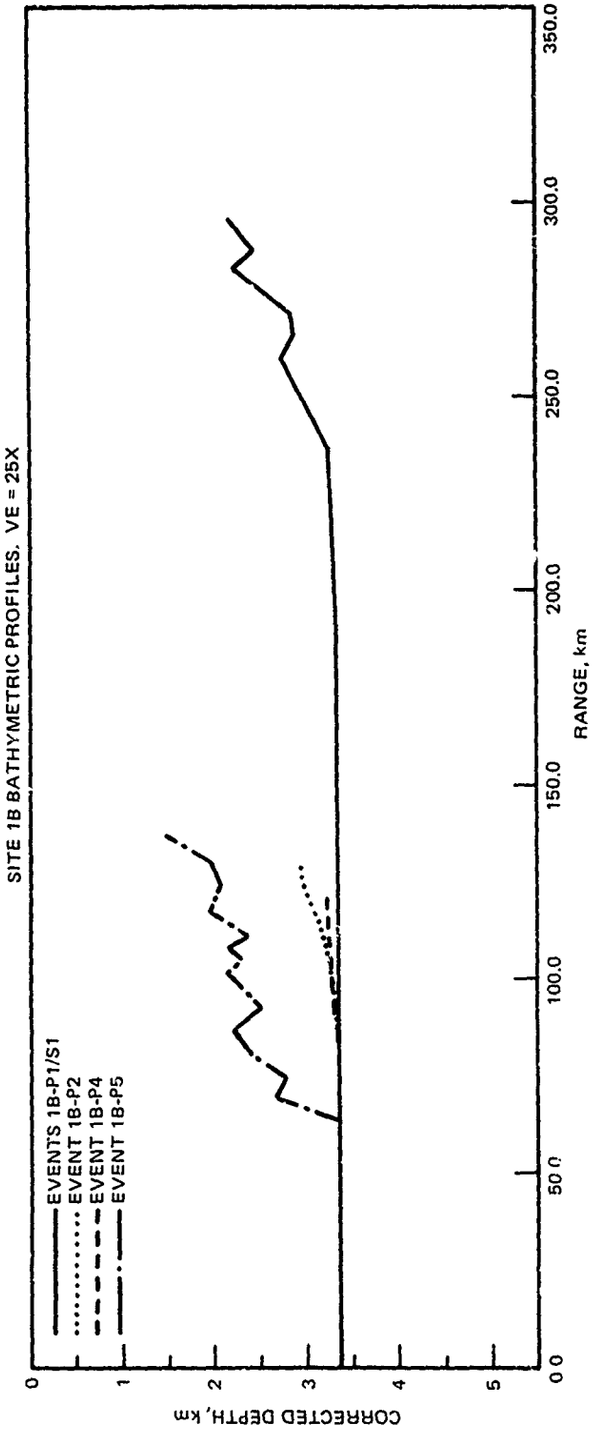

Figure A-3. (U) Long range bathymetry for events 1BP1, 1BS1, 1BP2, 1BP4, and 1BP5. (U)

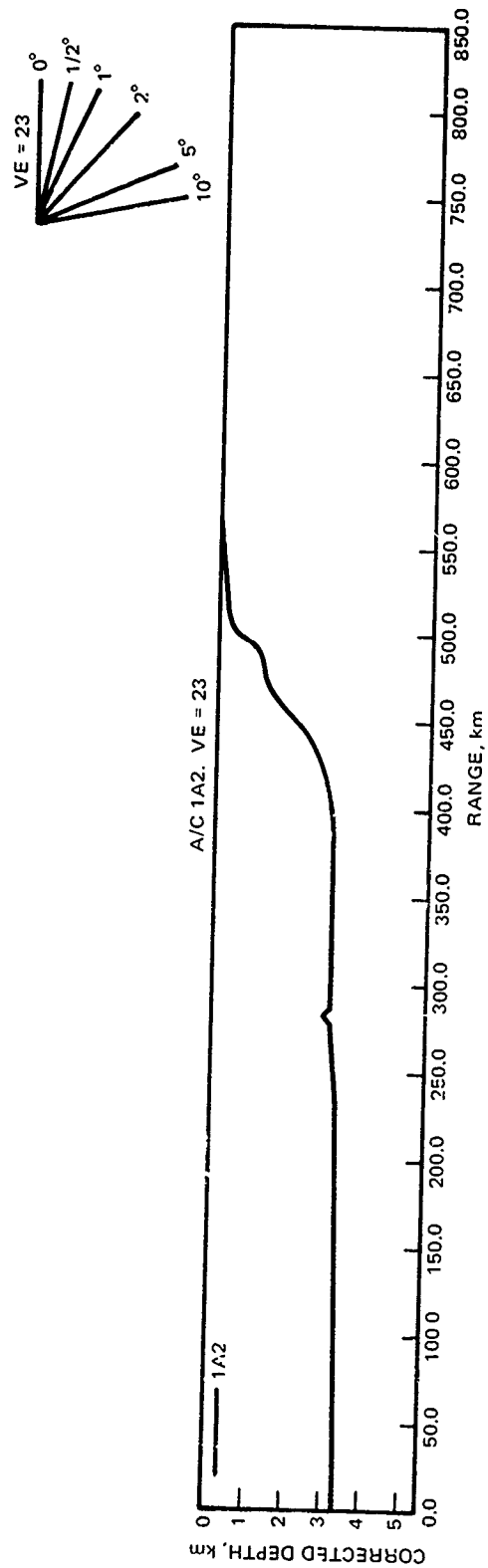

Figure A-4. (U) Long range bathymetry for event 1AA2. (U)

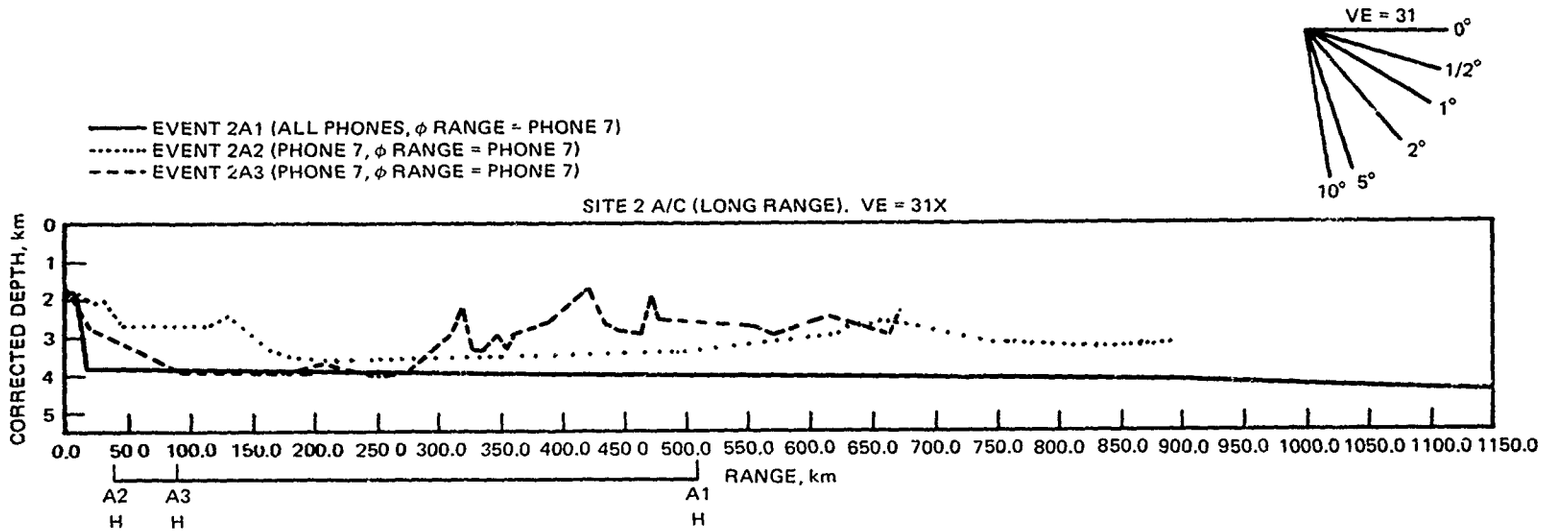

Figure A-5. (U) Long range bathymetry for events 2A1, 2A2, and 2A3. (U)

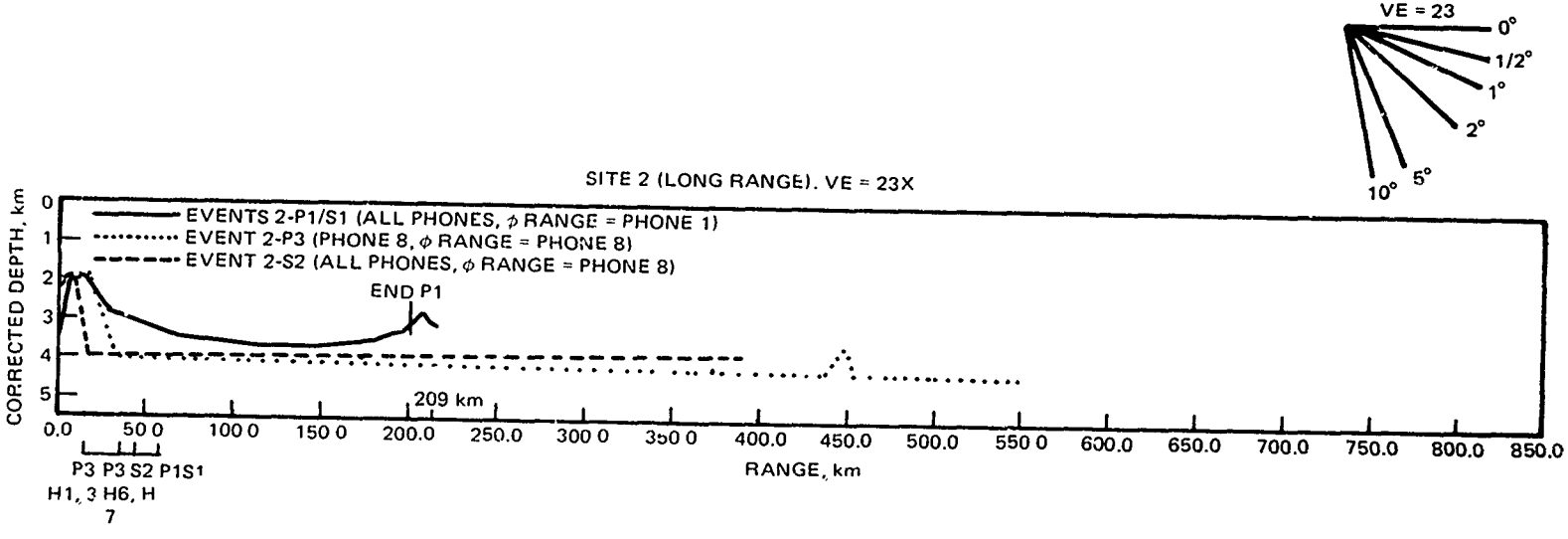

Figure A-6. (U) Long range bathymetry for events 2P1, 2S1, 2P3, and 2S2. (U)

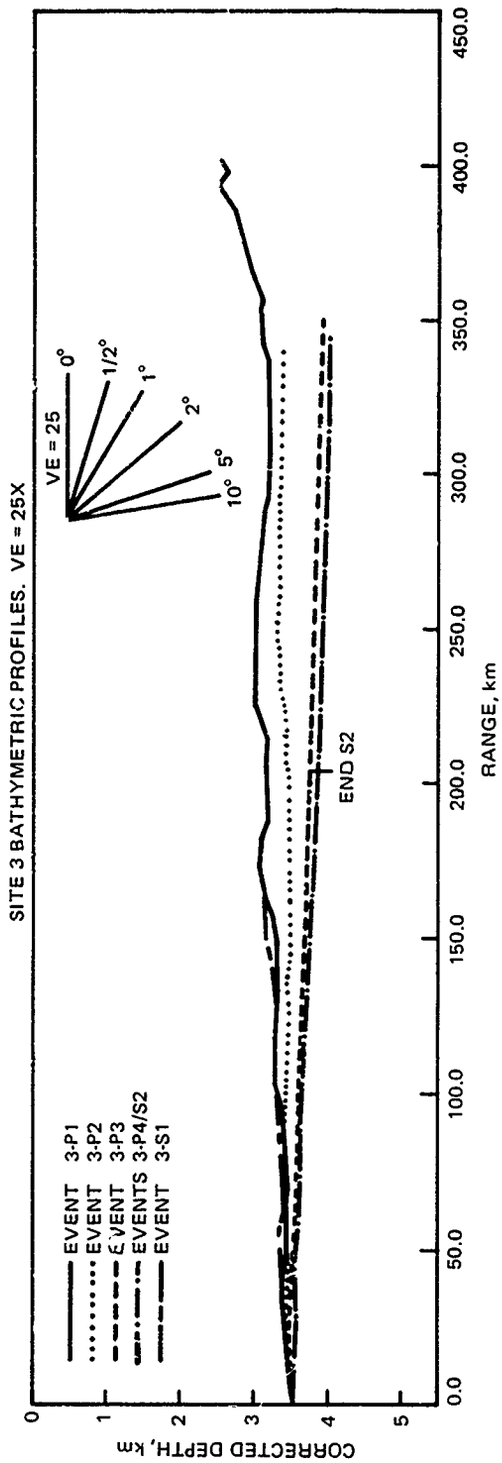

Figure A-7. (U) Long range bathymetry for events 3P1, 3P2, 3P3, 3P4, 3S2, and 3S1. (U)

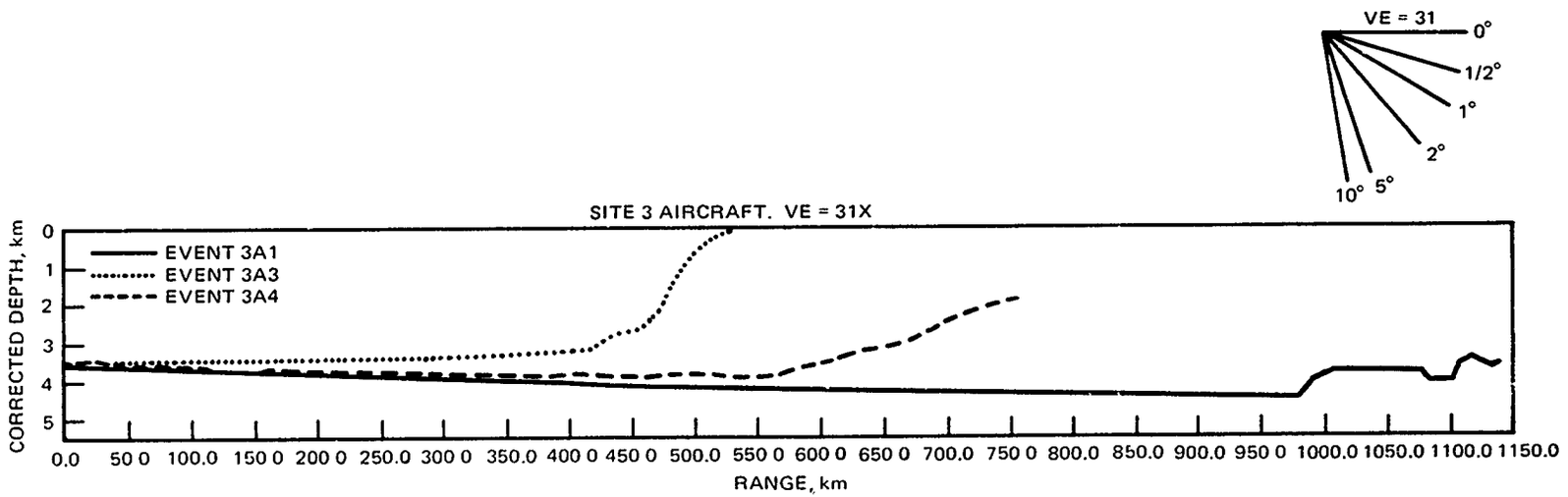

Figure A-8. (U) Long range bathymetry for events 3A1, 3A3, and 3A4. (U)

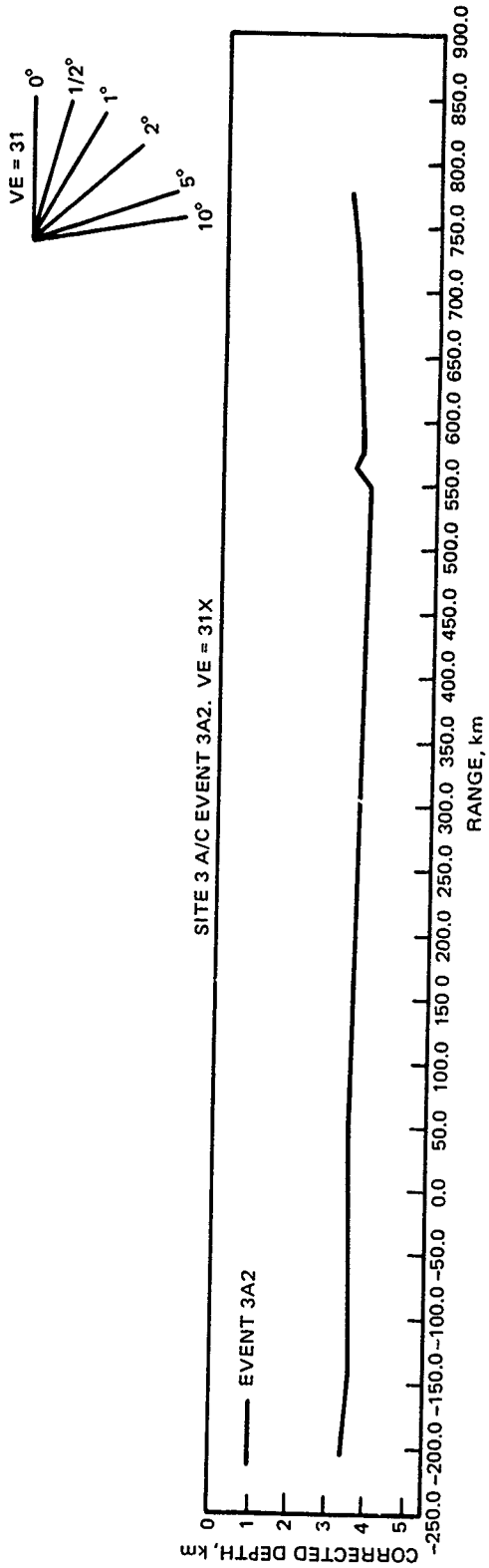

Figure A-9. (U) Long range bathymetry for event 3A2. (U)

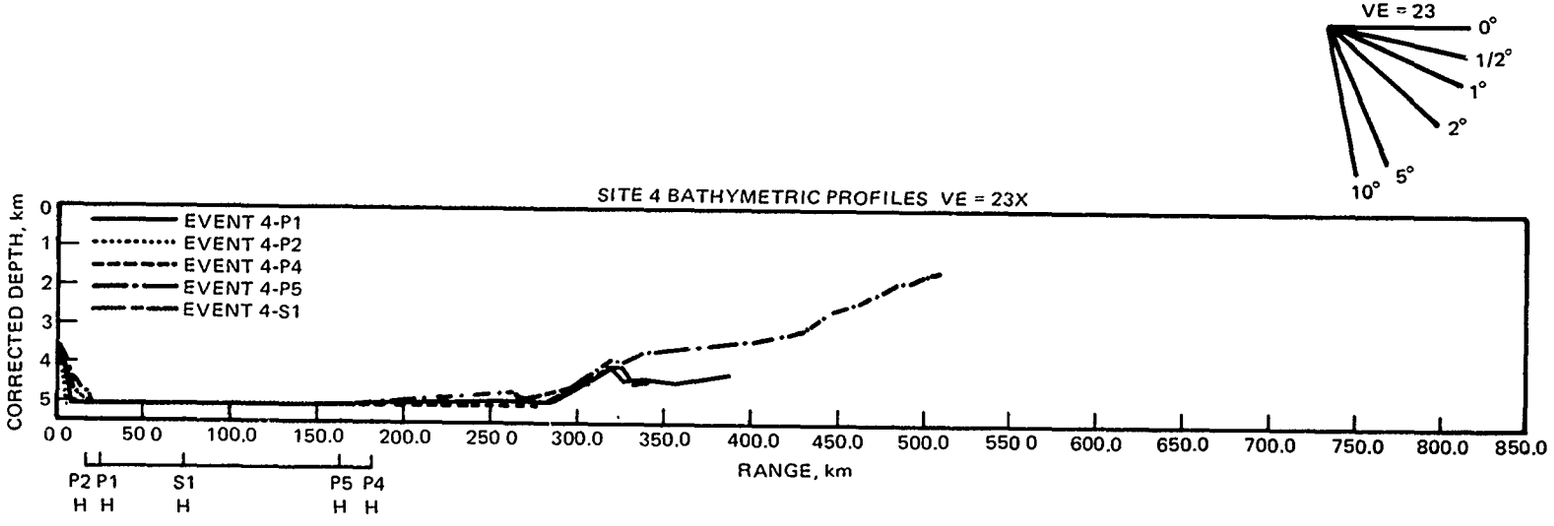

Figure A-10. (U) Long range bathymetry for events 4P1, 4P2, 4P4, 4P5, and 4S1. (U)

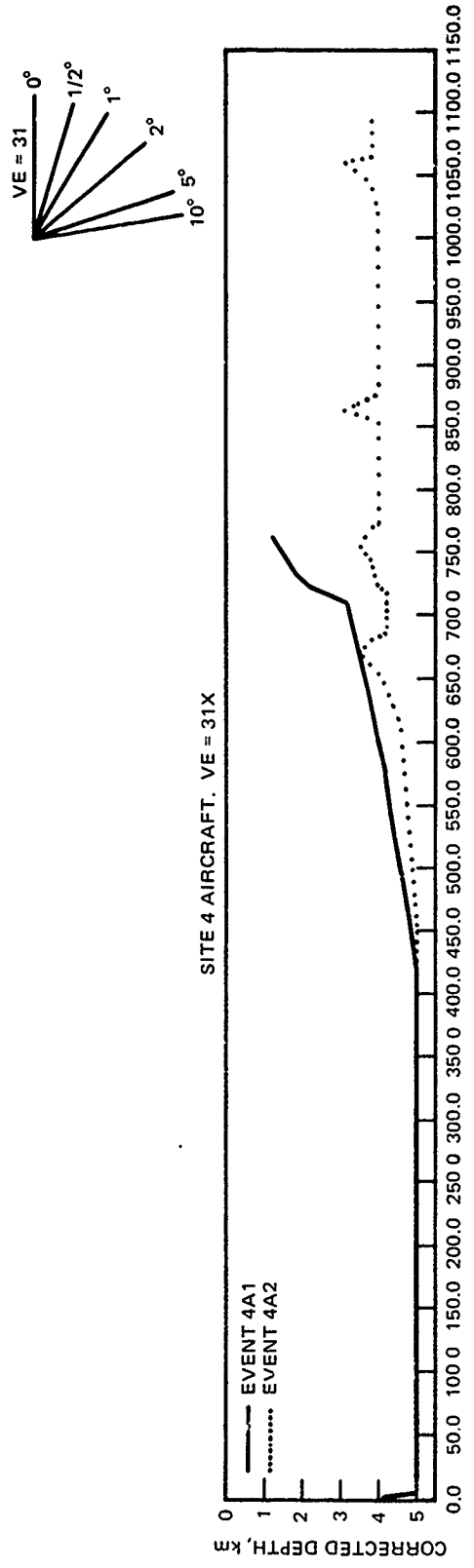

Figure A-11. (U) Long range bathymetry for events 4A1 and 4A2. (U)

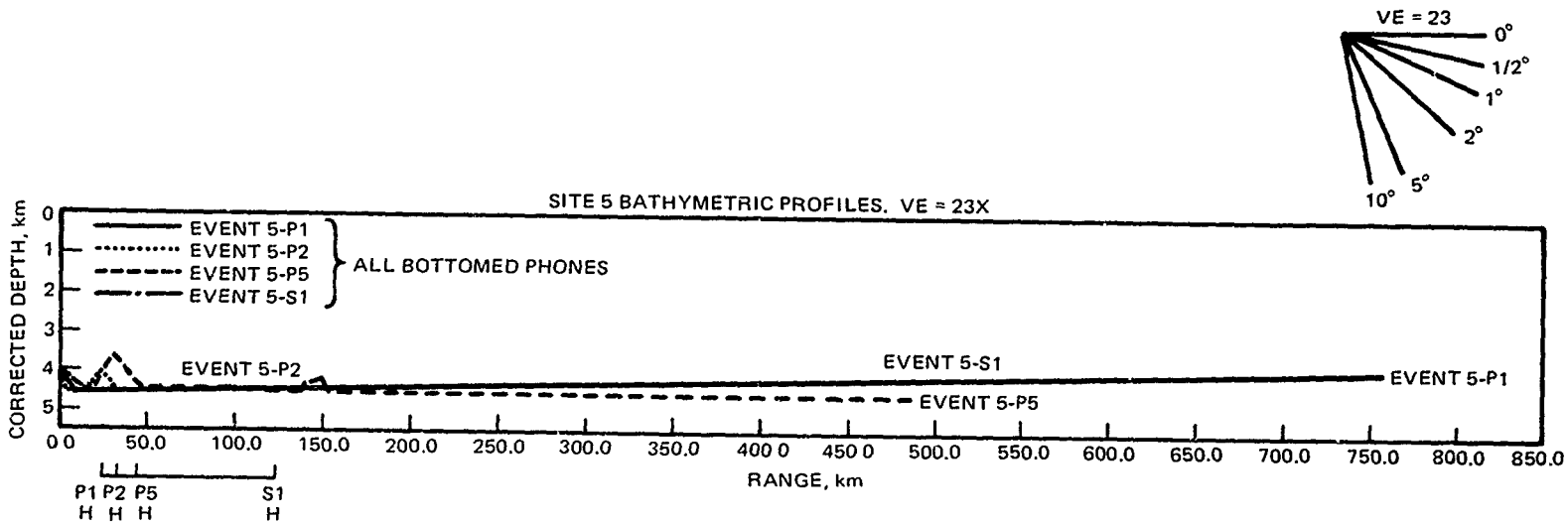

Figure A-12. (U) Long range bathymetry for events 5P1, 5P2, 5P5, and 5S1. (U)

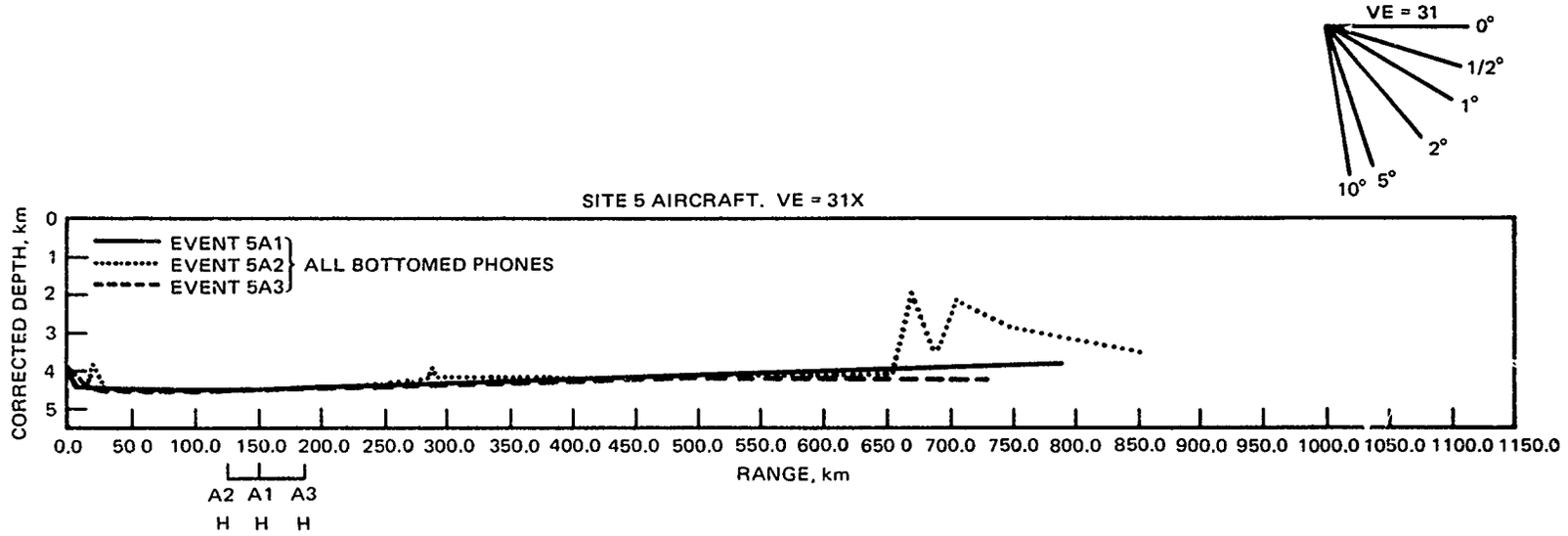

Figure A-13. (U) Long range bathymetry for events 5A1, 5A2, and 5A3. (U)

APPENDIX B: NORMAL MODE ANALYSIS OF VARIABILITY (U)

(C) In an endeavor to explain the variability of the scatter of raw CW data, a multilayered normal mode model (ref 14) was used to make propagation loss calculations for Site 1B. The sound speed input to this model was based on the Fenner (ref 10) representative profile for Site 1B. The sub-bottom inputs to the model were based on the sub-bottom structure as derived by Hamilton and modified by ARL/UT (ref 7).

(C) Figures B-1 and B-2 compare the normal mode theoretical results with experimental data at 25 Hz over range intervals of 25 to 75 km and 225 to 275 km, respectively. The theoretical propagation losses at 25 Hz were calculated for range increments of 100 m. The adequacy of this sampling was checked by recalculating at a 50-km interval and noting that there was no significant change in the resulting pattern. This comparison of experiment and theory demonstrates that the experimental variability is not excessive, is to be expected, and may be regarded as typical of bottom-limited propagation involving large numbers of multipaths in a low-bottom-loss environment.

(C) It is also of interest to compare the variability of BEARING STAKE data to the variability of information applicable to other ocean areas. Normal mode calculations had previously been made for convergence zone propagation in the Atlantic and Pacific (ref 14). The calculations were made over the range interval 463–566 km at 25 and 50 Hz. Therefore, normal mode calculations were made over the same range interval for BEARING STAKE. Figure B-2 shows the resulting curve for 25 Hz, figure B-4 for 50 Hz. (In order to make the analysis herein complete, calculations were also made at 50 Hz over the range interval 25 to 70 km and plotted in figure B-5 for comparison with figure B-1.)

(U) Before discussing the above BEARING STAKE normal mode calculation results, several previous studies/work should be mentioned to provide a convenient method of characterizing the BEARING STAKE data. In reference 15, Gordon examined the effect of rapid increases in propagation loss (fades) on the beamformer of linear arrays. It was determined that such fades can decrease array signal gain by several decibels and can also cause bearing errors. Furthermore, in reference 16, Gordon suggested that the variability in long range propagation could be characterized by counting the number of fades in some range interval and then dividing the interval by the number of fades to obtain an average distance between fades.

(C) As can be seen in figures B-1 to B-5, the normal mode results for BEARING STAKE indicate that the Northwest Indian Ocean acoustic environment is also characterized by a large number of fades. Hence, the range intervals between fades for the BEARING STAKE results were calculated and summarized in table B-1 along with range intervals determined for the Atlantic and Pacific. The salient feature of table B-1 is that there is a slight increase in fade interval with range. This can be attributed to the "stripping" off of arrival paths at longer ranges due to bottom loss. There is also a consistent decrease in the fade interval at 50 Hz when compared to 25 Hz.

---

14. Naval Ocean Systems Center TR 393, "Underwater Sound Propagation Loss Program: Computation By Normal Modes For Layered Oceans and Sediments," by D. F. Gordon (in publication)
15. Gordon, D. F., and Floyd, E. R., "Acoustic Propagation Effects in Beamforming of Long Arrays (U)," JUA (USN) vol. 29, January 1979 (CONFIDENTIAL)
16. Gordon, D. F., "Multipath Interference Nulls in Long Range, Low-Frequency, Acoustic Propagation By Normal Modes," article submitted to JASA

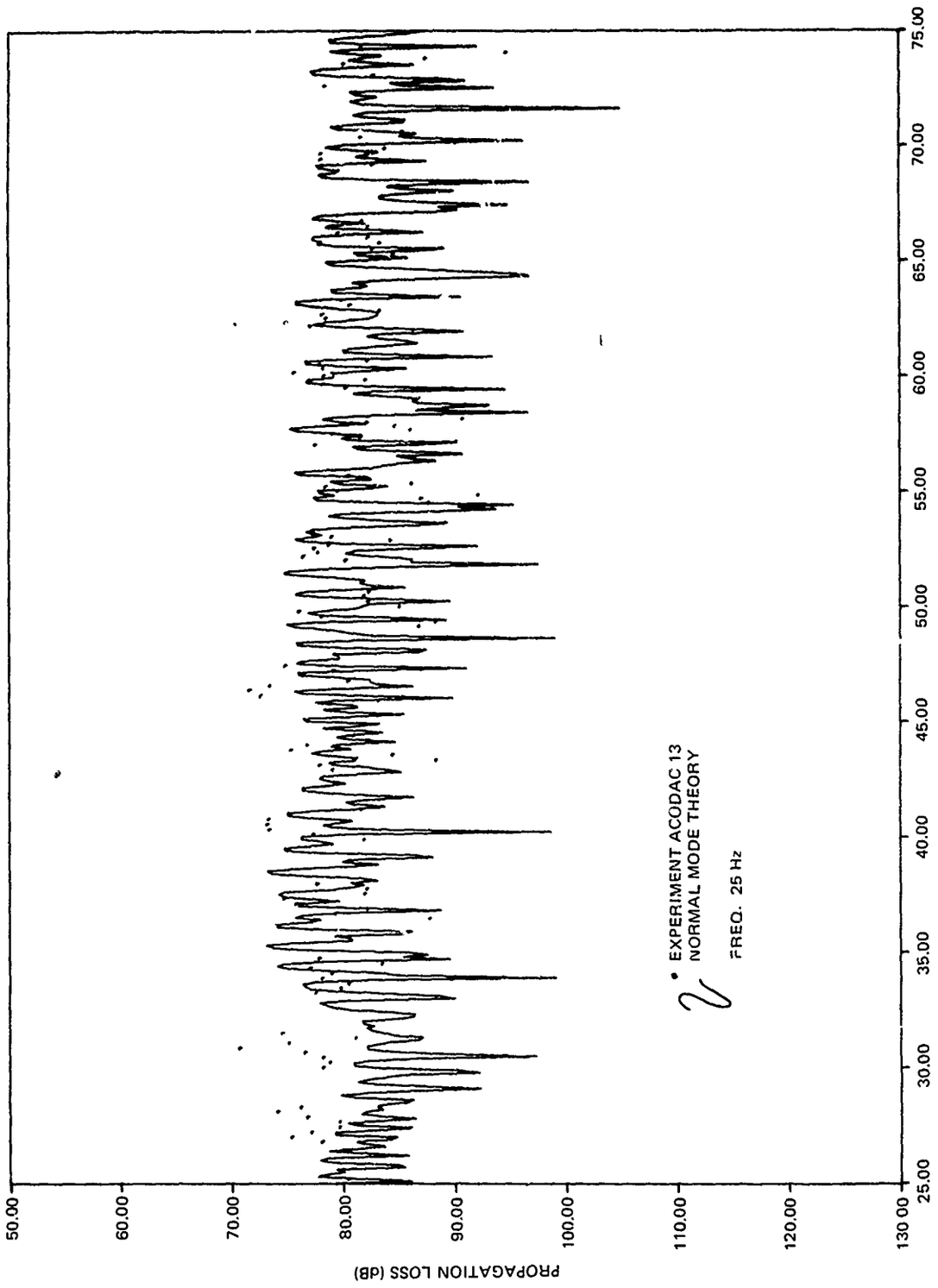

Figure B-1. (C) Theoretical and experimental propagation loss at 25 Hz for a receiver on the ocean bottom over the range interval 25–75 km. (C)

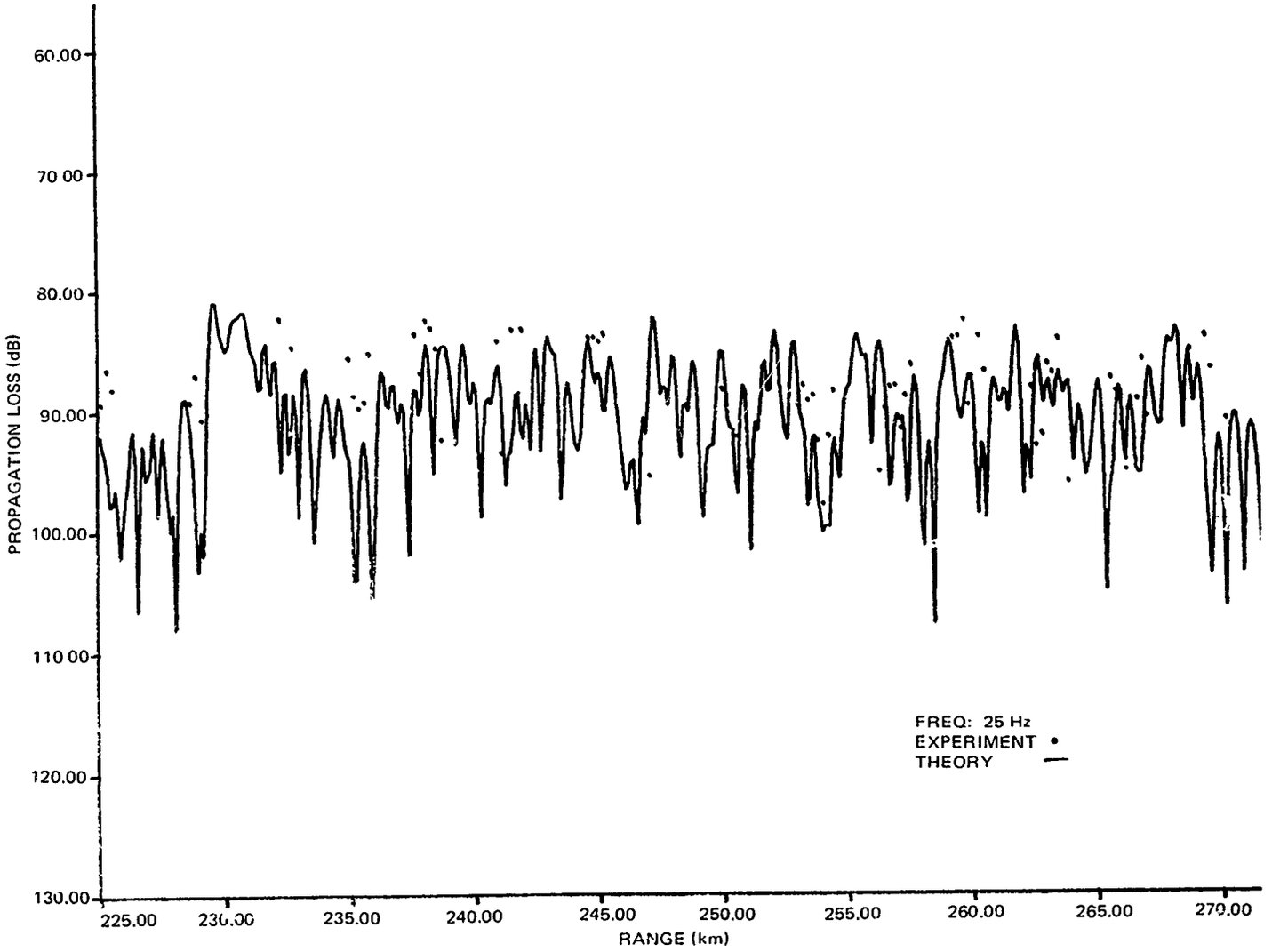

Figure B-2. (C) Theoretical and experimental propagation loss at 25 Hz for a receiver on the ocean bottom over the range interval 225–275 km. (C)

CONFIDENTIAL

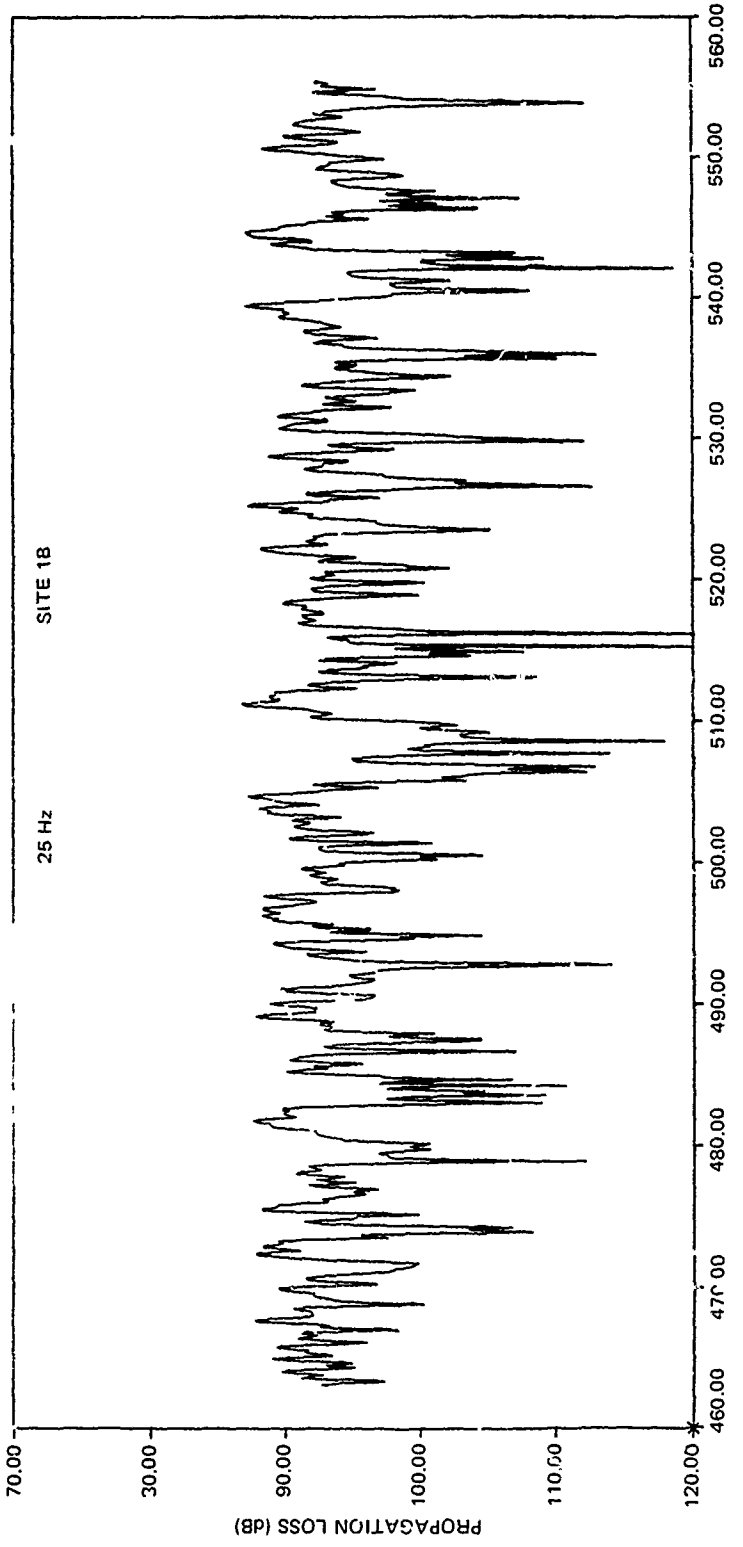

Figure B-3. (C) Propagation loss calculated by normal mode model for Site 1B at 25 Hz over the range interval 460–560 km. (C)

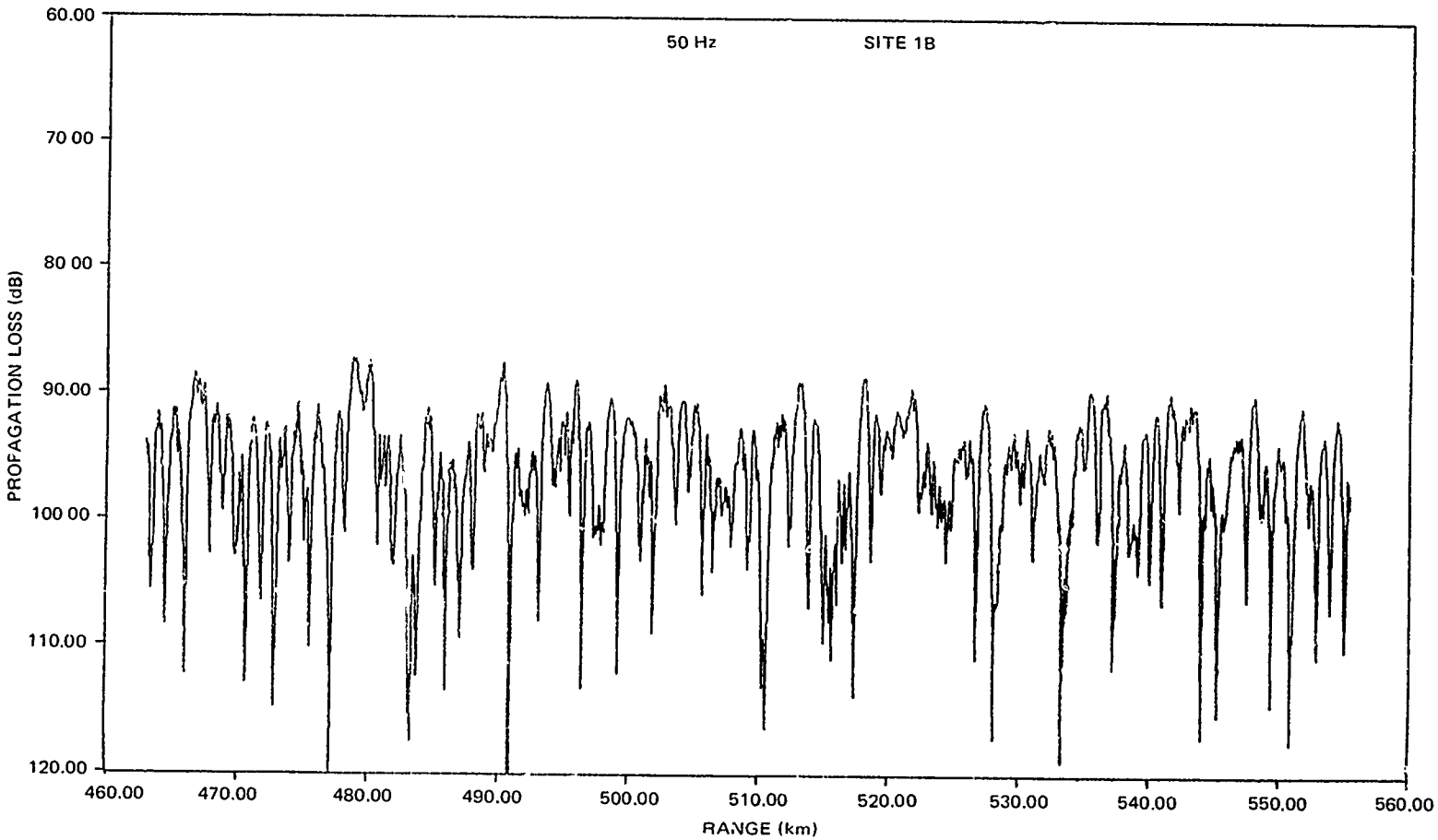

Figure B-4. (C) Propagation loss calculated by normal mode model for Site 1B at 50 Hz over the range interval 460–560 km. (C)

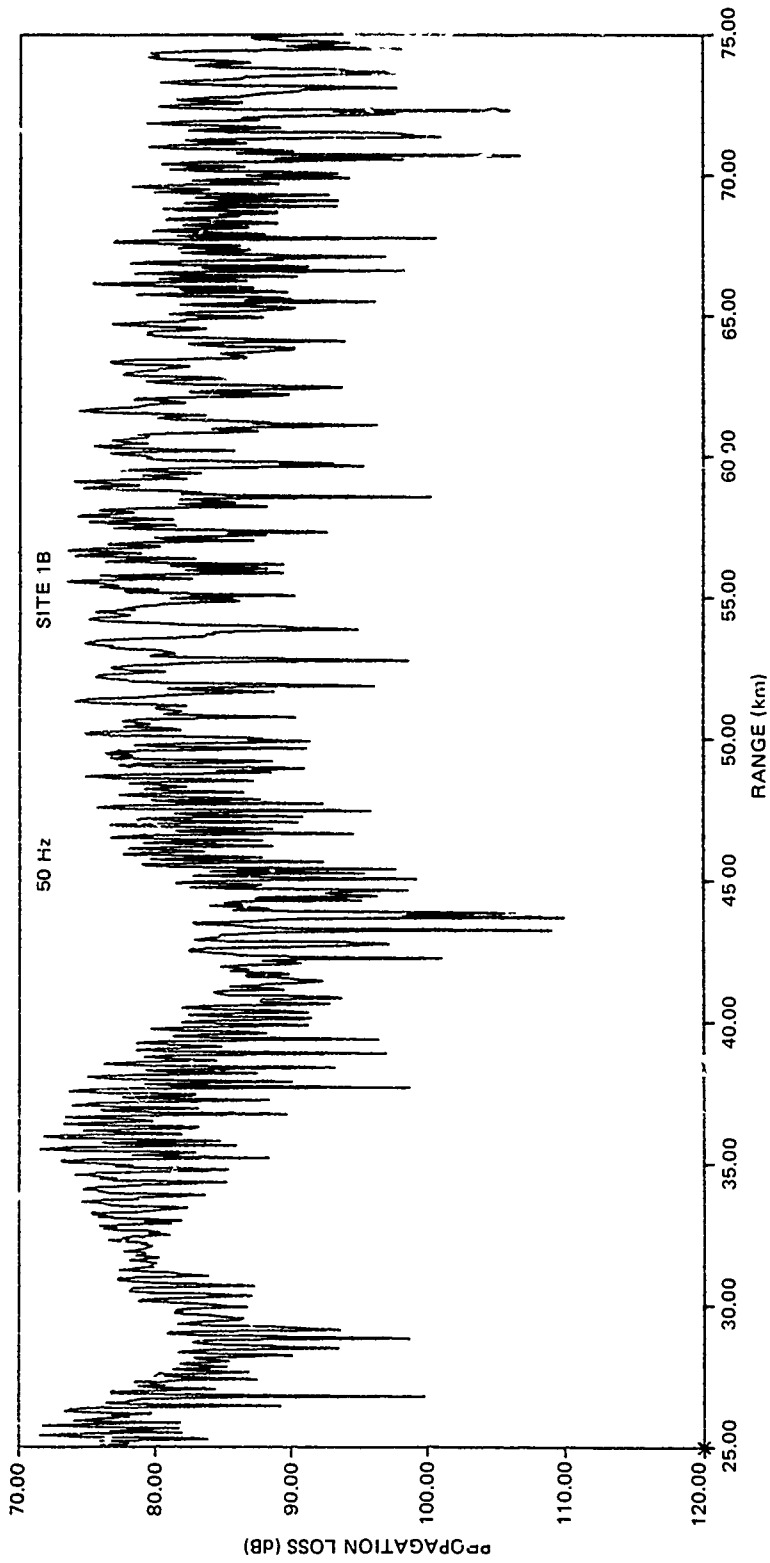

Figure B-5. (C) Propagation loss calculated by normal mode model for Site 1B at 50 Hz over the range interval 25–75 km. (C)

Table B-1. (C) Distance (km) between 5- and 10-dB fades at 25 and 50 Hz over various range intervals for Site 1B and other ocean areas. (C)

		Site 1B					Other Oceans
		Range Interval (km)					
Freq (Hz)	dB Loss Fades	25-75	75-125	125-175	175-225	225-275	463-556
25	5	0.9	0.8	0.9	0.9	1.1	5.4 to 16.3
25	10	1.4	1.8	1.9	2.0	2.0	10.3 to 20.6
50	5	0.4	0.5	0 5	0.6	0.7	5.2 to 20.6
50	10	0.8	1.0	1.0	1.3	1.3	6.9 to 30.8

(C) The fade intervals for the Atlantic and Pacific Oceans for the range interval of 463 to 556 km, shown in table B-1, indicate that fades in propagation appear to occur at least three times as often for the bottom-limited conditions in the Indian Ocean as compared to convergence zone propagation in the Atlantic or Pacific Ocean. This, in turn, suggests that beamforming problems may be more severe in the Indian Ocean than other areas.

(C) Figures B-1 to B-5 also indicate why the variability of the experimental data must be treated in a statistical manner. First, note that the experimental data are undersampled, even at 25 Hz. For example, the nominal range interval between successive experimental observations was about 0.5 km for Site 1B. The fade intervals according to table B-1 are 1.4 and 2.0 km for th3 25–75-km and 225–275-km range intervals, respectively. Thus, the experimental data are undersampled, with only three or four measurements over each fade range interval. At the higher frequencies of 140 and 290 Hz, it is probable that the experimental data were sampled less than once over a fade interval.

(U) Hence, it is apparent why the raw CW data appear jumbled and ragged and devoid of any regular structure except for a general increase in loss with increasing range. The normal mode calculation exhibits a similar lack of structure except at the short ranges of figure B-5, where a slow modulation appears Indeed, the modal result is even more jumbled and ragged than the experimental data.

(U) The experimental data represent a nearly random statistical sampling which is sparse compared to the theoretical fade interval. At the present state of the art, it is believed that the best procedure in treating the experimental data is to compute average values of propagation loss. The variability of the data about these average values can be described in terms of statistical models of the variance.

(U) INITIAL DISTRIBUTION (U)

DEPUTY UNDER SECRETARY OF DEFENSE R&E
(TACT, WARFARE PROGRAMS)
DIR NAVAL WARFARE

ARPA RESEARCH CENTER
UNIT 1
T KOOIJ

ASSISTANT SECRETARY OF THE NAVY (RE&S)
DEP ASST SECRETARY (SYSTEMS)
G CANN

CHIEF OF NAVAL OPERATIONS
NOP-095
NOP-098
NOP-951 (2)
NOP-951F (2)
NOP-952 (2)

CHIEF OF NAVAL MATERIAL
NMT-08T24 (GR SPALDING)

NAVAL ELECTRONIC SYSTEMS COMMAND
CODE 320 (J SINSKY)
PME-124-20 (R KNUDSEN)
PME-124-30
PME-124-60 (4)

NAVAL SEA SYSTEMS COMMAND
NSEA-06R (CD SMITH)

NAVAL AIR SYSTEMS COMMAND
NAIR-370

OFFICE OF NAVAL RESEARCH
ONR-102B

NAVAL RESEARCH LABORATORY
CODE 8108
CODE 8160 (BB ADAMS)

NAVAL INTELLIGENCE SUPPORT CENTER
CODE 222

NAVAL POSTGRADUATE SCHOOL
LIBRARY

NAVAL AIR DEVELOPMENT CENTER
CODE 303 (J HOWARD) (2)

NAVAL OCEANOGRAPHY COMMAND

NAVAL OCEAN RESEARCH AND DEVELOPMENT
ACTIVITY
CODE 110 (TECH DIRECTOR) (2)
CODE 320 (2)
CODE 600 (Dr RD GAUL)
CODE 200 (CDR T MCCLOSKEY)
CODE 340 (DR S MARSHALL)
CODE 360 (DR H EPPERT)

NAVAL OCEANOGRAPHIC OFFICE
CODE 3410 (J CARROLL)
CODE 3400 (WH GEDDES)

NAVAL OCEAN RESEARCH AND DEVELOPMENT
ACTIVITY LIAISON OFFICE

COMMANDER IN CHIEF U.S.
ATLANTIC FLEET
PACIFIC FLEET
COMMANDER
CODE 352

COMMANDER THIRD FLEET
N-32

COMMANDER SEVENTH FLEET
N34

THE UNIVERSITY OF TEXAS
APPLIED RESEARCH LABORATORY
S MITCHELL (2)

WOODS HOLE OCEANOGRAPHIC INSTITUTE
E HAYES

BELL TELEPHONE LABORATORIES
WHIPPANY, NJ 07981
R LAUVER
PENNOTTI

WESTERN ELECTRIC COMPANY
PO BOX 20046
GELFORD CENTER
GREENBORO, NC 27420
R SCUDDER (3)

PLANNING SYSTEMS, INC.
7900 WESTPARK DRIVE
MC LEAN, VA 22101
DR L SOLOMON

TRW, INC.
7600 COLSHIRE DR
MC LEAN, VA 22101
R MURAWSKI

APPLIED HYDROACOUSTICS, INC.
656 QUINCE ORCHARD RD
GAITHERSBERG, MD 20760
F RYDER

COMPUTER SCIENCES CORP.
2251 SAN DIEGO AVENUE
SAN DIEGO, CA 92110

DEFENSE DOCUMENTATION CENTER (2)

DEPARTMENT OF THE NAVY
OFFICE OF NAVAL RESEARCH
875 NORTH RANDOLPH STREET
SUITE 1425
ARLINGTON VA 22203-1995

IN REPLY REFER TO:

5510/1
Ser 321OA/011/06
31 Jan 06

MEMORANDUM FOR DISTRIBUTION LIST

Subj: DECLASSIFICATION OF LONG RANGE ACOUSTIC PROPAGATION PROJECT (LRAPP) DOCUMENTS

Ref: (a) SECNAVINST 5510.36

Encl: (1) List of DECLASSIFIED LRAPP Documents

1. In accordance with reference (a), a declassification review has been conducted on a number of classified LRAPP documents.

2. The LRAPP documents listed in enclosure (1) have been downgraded to UNCLASSIFIED and have been approved for public release. These documents should be remarked as follows:

   Classification changed to UNCLASSIFIED by authority of the Chief of Naval Operations (N772) letter N772A/6U875630, 20 January 2006.

   DISTRIBUTION STATEMENT A: Approved for Public Release; Distribution is unlimited.

3. Questions may be directed to the undersigned on (703) 696-4619, DSN 426-4619.

BRIAN LINK
By direction

Subj: DECLASSIFICATION OF LONG RANGE ACOUSTIC PROPAGATION PROJECT (LRAPP) DOCUMENTS

DISTRIBUTION LIST:

NAVOCEANO (Code N121LC – Jaime Ratliff)
NRL Washington (Code 5596.3 – Mary Templeman)
PEO LMW Det San Diego (PMS 181)
DTIC-OCQ (Larry Downing)
ARL, U of Texas
Blue Sea Corporation (Dr.Roy Gaul)
ONR 32B (CAPT Paul Stewart)
ONR 321OA (Dr. Ellen Livingston)
APL, U of Washington
APL, Johns Hopkins University
ARL, Penn State University
MPL of Scripps Institution of Oceanography
WHOI
NAVSEA
NAVAIR
NUWC
SAIC

Declassified LRAPP Documents

Report Number	Personal Author	Title	Publication Source (Originator)	Pub. Date	Current Availability	Class.
Unavailable	Penrod, C. S., et al.	MOORED SURVEILLANCE SYSTEM FIELD VALIDATION TEST SENSOR PERFORMANCE ANALYSIS. VOLUME I. DATA COLLECTION AND MESUREMENT SYSTEM DESCRIPTION	University of Texas, Applied Research Laboratories	781231	ADC018009	C
Unavailable	Watkins, S. L., et al.	MOORED SURVEILLANCE SYSTEM FIELD VALIDATION TEST SENSOR PERFORMANCE ANALYSIS. VOLUME III. VERNIER RESOLUTION DATA PRODUCTS	University of Texas, Applied Research Laboratories	781231	ADC018373	C
Unavailable	Watkins, S. L., et al.	MOORED SURVEILLANCE SYSTEM FIELD VALIDATION TEST SENSOR PERFORMANCE ANALYSIS. VOLUME II. STANDARD RESOLUTION DATA PRODUCTS	University of Texas, Applied Research Laboratories	781231	ADC018374	C
NORDATN44	Bucca, P. J.	ENVIRONMENTAL VARIABILITY DURING THE CHURCH STROKE II CRUISE FIVE EXERCISE (U)	Naval Ocean R&D Activity	790201	ADC020353; NS; AU; ND	C
NADC7820830	Balonis, R. M.	TEST STEERED VERTICAL LINE ARRAY (TSVLA) MEASUREMENTS FOR BEARING STAKE SURVEYS (U)	Naval Air Systems Command	790301	ADC018003; NS; ND	C
USIControl674779	Williams, W., et al.	REPORT OF THE LRAPP EXERCISE PLANNING WORKSHOP TRACOR INC ROCKVILLE MD 16 - 17 OCTOBER 1978 (U)	Underwater Systems, Inc.	790302	NS; ND	C
NOSCTR357	Hamilton, E. L., et al.	GEOACOUSTIC MODELS OF THE SEAFLOOR: GULF OF OMAN, ARABIAN SEA, AND SOMALI BASIN (U)	Naval Ocean Systems Center	790615	ND	C
Unavailable	Unavailable	RAPIDLY DEPLOYABLE SURVEILLANCE SYST (RDSS) ACOUSTIC VALIDATION TEST (AVT) EXERCISE PLAN (U)	Naval Electronic Systems Command	790625	AU	C
LRAPPRC79027	Brunson, B. A., et al.	GULF OF MEXICO AND CARIBBEAN SEA DATA AND MODEL BASE REPORT (U)	Tracor, Inc.	790701	ADC019153; NS; ND	C
Unavailable	Unavailable	BEARING STAKE BMS DATA QUALITY ASSESSMENT REPORT (U)	University of Texas, Applied Research Laboratories	790705	AU	C
PME12430	Unavailable	RAPIDLY DEPLOYABLE SURVEILLANCE SYSTEM (RDSS) ACOUSTIC VALIDATION TEST (AVT) DATA REDUCTION AND ANALYSIS PLAN (U)	Naval Electronic Systems Command	790815	NS; AU	C
Unavailable	Unavailable	RAPIDLY DEPLOYABLE SURVEILLANCE SYSTEM (RDSS) ACOUSTIC VALIDATION TEST (AVT) EXERCISE PLAN (U)	Naval Electronic Systems Command	790917	AU	C
NOSCTR467	Pedersen, M. A., et al.	PROPAGATION LOSS ASSESSMENT OF THE BEARING STAKE EXERCISE (U)	Naval Ocean Systems Center	790928	ADC020845; NS; AU; ND	C
NOSCTR466	Anderson, A. L., et al.	BEARING STAKE ACOUSTIC ASSESSMENT (U)	Naval Ocean Systems Center	790928	ADC020797; NS; AU; ND	C